Biosynthesis of a bacterial meroterpenoid reveals a non-canonical class II meroterpenoid cyclase

Zengyuan Wang,[a] Tyler A. Alsup,[b] Xingming Pan,[a] Lu-Lu Li,[a] Jupeng Tian,[a] Ziyi Yang,[a] Xiaoxu Lin,[a] Hui-Min Xu,[c] Jeffrey D. Rudolf,[b] and Liao-Bin Dong*[,a]

[a]State Key Laboratory of Natural Medicines, School of Traditional Chinese Pharmacy, China Pharmaceutical University, Nanjing 211198, China

[b]Department of Chemistry, University of Florida, Gainesville, Florida 32611, United States

[c]The Public Laboratory Platform, China Pharmaceutical University, Nanjing 211198, China

Corresponding to: ldong@cpu.edu.cn (L.-B. D.)

This PDF file includes:

Supplementary Experimental Procedures

Supplementary Tables S1 to S23

Supplementary Figures S1 to S134

Table of Contents

Experimental Procedures

General experimental procedures.

All ^{1}H, ^{13}C, and 2D NMR (^{1}H-^{1}H COSY, HSQC, HMBC, and ROESY) experiments were run on a Bruker AVANCE NEO at 400 MHz for ^{1}H and 100 MHz for ^{13}C nuclei. Chemical shifts (δ) were given in parts per million (ppm) with reference to the solvent signals and coupling constants were expressed in hertz (Hz). Preparative HPLC was carried out on an Agilent 1260 Prep Infinity LC with a VWD detector equipped with an Agilent Eclipse XDB-C18 column (250 mm × 21.2 mm, 7 μm). LC-MS was performed on an Agilent 1260 Infinity LC coupled to an MSD IQ equipped with an Agilent Poroshell 120 EC-C18 column (50 mm × 4.6 mm, 2.7 μm). Optical rotations were obtained using an AUTOPOL IV automatic polarimeter (Rudolph Research Analytical). HRESIMS data were obtained using an Agilent G6230 Q-TOF mass instrument. UV spectra were acquired in MeOH with a Shimadzu UV-2600i UV-VIS spectrophotometer. X-ray crystal data were collected using a Bruker D8 VENTURE diffractometer. Fractions were monitored by TLC and spots were visualized by heating silica gel plates sprayed with 10% H_2SO_4 in EtOH. All of the solvents were analytically pure. Other chemicals, biochemical, and media components were purchased from standard commercial sources.

Culture conditions.

E. coli strains harboring plasmids were grown in lysogeny broth (LB) with appropriate antibiotic selection. Wild-type (*Streptomyces albus* J1074, *Streptomyces lividans* SBT18 and *Amycolatopsis tolypomycina* NRRL B-24205) and recombinant actinomycete strains were cultured in solid MS medium. *E. coli-Streptomyces* conjugations were plated onto solid ISP4 medium supplemented with 20 mM $MgCl_2$. Fermentation of wild-type and recombinant actinomycete strains were conducted using fermentation medium of PTMM.[1–3] Briefly, fresh spores of actinomycete strains were inoculated into 250 mL baffled flasks containing 50 mL of Tryptone Soy Broth (TSB) sterile seed medium and cultivated for 2–3 days at 28 °C on a rotary shaker (230 rpm). After that, 4% (v/v) seed culture were transferred into 2.5 L baffled Erlenmeyer flasks filled with 500 mL of fermentation medium, and incubated at 28 °C and 230 rpm for 7 days.

MS medium: 20 g D-mannitol, 20 g soya flour, 3 g $CaCO_3$, and 20 g agar in 1 L of deionized water, pH 7.2.

ISP4 medium: 10 g starch soluble, 1 g K_2HPO_4, 1 g $MgSO_4$, 1 g NaCl, 2 g $(NH_4)_2SO_4$, 2 g $CaCO_3$, 1 mg $FeSO_4$, 1 mg $MnCl_2$, 1 mg $ZnSO_4$, and 20 g agar in 1 L of deionized water, pH 7.2.

PTMM medium: 40 g dextrin, 40 g lactose, 5 g yeast extract, 5 g MOPS, and 10 mL trace elements (40 mg $ZnCl_2$, 200 mg $FeCl_3{\cdot}6H_2O$, 10 mg $CuCl_2$, 10 mg $MnCl_2{\cdot}4H_2O$, 10 mg $Na_2B_4O_7{\cdot}10H_2O$, and 10 mg $(NH_4)_6Mo_7O_{24}{\cdot}4H_2O$ in 1 L of deionized water) in 1 L of deionized water, pH 7.3.

Gene cloning and plasmid construction.

The sequences of synthetic promoters, ribosome binding sites (RBS), and terminators were designed based on a prior publication,[4] and were synthesized by General Biosystems (Anhui, China). Combinations of promoters and RBSs were organized to ensure that no additional sequences were present between promoter and RBS sequences (P12R10, P3R5, P9R7, and P10R10). The synthetic promoter-RBS parts and terminator parts (T2, T9, T4, and T10) were assembled onto the pRSFDuet-1 plasmid by General biosystems (Anhui, China), resulting in the construction of plasmids pRSFDuet-P12R10, pRSFDuet-P3R5, pRSFDuet-P9R7, and pRSFDuet-P10R10. Genomic DNA from *A. tolypomycina* was extracted according to the protocol of DC103 kit (Vazyme).

Each CDS (Coding sequence) in the *ato* gene cluster was amplified by polymerase chain reaction (PCR) from genomic DNA using the corresponding primers (Table S4). Genes *atoA*, *atoE*, *and atoF* were inserted into the *Nde*I restriction site within the pRSFDuet-P12R10 vector to construct plasmids pLDW1001, pLDW1002, and pLDW1003. Gene *atoB* was inserted into the *Pst*I restriction site within the pRSFDuet-P9R7 vector to construct pLDW1004. Gene *atoC* was inserted into the *Hind*III restriction site within the pRSFDuet-P3R5 vector to afford pLDW1005. Subsequently, plasmid pLDW1006 was constructed by inserting gene *atoD* into the *Afl*II restriction site of the pRSFDuet-P10R10 vector resulting in pRSFDuet-P10R10-*atoD*.

The PCR pruduct P3R5-*atoC*-T9, cloned from pLDW1005, was inserted into the *EcoR*V and *BamH*I sites of pSET152 vector to generate pLDW1007. Subsequently, the PCR pruducts P3R5-*atoC*-T9 and P10R10-*atoD*-T10 were cloned from pLDW1005 and pLDW1006, respectively, and inserted into the *EcoR*V and *BamH*I sites of pSET152 vector to afford pLDW1008. The PCR products of P3R5-*atoC*-T9 and P12R10-*atoE*-T2 were assembled into the linearized pSET152 vector, resulting in pLDW1009. The P3R5-*atoC*-T9 and P12R10-*atoF*-T2 fragments were cloned into the *EcoR*V and *BamH*I sites of pSET152 vector to create pLDW1010. The P3R5-*atoC*-T9, P10R10-*atoD*-T10, and P12R10-*atoE*-T2 fragments were assembled into the linearized pSET152 vector, resulting in pLDW1011. The P3R5-*atoC*-T9, P12R10-*atoE*-T2, and P12R10-*atoF*-T2 fragments were assembled into the linearized pSET152 vector, resulting in pLDW1012. The P3R5-*atoC*-T9, P10R10-*atoD*-T10, and P12R10-*atoF*-T2 fragments were assembled into the linearized pSET152 vector, resulting in pLDW1013. The P3R5-*atoC*-T9, P10R10-*atoD*-T10, P12R10-*atoE*-T2, and P12R10-*atoF*-T2 fragments were assembled into the linearized pSET152 vector, resulting in pLDW1014. The P9R7-atoB-T4, P3R5-*atoC*-T9, P10R10-*atoD*-T10, P12R10-*atoE*-T2, and P12R10-*atoF*-T2 fragments were assembled into the linearized pSET152 vector, resulting in pLDW1015. The P12R10-*atoA*-T2, P9R7-atoB-T4, P3R5-*atoC*-T9, P10R10-*atoD*-T10, P12R10-*atoE*-T2, and P12R10-*atoF*-T2 fragments were assembled into the linearized pSET152 vector, resulting in pLDW1016.

Genes *atoA*, *atoB*, *atoE*, and several class II meroterpenoid cyclase (MTC) genes (*SerTC*, *SmaTC*, *UtaTC*, *CcrTC*, *SsyTC*, *AxyTC*, and *PshTC*) were inserted into the *Nde*I and *Xho*I restriction sites within the pET-28a(+) vector, resulting in the construction of expression vectors pLDW1017–pLDW1019 and pLDW1021–pLDW1027.

Heterologous expression, extraction, and LC-MS analysis.

Plasmids pLDW1007–pLDW1016 were individually transformed into *E. coli* ET12567/pUZ8002 and introduced into *S. albus* J1074 by intergeneric conjugation according to the standard methods.[5] Positive colonies were selected with 20 μg/mL nalidixic acid and 50

μg/mL apramycin after 5–7 days cultivation and subsequently identified through PCR with corresponding primers. Finally, recombinant strains were constructed and named *S. albus* DLW1002–DLW1011, respectively. Likewise, the recombinant plasmid pDLW1014 was transferred into *S. lividans* SBT18 in the same manner to obtain *S. lividans* DLW1012.

All recombinant *Streptomyces* strains were fermented in PTMM medium. The broth and mycelium were separated by centrifugation at 3750 rpm for 15 min. The broth was then extracted three times with ethyl acetate (EtOAc), while the mycelium was extracted with acetone. After removing the solvent, the residual solution was further extracted with EtOAc. The organic phase of broth and mycelium extracts were combined and evaporated. The resulting residues were dissolved in CH_3OH and filtered through a 0.22 μm filter for subsequent LC-MS analysis. LC-MS analysis was performed using an 18 min solvent gradient (0.8 mL/min) from 10%–100% CH_3CN in H_2O containing 0.1% formic acid.

Isolation of atolypene A, C and D (1–3) from the *S.albus* DLW1011 overexpressing *atoABCDEF*.

The heterologous strain of *S. albus* DLW1011 harboring gens *atoABCDEF* was fermented on a 7.5-L large scale in PTMM medium. After a 7-day fermentation, the broth and mycelium were separated by centrifugation at 3750 rpm for 20 min. The broth was then extracted three times with EtOAc, while the mycelium was extracted with acetone. After removing the solvent, the residual mycelium solution was further extracted with EtOAc. The extracts from broth and mycelium were combined after concentration in vacuo. The crude extracts were then adsorbed onto C18 reverse-phase resin and fractionated by MPLC, eluting with a gradient of CH_3OH-H_2O (60:40–100:0) to give six fractions (Fr.01–Fr.06). Fr.02, which contained atolypene A (**1**), was further purified by reverse-phase preparative HPLC (65% CH_3CN, 17 mL/min) to yield 14 mg (t_R = 22 min; Figures S7 and S8). Fr.04 was purified by preparative HPLC eluted with 30–100% CH_3CN at a flow rate of 17 mL/min for 35 min, affording atolypene C (**2**) (9 mg; t_R = 25 min; Figures S9–S15) and atolypene D (**3**) (16 mg; t_R = 27 min; Figures S16–S21).

Atolypene A (**1**): white powder; ^{1}H NMR (400 MHz, CD_3OD): δ_H 5.73 (1H, m), 5.16 (1H, t, *J* = 6.6 Hz), 3.55 (1H, m), 2.53 (1H, m), 2.36 (1H, m), 2.30 (1H, m), 2.14 (1H, m), 2.12 (1H, m), 2.06 (1H, m), 2.24 (1H, m), 2.19 (1H, m), 1.98 (1H, m), 1.97 (1H, m), 1.95 (1H, m), 1.95 (1H, m), 1.94 (1H, m), 1.90 (1H, m), 1.79 (1H, m), 1.67 (1H, m), 1.65 (3H, s), 1.60 (1H, m), 1.59 (1H, m), 1.49 (1H, m), 1.47 (1H, m), 1.45 (1H, m), 1.34 (1H, m), 1.24 (3H, s), 1.21 (3H, s), 1.13 (1H, m), 1.03 (3H, s), 0.98 (3H, d, *J* = 7.1 Hz), 0.90 (3H, s) ppm. ^{13}C NMR (100 MHz, CD_3OD): δ_C 217.8, 174.6, 144.1, 139.2, 123.3, 122.4, 56.1, 51.6, 51.3, 45.7, 39.8, 39.0, 38.3, 37.2, 36.5, 33.9, 33.5, 32.7, 29.4, 26.5, 25.0, 24.8, 24.7, 23.3, 21.4, 16.6, 15.7, 14.9 ppm.

Atolypene C (**2**): white powder; $[\alpha]_D^{20}$ +22.5 (*c* 0.12, MeOH); UV (MeOH) λ_{max} nm (log ε): 208 (2.6); ^{1}H NMR (400 MHz) and ^{13}C NMR (100 MHz) data (CD_3OD), see **Table S5**; HRESIMS (negative mode) *m/z* 484.3438 [M – H]$^-$ (calcd for $C_{30}H_{46}NO_4^-$, 484.3432).

Atolypene D (**3**): white powder; $[\alpha]_D^{20}$ +6.0 (*c* 0.04, MeOH); UV (MeOH) λ_{max} nm (log ε): 206 (2.9); ^{1}H NMR (400 MHz) and ^{13}C NMR (100 MHz) data (CD_3OD), see **Table S6**; HRESIMS (negative mode) *m/z* 443.3169 [M – H]$^-$ (calcd for $C_{28}H_{43}O_4^-$, 443.3167).

Isolation of 4 and 5 from the *S.albus* DLW1005 overexpressing *atoCF*.

The heterologous strain of *S. albus* DLW1005, harboring gens *atoCF*, was fermented on a 10-L scale in PTMM medium. Following the procedure described above, the EtOAc fraction was adsorbed onto C18 reverse-phase resin and fractionated by MPLC, eluting with a gradient of CH_3OH-H_2O (50:50–100:0) to give four fractions (Fr.01- Fr.04). Fr.02 was subjected to silica gel CC and eluted with petroleum ether-EtOAc (10:1–5:1) to yiled **4** (11 mg; Figures S22–S27) and **5** (7 mg; Figures S28–S33).

Compound **4**: colorless oil; $[\alpha]_D^{20}$ +7.0 (*c* 0.01, MeOH); UV (MeOH) λ_{max} nm (log ε): 203 (1.7); ^{1}H NMR (400 MHz) and ^{13}C NMR (100 MHz) data (CD_3OD), see **Table S7**; HRESIMS (negative mode) *m/z* 405.3005 [M – H]$^-$ (calcd for $C_{25}H_{41}O_4^-$, 405.3010).

Compound **5**: colorless oil; $[\alpha]_D^{20}$ +12.0 (*c* 0.03, MeOH); UV (MeOH) λ_{max} nm (log ε): 212 (2.8); ^{1}H NMR (400 MHz) and ^{13}C NMR (100 MHz) data (CD_3OD), see **Table S8**; HRESIMS (negative mode) *m/z* 415.3187 [M + Na]$^+$ (calcd for $C_{25}H_{44}NaO_3^+$, 415.3183).

Isolation of 6–10 from the *S.albus* DLW1008 overexpressing *atoCDF*.

The heterologous strain of *S. albus* DLW1008, harboring gens *atoCDF*, was fermented on a 40-L large scale in PTMM medium. Following the procedure described above, the crude extracts were adsorbed onto C18 reverse-phase resin and fractionated by MPLC, eluting with a gradient of CH_3OH-H_2O (40:60–100:0) to give five fractions (Fr.01–Fr.05). Fr.02 was purified by preparative HPLC that was eluted with 60% CH_3CN at the flow rate of 17 mL/min for 25 min to afford **6** (68 mg; t_R = 16 min; Figures S34–S39). Fr.03 was subjected to silica gel CC and eluted with petroleum ether-EtOAc (10:1–1:1) to yiled **7** (5 mg; Figures S41–S46), **8** (221 mg; Figures S47–S52) and **9** (450 mg; Figures S53–S58). Fr. 04 was subjected to silica gel CC, eluting with petroleum ether-EtOAc (5:1), and further purified by preparative HPLC (CH_3CN-H_2O, 85:15) to yield **10** (330 mg; t_R = 20 min; Figures S59–S64).

Compound **6**: colorless oil; $[\alpha]_D^{20}$ +8.0 (*c* 0.10, MeOH); UV (MeOH) λ_{max} nm (log ε): 210 (2.7); ^{1}H NMR (400 MHz) and ^{13}C NMR (100 MHz) data (CD_3OD), see **Table S9**; HRESIMS (negative mode) *m/z* 462.3580 [M – H]$^-$ (calcd for $C_{28}H_{48}NO_4^-$, 462.3589).

Compound **7**: colorless oil; $[\alpha]_D^{20}$ +7.0 (*c* 0.03, MeOH); UV (MeOH) λ_{max} nm (log ε): 204 (2.1); ^{1}H NMR (400 MHz) and ^{13}C NMR (100 MHz) data (CD_3OD), see **Table S10**; HRESIMS (negative mode) *m/z* 504.3673 [M – H]$^-$ (calcd for $C_{30}H_{50}NO_5^-$, 504.3694).

Compound **8**: colorless oil; $[\alpha]_D^{20}$ +5.9 (*c* 0.22, MeOH); UV (MeOH) λ_{max} nm (log ε): 205 (2.6); ^{1}H NMR (400 MHz) and ^{13}C NMR (100 MHz) data (CD_3OD), see **Table S11**; HRESIMS (negative mode) *m/z* 463.3425 [M – H]$^-$ (calcd for $C_{28}H_{47}O_5^-$, 463.3429).

Compound **9**: colorless oil; $[\alpha]_D^{20}$ +35.0 (*c* 0.04, MeOH); UV (MeOH) λ_{max} nm (log ε): 213 (3.0); ^{1}H NMR (400 MHz) and ^{13}C NMR (100 MHz) data (CD_3OD), see **Table S12**; HRESIMS (negative mode) *m/z* 407.3161 [M – H]$^-$ (calcd for $C_{25}H_{43}O_4^-$, 407.3167).

Compound **10**: colorless oil; $[\alpha]_D^{20}$ +15.0 (*c* 0.05, MeOH); UV (MeOH) λ_{max} nm (log ε): 212 (2.9); ^{1}H NMR (400 MHz) and ^{13}C NMR (100 MHz) data (CD_3OD), see **Table S13**; HRESIMS (negative mode) *m/z* 433.3313 [M – H]$^-$ (calcd for $C_{27}H_{45}O_4^-$, 433.3323).

Isolation of atolypene E–G (11–13) from the *S.lividans* DLW1012 overexpressing *atoCDEF*.

The heterologous strain of *S. lividans* DL1012, harboring gens *atoCDEF*, was fermented on a 7.5-L large scale in PTMM medium. Following the procedure described above, the crude extracts were adsorbed onto C18 reverse phase resin and fractionated by MPLC, eluting with a gradient of CH_3OH-H_2O (60:40–100:0) to give six fractions (Fr.01–Fr.06). Fr.02 was further purified by preparative HPLC eluted with 30–100% CH_3CN at the flow rate of 17 mL/min for 25 min to afford atolypene E (**11**) (6 mg; t_R = 15 min; Figures S82–S87). Fr.03 that contained atolypene F (**12**) was further purified by preparative HPLC (75% CH_3CN, 17 mL/min) to yield 5 mg (t_R = 22 min; Figures S88–S93). Fr.05 was subjected to silica gel CC and eluted with petroleum ether-EtOAc (5:1) to yiled atolypene E (**13**) (15 mg; Figures S94–S99).

Atolypene E (**11**): white powder; $[\alpha]_D^{20}$ +38.3 (*c* 0.06, MeOH); UV (MeOH) λ_{max} nm (log ε): 206 (2.6); ^{1}H NMR (400 MHz) and ^{13}C NMR (100 MHz) data (CD_3OD), see **Table S16**; HRESIMS (negative mode) *m/z* 444.3492 [M – H]$^-$ (calcd for $C_{28}H_{46}NO_3^-$, 444.3483).

Atolypene F (**12**): white powder; $[\alpha]_D^{20}$ +45.0 (*c* 0.06, MeOH); UV (MeOH) λ_{max} nm (log ε): 207 (2.4); ^{1}H NMR (400 MHz) and ^{13}C NMR (100 MHz) data (CD_3OD), see **Table S17**; HRESIMS (negative mode) *m/z* 486.3584 [M – H]$^-$ (calcd for $C_{30}H_{48}NO_4^-$, 486.3589).

Atolypene G (**13**): colorless waxy solid; $[\alpha]_D^{20}$ +54.6 (*c* 0.03, MeOH); UV (MeOH) λ_{max} nm (log ε): 209 (2.9); ^{1}H NMR (400 MHz) and ^{13}C NMR (100 MHz) data (CD_3OD), see **Table S18**; HRESIMS (negative mode) *m/z* 415.3214 [M – H]$^-$ (calcd for $C_{27}H_{43}O_3^-$, 415.3218).

Synthesis of Mosher esters of 9.

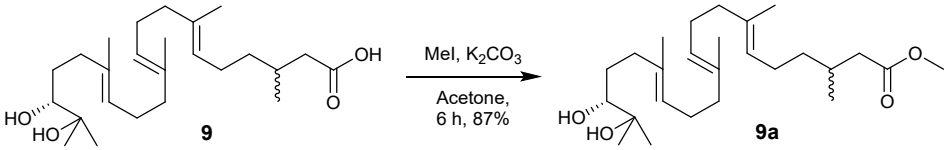

To a stirred solution of **9** (61.4 mg, 0.150 mmol) and K_2CO_3 (104.0 mg, 0.750 mmol) in dry acetone (1 mL) was added MeI (93.4 μL, 1.500 mmol). The reaction mixture was stirred at room temperature for 6 h. After removing of acetone under reduced pressure, the reaction mixture was extracted with EtOAc (3 × 10 mL) and dried over anhydrous Na_2SO_4. The crude product was concentrated in vacuo and purified by silica gel CC, eluting with petroleum ether-EtOAc (4:1) to yiled **9a** (55.0 mg; 87%; Figures S65 and S66).

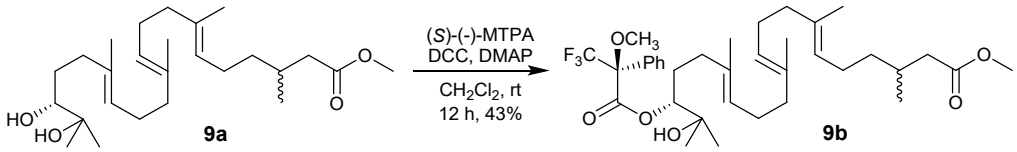

The synthesis of Mosher esters of compound **9a** was carried out using previously published methods.[6]

A mixture of **9a** (20.0 mg, 0.047 mmol), (*S*)-(-)-MTPA (44.0 mg, 0.188 mmol), DCC (39.0 mg, 0.189 mmol), and DMAP (17.0 mg, 0.139 mmol) was dissolved in anhydrous CH_2Cl_2 (1 mL), which was stirred under N_2 at room temperature for 12 h. After concentration in vacuo, the crude product was subjected to silica gel CC and eluted with petroleum ether-EtOAc (10:1) to yiled **9b** (13 mg; 43%; Figures S69–S71).

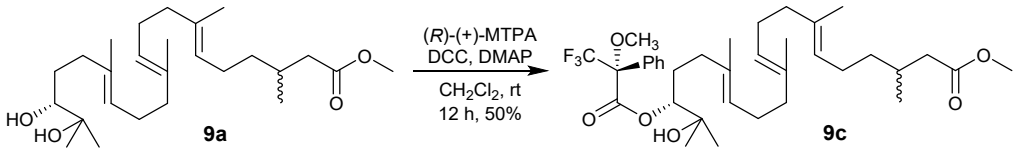

Consistent with the above process, a mixture of **9a** (25.0 mg, 0.059 mmol), (*R*)-(+)-MTPA (55.0 mg, 0.235 mmol), DCC (48.7 mg, 0.236 mmol), and DMAP (21.0 mg, 0.172 mmol) was dissolved in anhydrous CH_2Cl_2 (1 mL), which was stirred under N_2 at room temperature for 12 h. After concentration in vacuo, the crude product was subjected to silica gel CC and eluted with petroleum ether-EtOAc (10:1) to yiled **9c** (19 mg; 50%; Figures S72–S74).

Compound **9a**: colorless oil; $[\alpha]_D^{20}$ +12.0 (*c* 0.13, MeOH); UV (MeOH) λ_{max} nm (log ε): 215 (3.1); ^{1}H NMR (400 MHz) and ^{13}C NMR (100 MHz) data (CD_3OD), see **Table S14**; HRESIMS (positive mode) *m/z* 445.3275 [M + Na]$^+$ (calcd for $C_{26}H_{46}NaO_4^+$, 445.3288).

Compound **9b**: colorless oil; $[\alpha]_D^{20}$ –12.4 (*c* 0.13, MeOH); UV (MeOH) λ_{max} nm (log ε): 218 (3.4); ^{1}H NMR (400 MHz) and ^{13}C NMR (100 MHz) data (CD_3OD), see **Table S14**; HRESIMS (positive mode) *m/z* 661.3680 [M + Na]$^+$ (calcd for $C_{36}H_{53}F_3NaO_6^+$, 661.3686).

Compound **9c**: colorless oil; $[\alpha]_D^{20}$ +31.6 (*c* 0.18, MeOH); UV (MeOH) λ_{max} nm (log ε): 221 (3.6); ^{1}H NMR (400 MHz) and ^{13}C NMR (100 MHz) data (CD_3OD), see **Table S14**; HRESIMS (positive mode) *m/z* 661.3679 [M + Na]$^+$ (calcd for $C_{36}H_{53}F_3NaO_6^+$, 661.3686).

Synthesis of Mosher esters of 10.

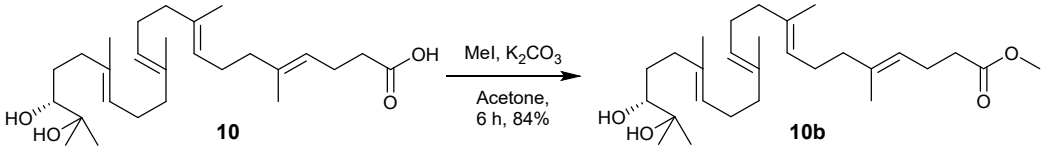

To a stirred solution of **10** (30 mg, 0.069 mmol) and K_2CO_3 (47.8.0 mg, 0.346 mmol) in dry acetone (1 mL) was added MeI (22.0 μL, 0.345 mmol). The reaction mixture was stirred at room temperature for 6 h. After removing of acetone under reduced pressure, the reaction mixture was extracted with EtOAc (3 × 10 mL) and dried over anhydrous Na_2SO_4. The crude product was concentrated in vacuo and purified by silica gel CC, eluting with petroleum ether-EtOAc (5:1) to yiled **10b** (26.0 mg; 84%; Figures S67 and S68).

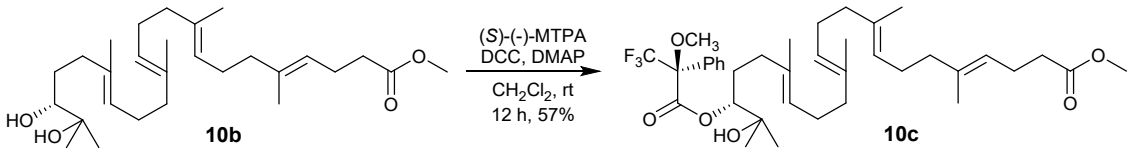

A mixture of **10b** (13.0 mg, 0.029 mmol), (*S*)-(-)-MTPA (13.0 mg, 0.029 mmol), DCC (24.0 mg, 0.117 mmol), and DMAP (15.0 mg, 0.123 mmol) was dissolved in anhydrous CH_2Cl_2 (1 mL), which was stirred under N_2 at room temperature for 12 h. After concentration in vacuo, the crude product was subjected to silica gel CC and eluted with petroleum ether-EtOAc (11:1) to yiled **10c** (11.0 mg; 57%; Figures S75–S77).

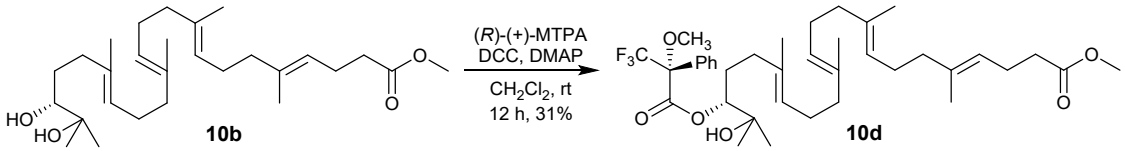

A mixture of **10b** (13.0 mg, 0.029 mmol), (*R*)-(+)-MTPA (30.0 mg, 0.128 mmol), DCC (24.0 mg, 0.117 mmol), and DMAP (15.0 mg, 0.123 mmol) was dissolved in anhydrous CH_2Cl_2 (1 mL), which was stirred under N_2 at room temperature for 12 h. After concentration in vacuo, the crude product was subjected to silica gel CC and eluted with petroleum ether-EtOAc (11:1) to yiled **10d** (6.0 mg; 31%; Figures S78 and S79).

Compound **10b**: colorless oil; $[\alpha]_D^{20}$ +6.7 (*c* 0.03, MeOH); UV (MeOH) λ_{max} nm (log ε): 212 (2.8); ^{1}H NMR (400 MHz) and ^{13}C NMR (100 MHz) data (CD_3OD), see **Table S15**; HRESIMS (positive mode) *m/z* 471.3454 $[M + Na]^+$ (calcd for $C_{28}H_{48}NaO_4^+$, 471.3445).

Compound **10c**: colorless oil; $[\alpha]_D^{20}$ –13.8 (*c* 0.15, MeOH); UV (MeOH) λ_{max} nm (log ε): 218 (3.2); ^{1}H NMR (400 MHz) and ^{13}C NMR (100 MHz) data (CD_3OD), see **Table S15**; HRESIMS (positive mode) *m/z* 687.3832 $[M + Na]^+$ (calcd for $C_{38}H_{55}F_3NaO_6^+$, 687.3843).

Compound **10d**: colorless oil; $[\alpha]_D^{20}$ +19.0 (*c* 0.04, MeOH); UV (MeOH) λ_{max} nm (log ε): 215 (3.1); ^{1}H NMR (400 MHz) and ^{13}C NMR (100 MHz) data (CD_3OD), see **Table S15**; HRESIMS (positive mode) *m/z* 687.3833 $[M + Na]^+$ (calcd for $C_{38}H_{55}F_3NaO_6^+$, 687.3843).

Chemical synthesis of 10a.

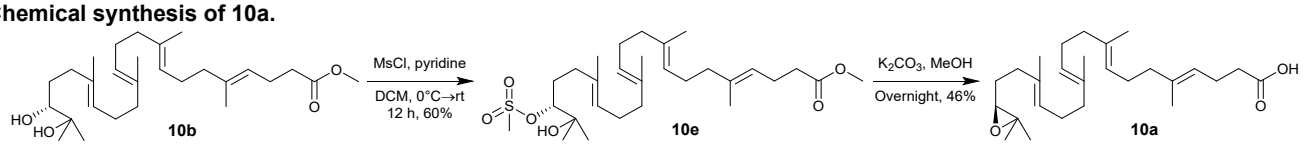

Compound **10a** was synthesized with slight modifications from previously published methods.[7,8]

To a solution of **10b** (35.1 mg, 0.078 mmol) and pyridine (94.5 μL, 1.175 mmol) in dry CH_2Cl_2 (1 mL) at 0 °C, MsCl (30.2 μL, 0.390 mmol) was added, and the reaction mixture was stirred at room temperature for 12 h. The solvent was then removed under reduced pressure, and the residue was purified by preparative HPLC, eluting with 90% CH_3CN for 30 min at a flow rate of 17 mL/min to afford **10e** (24.7 mg, 60%; t_R = 18 min; Figures S111 and S112).

A stirred solution of **10e** (24.7 mg, 0.047 mmol) and K_2CO_3 (64.9 mg, 0.470 mmol) in 1 mL MeOH at room temperature for overnight. Then, the solvent was removed under vacuum, and the residue was diluted with ice water (10 mL), followed by extraction with EtOAc (3 × 10 mL). The combined organic layer was dried over Na_2SO_4, and concentrated under vacuum, and the residue was purified by preparative HPLC, eluting with 95% CH_3CN for 30 min at a flow rate of 17 mL/min to afford **10a** (9.0 mg, 46%; t_R = 19 min; Figures S113–S118).

Compound **10e**: colorless oil; $[\alpha]_D^{20}$ –3.3 (*c* 0.03, MeOH); UV (MeOH) λ_{max} nm (log ε): 213 (2.9); ^{1}H NMR (400 MHz) and ^{13}C NMR (100 MHz) data (CD_3OD), see **Table S20**; HRESIMS (positive mode) *m/z* 549.3219 $[M + Na]^+$ (calcd for $C_{29}H_{50}NaO_6S^+$, 549.3220).

Compound **10a**: colorless oil; $[\alpha]_D^{20}$ –7.7 (*c* 0.03, MeOH); UV (MeOH) λ_{max} nm (log ε): 211 (2.8); ^{1}H NMR (400 MHz) and ^{13}C NMR (100 MHz) data (CD_3OD), see **Table S21**; HRESIMS (positive mode) *m/z* 417.3366 $[M + H]^+$ (calcd for $C_{27}H_{45}O_3^+$, 417.3363).

X-ray crystallographic analysis of 2 and 12.

Crystallographic data for ***2***: $C_{31}H_{51}NO_5$, M = 517.72, *a* = 13.5566(3) Å, *b* = 6.1185(2) Å, *c* = 34.8632 (8) Å, α = 90°, β = 91.6810 (10)°, γ = 90°, *V* = 2890.52(13) Å3, *T* = 193.00 K, space group *C2*, *Z* = 4, λ(CuKα) = 1.54178, 42594 reflections collected, 5296 independent reflections (R_{int} = 0.0446, R_{sigma} =0.0263). The final *R1* values were 0.0335 ($I > 2\sigma(I)$). The final *wR(F²)* values were 0.0880 ($I > 2\sigma(I)$). The final *R1* values were 0.0347 (all data). The final *wR(F²)* values were 0.0892 (all data). The goodness of fit on F^2 was 1.068. Flack parameter = -0.03(5). Crystallographic data for **2** has been deposited into Cambridge Crystallographic Data Center as supplementary publications (number: CCDC 2309354).

Crystallographic data for ***12***: $C_{30}H_{51}NO_5$, M = 505.71, *a* = 7.2412(2) Å, *b* = 12.2368(4) Å, *c* = 34.0916 (10) Å, α = 90°, β = 90°, γ = 90°, *V* = 3020.83(16) Å3, *T* = 200.00(10) K, space group $P2_12_12_1$ (no. 19), *Z* = 4, λ(CuKα) = 1.54178, 15374 reflections collected, 5945 independent reflections (R_{int} = 0.0398, R_{sigma} =0.0360). The final *R1* values were 0.0701 ($I > 2\sigma(I)$). The final *wR(F²)* values were 0.1735 ($I > 2\sigma(I)$). The final *R1* values were 0.0773 (all data). The final *wR(F²)* values were 0.1770 (all data). The goodness of fit on F^2 was 1.198. Flack parameter = -0.07(13). Crystallographic data for **12** has been deposited into Cambridge Crystallographic Data Center as supplementary publications (number: CCDC 2314937).

Expression of AtoE and AtoE-mutants in *Streptomyces* and purification.

AtoE was heterologously overproduced in *S. albus* J1074 for enzyme activity assays. Plasmid pUWL201PWT was used as an *E. coli-Streptomyces* expression shuttle vector to overexpress *atoE* in *Streptomyces*.[2] The full-length *atoE* gene together with an N-terminal His_6-tag sequence was amplified by PCR from pLDW1019 using the *PWTatoE_F* and *PWTatoE_R* primers. Thus, *atoE* was cloned into the *Nde*I and *Hind*III sites of pUWL201PWT to afford pLDW1020. Plasmid pLDW1020 was transformed into *E. coli* ET12567/pUZ8002 and introduced into *S. albus* J1074 by intergeneric conjugation. Positive colonies were selected using 10 μg/mL thiostrepton and named *S. albus* DLW1016. Fresh spores of DLW1016 were inoculated into TSB seed medium supplemented with 10 μg/mL thiostrepton and cultured for 2 days. Seven liters of YEME medium (3 g yeast extract, 3 g malt extract, 5 g peptone and 10 g glucose in 1 L of deionized water, pH 7.2) was inoculated with 5% (v/v) seed culture supplemented with 10 μg/mL thiostrepton and incubated at 28 °C for 2 days. After harvesting the cells by centrifugation at 3750 rpm for 30 min at 4 °C, the pellet was resuspended in lysis buffer (50 mM Tris, 300 mM NaCl, 0.8 mM TCEP and 10% glycerol) and 1 mg/mL lysozyme and 0.5 mg/mL of phenylmethylsulfonyl fluoride (protease inhibitor) were added. After incubation on ice for 2 h, the pellet was lysed by sonication, and centrifuged at 15,000 rpm for 60 min at 4 °C. The supernatant containing AtoE was purified by nickel-affinity chromatography using an ÄKTAxpress system (GE Healthcare Life Sciences) equipped with a HisTrap column. The resultant protein with an N-terminal His_6-tag was desalted using a HiPrep desalting column (GE Healthcare Biosciences) and concentrated using an Amicon Ultra-15 concentrator (Millipore) in 50 mM Tris, pH 7.5, containing 100 mM NaCl, and 10% glycerol. Fractions containing the target protein were pooled, concentrated, aliquoted, and flash-frozen for storage at –80 °C. Protein concentrations were determined from the absorbance at 280 nm using a molar absorptivity constant of each protein.

The protein purification of AtoE-mutants was performed according to the aforementioned procedure.

Expression and purification of AtoA.

Plasmid pLDW1017 was transformed into the BL21 (DE3) to generate *E. coli* strain DLW1013. An overnight culture of 5 mL of DLW1013 was used to incubate 1 L LB medium in 2 L non-beveled Erlenmeyer flask, supplemented with 50 μg/mL, kanamycin, and 1 mL/L trace element (aqueous solution of 50 mM $FeCl_3$, 20 mM $CaCl_2$, 10 mM $MnSO_4$, 10 mM $ZnSO_4$, 2 mM $CoSO_4$, 2 mM $CuCl_2$, 2 mM $NiCl_2$, 2 mM Na_2MoO_4, 2 mM H_3BO_3). The cultures were shaken at 230 rpm and 37 °C until an optical density (OD_{600}) of 0.6–0.8 was reached. The cultures were cooled to 4 °C, and the gene expression was induced with the addition of 0.25 mM IPTG, and the cells were grown around 18 h at 18 °C with shaking. After harvesting the cells by centrifugation at 3750 rpm for 20 min at 4 °C, the pellet was resuspended in lysis buffer (50 mM Tris, pH 8.0, containing 300 mM NaCl and 10% glycerol), lysed by sonication, and centrifuged at 15,000 rpm for 30 min at 4 °C. The supernatant was purified by nickel-affinity chromatography using an ÄKTAxpress system (GE Healthcare Life Sciences) equipped with a HisTrap column. The resultant protein with an N-terminal His_6-tag was desalted using a HiPrep desalting column (GE Healthcare Biosciences) and concentrated using an Amicon Ultra-15 concentrator (Millipore) in 50 mM Tris, pH 8.0, containing 100 mM NaCl, and 10% glycerol. Protein concentrations were determined from the absorbance at 280 nm using a molar absorptivity constant of each protein. Individual aliquots of each protein were stored at –80 °C until use.

Expression and purification of AtoB and selected class II MTCs.

Plasmids pLDW1018 and pLDW1021–pLDW1027 were transformed into the BL21 (DE3) to generate *E. coli* strain DLW1014 and DLW1017–DLW1023, respectively. These recombinant strains were inoculated into 5 mL of LB containing kanamycin. After overnight incubation, the cultures were scaled up by inoculating 5 mL into 1 L of LB medium and grown at 37 °C with shaking at 230 rpm until an OD_{600} of 0.6–0.8 was reached. The cultures were then cooled to 4 °C, and gene expression was induced by adding 0.25 mM IPTG. The cells were further incubated for approximately 18 h at 18 °C with shaking. After harvesting the cells by centrifugation at 3750 rpm for 20 min at 4 °C, the pellet was resuspended in lysis buffer (50 mM Tris, pH 8.0, containing 300 mM NaCl and 10% glycerol), lysed by sonication, and centrifuged at 15,000 rpm for 30 min at 4 °C. The supernatant was purified by nickel-affinity chromatography using an ÄKTAxpress system (GE Healthcare Life Sciences) equipped with a HisTrap column. The resultant protein with an N-terminal His_6-tag was desalted using a HiPrep desalting column (GE Healthcare Biosciences) and concentrated using an Amicon Ultra-15 concentrator (Millipore) in 50 mM Tris, pH 8.0, containing 100 mM NaCl, and 10% glycerol. For the purification of SerTC, the concentration step was performed in a buffer containing 50 mM Tris, pH 8.0, 300 mM NaCl, and 10% glycerol. Protein concentrations were determined from the absorbance at 280 nm using a molar absorptivity constant of each protein. Individual aliquots of each protein were stored at –80 °C until use.

In vitro enzymatic assay of AtoA.

The in vitro reaction of AtoA were carried out in a 100 μL reaction system containing 50 mM Tris, pH 8.0, 5 μM Opt13, 10 mM $Na_2HPO_3{\cdot}5H_2O$, 10 μM AtoA, 500 μM substrates **11** or **12**, 1 mM $NADP^+$, and redox partners (i) 5 μM CamA, 10 μM CamB; (ii) 5 μM Fdx, 5 μM FdR; or (iii) 5 μM RhfRed. After incubation at 30°C for 12 h, the reactions were extracted with 100 μL EtOAc, which were then dried and directly subjected to LC-MS analysis.

In vitro enzymatic assay of AtoB.

The in vitro reactions of AtoB were conducted in a 100 μL reaction system containing 50 mM Tris·HCl (pH 8.0) with 50 mM NaCl, 3 mM sodium pyruvate, 10 μM pyridoxal phosphate (PLP), 10 μM AtoB, and 500 μM substrate **6**. After incubation at 30°C for 12 h, the reactions were extracted with 100 μL EtOAc, which were then dried and directly subjected to LC-MS analysis.

Preparative scale assays of AtoB were performed using 10 mg **6**, followed by extraction with EtOAc (3 × 200 mL). The EtOAc layer was purified by preparative HPLC, eluting with 30–100% CH_3CN for 25 min at a flow rate of 17 mL/min to afford **14** (1.2 mg; t_R = 15 min; Figures S104–S109).

To determine the reversible activity of AtoB, the conversion of **14** into **6** was conducted in a 100 μL reaction mixture containing 1 mM L-alanine (L-Ala), 10 μM PLP, 10 μM AtoB, 500 μM substrate **14**, and 50 mM Tris·HCl (pH 8.0) with 50 mM NaCl.

Compound **14**: colorless oil; $[\alpha]_D^{20}$ +6.1 (*c* 0.01, MeOH); UV (MeOH) λ_{max} nm (log ε): 212 (2.9); ^{1}H NMR (400 MHz) and ^{13}C NMR (100 MHz) data (CD_3OD), see **Table S19**; HRESIMS (negative mode) *m/z* 461.3274 $[M - H]^-$ (calcd for $C_{28}H_{48}NO_4^-$, 461.3272).

In vitro enzymatic assay of AtoE, AtoE-mutants, and selected class II MTCs.

The in vitro reactions catalyzed by AtoE, AtoE-mutants, and selected class II MTCs were conducted out in a 100 µL reaction system containing 50 mM Tris (pH 8.0), 10 µM enzyme, and 0.5 mM substrate **10a**. After incubation at 30 °C for 12 h, the reactions were extracted with EtOAc (3 × 100 µL), which were then dried and directly subjected to LC-MS analysis.

Preparative scale assays of SerTC were performed using 6 mg **10a**, followed by extraction with EtOAc (3 × 200 mL). The EtOAc layer was purified by preparative HPLC, eluting with 75% CH_3CN for 30 min at a flow rate of 17 mL/min to afford **15** (2.0 mg; t_R = 19 min; Figures S128–S133).

Atolypene H (**15**): white powder; $[\alpha]_D^{20}$ +9.7 (*c* 0.02, MeOH); UV (MeOH) λ_{max} nm (log ε): 206 (2.2); ^{1}H NMR (400 MHz) and ^{13}C NMR (100 MHz) data (CD_3OD), see **Table S23**; HRESIMS (negative mode) *m/z* 415.3218 $[M - H]^-$ (calcd for $C_{27}H_{43}O_3^-$, 415.3218).

Bioinformatics analysis.

The amino acid sequence of AtoE was used as the BLAST search query to identify putative AtoE-like MTCs in bacteria. The FASTA sequences of BLAST hits were collected and used to perform a multiple sequence alignment and phylogenetic reconstruction in MEGA X.[9] An unrooted maximum-likelihood tree was assembled with 1000 bootstrap replicants and visualized and colored using iTOL.[10] Analysis of catalytic motifs was performed by clade using MEME Suite (meme-suite.org/meme/). UniProt IDs of identified AtoE-like MTCs were used to generate a genome neighborhood diagram with EFI-GNT with a genome window of 20 genes.[11] Homologous gene clusters were selected, and Clinker was used to visualize the percent identity of each gene between the clusters.[12] A connectivity threshold of 0.3 (corresponding to 30% identity) was chosen, and connections were given for genes sharing at least 30% identity. Gene color was assigned based on predicted function.

Table S1. Predicted gene functions and blast results of *ato* BGC.

Protein	Accession numbers	Size (aa)	BlastP homologs	Identity/ Positives (%)	Proposed function
AtoA	WP_208613467	394	WP_229880587	52/68	Cytochrome P450
AtoB	WP_091316340	327	WP_141924886	47/59	Aminotransferase
AtoC	WP_091316341	327	WP_086885075	55/66	Polyprenyl synthetase
AtoD	WP_244170484	300	WP_014058158	55/62	UbiA family prenyltransferase
AtoE	WP_091316343	534	WP_202237234	49/59	Sesterterpene cyclase
AtoF	WP_091316344	432	WP_280882156	52/63	Epoxidase

Table S2. Strains used in this study.

Strains	Genotype, Description	Sources (Reference)
E. coli DH5α	Host strain for general cloning	General biosystems (Anhui, China)
E. coli BL21 (DE3)	Heterologous host for protein expression	General biosystems (Anhui, China)
E. coli ET12567/pUZ8002	Methylation-deficient *E. coli* host for intergeneric conjugation	[13]
Amycolatopsis tolypomycina NRRL B-24205	*Actinomycetes* used to extract the genome as a PCR template	[14]
Streptomyces albus J1074	Host strain for heterologous expression	[15]
Streptomyces lividans SBT18	Host strain for heterologous expression	[16]
S. albus DLW1001	*S. albus* J1074 integrated with empty pSET152 vector	This study
S. albus DLW1002	*S. albus* J1074 integrated with pLDW1007	This study
S. albus DLW1003	*S. albus* J1074 integrated with pLDW1008	This study
S. albus DLW1004	*S. albus* J1074 integrated with pLDW1009	This study
S. albus DLW1005	*S. albus* J1074 integrated with pLDW1010	This study
S. albus DLW1006	*S. albus* J1074 integrated with pLDW1011	This study
S. albus DLW1007	*S. albus* J1074 integrated with pLDW1012	This study
S. albus DLW1008	*S. albus* J1074 integrated with pLDW1013	This study
S. albus DLW1009	*S. albus* J1074 integrated with pLDW1014	This study
S. albus DLW1010	*S. albus* J1074 integrated with pLDW1015	This study
S. albus DLW1011	*S. albus* J1074 integrated with pLDW1016	This study
S. lividans DLW1012	*S. lividans* SBT18 integrated with pLDW1014	This study
E. coli DLW1013	*E. coli* BL21 harboring pLDW1017	This study
E. coli DLW1014	*E. coli* BL21 harboring pLDW1018	This study
E. coli DLW1015	*E. coli* BL21 harboring pLDW1019	This study
S. albus DLW1016	*S. albus* J1074 containing pLDW1020 for AtoE protein expression	This study
E. coli DLW1017	*E. coli* BL21 harboring pLDW1021	This study
E. coli DLW1018	*E. coli* BL21 harboring pLDW1022	This study
E. coli DLW1019	*E. coli* BL21 harboring pLDW1023	This study
E. coli DLW1020	*E. coli* BL21 harboring pLDW1024	This study
E. coli DLW1021	*E. coli* BL21 harboring pLDW1025	This study
E. coli DLW1022	*E. coli* BL21 harboring pLDW1026	This study
E. coli DLW1023	*E. coli* BL21 harboring pLDW1027	This study

Table S3. Plasmids used in this study.

Plasmid	Description	Source (Reference)
pSET152	*E. coli-Streptomyces* integrating vector, including the promoter ermE, Apr^r	[17]
pUWL201PWT	*E. coli-Streptomyces* expression shuttle vector, Tsr^r	[18]
pET-28a(+)	Protein co-expression vector used in *E. coli*, encoding N-terminal 6× His tag, Kan^r	Novagen
pRSF-Duet-1	Protein co-expression vector used in *E. coli*, N-terminal 6× His tag, Kan^r	Novagen
pLDW1001	pRSF-Duet-1 harboring *atoA,* P12R10, and T2, Kan^r	This study
pLDW1002	pRSF-Duet-1 harboring *atoE,* P12R10, and T2, Kan^r	This study
pLDW1003	pRSF-Duet-1 harboring *atoF,* P12R10, and T2, Kan^r	This study
pLDW1004	pRSF-Duet-1 harboring *atoB,* P9R7, and T4, Kan^r	This study
pLDW1005	pRSF-Duet-1 harboring *atoC,* P3R5, and T9, Kan^r	This study
pLDW1006	pRSF-Duet-1 harboring *atoD,* P10R10, and T10, Kan^r	This study
pLDW1007	pSET152 harboring P3R5-*atoC*-T9	This study
pLDW1008	pSET152 harboring *atoC* and *atoD,* along with their respective promoters, RBS, and terminators.	This study
pLDW1009	pSET152 harboring *atoC* and *atoE*, along with their respective promoters, RBS, and terminators.	This study
pLDW1010	pSET152 harboring *atoC* and *atoF*, along with their respective promoters, RBS, and terminators.	This study
pLDW1011	pSET152 harboring *atoC*, *atoD*, and *atoE*, along with their respective promoters, RBS, and terminators.	This study
pLDW1012	pSET152 harboring *atoC*, *atoE*, and *atoF*, along with their respective promoters, RBS, and terminators.	This study
pLDW1013	pSET152 harboring *atoC*, *atoD*, and *atoF*, along with their respective promoters, RBS, and terminators.	This study
pLDW1014	pSET152 harboring *atoC*, *atoD*, *atoE*, and *atoF*, along with their respective promoters, RBS, and terminators.	This study
pLDW1015	pSET152 harboring *atoB*, *atoC*, *atoD*, *atoE*, and *atoF*, along with their respective promoters, RBS, and terminators.	This study
pLDW1016	pSET152 harboring *atoA*, *atoB*, *atoC*, *atoD*, *atoE*, and *atoF*, along with their respective promoters, RBS, and terminators.	This study
pLDW1017	pET-28a(+) harboring *atoA*	This study
pLDW1018	pET-28a(+) harboring *atoB*	This study
pLDW1019	pET-28a(+) harboring *atoE*	This study
pLDW1020	pUWL201PWT harboring *atoE* gene together with an N-terminal His_6-tag	This study
pLDW1021	pET-28a(+) harboring *SerTC*	This study
pLDW1022	pET-28a(+) harboring *SmaTC*	This study
pLDW1023	pET-28a(+) harboring *UtaTC*	This study
pLDW1024	pET-28a(+) harboring *CcrTC*	This study
pLDW1025	pET-28a(+) harboring *SsyTC*	This study
pLDW1026	pET-28a(+) harboring *AxyTC*	This study
pLDW1027	pET-28a(+) harboring *PshTC*	This study

Table S4. Primers used in this study.

Primers	Nucleotide Sequence (5´–3´)
For construction of pLDW1001	
pRSFDuet-atoA-F	AGAAGGAGGTTAACACATATGATGTCCCTGCCTGCCTTCC
pRSFDuet-atoA-R	GAATTTGGTACCGAGCATATGctaccaggtgatcggtagctcg
For construction of pLDW1002	
pRSFDuet-atoE-F	AGAAGGAGGTTAACACATATGATGCCTGAGACGGATCTGCTCGACG
pRSFDuet-atoE-R	GAATTTGGTACCGAGCATATGTCATCGCGCCGCCTCCCG
For construction of pLDW1003	
pRSFDuet-atoF-F	AGAAGGAGGTTAACACATATGATGACCGACGTACTCGTGTGC
pRSFDuet-atoF-R	GAATTTGGTACCGAGCATATGTCACACGCCGGAGGACCA
For construction of pLDW1004	
pRSFDuet-atoB-F	AGAAGGAGGTACCAACTGCAGATGGACACAGAACGGCTGCG
pRSFDuet-atoB-R	GATTTTTTTTATCTGCTGCAGTCATGCGGGGAACTCCGC
For construction of pLDW1005	
pRSFDuet-atoC-F	CAGAAGGAGATTATAAAGCTTATGAGCATCGCCCTGGAAC
pRSFDuet-atoC-R	TTTTTTGGTACCGAGAAGCTTTCACCGCTCCCGATCGAC
For construction of pLDW1006	
pRSFDuet-atoD-F	AGAAGGAGGTTAACACTTAAGATGCTGTCGGCACACGTGC
pRSFDuet-atoD-R	TTCCTGACTCATAACCTTAAGTCAGGCATGGCGTCCCTC
For construction of pLDW1007	
pSET-atoC-F	GGTATCGATAAGCTTAGTGGAGGCTACCTCACAATGG
pSET-atoC-R	CAGGTCGACTCTAGAGGACCAAAAAAAAAAAAGACGC
For construction of pLDW1008	
152-AtoCDup-F	GGTATCGATAAGCTTGATATCAGTGGAGGCTACCTCACAATGG
152-AtoCDup-R	AGCCCTGCTAGGACCAAAAAAAAAAAAGACGC
152-AtoCDdown-F	TTTTTGGTCCTAGCAGGGCTCCAAAACTAACG
152-AtoCDdown-R	CAGGTCGACTCTAGAGGATCCAAAGCAAGCAAAGAAAAAAGGC
For construction of pLDW1009	
152-AtoCDup-F	GGTATCGATAAGCTTGATATCAGTGGAGGCTACCTCACAATGG
152-ProsAtoCEUP-R	CCCGCACAGGACCAAAAAAAAAAAAGACGC
152-ProsAtoCEDown-F	TTTTTTTGGTCCTGTGCGGGCTCTAACACGTC
152-ProsAtoCEDown-R	CAGGTCGACTCTAGAGGACCAAAACGAAAAAAGACGC
For construction of pLDW1011	
152-AtoCDup-F	GGTATCGATAAGCTTGATATCAGTGGAGGCTACCTCACAATGG
152-ProsAtoCEDown-R	CAGGTCGACTCTAGAGGACCAAAACGAAAAAAGACGC
For construction of pLDW1012	
152-AtoCDup-F	GGTATCGATAAGCTTGATATCAGTGGAGGCTACCTCACAATGG
152-ProsAtoCEUP-R	CCCGCACAGGACCAAAAAAAAAAAAGACGC
152-ProsAtoCEDown-F	TTTTTTTGGTCCTGTGCGGGCTCTAACACGTC
152-ProsAtoCEDown-R	CAGGTCGACTCTAGAGGACCAAAACGAAAAAAGACGC
For construction of pLDW1013	
152-AtoCDup-F	GGTATCGATAAGCTTGATATCAGTGGAGGCTACCTCACAATGG
152-ProsAtoCDF-R	GTTAGAGCCCGCACAAAAGCAAGCAAAGAAAAAAGGC
152-ProsAtoCDF-F	GCTTTTGTGCGGGCTCTAACACGTCC
152-ProsAtoCEDown-R	CAGGTCGACTCTAGAGGACCAAAACGAAAAAAGACGC
For construction of pLDW1014	
152-AtoCDup-F	GGTATCGATAAGCTTGATATCAGTGGAGGCTACCTCACAATGG
152-ProsAtoCDEF-R	CCGCACAGGACCAAAACGAAAAAAGACGCTTTTC
152-ProsAtoCDEF-F	TTCGTTTTGGTCCTGTGCGGGCTCTAACACGTCC
152-ProsAtoCEDown-R	CAGGTCGACTCTAGAGGACCAAAACGAAAAAAGACGC
For construction of pLDW1015	
152-AtoBCDEF-1F	GGTATCGATAAGCTTGATATCCAGGTCGGCTGGTTGGCT
152-ProsAtoCDEF-R	CCGCACAGGACCAAAACGAAAAAAGACGCTTTTC
152-ProsAtoCDEF-F	TTCGTTTTGGTCCTGTGCGGGCTCTAACACGTCC
152-ProsAtoCEDown-R	CAGGTCGACTCTAGAGGACCAAAACGAAAAAAGACGC
For construction of pLDW1016	
152-AtoABCDEFup-F	GGTATCGATAAGCTTGATATCTGTGCGGGCTCTAACACGTC
152-AtoABCDEFup-R	CAACCAGCCGACCTGGGACCAAAACGAAAAAAGACGC
152-AtoBCDEFdown-F	TTTCGTTTTGGTCCCAGGTCGGCTGGTTGGCT

152-ProsAtoCEDown-R	CAGGTCGACTCTAGAGGACCAAAACGAAAAAAGACGC
For construction of pLDW1017	
28a-atoA-F	GTGCCGCGCGGCAGCATGTCCCTGCCTGCCTTCC
28a-atoA-R	GTGGTGGTGGTGGTGCTACCAGGTGATCGGTAGCTCG
For construction of pLDW1018	
28a-atoB-F	GTGCCGCGCGGCAGCATGGACACAGAACGGCTGCG
28a-atoB-R	GTGGTGGTGGTGGTGTCATGCGGGGAACTCCGC
For construction of pLDW1019	
28a-AtoE-F	GTGCCGCGCGGCAGCATGCCTGAGACGGATCTGCTC
28a-AtoE-R	GTGGTGGTGGTGGTGTCATCGCGCCGCCTCCCG
For construction of pLDW1020	
pUWLNdeI-AtoE-F	AAAGAGGAGAAATTACATATGATGGGCAGCAGCCATCATC
pUWLHindIII-AtoE-R	GGACCAAAACGAAAAAAGACGCTCATCGCGCCGCCTCCCG
For construction of pLDW1021	
28a-SerTC-F	GTGCCGCGCGGCAGCATGACCTTCCTACGCGCGG
28a-SerTC-R	GTGGTGGTGGTGGTGTCATCGCGCCACCGCCTT
For construction of pLDW1022	
28a-SmaTC-F	GTGCCGCGCGGCAGCATGCCCCCTTCCGCCTTG
28a-SmaTC-R	GTGGTGGTGGTGGTGTGGCCTGCCTCCTTCGCC
For construction of pLDW1023	
28a-UtaTC-F	GTGCCGCGCGGCAGCATGACTTCGGTGCACGTCGA
28a-UtaTC-R	GTGGTGGTGGTGGTGCGAAGTCGTGTCCCGCCG
For construction of pLDW1024	
28a-CcrTC-F	GTGCCGCGCGGCAGCGTGAATTCCACGGAGCTGACCG
28a-CcrTC-R	GTGGTGGTGGTGGTGTGTCCGCTCGGCCTGCCG
For construction of pLDW1025	
28a-SsyTC-F	GTGCCGCGCGGCAGCATGACAGCCGTGTCCGACG
28a-SsyTC-R	GTGGTGGTGGTGGTGTCAGGCGACCATACCCGG
For construction of pLDW1026	
28a-AxyTC-F	GTGCCGCGCGGCAGCATGACGGAACTCGCACTCGA
28a-AxyTC-R	GTGGTGGTGGTGGTGTCACTCATGGCCCGCTCC
For construction of pLDW1027	
28a-PshTC-F	GTGCCGCGCGGCAGCGTGACCAGGGCCGGGGAA
28a-PshTC-R	GTGGTGGTGGTGGTGTCATCGGCACCCGGCCTC

Table S5. Summary of ^{1}H NMR (400 MHz) and ^{13}C NMR (100 MHz) data for atolypene C (**2**) in methanol-d_4 (δ in ppm, J in Hz).

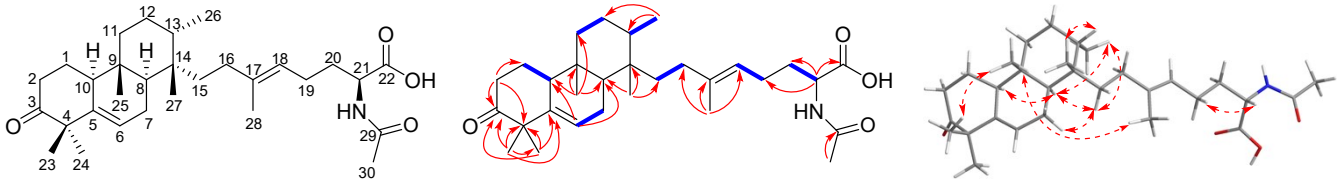

Chemical structure of **2** and ^{1}H-^{1}H COSY ( ), key HMBC correlations ( ), and key ROESY correlations ( ).

No.	δ_C, type	δ_H, mult. (J, Hz)
1a	23.1, CH_2	1.95, m
1b		1.58, m
2a	38.9, CH_2	2.52, m
2b		2.35, m
3	217.8, C	
4	51.1, C	
5	143.8, C	
6	122.3, CH	5.73, m
7a	24.6, CH_2	2.05, m
7b		1.95, overlapped
8	45.5, CH	1.47, m
9	37.1, C	
10	51.4, CH	2.29, m
11a	33.4, CH_2	1.58, overlapped
11b		1.47, overlapped
12a	26.4, CH_2	1.97, overlapped
12b		1.34, m
13	36.4, CH	1.68, m
14	38.2, C	
15a	39.7, CH_2	1.47, overlapped
15b		1.13, m
16a	33.8, CH_2	1.95, 2H, overlapped
16b		
17	139.0, C	
18	123.4, CH	5.14, t (7.2)
19a	25.3, CH_2	2.08, m
19b		1.96, overlapped
20a	32.7, CH_2	1.85, m
20b		1.69, overlapped
21	53.4, CH	4.33, q (4.6)
22	176.1, C	
23	29.2, CH_3	1.24, s
24	24.6, CH_3	1.21, s
25	15.6, CH_3	0.90, s
26	14.7, CH_3	0.99, d (7.0)
27	21.2, CH_3	1.03, s
28	16.3, CH_3	1.61, s
29	173.4, C	
30	22.4, CH_3	1.99, s

Table S6. Summary of ^{1}H NMR (400 MHz) and ^{13}C NMR (100 MHz) data for atolypene D (**3**) in methanol-d_4 (δ in ppm, J in Hz).

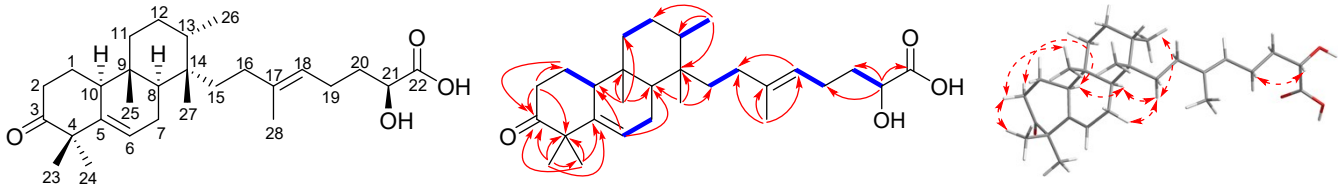

Chemical structure of **3** and ^{1}H-^{1}H COSY ( ), key HMBC correlations ( ), and key ROESY correlations ( ).

No.	δ_C, type	δ_H, mult. (J, Hz)
1a	23.1, CH_2	1.95, m
1b		1.60, m
2a	38.9, CH_2	2.53, m
2b		2.36, m
3	217.8, C	
4	51.1, C	
5	143.8, C	
6	122.3, CH	5.73, m
7a	24.6, CH_2	2.12, m
7b		1.95, overlapped
8	45.5, CH	1.46, m
9	37.1, C	
10	51.4, CH	2.29, m
11a	33.4, CH_2	1.59, overlapped
11b		1.49, overlapped
12a	26.4, CH_2	1.97, overlapped
12b		1.34, m
13	36.4, CH	1.67, m
14	38.1, C	
15a	39.7, CH_2	1.47, overlapped
15b		1.13, m
16a	33.9, CH_2	1.48, 2H, overlapped
16b		
17	138.3, C	
18	124.0, CH	5.16, t (7.2)
19a	24.6, CH_2	2.12, overlapped
19b		1.95, overlapped
20a	35.6, CH_2	1.77, m
20b		1.66, overlapped
21	71.2, CH	4.07, q (4.0)
22	178.5, C	
23	29.2, CH_3	1.24, s
24	24.6, CH_3	1.21, s
25	15.6, CH_3	0.90, s
26	14.7, CH_3	0.99, d (7.0)
27	21.2, CH_3	1.03, s
28	16.3, CH_3	1.64, s

Table S7. Summary of ^{1}H NMR (400 MHz) and ^{13}C NMR (100 MHz) data for **4** in methanol-d_4 (δ in ppm, J in Hz).

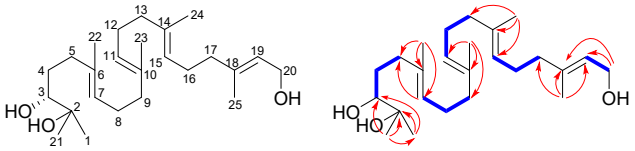

Chemical structure of **4** and ^{1}H-^{1}H COSY ( ), and key HMBC correlations ( ).

No.	δ_C, type	δ_H, mult. (J, Hz)
1	24.9, CH_3	1.13, s
2	73.8, C	
3	79.1, CH	3.23, dd (10.5, 1.6)
4a	30.8, CH_2	1.71, m
4b		1.34, m
5a	37.9, CH_2	2.25, m
5b		2.00, m
6	136.2, C	
7	125.5, CH	5.18, m
8a	27.4, CH_2	2.09, 2H, m
8b		
9a	40.9, CH_2	2.09, overlapped
9b		2.00, overlapped
10	136.0, C	
11	125.5, CH	5.12, m
12a	27.6, CH_2	2.09, overlapped
12b		2.00, overlapped
13a	40.9, CH_2	2.09, overlapped
13b		2.00, overlapped
14	135.9, C	
15	125.5, CH	5.12, overlapped
16a	27.7, CH_2	2.09, overlapped
16b		2.00, overlapped
17a	40.8, CH_2	2.09, 2H, overlapped
17b		
18	139.5, C	
19	124.6, CH	5.36, m
20a	59.4, CH_2	4.08, 2H, d (6.8)
20b		
21	25.7, CH_3	1.16, s
22	16.2, CH_3	1.62, s
23	16.1, CH_3	1.61, s
24	16.0, CH_3	1.60, s
25	16.3, CH_3	1.67, s

Table S8. Summary of ^{1}H NMR (400 MHz) and ^{13}C NMR (100 MHz) data for **5** in methanol-d_4 (δ in ppm, J in Hz).

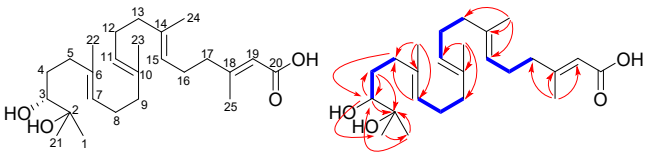

Chemical structure of **5** and ^{1}H-^{1}H COSY ( ), and key HMBC correlations ( ).

No.	δ_C, type	δ_H, mult. (J, Hz)
1	25.0, CH_3	1.13, s
2	73.8, C	
3	79.1, CH	3.24, dd (10.5, 1.4)
4a	30.9, CH_2	1.70, m
4b		1.34, m
5a	37.9, CH_2	2.25, m
5b		2.00, m
6	136.0, C	
7	125.6, CH	5.18, t (6.8)
8a	27.4, CH_2	2.09, m
8b		2.00, overlapped
9a	40.8, CH_2	2.09, overlapped
9b		2.00, overlapped
10	136.0, C	
11	125.4, CH	5.12, m
12a	27.1, CH_2	2.19, 2H, m
12b		
13a	40.8, CH_2	2.09, overlapped
13b		2.00, overlapped
14	137.0, C	
15	124.4, CH	5.12, overlapped
16a	27.7, CH_2	2.09, overlapped
16b		2.00, overlapped
17a	41.9, CH_2	2.19, 2H, overlapped
17b		
18	159.8, C	
19	118.0, CH	4.87, overlapped
20	171.3, C	
21	25.6, CH_3	1.16, s
22	16.1, CH_3	1.62, s
23	16.1, CH_3	1.61, s
24	16.2, CH_3	1.60, s
25	18.9, CH_3	2.12, s

Table S9. Summary of ^{1}H NMR (400 MHz) and ^{13}C NMR (100 MHz) data for **6** in methanol-d_4 (δ in ppm, J in Hz).

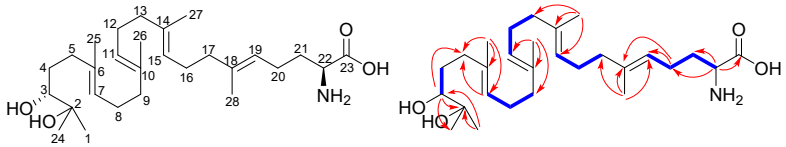

Chemical structure of **6** and ^{1}H-^{1}H COSY ( ), and key HMBC correlations ( ).

No.	δ_C, type	δ_H, mult. (J, Hz)
1	24.9, CH_3	1.13, s
2	73.8, C	
3	79.1, CH	3.24, dd (10.5, 1.6)
4a	30.9, CH_2	1.71, m
4b		1.34, m
5a	37.9, CH_2	2.25, m
5b		2.00, m
6	135.9, C	
7	125.6, CH	5.17, m
8a	27.6, CH_2	2.00, 2H, overlapped
8b		
9a	40.8, CH_2	2.09, overlapped
9b		2.00, overlapped
10	136.1, C	
11	125.4, CH	5.12, m
12a	27.7, CH_2	2.09, overlapped
12b		2.00, overlapped
13a	40.9, CH_2	2.09, overlapped
13b		2.00, overlapped
14	136.1, C	
15	125.5, CH	5.12, overlapped
16a	27.7, CH_2	2.09, overlapped
16b		2.00, overlapped
17a	40.9, CH_2	2.19, 2H, overlapped
17b		
18	137.9, C	
19	123.8, CH	5.17, overlapped
20a	25.0, CH_2	2.14, 2H, m
20b		
21a	32.7, CH_2	1.89, m
21b		1.82, m
22	56.1, CH	3.53, dd (6.8, 5,2)
23	174.5, C	
24	25.6, CH_3	1.16, s
25	16.2, CH_3	1.62, s
26	16.2, CH_3	1.60, overlapped
27	16.2, CH_3	1.60, overlapped
28	16.2, CH_3	1.65, s

Table S10. Summary of ^{1}H NMR (400 MHz) and ^{13}C NMR (100 MHz) data for **7** in methanol-d_4 (δ in ppm, J in Hz).

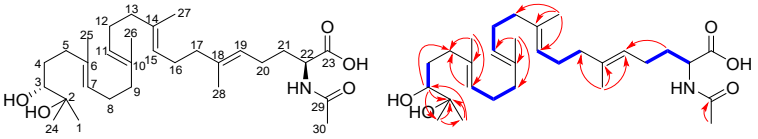

Chemical structure of **7** and ^{1}H-^{1}H COSY ( ), and key HMBC correlations ( ).

No.	δ_C, type	δ_H, mult. (J, Hz)
1	25.0, CH_3	1.12, s
2	73.8, C	
3	79.1, CH	3.23, d (10.5)
4a	30.9, CH_2	1.70, m
4b		1.34, m
5a	38.0, CH_2	2.25, m
5b		2.00, m
6	135.8, C	
7	125.6, CH	5.18, m
8a	27.7, CH_2	2.09, m
8b		2.00, overlapped
9a	40.9, CH_2	2.09, overlapped
9b		2.00, overlapped
10	136.0, C	
11	125.4, CH	5.12, m
12a	27.6, CH_2	2.09, overlapped
12b		2.00, overlapped
13a	40.9, CH_2	2.09, overlapped
13b		2.00, overlapped
14	136.0, C	
15	125.5, CH	5.12, overlapped
16a	27.7, CH_2	2.09, overlapped
16b		2.00, overlapped
17a	40.9, CH_2	2.09, overlapped
17b		2.00, overlapped
18	137.6, C	
19	124.1, CH	5.13, overlapped
20a	25.3, CH_2	2.09, 2H, overlapped
20b		
21a	32.8, CH_2	1.85, m
21b		1.71, m
22	53.7, CH	4.32, q (4.4)
23	ND	
24	25.7, CH_3	1.16, s
25	16.2, CH_3	1.62, s
26	16.1, CH_3	1.60, s
27	16.1, CH_3	1.60, s
28	16.1, CH_3	1.60, s
29	173.3, C	
30	22.4, CH_3	1.99, s

ND: Not detected

Table S11. Summary of ^{1}H NMR (400 MHz) and ^{13}C NMR (100 MHz) data for **8** in methanol-d_4 (δ in ppm, J in Hz).

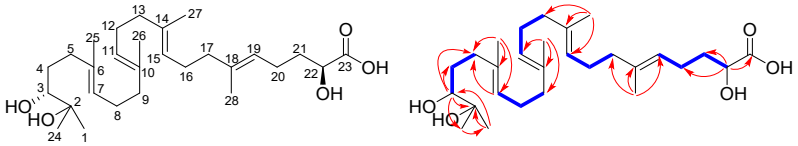

Chemical structure of **8** and ^{1}H-^{1}H COSY ( ), and key HMBC correlations ( ).

No.	δ_C, type	δ_H, mult. (J, Hz)
1	25.0, CH_3	1.13, s
2	73.8, C	
3	79.1, CH	3.23, dd (10.6, 1.6)
4a	30.9, CH_2	1.71, m
4b		1.33, m
5a	37.9, CH_2	2.25, m
5b		2.00, m
6	135.8, C	
7	125.6, CH	5.18, m
8a	27.8, CH_2	2.09, m
8b		2.00, overlapped
9a	40.9, CH_2	2.09, overlapped
9b		2.00, overlapped
10	135.9, C	
11	125.5, CH	5.12, m
12a	27.7, CH_2	2.09, overlapped
12b		2.00, overlapped
13a	40.9, CH_2	2.09, overlapped
13b		2.00, overlapped
14	136.0, C	
15	125.4, CH	5.12, overlapped
16a	27.6, CH_2	2.09, overlapped
16b		2.00, overlapped
17a	40.9, CH_2	2.09, overlapped
17b		2.00, overlapped
18	137.2, C	
19	124.6, CH	5.15, m
20a	24.6, CH_2	2.14, 2H, m
20b		
21a	35.6, CH_2	1.77, m
21b		1.67, m
22	70.9, CH	4.09, q (4.1)
23	178.1, C	
24	25.6, CH_3	1.16, s
25	16.1, CH_3	1.62, s
26	16.1, CH_3	1.61, s
27	16.1, CH_3	1.61, s
28	16.2, CH_3	1.63, s

Table S12. Summary of ^{1}H NMR (400 MHz) and ^{13}C NMR (100 MHz) data for **9** in methanol-d_4 (δ in ppm, J in Hz).

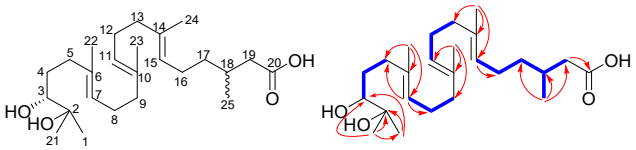

Chemical structure of **9** and ^{1}H-^{1}H COSY ( ), and key HMBC correlations ( ).

No.	δ_C, type	δ_H, mult. (J, Hz)
1	25.2, CH_3	1.13, s
2	73.9, C	
3	79.2, CH	3.24, dd (10.5, 1.5)
4a	31.0, CH_2	1.70, m
4b		1.34, m
5a	38.1, CH_2	2.27, m
5b		2.00, m
6	136.2, C	
7	125.6, CH	5.18, t (7.0)
8a	27.9, CH_2	2.09, m
8b		1.99, m
9a	41.0, CH_2	2.09, overlapped
9b		1.99, overlapped
10	136.1, C	
11	125.7, CH	5.12, m
12a	27.7, CH_2	2.09, overlapped
12b		2.00, overlapped
13a	41.0, CH_2	2.09, overlapped
13b		1.99, overlapped
14	136.0, C	
15	125.7, CH	5.12, overlapped
16a	26.5, CH_2	2.03, 2H, m
16b		
17a	38.0, CH_2	1.37, m
17b		1.24, m
18	31.3, CH	1.93, m
19a	42.9, CH_2	2.27, overlapped
19b		2.08, overlapped
20	177.5, C	
21	25.7, CH_3	1.16, s
22	16.3, CH_3	1.60, s
23	16.4, CH_3	1.62, s
24	16.4, CH_3	1.62, s
25	20.2, CH_3	0.96, d (6.6)

Table S13. Summary of ^{1}H NMR (400 MHz) and ^{13}C NMR (100 MHz) data for **10** in methanol-d_4 (δ in ppm, J in Hz).

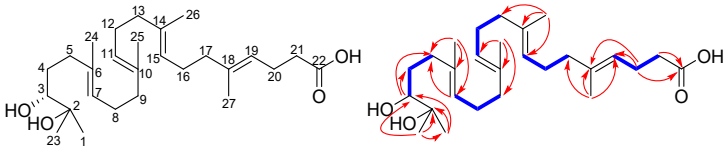

Chemical structure of **10** and ^{1}H-^{1}H COSY ( ), and key HMBC correlations ( ).

No.	δ_C, type	δ_H, mult. (J, Hz)
1	25.0, CH_3	1.13, s
2	73.8, C	
3	79.1, CH	3.24, dd (10.6, 1.6)
4a	30.8, CH_2	1.71, m
4b		1.34, m
5a	37.9, CH_2	2.24, m
5b		1.99, m
6	135.8, C	
7	125.5, CH	5.18, m
8a	27.7, CH_2	2.08, m
8b		1.99, m
9a	40.9, CH_2	2.08, overlapped
9b		1.99, overlapped
10	135.9, C	
11	125.5, CH	5.11, m
12a	27.6, CH_2	2.08, overlapped
12b		1.99, overlapped
13a	40.8, CH_2	2.08, overlapped
13b		1.99, overlapped
14	136.0, C	
15	125.4, CH	5.11, overlapped
16a	27.6, CH_2	2.08, overlapped
16b		1.99, overlapped
17a	40.8, CH_2	2.08, overlapped
17b		1.99, overlapped
18	137.4, C	
19	124.0, CH	5.14, overlapped
20a	24.7, CH_2	2.29, 2H, m
20b		
21a	35.5, CH_2	2.29, 2H, overlapped
21b		
22	177.8, C	
23	25.6, CH_3	1.16, s
24	16.2, CH_3	1.62, s
25	16.1, CH_3	1.61, s
26	16.1, CH_3	1.61, s
27	16.2, CH_3	1.64, s

Table S14. Summary of [1]H NMR (400 MHz) and [13]C NMR (100 MHz) data for **9a**, **9b**, and **9c** in methanol-d_4 (δ in ppm, J in Hz).

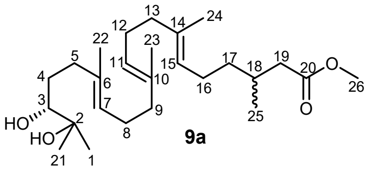

9a

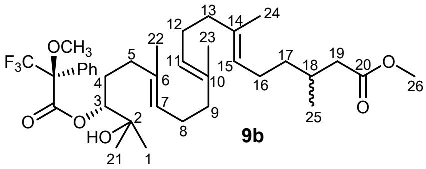

9b

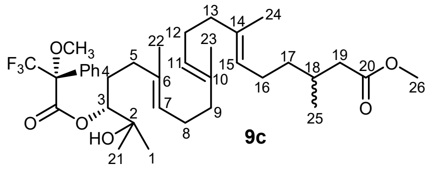

9c

	9a		9b		9c	
No.	δ_C, type	δ_H, mult. (J, Hz)	δ_C, type	δ_H, mult. (J, Hz)	δ_C, type	δ_H, mult. (J, Hz)
1	25.0, CH_3	1.13, s	26.1, CH_3	1.08, s	25.0, CH_3	1.16, s
2	73.8, C		72.5, C		72.7, C	
3	79.1, CH	3.24, dd (10.6, 1.6)	83.4, CH	4.99, d (10.6)	83.3, CH	5.02, m
4a	30.9, CH_2	1.70, m	30.9, CH_2	1.98, m	30.9, CH_2	1.82, m
4b		1.34, m		1.62, m		1.49, m
5a	37.8, CH_2	2.25, m	37.5, CH_2	1.99, 2H, m	37.2, CH_2	1.82, 2H, overlapped
5b		2.01, m				
6	136.1, C		136.1, C		136.1, C	
7	125.4, CH	5.18, td (7.0, 0.9)	125.5, CH	5.12, m	126.3, CH	5.03, m
8a	27.8, CH_2	2.09, m	27.8, CH_2	2.09, m	27.6, CH_2	2.07, m
8b		2.01, overlapped		2.00, m		1.99, m
9a	40.9, CH_2	2.09, overlapped	40.7, CH_2	2.09, 2H, overlapped	40.7, CH_2	2.07, 2H, m
9b		2.01, overlapped				
10	136.0, C		135.7, C		135.7, C	
11	125.5, CH	5.11, m	125.6, CH	5.12, overlapped	125.6, CH	5.12, m
12a	27.6, CH_2	2.09, overlapped	27.6, CH_2	2.09, overlapped	27.6, CH_2	2.07, overlapped
12b		2.01, overlapped		2.00, overlapped		1.99, overlapped
13a	40.9, CH_2	2.09, overlapped	40.9, CH_2	1.99, 2H, overlapped	40.9, CH_2	1.99, 2H, overlapped
13b		2.01, overlapped				
14	135.9, C		134.9, C		134.8, C	
15	125.5, CH	5.11, overlapped	126.4, CH	5.12, overlapped	125.5, CH	5.12, overlapped
16a	26.3, CH_2	2.01, 2H, overlapped	26.3, CH_2	2.02, 2H, overlapped	26.3, CH_2	2.02, 2H, m
16b						
17a	38.0, CH_2	1.35, overlapped	37.8, CH_2	1.35, m	37.8, CH_2	1.35, m
17b		1.24, m		1.23, m		1.23, m
18	31.2, CH	1.93, m	31.1, CH	1.93, m	31.1, CH	1.93, m
19a	42.3, CH_2	2.33, dd (14.8, 6.1)	42.3, CH_2	2.32, dd (14.8, 6.1)	42.3, CH_2	2.32, dd (14.8, 6.0)
19b		2.14, m		2.13, m		2.13, m
20	175.4, C		175.4, C		175.3, C	
21	25.6, CH_3	1.16, s	25.2, CH_3	1.12, s	26.3, CH_3	1.20, s
22	16.1, CH_3	1.61, s	16.0, CH_3	1.59, s	16.0, CH_3	1.52, s
23	16.2, CH_3	1.61, s	16.1, CH_3	1.60, s	16.1, CH_3	1.60, s
24	16.2, CH_3	1.62, s	16.1, CH_3	1.60, s	16.1, CH_3	1.60, s
25	20.0, CH_3	0.94, d (6.7)	20.0, CH_3	0.93, d (6.7)	20.0, CH_3	0.93, d (6.7)
26	51.9, CH_3	3.65, s	51.9, CH_3	3.64, s	51.9, CH_3	3.64, s

Table S15. Summary of ^{1}H NMR (400 MHz) and ^{13}C NMR (100 MHz) data for **10b**, **10c**, and **10d** in methanol-d_4 (δ in ppm, J in Hz).

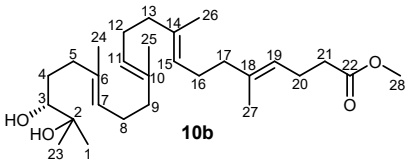

10b

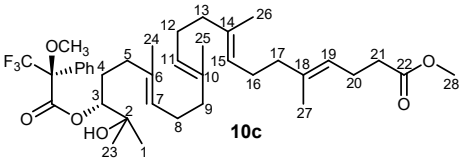

10c

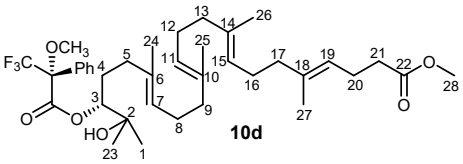

10d

	10b		**10c**		**10d**	
No.	δ_C, type	δ_H, mult. (J, Hz)	δ_C, type	δ_H, mult. (J, Hz)	δ_C, type	δ_H, mult. (J, Hz)
1	25.0, CH_3	1.13, s	26.1, CH_3	1.08, s	26.3, CH_3	1.16, s
2	73.8, C		72.5, C		72.7, C	
3	79.1, CH	3.24, d (10.5)	83.4, CH	4.99, d (10.0)	83.3, CH	5.02, m
4a	30.9, CH_2	1.71, m	29.6, CH_2	1.93, m	29.8, CH_2	1.83, m
4b		1.34, m		1.61, m		1.48, m
5a	38.0, CH_2	2.25, m	37.5, CH_2	1.99, 2H, m	37.2, CH_2	1.83, 2H, overlapped
5b		1.99, m				
6	135.9, C		134.9, C		134.9, C	
7	125.5, CH	5.18, t (6.9)	126.4, CH	5.11, m	126.3, CH	5.03, m
8a	27.8, CH_2	2.08, m	27.7, CH_2	2.08, m	27.7, CH_2	2.08, m
8b		1.99, overlapped		1.99, m		1.99, m
9a	40.9, CH_2	2.08, overlapped	40.9, CH_2	2.08, overlapped	40.9, CH_2	2.08, overlapped
9b		1.99, overlapped		1.99, overlapped		1.98, overlapped
10	136.0, C		135.7, C		135.7, C	
11	125.5, CH	5.11, m	125.6, CH	5.11, m	125.6, CH	5.11, m
12a	27.7, CH_2	2.08, overlapped	27.6, CH_2	2.08, overlapped	27.6, CH_2	2.08, overlapped
12b		1.99, overlapped		1.99, overlapped		1.99, overlapped
13a	40.9, CH_2	2.08, overlapped	40.8, CH_2	2.08, overlapped	40.8, CH_2	2.08, overlapped
13b		1.99, overlapped		1.99, overlapped		1.99, overlapped
14	136.1, C		136.0, C		136.0, C	
15	125.5, CH	5.11, overlapped	125.3, CH	5.11, overlapped	125.3, CH	5.11, overlapped
16a	27.5, CH_2	2.08, overlapped	27.5, CH_2	2.08, overlapped	27.5, CH_2	2.08, overlapped
16b		1.99, overlapped		1.99, overlapped		1.99, overlapped
17a	40.8, CH_2	2.08, overlapped	40.7, CH_2	2.08, overlapped	40.7, CH_2	2.08, overlapped
17b		1.99, overlapped		1.99, overlapped		1.99, overlapped
18	137.6, C		137.7, C		137.7, C	
19	123.7, CH	5.11, overlapped	123.7, CH	5.11, overlapped	123.7, CH	5.11, overlapped
20a	24.5, CH_2	2.29, 2H, m	24.5, CH_2	2.31, 2H, m	24.5, CH_2	2.32, 2H, m
20b						
21a	35.1, CH_2	2.29, 2H, overlapped	35.1, CH_2	2.31, 2H, overlapped	35.1, CH_2	2.32, 2H, overlapped
21b						
22	175.5, C		175.5, C		175.5, C	
23	25.6, CH_3	1.16, s	25.2, CH_3	1.12, s	25.1, CH_3	1.20, s
24	16.2, CH_3	1.62, s	16.1, CH_3	1.60, s	16.1, CH_3	1.52, s
25	16.1, CH_3	1.60, s	16.1, CH_3	1.59, s	16.1, CH_3	1.60, s
26	16.1, CH_3	1.60, s	16.0, CH_3	1.59, s	16.0, CH_3	1.60, s
27	16.2, CH_3	1.63, s	16.1, CH_3	1.62, s	16.1, CH_3	1.63, s
28	52.0, CH_3	3.65, s	52.0, CH_3	3.64, s	52.0, CH_3	3.64, s

Table S16. Summary of ^{1}H NMR (400 MHz) and ^{13}C NMR (100 MHz) data for atolypene E (**11**) in methanol-d_4 (δ in ppm, J in Hz).

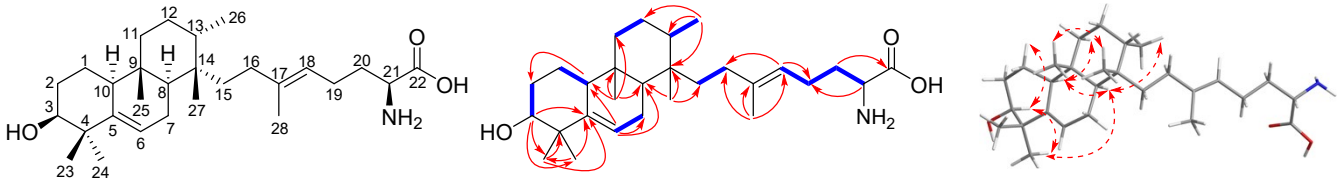

Chemical structure of **11** and ^{1}H-^{1}H COSY ( ), key HMBC correlations ( ), and key ROESY correlations ( ).

No.	δ_C, type	δ_H, mult. (J, Hz)
1a	19.7, CH_2	1.62, m
1b		1.47, m
2a	29.4, CH_2	1.86, m
2b		1.66, m
3	77.0, CH	3.44, t (2.7)
4	41.4, C	
5	143.7, C	
6	121.1, CH	5.57, br s
7a	24.5, CH_2	1.93, 2H, m
7b		
8	45.9, CH	1.28, m
9	37.0, C	
10	51.0, CH	2.02, m
11a	34.0, CH_2	1.55, m
11b		1.41, m
12a	26.5, CH_2	1.93, overlapped
12b		1.30, m
13	36.3, CH	1.64, overlapped
14	38.0, C	
15a	39.8, CH_2	1.49, overlapped
15b		1.10, m
16a	33.7, CH_2	1.93, 2H, overlapped
16b		
17	139.2, C	
18	123.3, CH	5.12, t (6.4)
19a	24.8, CH_2	2.13, 2H, m
19b		
20a	32.6, CH_2	1.99, m
20b		1.81, m
21	56.0, CH	3.53, m
22	173.1, C	
23	29.8, CH_3	1.02, s
24	26.0, CH_3	1.12, s
25	16.3, CH_3	0.92, s
26	14.8, CH_3	0.95, d (7.1)
27	21.5, CH_3	1.02, s
28	16.4, CH_3	1.65, s

Table S17. Summary of ^{1}H NMR (400 MHz) and ^{13}C NMR (100 MHz) data for atolypene F (**12**) in methanol-d_4 (δ in ppm, J in Hz).

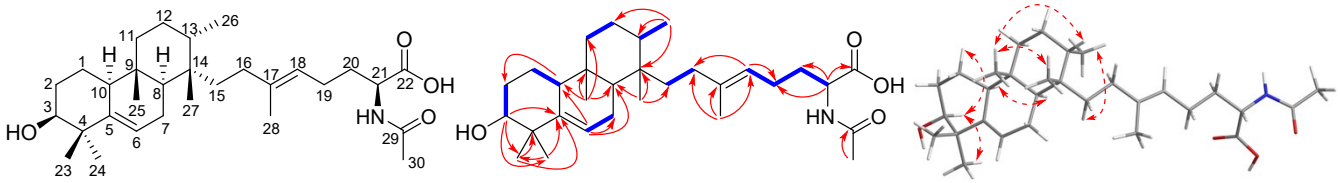

Chemical structure of **12** and ^{1}H-^{1}H COSY ( ), key HMBC correlations ( ), and key ROESY correlations ( ).

No.	δ_C, type	δ_H, mult. (J, Hz)
1a	19.7, CH_2	1.62, m
1b		1.47, m
2a	29.3, CH_2	1.89, m
2b		1.67, m
3	77.0, CH	3.44, t (2.6)
4	41.4, C	
5	143.6, C	
6	121.7, CH	5.58, br s
7a	24.5, CH_2	1.93, 2H, m
7b		
8	45.9, CH	1.46, overlapped
9	37.0, C	
10	50.9, CH	2.01, m
11a	34.0, CH_2	1.55, m
11b		1.40, m
12a	26.5, CH_2	1.93, m
12b		1.30, m
13	36.3, CH	1.63, overlapped
14	38.1, C	
15a	39.8, CH_2	1.48, overlapped
15b		1.13, m
16a	33.9, CH_2	1.93, 2H, overlapped
16b		
17	139.0, C	
18	123.3, CH	5.13, t (7.2)
19a	25.3, CH_2	2.09, 2H, m
19b		
20a	32.7, CH_2	1.85, overlapped
20b		1.71, m
21	53.4, CH	4.32, q (4.6)
22	175.9, C	
23	29.8, CH_3	1.02, s
24	26.0, CH_3	1.12, s
25	16.3, CH_3	0.92, s
26	14.8, CH_3	0.96, d (7.1)
27	21.5, CH_3	1.02, s
28	16.3, CH_3	1.60, s
29	173.4, C	
30	22.4, CH_3	1.99, s

Table S18. Summary of ^{1}H NMR (400 MHz) and ^{13}C NMR (100 MHz) data for atolypene G (**13**) in methanol-d_4 (δ in ppm, J in Hz).

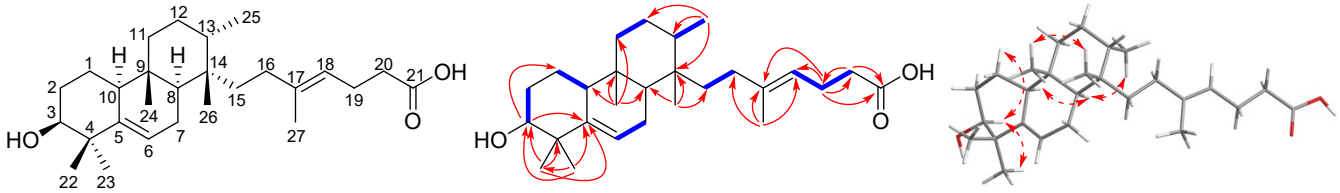

Chemical structure of **13** and ^{1}H-^{1}H COSY ( ), key HMBC correlations ( ), and key ROESY correlations ( ).

No.	δ_C, type	δ_H, mult. (J, Hz)
1a	19.7, CH_2	1.62, m
1b		1.47, m
2a	29.4, CH_2	1.90, m
2b		1.67, overlapped
3	77.0, CH	3.44, t (2.7)
4	41.4, C	
5	143.7, C	
6	121.1, CH	5.57, br s
7a	24.5, CH_2	1.92, 2H, m
7b		
8	45.9, CH	1.29, m
9	37.0, C	
10	51.0, CH	2.01, m
11a	34.0, CH_2	1.55, m
11b		1.40, m
12a	26.5, CH_2	1.93, overlapped
12b		1.30, m
13	36.3, CH	1.64, overlapped
14	38.0, C	
15a	39.8, CH_2	1.47, overlapped
15b		1.09, m
16a	33.8, CH_2	1.92, 2H, overlapped
16b		
17	138.8, C	
18	123.2, CH	5.14, t (6.6)
19a	24.7, CH_2	2.29, 2H, m
19b		
20a	35.4, CH_2	2.29, 2H, overlapped
20b		
21	177.6, C	
22	29.8, CH_3	1.02, s
23	26.0, CH_3	1.12, s
24	16.3, CH_3	0.92, s
25	14.8, CH_3	0.95, d (7.1)
26	21.5, CH_3	1.02, s
27	16.5, CH_3	1.64, s

Table S19. Summary of ^{1}H NMR (400 MHz) and ^{13}C NMR (100 MHz) data for **14** in methanol-d_4 (δ in ppm, J in Hz).

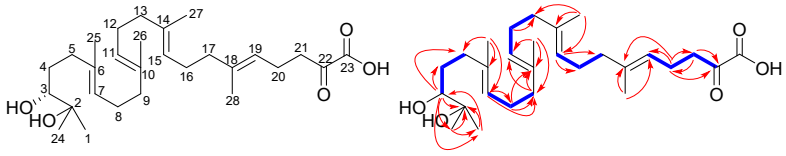

Chemical structure of **14** and ^{1}H-^{1}H COSY ( ), and key HMBC correlations ( ).

No.	δ_C, type	δ_H, mult. (J, Hz)
1	25.0, CH_3	1.13, s
2	73.8, C	
3	79.1, CH	3.24, dd (10.6, 1.6)
4a	30.9, CH_2	1.71, m
4b		1.33, m
5a	37.9, CH_2	2.27, m
5b		1.99, m
6	135.8, C	
7	125.6, CH	5.18, m
8a	27.6, CH_2	2.08, m
8b		1.99, m
9a	40.8, CH_2	1.99, 2H, overlapped
9b		
10	135.9, C	
11	125.5, CH	5.11, m
12a	27.7, CH_2	2.08, overlapped
12b		1.99, overlapped
13a	40.9, CH_2	1.99, 2H, overlapped
13b		
14	135.9, C	
15	125.5, CH	5.11, overlapped
16a	27.8, CH_2	2.08, 2H, overlapped
16b		
17a	40.9, CH_2	1.99, 2H, overlapped
17b		
18	137.0, C	
19	124.2, CH	5.16, overlapped
20a	22.9, CH_2	2.71, t (7.4)
20b		2.28, overlapped
21a	40.7, CH_2	2,71, overlapped
21b		2.08, overlapped
22	206.0, C	
23	ND	
24	25.6, CH_3	1.16, s
25	16.1, CH_3	1.62, s
26	16.1, CH_3	1.60, overlapped
27	16.1, CH_3	1.60, overlapped
28	16.2, CH_3	1.63, s

ND: Not detected

Table S20. Summary of ^{1}H NMR (400 MHz) and ^{13}C NMR (100 MHz) data for **10e** in methanol-d_4 (δ in ppm, J in Hz).

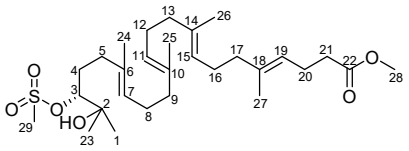

No.	δ_C, type	δ_H, mult. (J, Hz)
1	24.5, CH_3	1.21, s
2	72.9, C	
3	91.2, CH	4.47, dd (9.7, 2.3)
4a	30.5, CH_2	1.80, m
4b		1.32, m
5a	37.2, CH_2	2.22, m
5b		2.00, m
6	135.9, C	
7	125.5, CH	5.21, t (6.7)
8a	27.7, CH_2	2.08, m
8b		2.00, overlapped
9a	40.9, CH_2	2.08, overlapped
9b		2.00, overlapped
10	136.0, C	
11	125.5, CH	5.11, m
12a	27.7, CH_2	2.08, overlapped
12b		2.00, overlapped
13a	40.8, CH_2	2.08, overlapped
13b		2.00, overlapped
14	136.1, C	
15	125.5, CH	5.11, overlapped
16a	27.5, CH_2	2.08, overlapped
16b		2.00, overlapped
17a	40.7, CH_2	2.08, overlapped
17b		2.00, overlapped
18	137.6, C	
19	123.7, CH	5.11, overlapped
20a	24.7, CH_2	2.32, 2H, m
20b		
21a	35.1, CH_2	2.32, 2H, overlapped
21b		
22	175.5, C	
23	26.8, CH_3	1.22, s
24	16.2, CH_3	1.62, s
25	16.1, CH_3	1.60, s
26	16.1, CH_3	1.60, s
27	16.1, CH_3	1.63, s
28	52.0, CH_3	3.65, s
29	39.1, CH_3	3.14, s

Table S21. Summary of ^{1}H NMR (400 MHz) and ^{13}C NMR (100 MHz) data for **10a** in methanol-d_4 (δ in ppm, J in Hz).

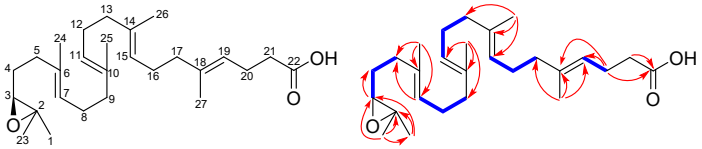

Chemical structure of **10a** and ^{1}H-^{1}H COSY ( ) and key HMBC correlations ( ).

No.	δ_C, type	δ_H, mult. (J, Hz)
1	18.9, CH_3	1.26, s
2	60.2, C	
3	65.8, CH	2.75, t (6.3)
4a	28.5, CH_2	1.61, 2H, m
4b		
5a	37.4, CH_2	2.12, 2H, m
5b		
6	135.1, C	
7	126.1, CH	5.18, t (6.9)
8a	27.6, CH_2	2.10, m
8b		2.00, m
9a	40.8, CH_2	2.10, overlapped
9b		2.00, overlapped
10	135.9, C	
11	125.4, CH	5.11, m
12a	27.6, CH_2	2.10, overlapped
12b		2.00, overlapped
13a	40.8, CH_2	2.10, overlapped
13b		2.00, overlapped
14	135.7, C	
15	125.6, CH	5.11, overlapped
16a	27.6, CH_2	2.10, overlapped
16b		2.00, overlapped
17a	40.8, CH_2	2.10, overlapped
17b		2.00, overlapped
18	137.4, C	
19	124.0, CH	5.14, m
20a	24.7, CH_2	2.29, 2H, m
20b		
21a	35.4, CH_2	2.29, 2H, overlapped
21b		
22	177.1, C	
23	25.1, CH_3	1.28, s
24	16.1, CH_3	1.63, s
25	16.1, CH_3	1.60, s
26	16.1, CH_3	1.60, s
27	16.1, CH_3	1.63, s

Table S22. AtoE-like MTCs used for phylogenetic analysis.[a]

Protein	Strain	UniProt ID	Length (AA)	Clade
AtoE	*Amycolatopsis tolypomycina* NRRL B-24205	A0A1H4ZTV5	534	III
Bra4	*Nocardia brasiliensis*	B1Q2P4	556	IV
PlaT2	*Streptomyces* sp. Tü6071	Q2I762	571	VI
TnlT2	*Streptomyces* sp. CB03234	A0A1Q5LS56	604	VI
TnlT2	*Streptomyces* sp. CB03238	A0A1X1NCL8	584	VI
Lon15	*Streptomyces argenteolus* A2	A9ZNV5	545	VII
	Actinobacteria bacterium OK074	A0A0N0MUW6	555	I
	Actinokineospora bangkokensis	A0A1Q9LNM5	551	I
	Actinosynnema mirum ATCC 29888	C6WK21	560	I
	Actinosynnema pretiosum	A0A290Z9G3	560	I
	Amycolatopsis panacis	A0A419HYZ8	555	I
	Amycolatopsis sp. WAC 04169	A0A429C6Z9	554	I
	Amycolatopsis sulphurea	A0A2A9G0G6	555	I
	Amycolatopsis thailandensis	A0A229S526	554	I
	Lentzea fradiae	A0A1G7K5R4	555	I
	Lentzea xinjiangensis	A0A1H9UYX0	555	I
	Nocardia sp. NRRL S-836	A0A0M8WFT9	555	I
	Pseudonocardia sp. Ae706_Ps2	A0A1Q8LD59	558	I
	Pseudonocardia sp. Ae717_Ps2	A0A1Q8LWS8	558	I
	Pseudonocardia sp. EV170527-09	A0A5B0HY15	558	I
	Pseudonocardia sp. HH130630-07	A0A1B1ZIR2	558	I
	Saccharopolyspora dendranthemae	A0A561V877	566	I
	Saccharopolyspora elongata	A0A4R4ZCL0	558	I
	Saccharopolyspora erythraea	A4FIP2	553	I
	Saccharopolyspora karakumensis	A0A4R5BC21	554	I
	Saccharopolyspora kobensis	A0A1H6ACW3	558	I
	Saccharopolyspora shandongensis	A0A1H3R7G8	558	I
	Saccharopolyspora sp. ASAGF58	A0A6H1RFA4	553	I
	Saccharopolyspora spinosa	A0A2N3Y4X7	553	I
	Saccharopolyspora terrae	A0A4R4VEZ1	554	I
	Umezawaea tangerina	A0A2T0STH2	563	I
	Streptomyces griseoaurantiacus	A0A7W2DXP5	546	II
	Streptomyces griseoaurantiacus M045	F3NDC3	503	II
	Streptomyces jietaisiensis	A0A1G7VIK1	594	II
	Streptomyces sp. WAC 01420	A0A429AHL0	546	II
	Streptomyces sp. WAC 01438	A0A3Q8VBC2	546	II
	Streptomyces antimycoticus	A0A499UX71	581	III
	Streptomyces autolyticus	A0A1P8XPB9	574	III
	Streptomyces hygroscopicus	A0A1S6R8W9	587	III
	Streptomyces iranensis	A0A061A395	715	III
	Streptomyces malaysiensis	A0A515GD19	575	III
	Streptomyces melanosporofaciens	A0A1H5BU00	568	III
	Streptomyces rapamycinicus ATCC 29253	A0A3L8QYP9	594	III
	Streptomyces sp. 11-1-2	A0A222SNY9	587	III
	Streptomyces sp. Amel2xB2	A0A327UPB0	618	III
	Streptomyces sp. M56	A0A2K8RH60	574	III
	Streptomyces sp. PRh5	A0A014LBY2	640	III
	Streptomyces sp. Z26	A0A498DR72	595	III
	Streptomyces violaceusniger	A0A4D4KW08	582	III
	Streptomyces violaceusniger Tü4113	G2P3W2	587	III
	Streptomycetaceae bacterium MP113-05	V6L1S5	477	III
	Nocardia arthritidis	A0A6G9YGF3	553	IV
	Nocardia terpenica	A0A164MNL0	556	IV

Nocardia terpenica	A0A291RHW6	556	IV
Nocardia terpenica	A0A6G9Z1W4	556	IV
Actinoplanes derwentensis	A0A1H1W8Y1	557	V
Labedaea rhizosphaerae	A0A4R6S0L8	567	V
Micromonospora aurantiaca DSM 43813	D9SZA3	566	V
Micromonospora ferruginea	A0A7L6B3A3	566	V
Micromonospora humi	A0A1C5GJ27	566	V
Micromonospora marina	A0A1C4VJH9	566	V
Micromonospora matsumotoense	A0A1C5AJ72	566	V
Micromonospora mirobrigensis	A0A1C4WX72	566	V
Micromonospora pisi	A0A495JV02	559	V
Micromonospora polyrhachis	A0A7W7WMV2	556	V
Micromonospora rifamycinica	A0A109IME3	566	V
Micromonospora sp. AMSO1212t	A0A6H9XDP7	566	V
Micromonospora sp. B006	A0A385AT49	566	V
Micromonospora sp. HM134	A0A518WDL6	566	V
Micromonospora sp. M42	W7VR86	565	V
Micromonospora sp. RP3T	A0A2T3VPR7	566	V
Micromonospora sp. TSRI0369	A0A1Q5HKX0	566	V
Micromonospora sp. XM-20-01	A0A505HSM1	566	V
Micromonospora tulbaghiae	A0A1C4UU69	566	V
Micromonospora wenchangensis	A0A246RSK5	566	V
Saccharothrix sp. NRRL B-16348	A0A0M8Y906	552	V
Saccharothrix syringae	A0A5Q0H4Q7	566	V
Saccharothrix texasensis	A0A3N1HHK0	552	V
Actinomadura litoris	A0A7K1KVG6	572	VI
Frankia sp. KB5	A0A1X1MKK4	571	VI
Saccharopolyspora antimicrobica	A0A1I5KZN7	558	VI
Saccharopolyspora elongata	A0A4R4Y7E8	588	VI
Streptacidiphilus jiangxiensis	A0A1H7KKC5	584	VI
Streptomyces broussonetiae	A0A6I6MUP5	571	VI
Streptomyces harbinensis	A0A1I6VN40	562	VI
Streptomyces olivaceus	A0A1D8SWY0	571	VI
Streptomyces paludis	A0A345HS54	552	VI
Streptomyces xiamenensis	A0A0F7G043	567	VI
Alloactinosynnema sp. L-07	A0A0H5DAM2	536	VII
Amycolatopsis coloradensis	A0A1R0KUQ2	572	VII
Amycolatopsis xylanica	A0A1H3CQ58	546	VII
Crossiella cryophila	A0A7W7FUZ7	564	VII
Kibdelosporangium aridum	A0A428ZRL1	645	VII
Kitasatospora viridis	A0A561UCI7	619	VII
Nonomuraea terrae	A0A4R4ZAM5	569	VII
Prauserella shujinwangii	A0A2T0LSJ8	554	VII
Saccharomonospora xinjiangensis	A0A4P7CC09	568	VII
Saccharopolyspora sp. ASAGF58	A0A6H1R8U3	570	VII
Sphaerisporangium rubeum	A0A7X0M9R3	561	VII
Streptomyces sporangiiformans	A0A505CX34	583	VII
Amycolatopsis antarctica	A0A263D1Y7	557	
Saccharopolyspora gloriosae	A0A840N7M9	571	
Streptomyces sp. SN-593	A0A7U3UW44	571	

[a] The proteins AtoE (Uniprot ID: A0A1H4ZTV5), SerTC (Uniprot ID: A4FIP2), SmaTC (Uniprot ID: A0A515GD19), UtaTC (Uniprot ID: A0A2T0STH2), CcrTC (Uniprot ID: A0A7W7FUZ7), SsyTC (Uniprot ID: A0A5Q0H4Q7), AxyTC (Uniprot ID: A0A1H3CQ58) and PshTC (Uniprot ID: A0A2T0LSJ8), which were characterized in this study, are highlighted in blue text.

Table S23. Summary of ^{1}H NMR (400 MHz) and ^{13}C NMR (100 MHz) data for atolypene H (**15**) in methanol-d_4 (δ in ppm, J in Hz).

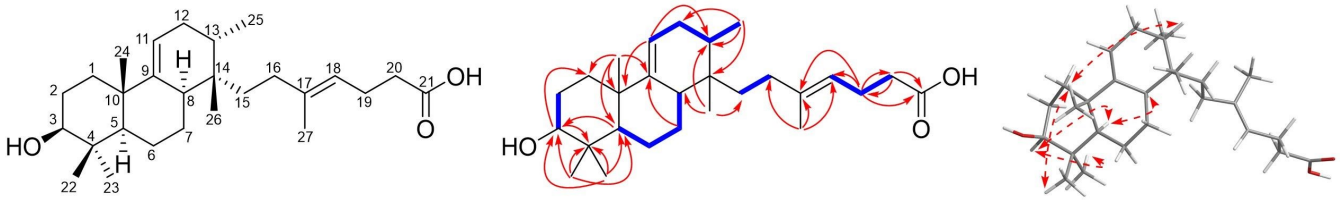

Chemical structure of **15** and ^{1}H-^{1}H COSY ( ), key HMBC correlations ( ), and key ROESY correlations ( ).

No.	δ_C, type	δ_H, mult. (J, Hz)
1a	40.6, CH_2	1.95, m
1b		1.32, m
2a	28.9, CH_2	1.70, m
2b		1.63, m
3	79.8, CH	3.13, dd (11.4, 4.7)
4	40.3, C	
5	45.6, CH	1.32, overlapped
6a	19.7, CH_2	1.71, m
6b		1.31, overlapped
7a	30.3, CH_2	1.32, 2H, overlapped
7b		
8	39.7, CH	2.02, m
9	151.3, C	
10	39.0, C	
11	115.9, CH	5.37, m
12a	31.4, CH_2	2.23, m
12b		1.71, overlapped
13	33.7, CH	1.61, m
14	36.6, C	
15a	38.0, CH_2	1.50, td (12.3, 4.3)
15b		1.33, overlapped
16a	34.3, CH_2	1.95, m
16b		1.85, td (12.7, 4.2)
17	138.7, C	
18	123.3, CH	5.15, t (6.7)
19a	24.8, CH_2	2.30, 2H, d (3.2)
19b		
20a	35.4, CH_2	2.30, 2H, overlapped
20b		
21	177.7, C	
22	15.8, CH_3	0.86, s
23	28.2, CH_3	0.95, s
24	25.8, CH_3	1.09, s
25	15.2, CH_3	0.81, d (7.0)
26	20.3, CH_3	0.73
27	16.3, CH_3	1.65, s

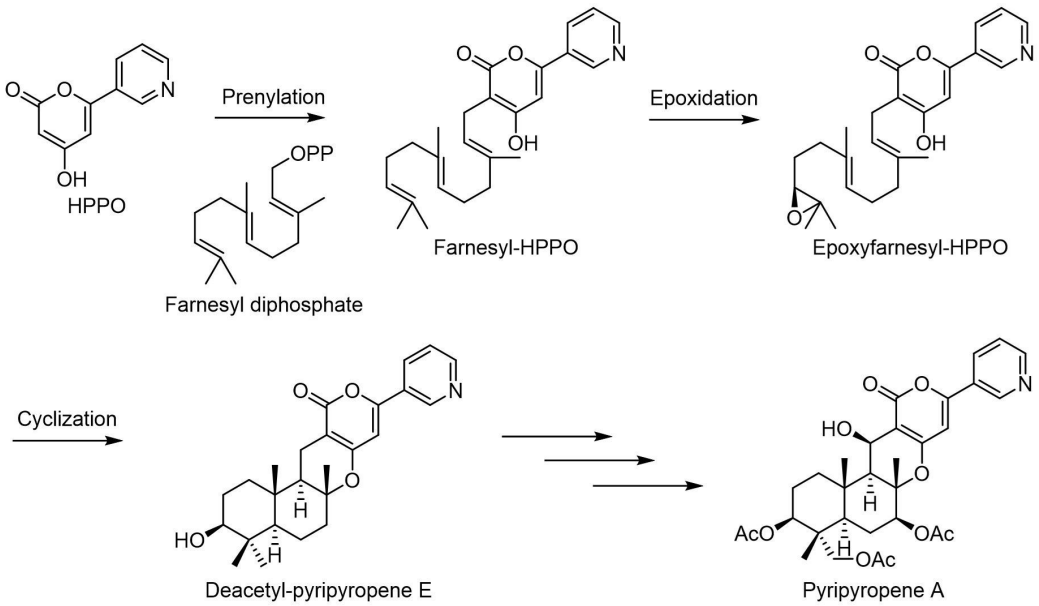

Figure S1. Biosynthetic pathway of pyripyropene A. The biosynthesis of pyripyropene A start with the assembly of the polyketide moiety, which is followed by prenylation of the polyketide, stereospecific epoxidation of the olefin of the prenyl chain, and cyclization of the terpenoid moiety to generate the core scaffold.[19]

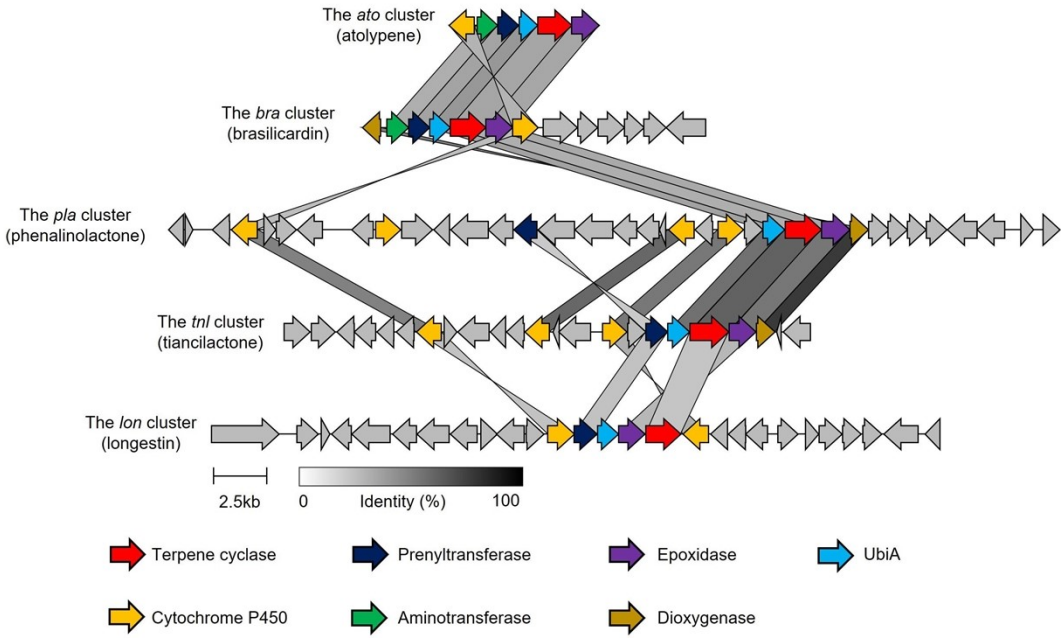

Figure S2. Schematic representation of the *ato* cluster and its homologous gene clusters and BLASTp comparisons of each gene product.

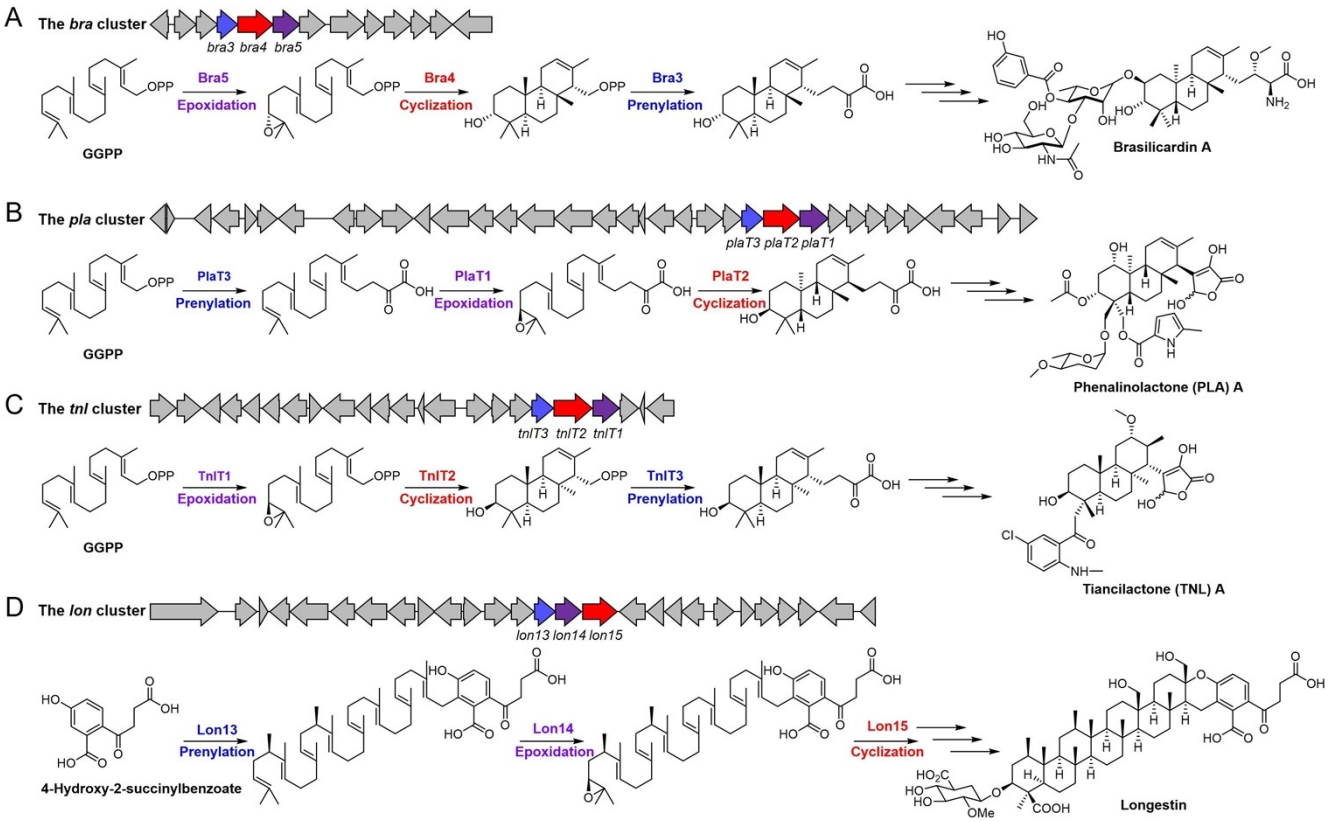

Figure S3. Proposed biosynthetic pathways of brasilicardin A,[20] phenalinolactone A,[21,22] tiancilactone A,[3] and longestin.[23]

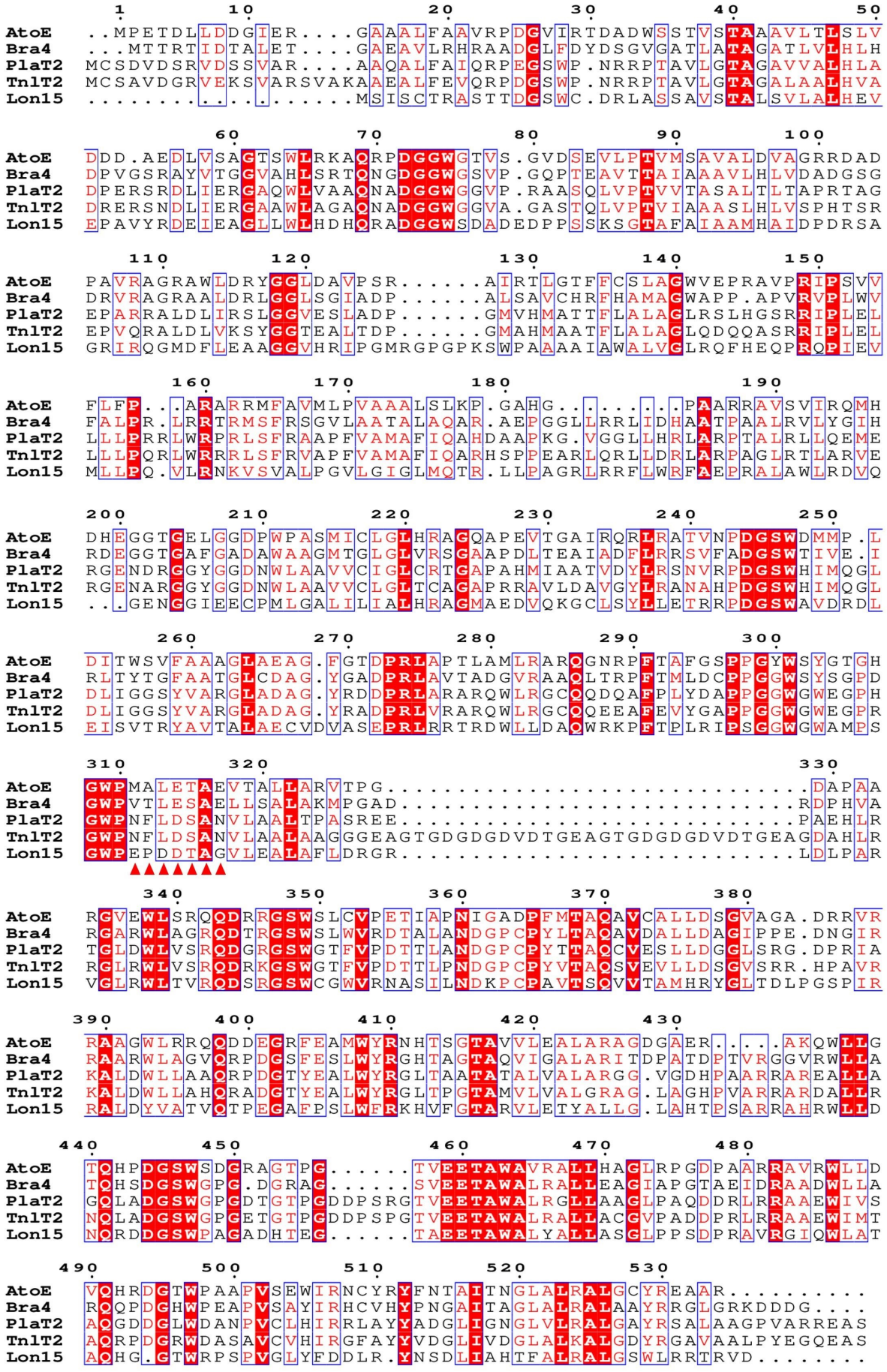

Figure S4. Amino acid sequence alignment of bacterial noncanonical class II MTCs. Alignment of amino acid sequences was conducted for bacterial noncanonical class II MTCs, including AtoE, Bra4, PlaT2, TnlT2, and Lon15. All these MTCs contain the noncanonical sequence motifs xxx(E/D)(T/S)xE, which are marked with red triangle symbols. The sequence alignment was generated by Clustal Omega and the figure drawn in EsPript 3.0.

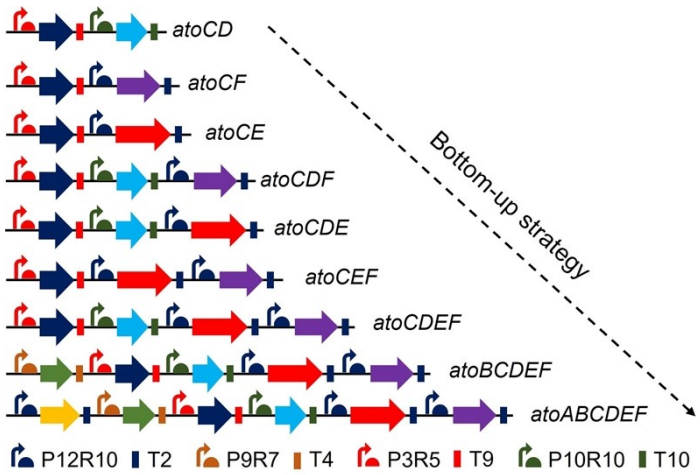

Figure S5. Reconstitution of the *ato* gene cluster. A bottom-up strategy was adopted for the comprehensive reconstruction of the *ato* genes, with all gene combinations meticulously constructed and integrated into the pSET152 vector.

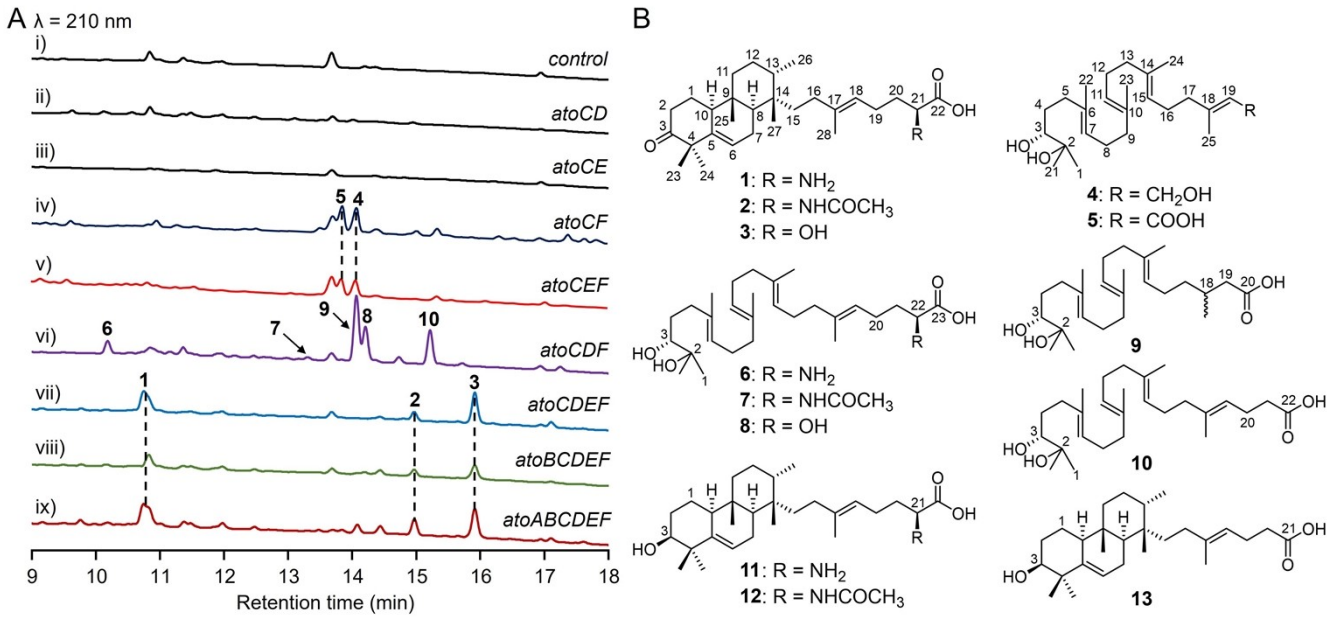

Figure S6. Analysis of metabolites from engineered *Streptomyces* strains. A) HPLC results (λ_{max} = 210 nm). *S. albus* J1074 with empty pSET152 was used as a control. B) Structures of the metabolites isolated in this study (**1**−**13**).

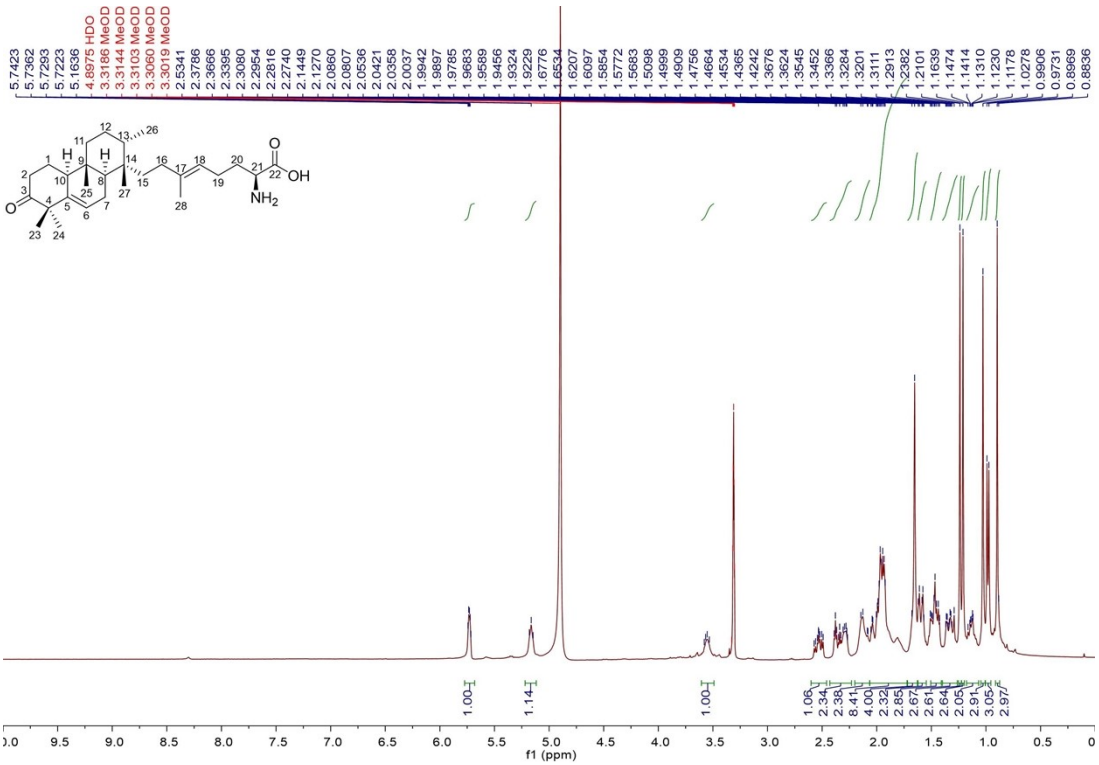

Figure S7. ^{1}H NMR spectrum of atolypene A (**1**) in methanol-d_4 (400 MHz).

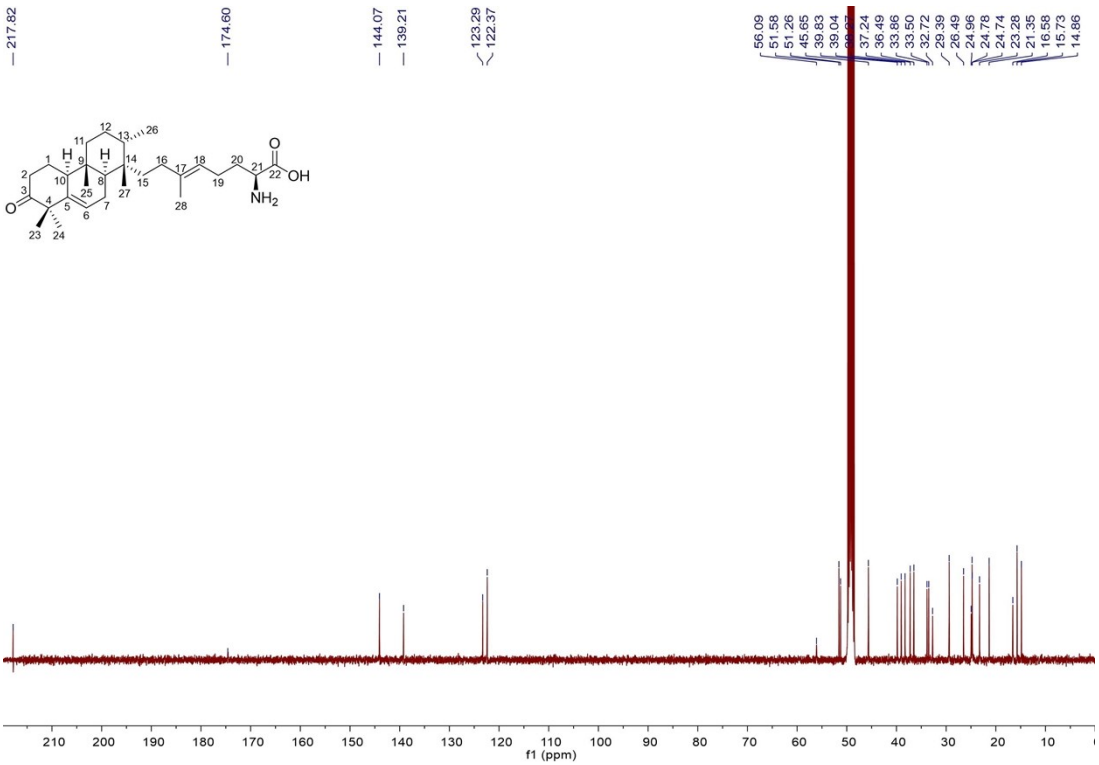

Figure S8. ^{13}C NMR spectrum of atolypene A (**1**) in methanol-d_4 (100 MHz).

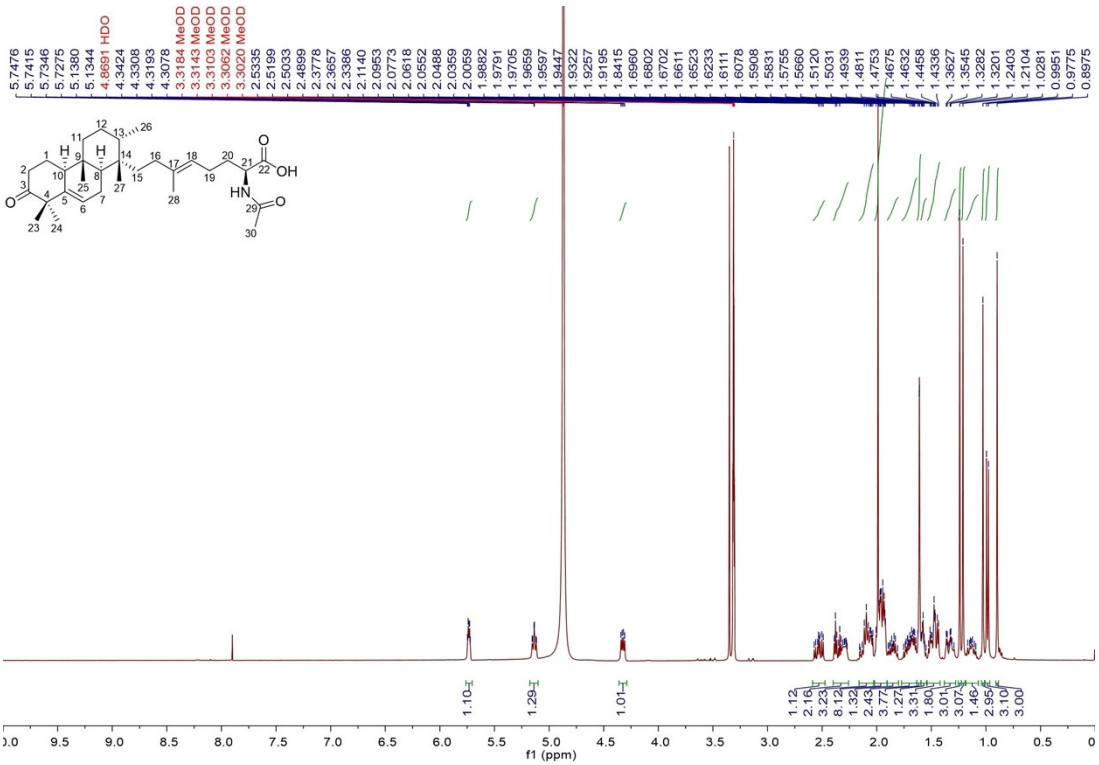

Figure S9. ^{1}H NMR spectrum of atolypene C (**2**) in methanol-d_4 (100 MHz).

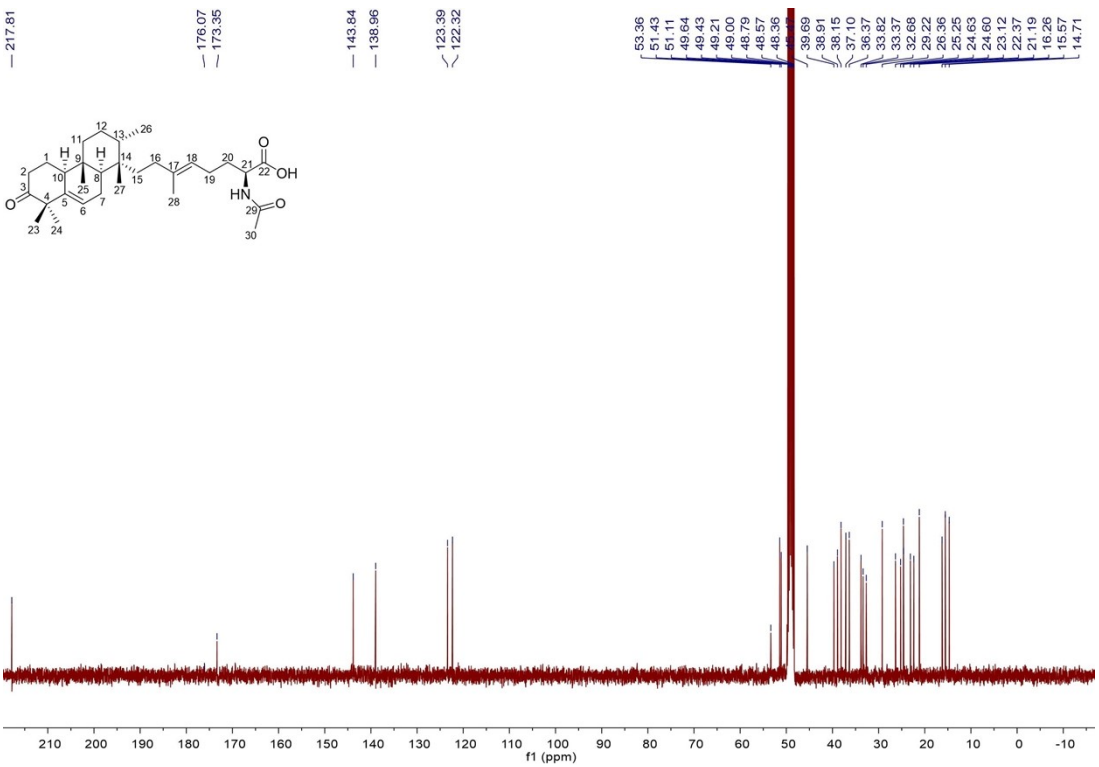

Figure S10. ^{13}C NMR spectrum of atolypene C (**2**) in methanol-d_4 (100 MHz).

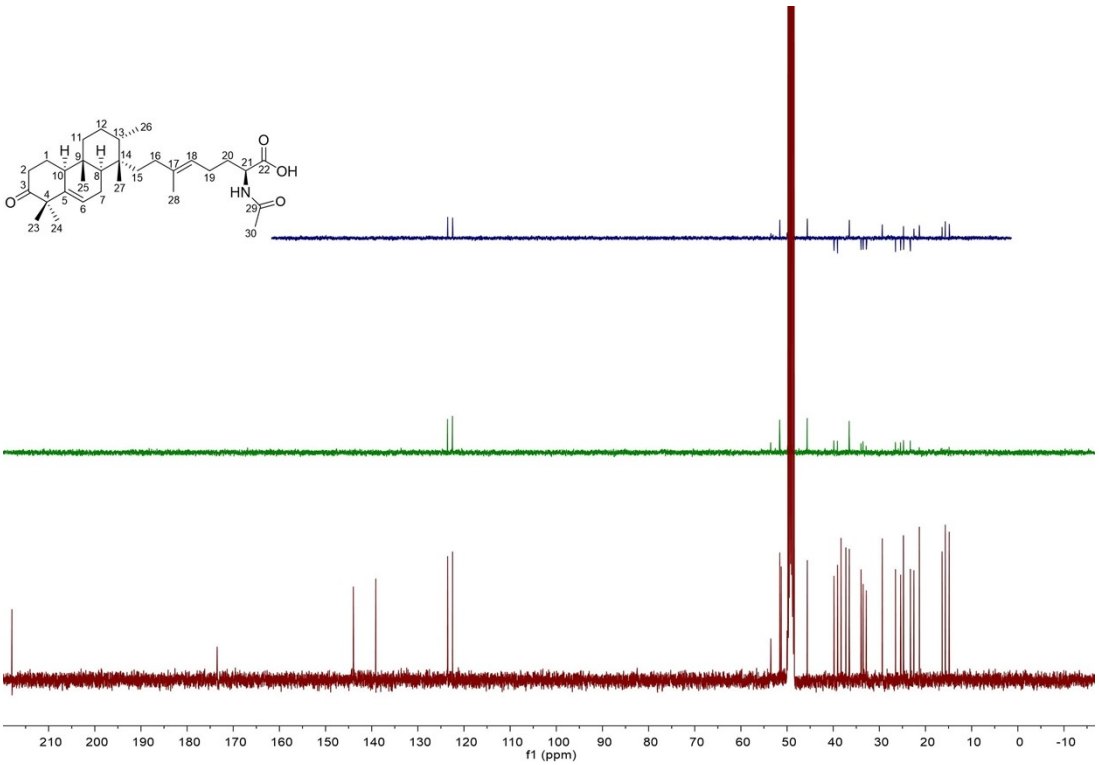

Figure S11. DEPT spectrum of atolypene C (**2**) in methanol-d_4.

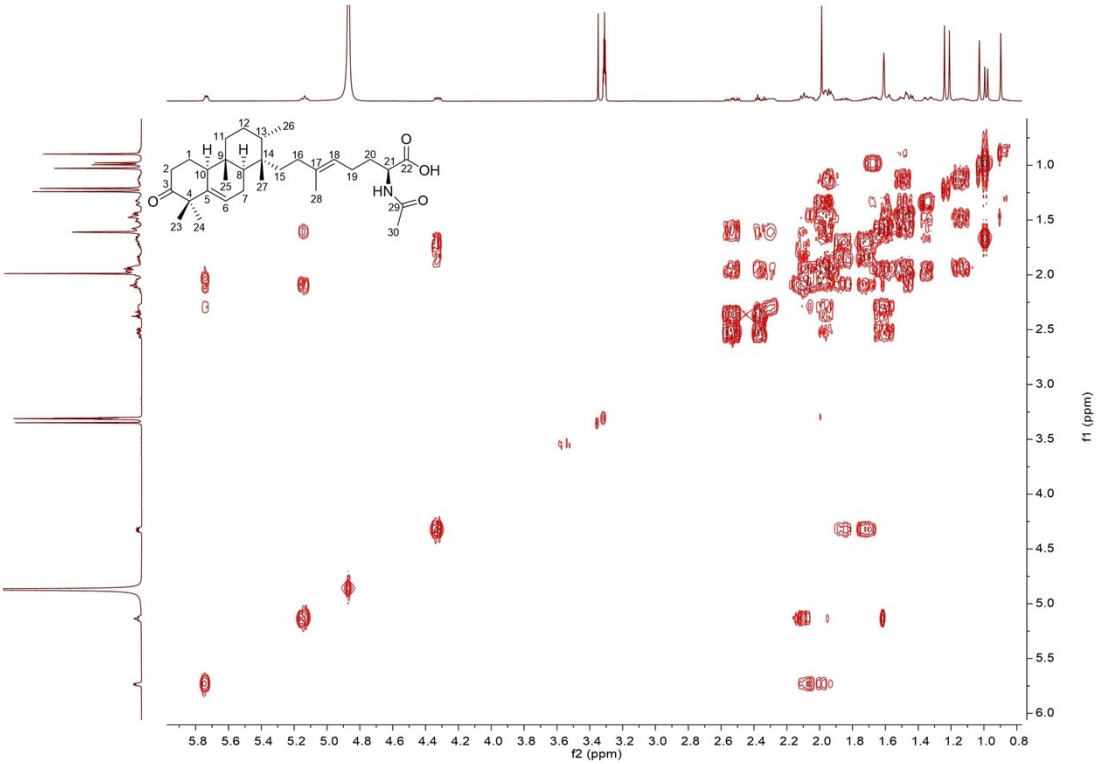

Figure S12. ^{1}H-^{1}H COSY spectrum of atolypene C (**2**) in methanol-d_4.

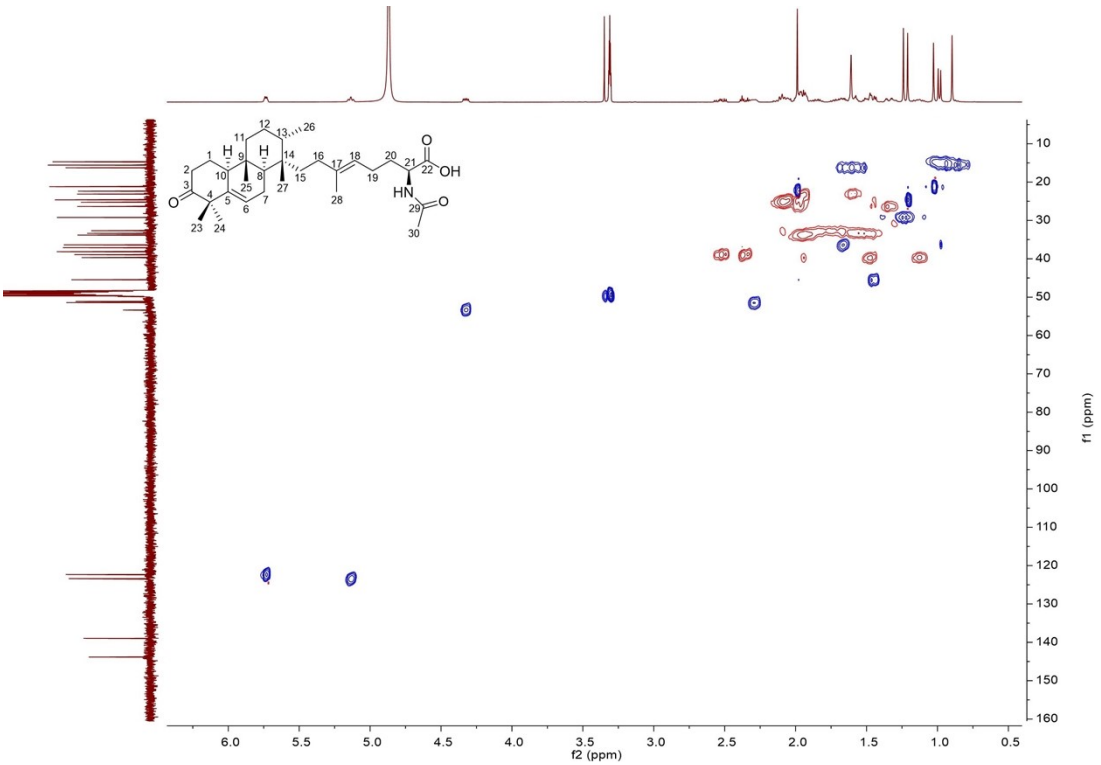

Figure S13. HSQC spectrum of atolypene C (**2**) in methanol-d_4.

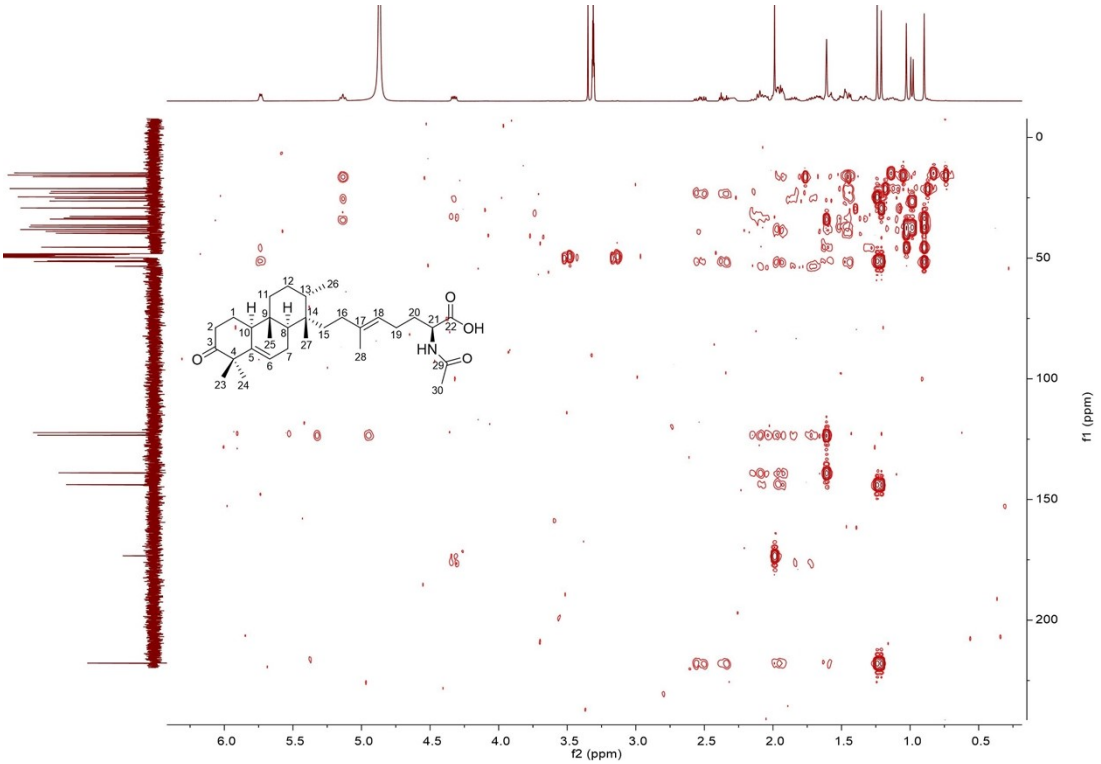

Figure S14. HMBC spectrum of atolypene C (**2**) in methanol-d_4.

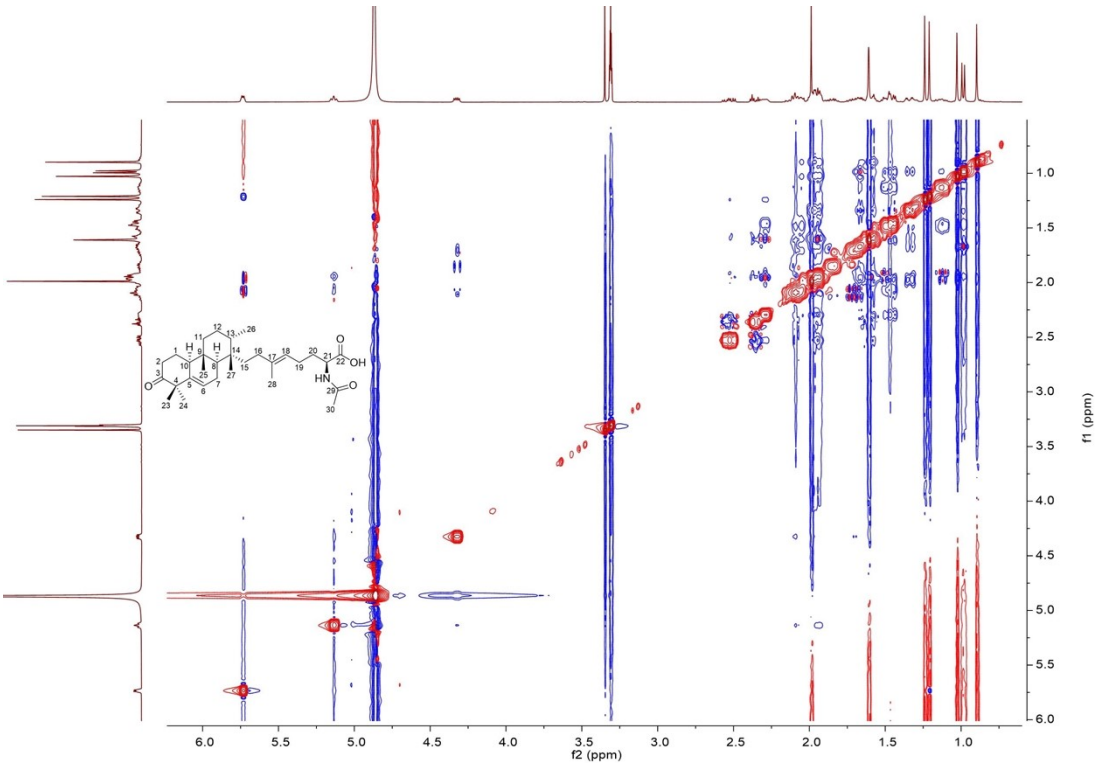

Figure S15. ROESY spectrum of atolypene C (**2**) in methanol-d_4.

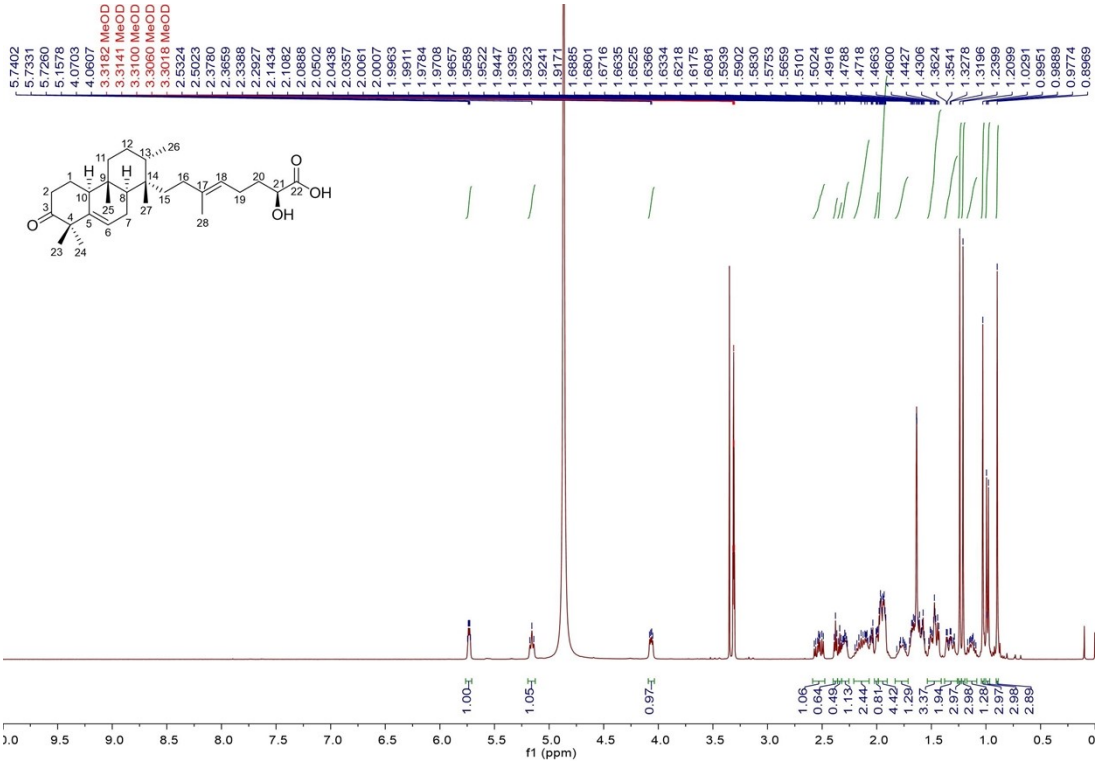

Figure S16. ^{1}H NMR spectrum of atolypene D (**3**) in methanol-d_4 (400 MHz).

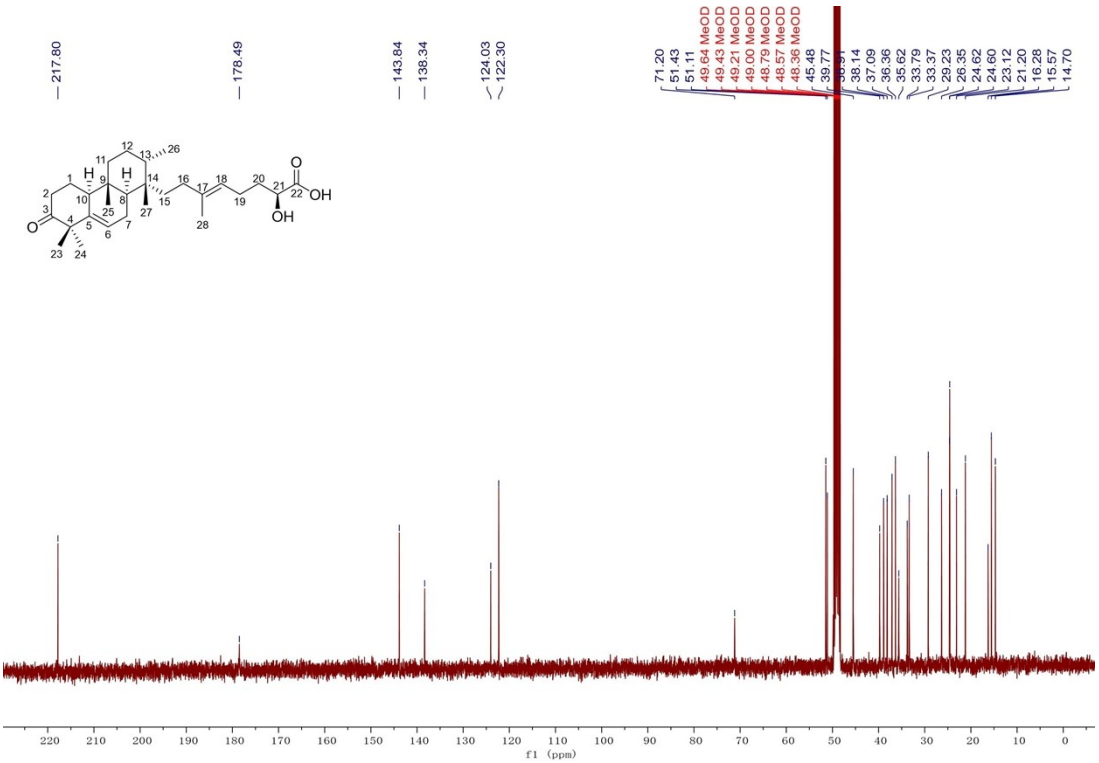

Figure S17. ^{13}C NMR spectrum of atolypene D (**3**) in methanol-d_4 (100 MHz).

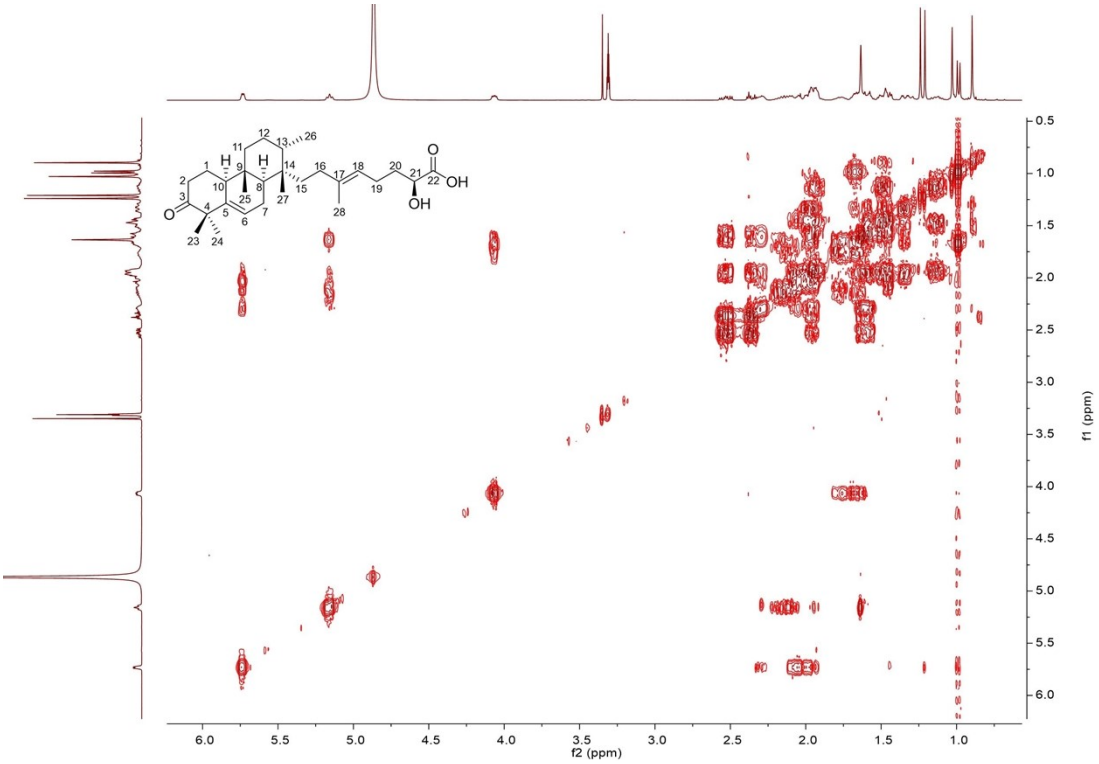

Figure S18. ^{1}H-^{1}H COSY spectrum of atolypene D (**3**) in methanol-d_4.

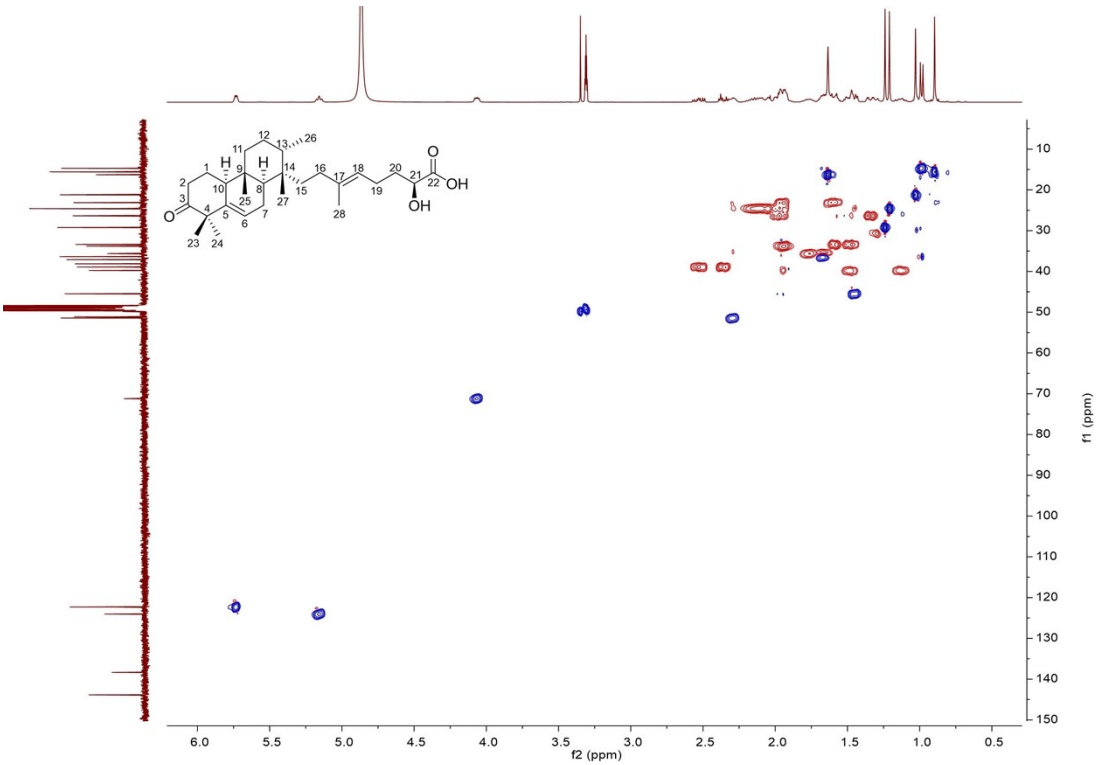

Figure S19. HSQC spectrum of atolypene D (**3**) in methanol-d_4.

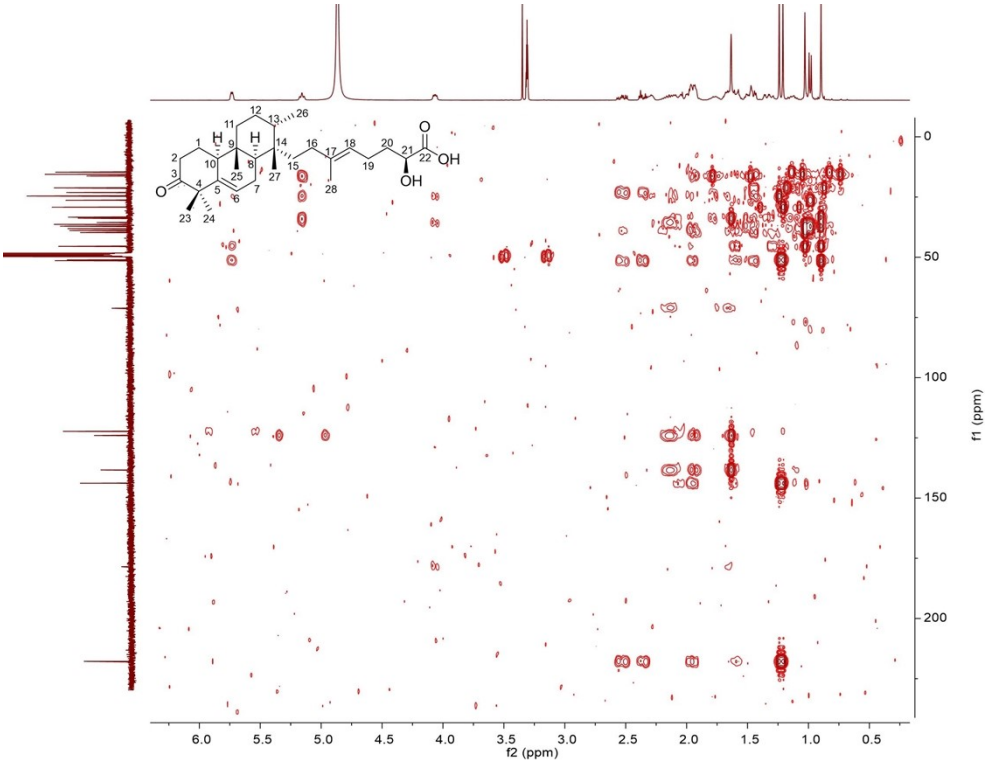

Figure S20. HMBC spectrum of atolypene D (**3**) in methanol-d_4.

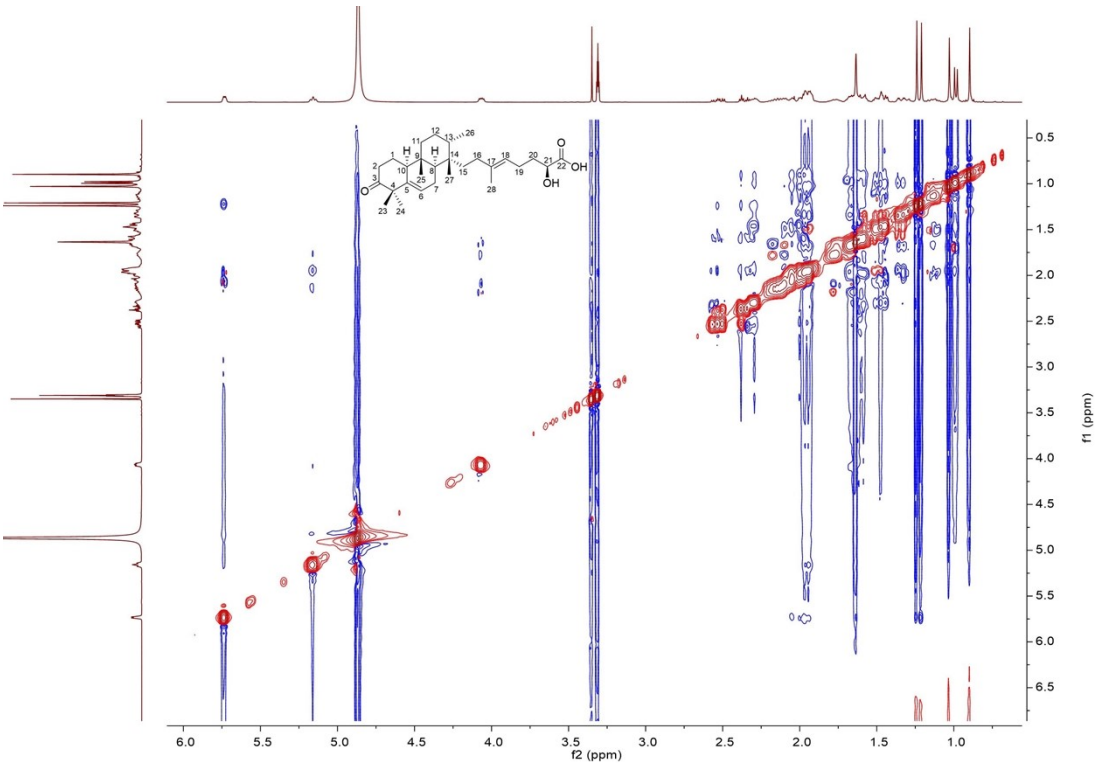

Figure S21. ROESY spectrum of atolypene D (**3**) in methanol-d_4.

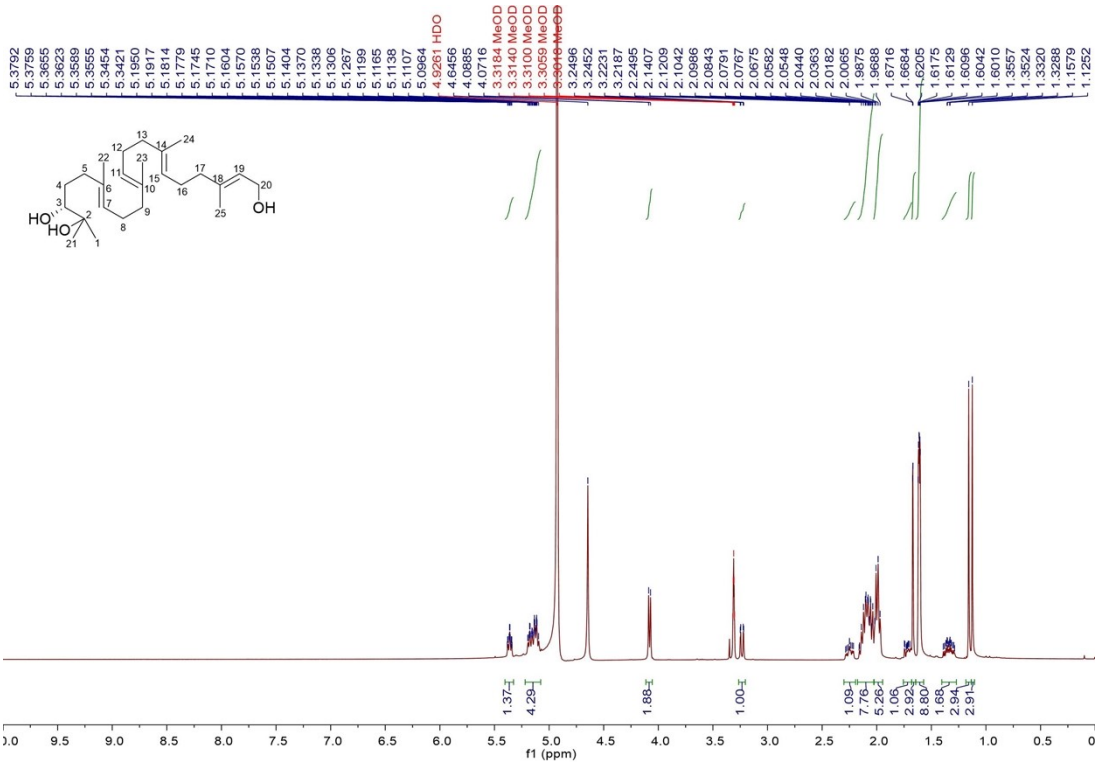

Figure S22. ^{1}H NMR spectrum of **4** in methanol-d_4 (400 MHz).

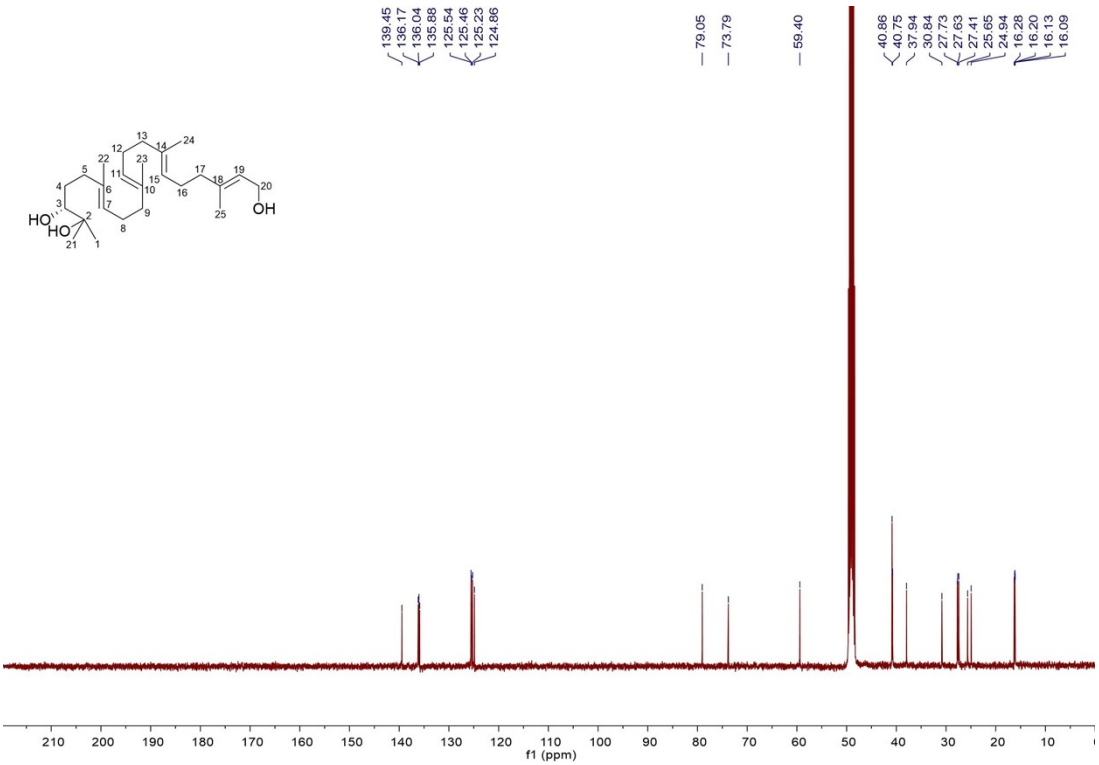

Figure S23. ^{13}C NMR spectrum of **4** in methanol-d_4 (100 MHz).

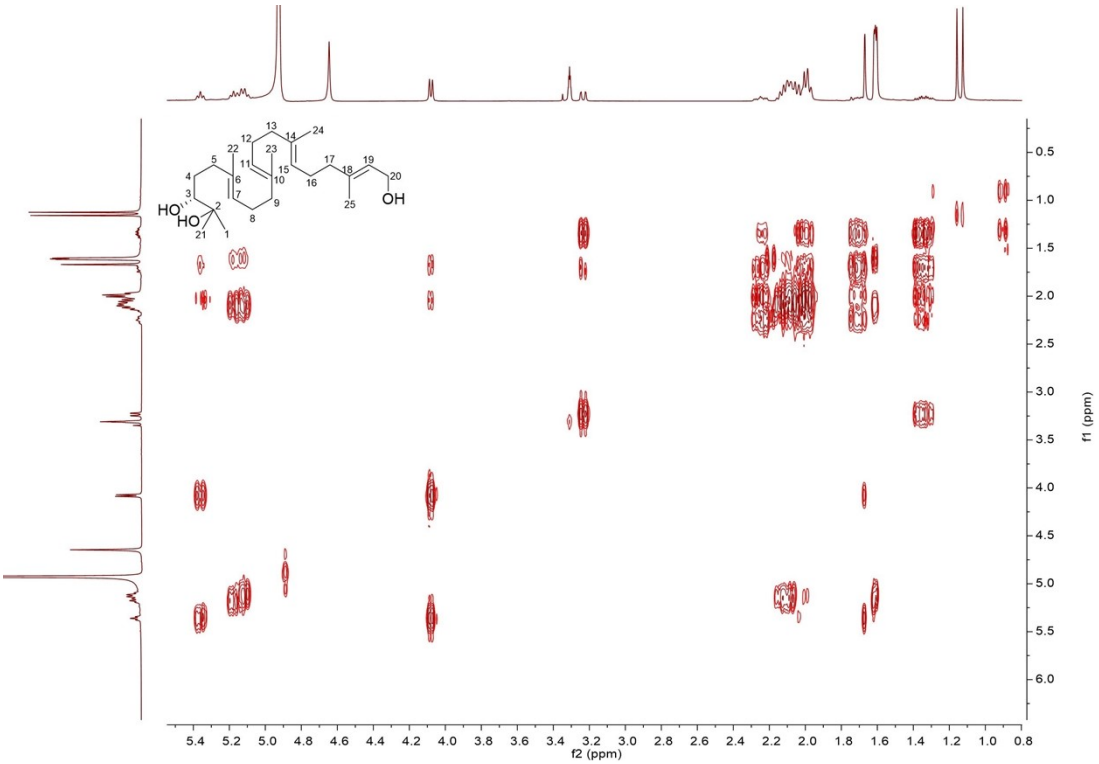

Figure S24. ^{1}H-^{1}H COSY spectrum of **4** in methanol-d_4.

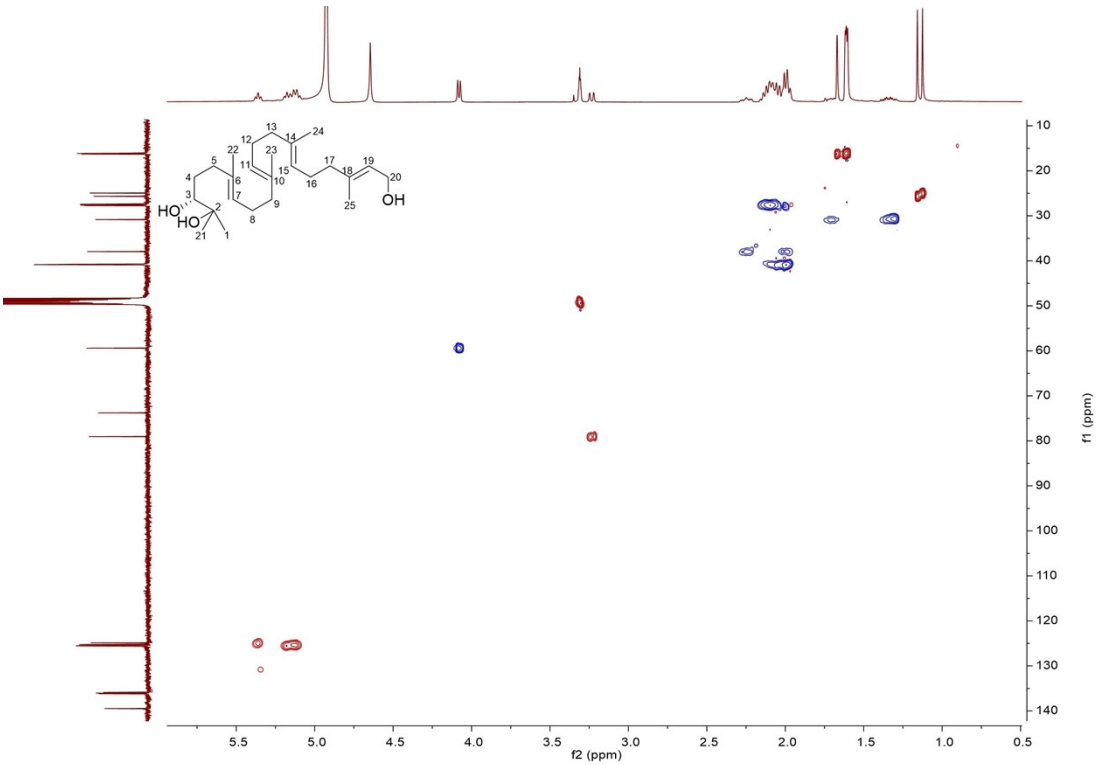

Figure S25. HSQC spectrum of **4** in methanol-d_4.

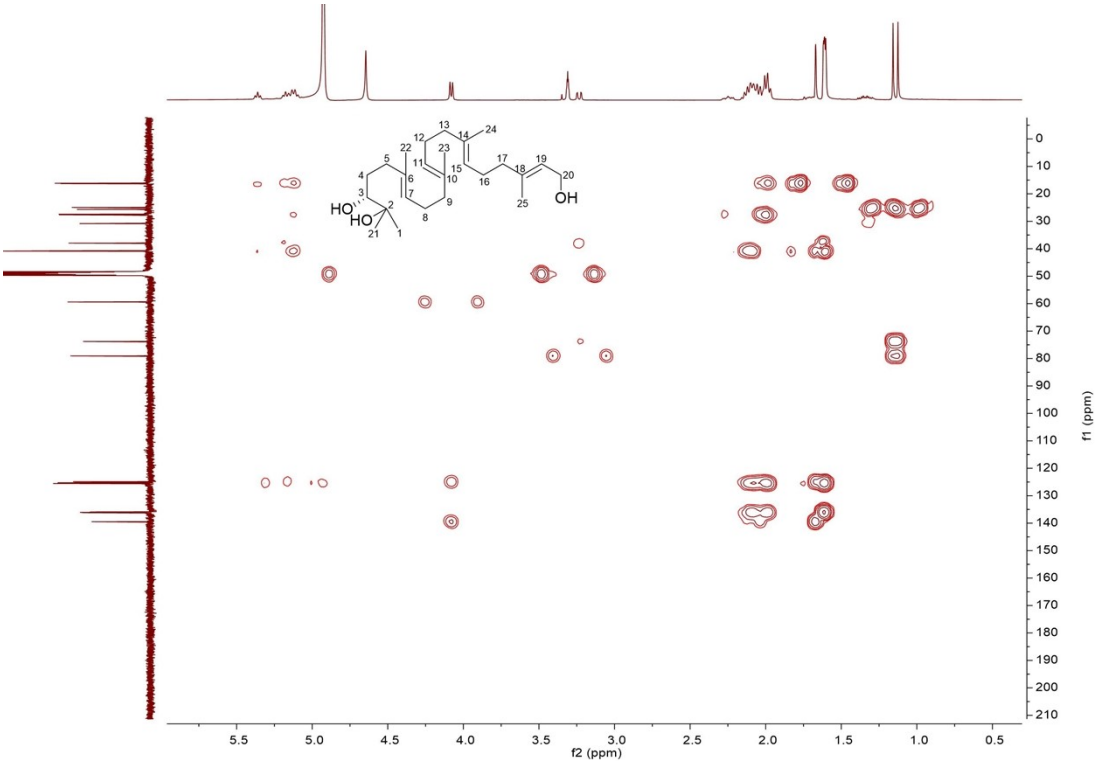

Figure S26. HMBC spectrum of **4** in methanol-d_4.

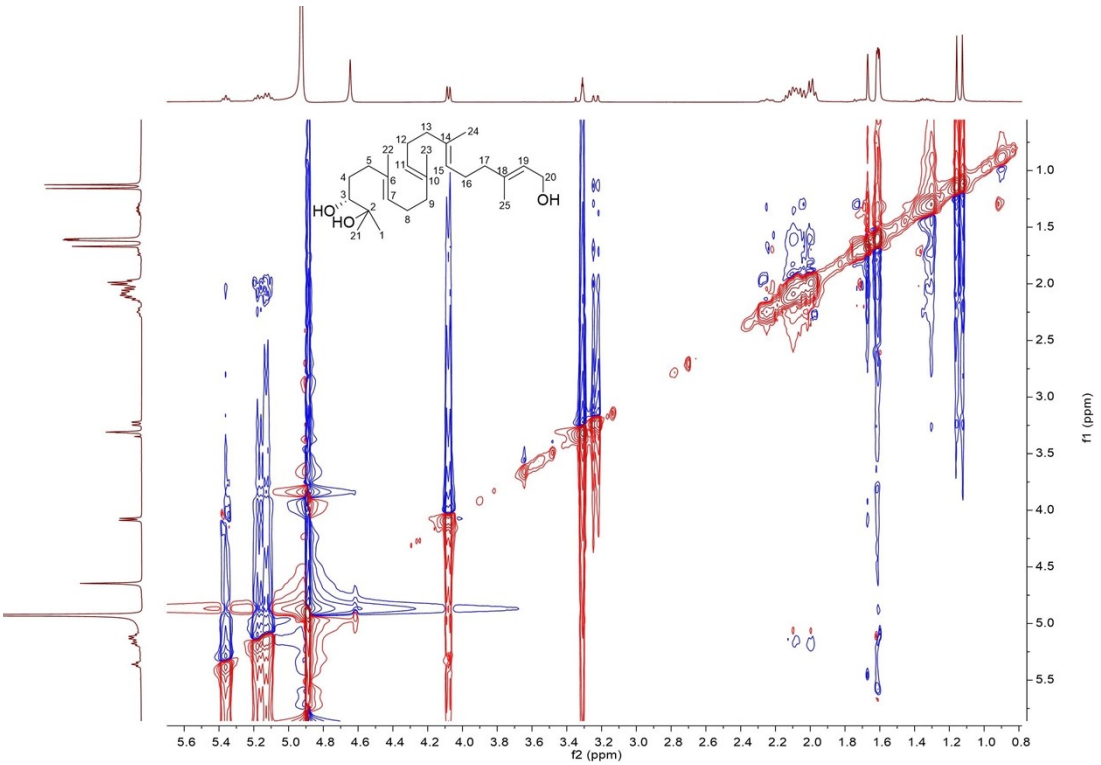

Figure S27. ROESY spectrum of **4** in methanol-d_4.

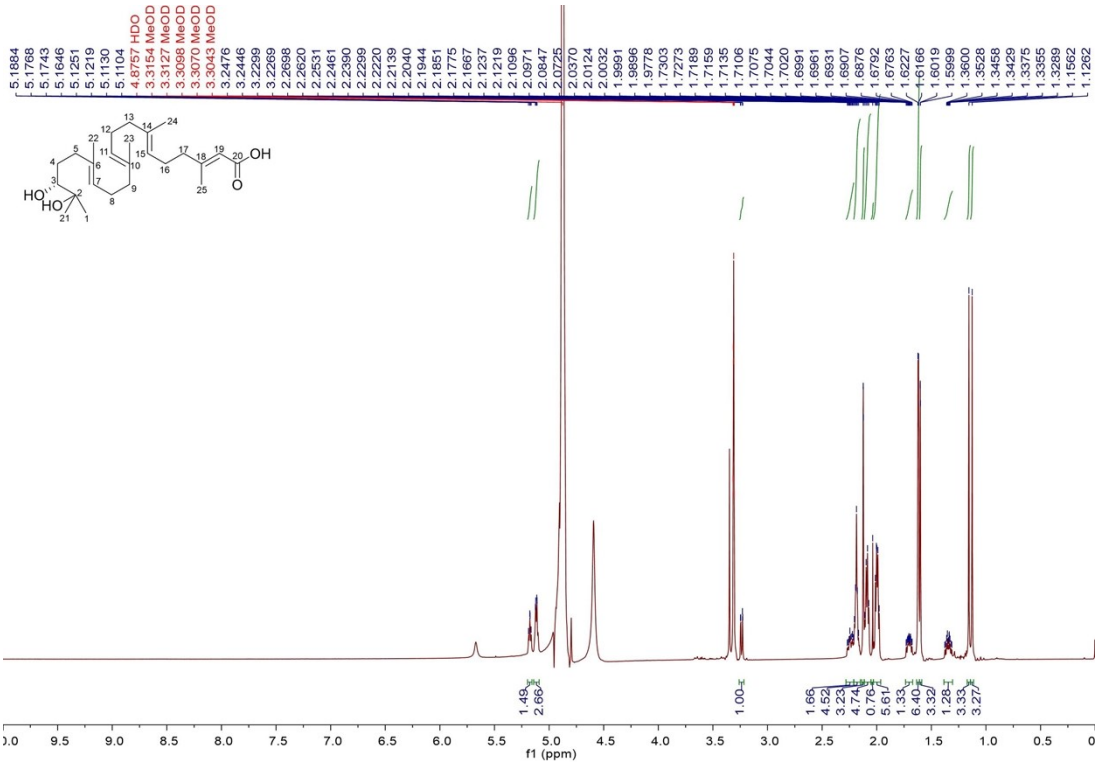

Figure S28. ^{1}H NMR spectrum of **5** in methanol-d_4 (400 MHz).

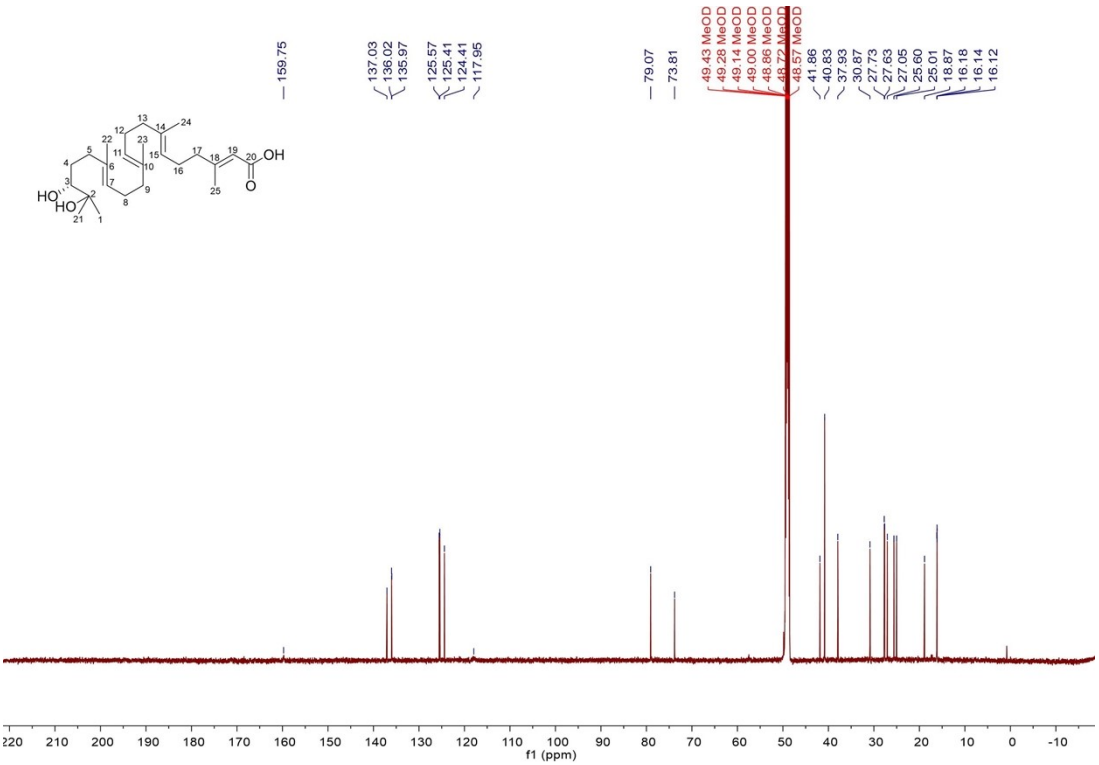

Figure S29. ^{13}C NMR spectrum of **5** in methanol-d_4 (100 MHz).

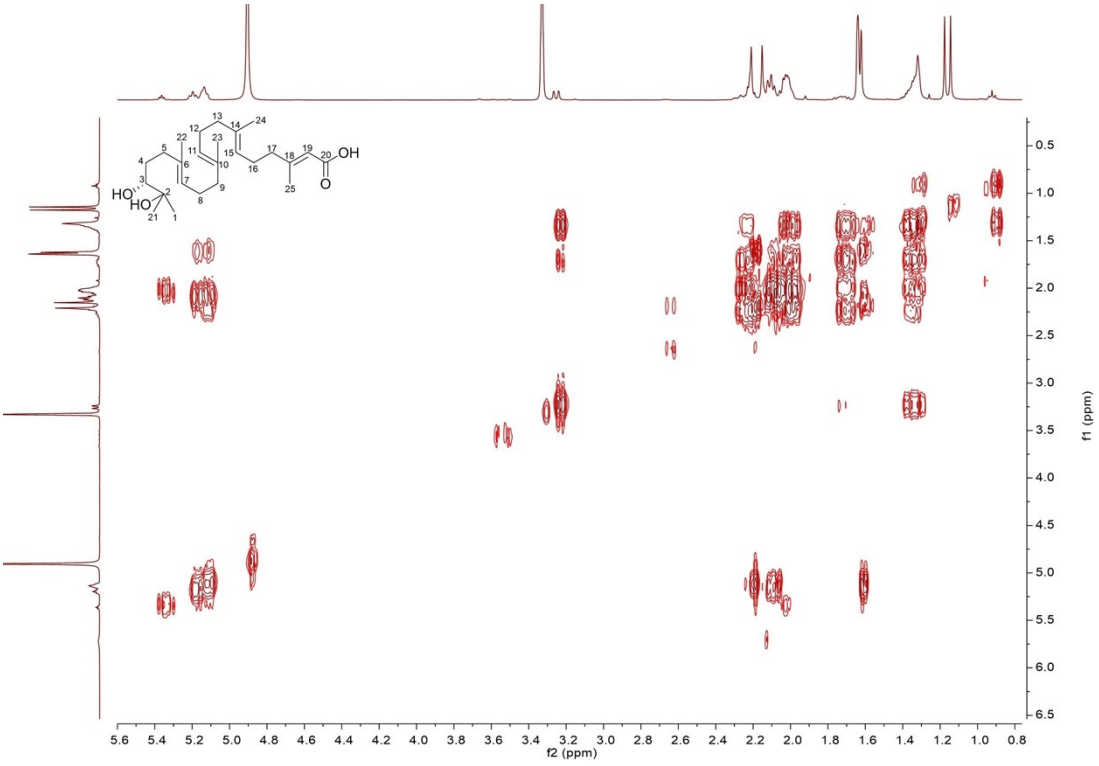

Figure S30. ^{1}H-^{1}H COSY spectrum of **5** in methanol-d_4.

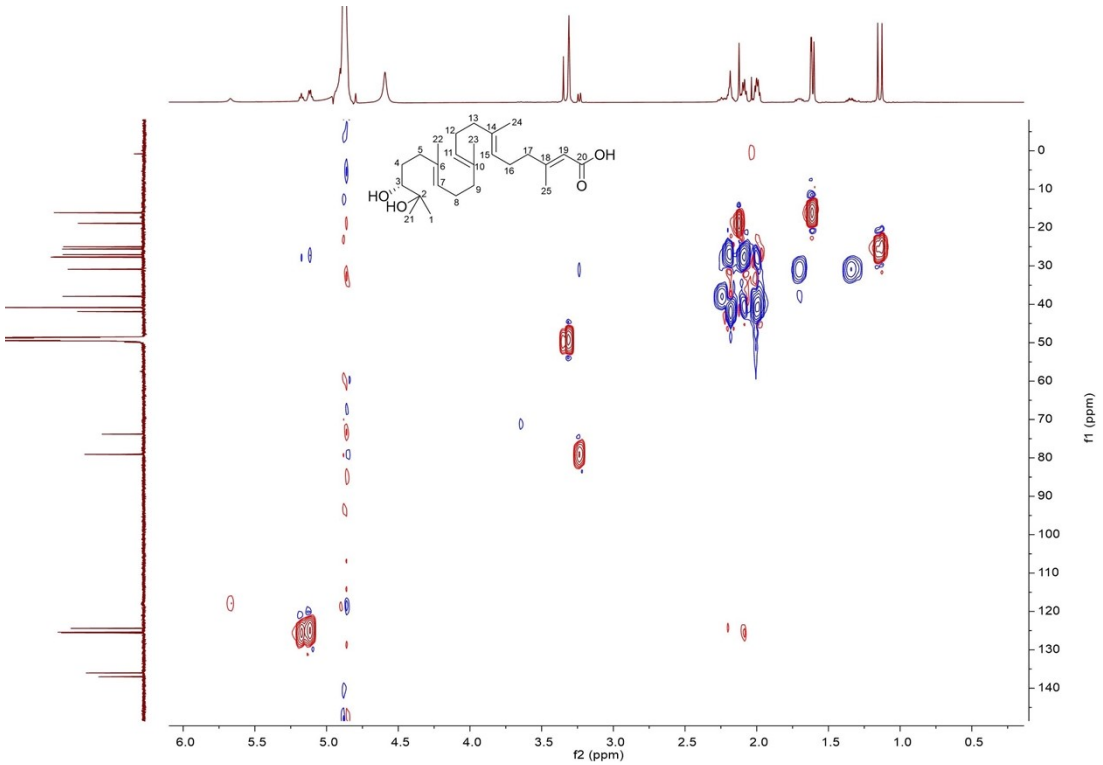

Figure S31. HSQC spectrum of **5** in methanol-d_4.

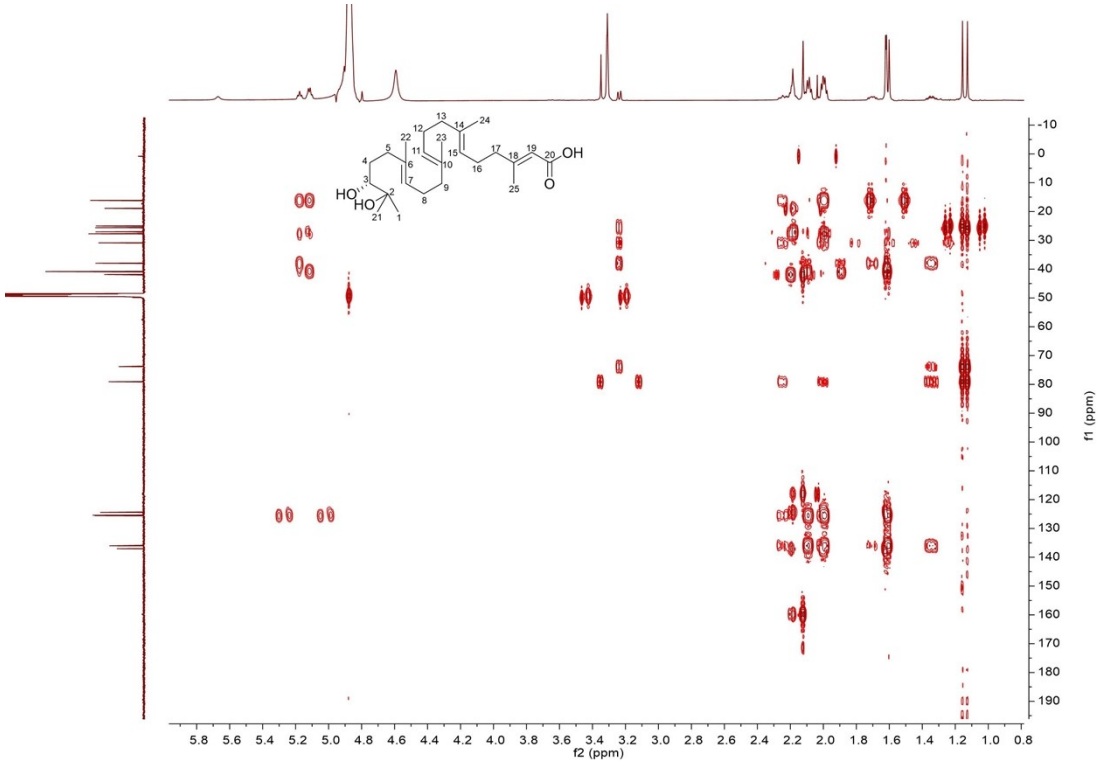

Figure S32. HMBC spectrum of **5** in methanol-d_4.

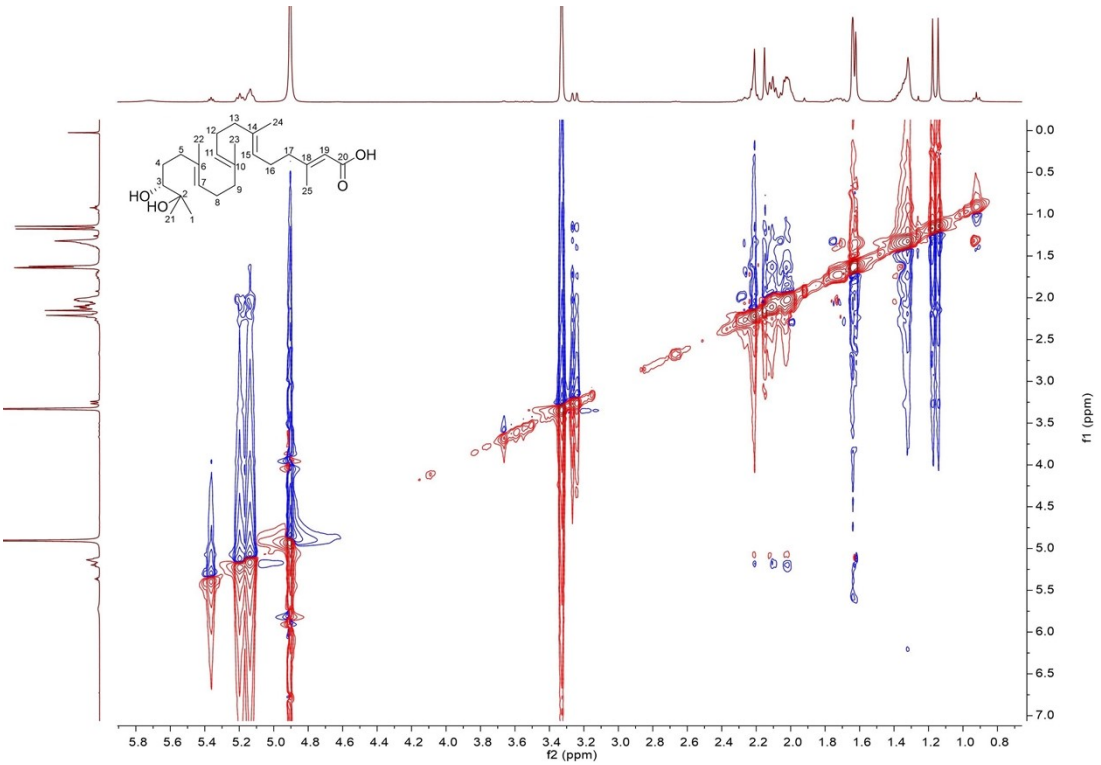

Figure S33. ROESY spectrum of **5** in methanol-d_4.

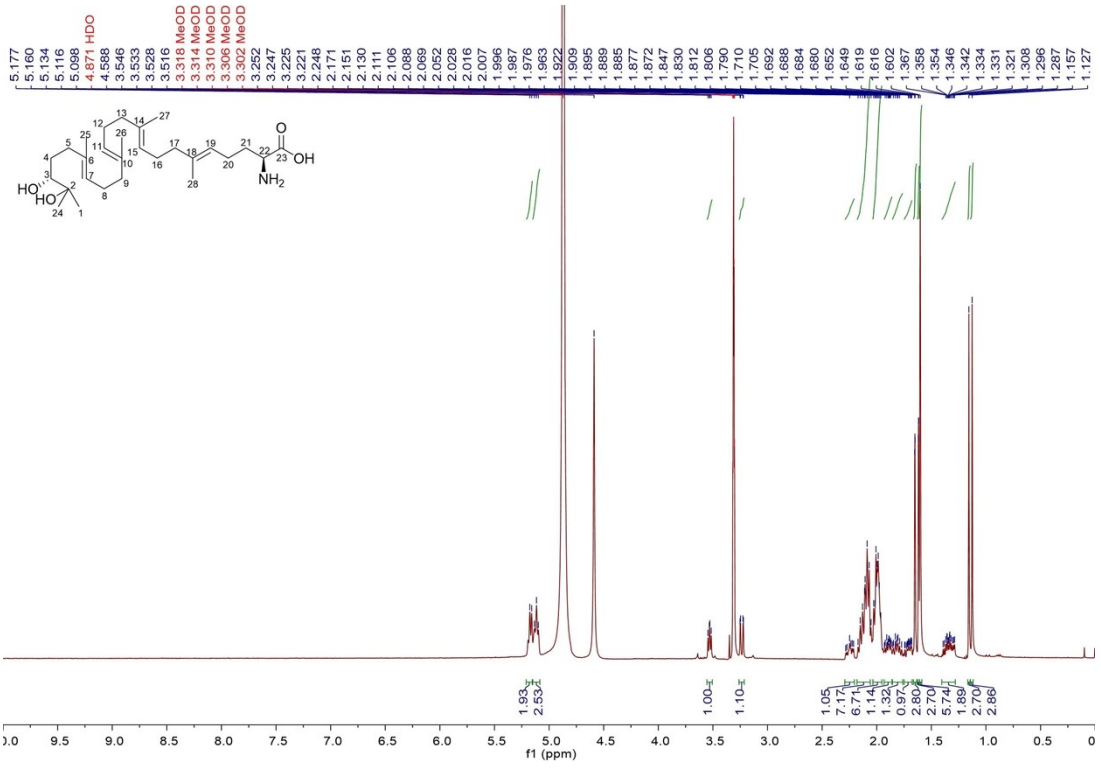

Figure S34. ^{1}H NMR spectrum of **6** in methanol-d_4 (400 MHz).

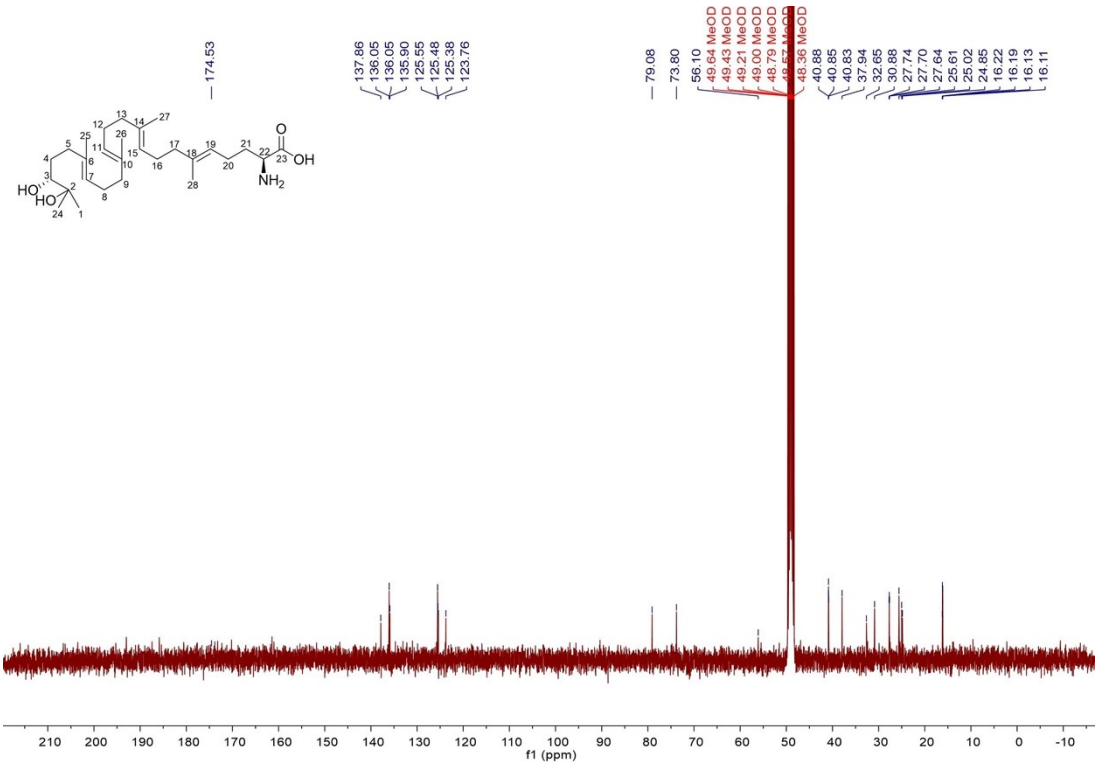

Figure S35. ^{13}C NMR spectrum of **6** in methanol-d_4 (100 MHz).

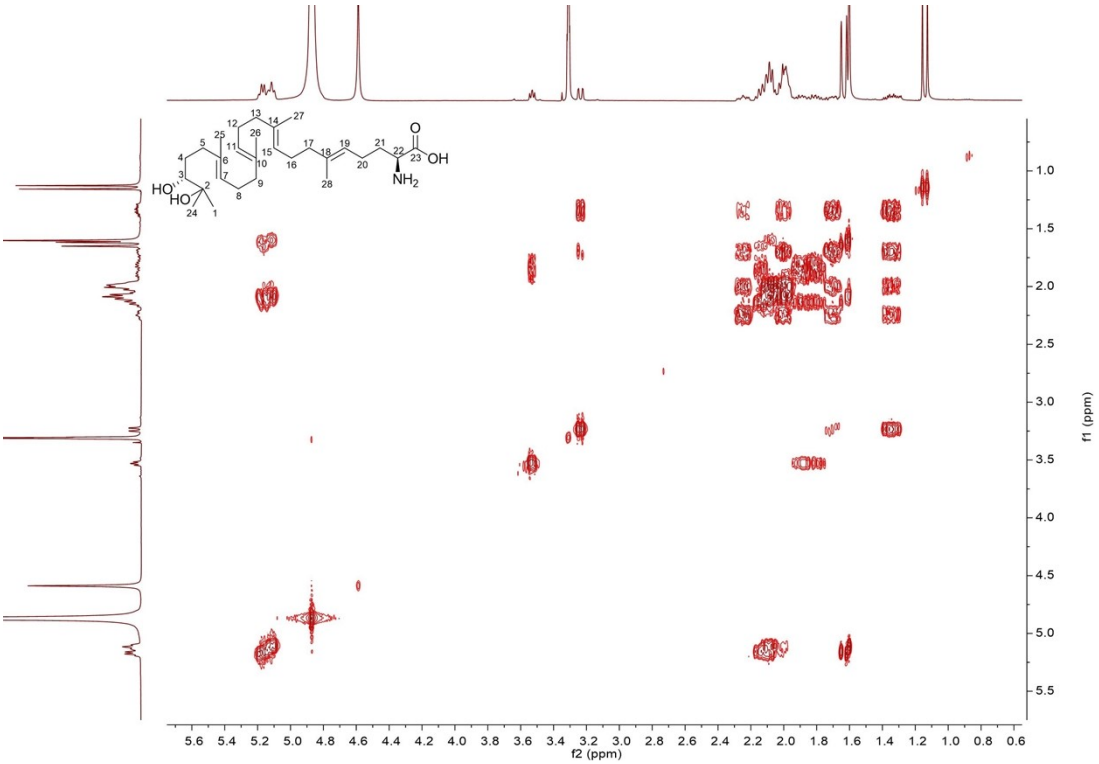

Figure S36. ^{1}H-^{1}H COSY spectrum of **6** in methanol-d_4.

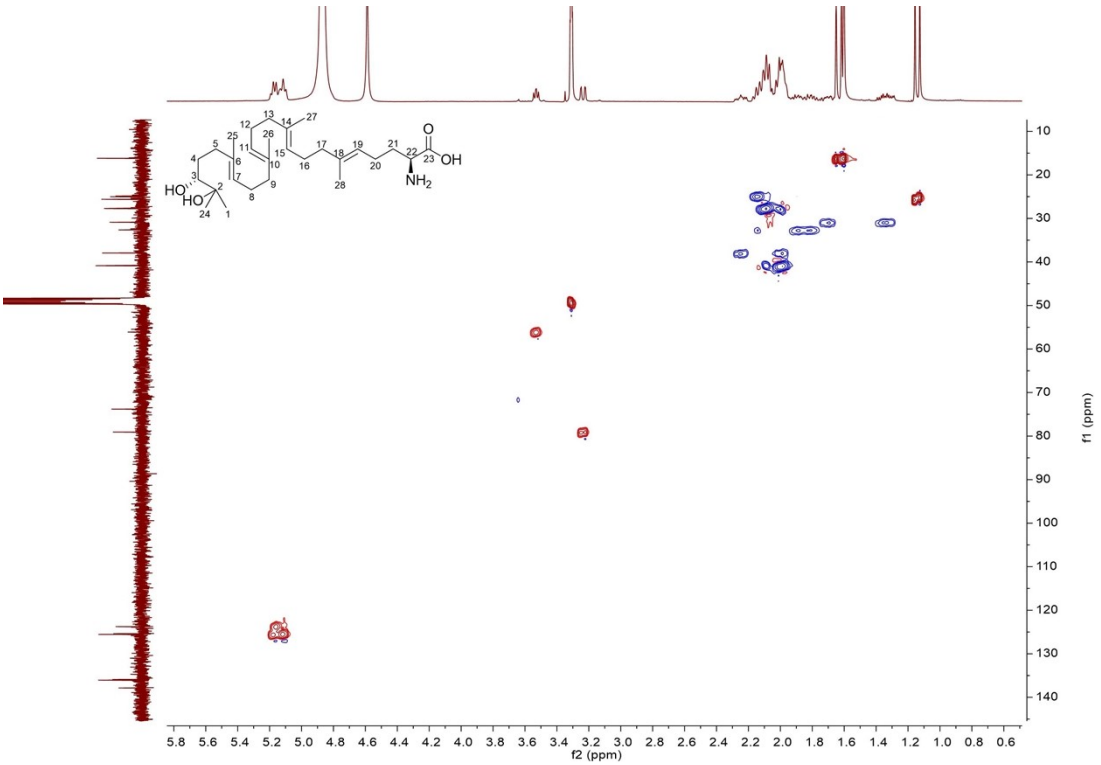

Figure S37. HSQC spectrum of **6** in methanol-d_4.

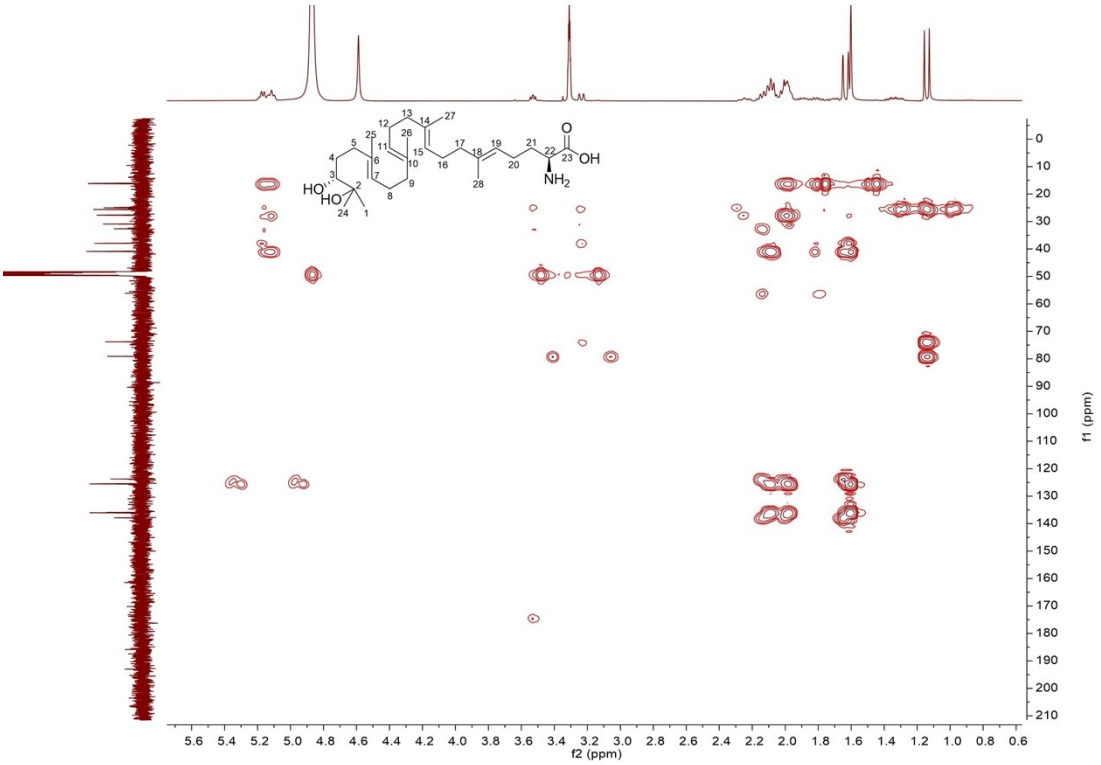

Figure S38. HMBC spectrum of **6** in methanol-d_4.

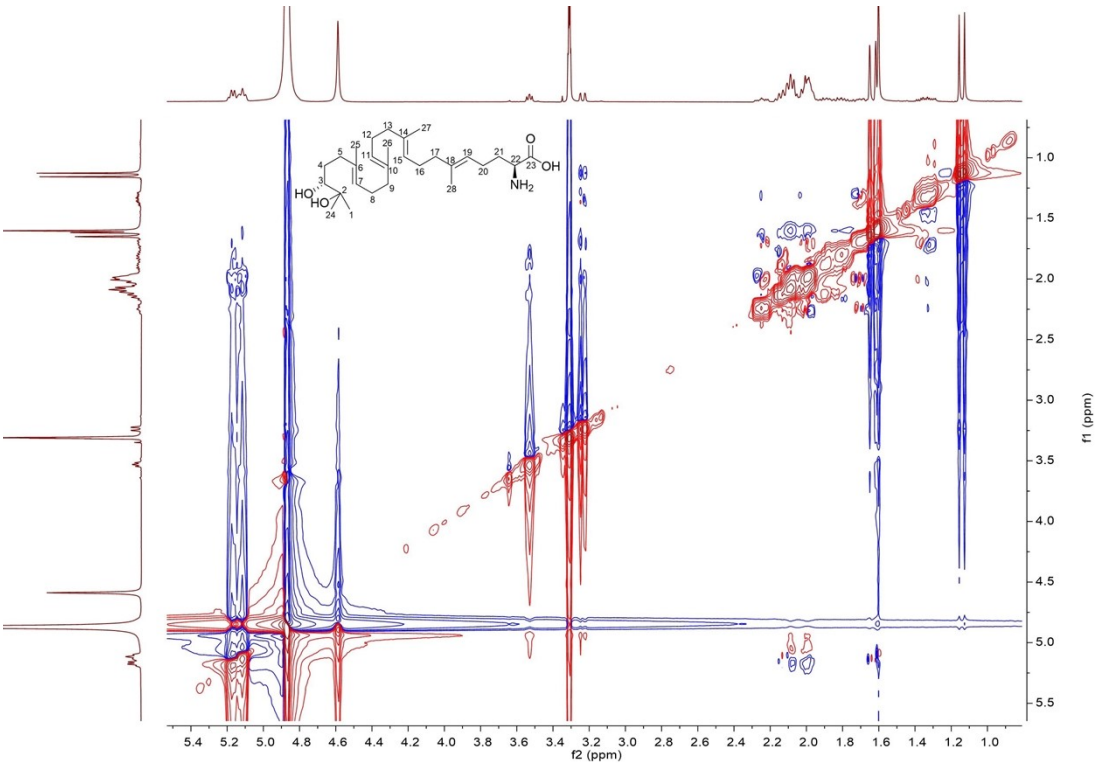

Figure S39. ROESY spectrum of **6** in methanol-d_4.

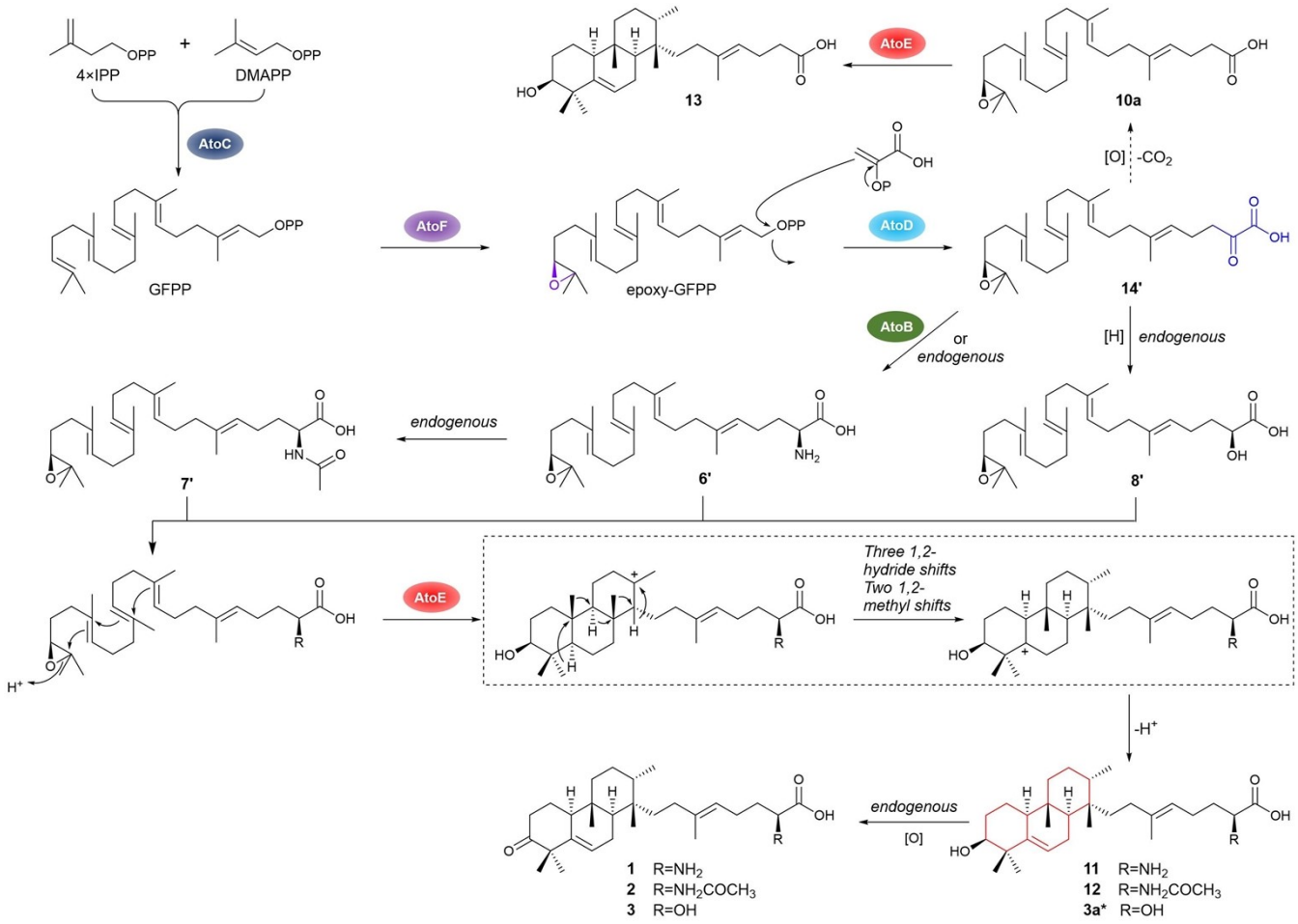

Figure S40. Proposed biosynthetic pathway of atolypenes. Compounds **6'**–**8'** and **14'** are the epoxide forms of **6**–**8** and **14**, respectively. **3a***: Not isolated.

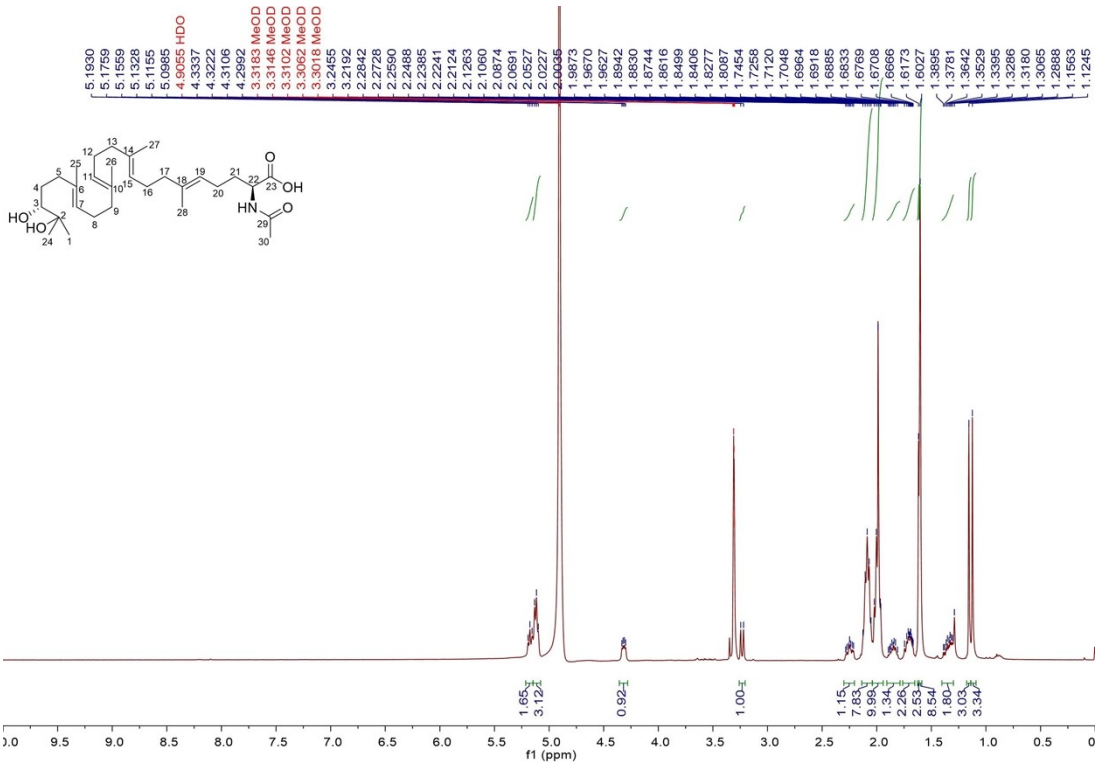

Figure S41. ^{1}H NMR spectrum of **7** in methanol-d_4 (400 MHz).

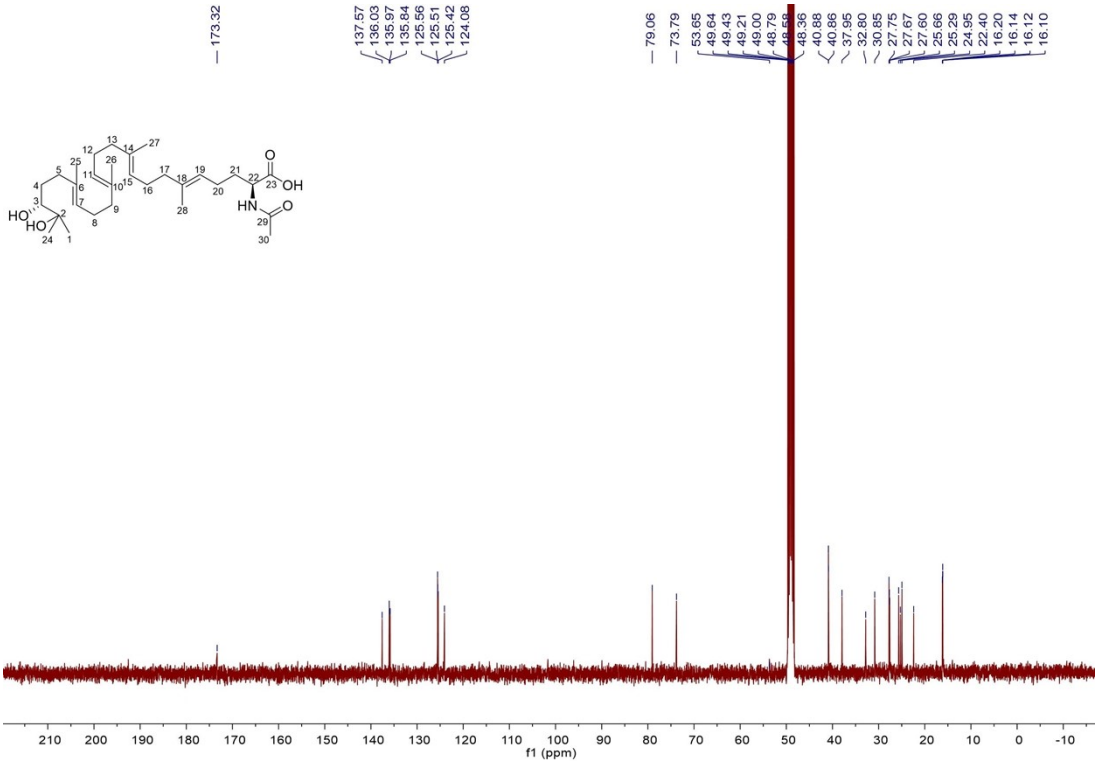

Figure S42. ^{13}C NMR spectrum of **7** in methanol-d_4 (100 MHz).

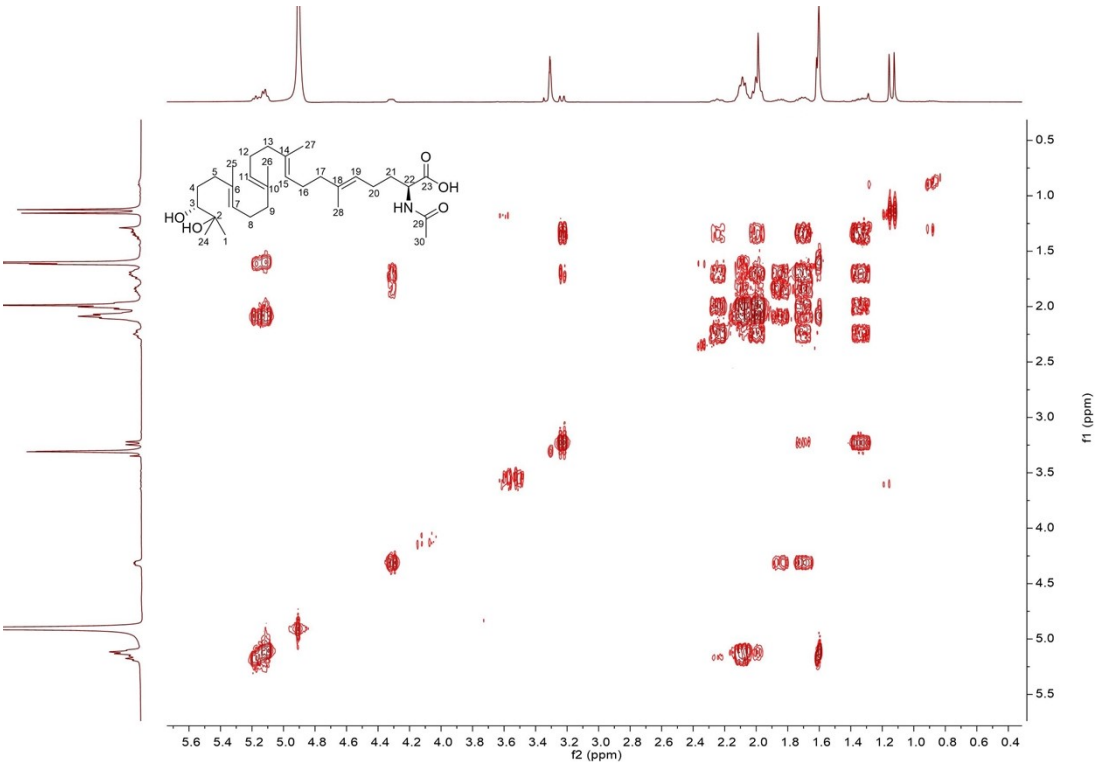

Figure S43. ^{1}H-^{1}H COSY spectrum of **7** in methanol-d_4.

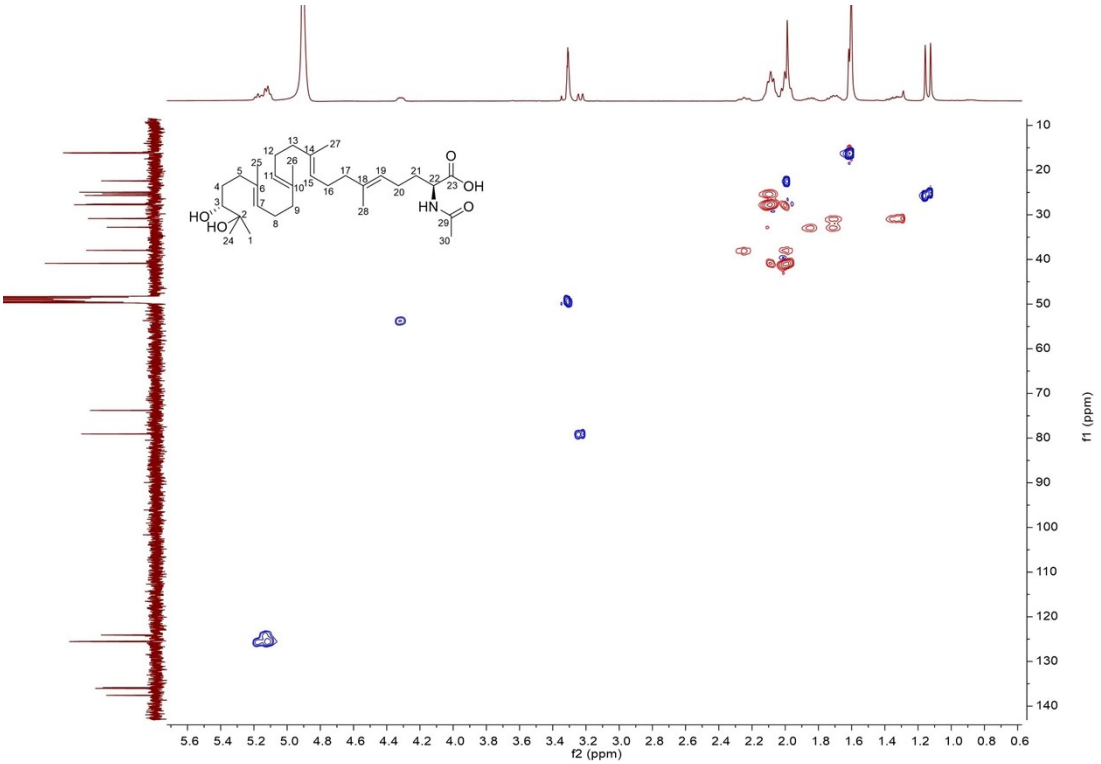

Figure S44. HSQC spectrum of **7** in methanol-d_4.

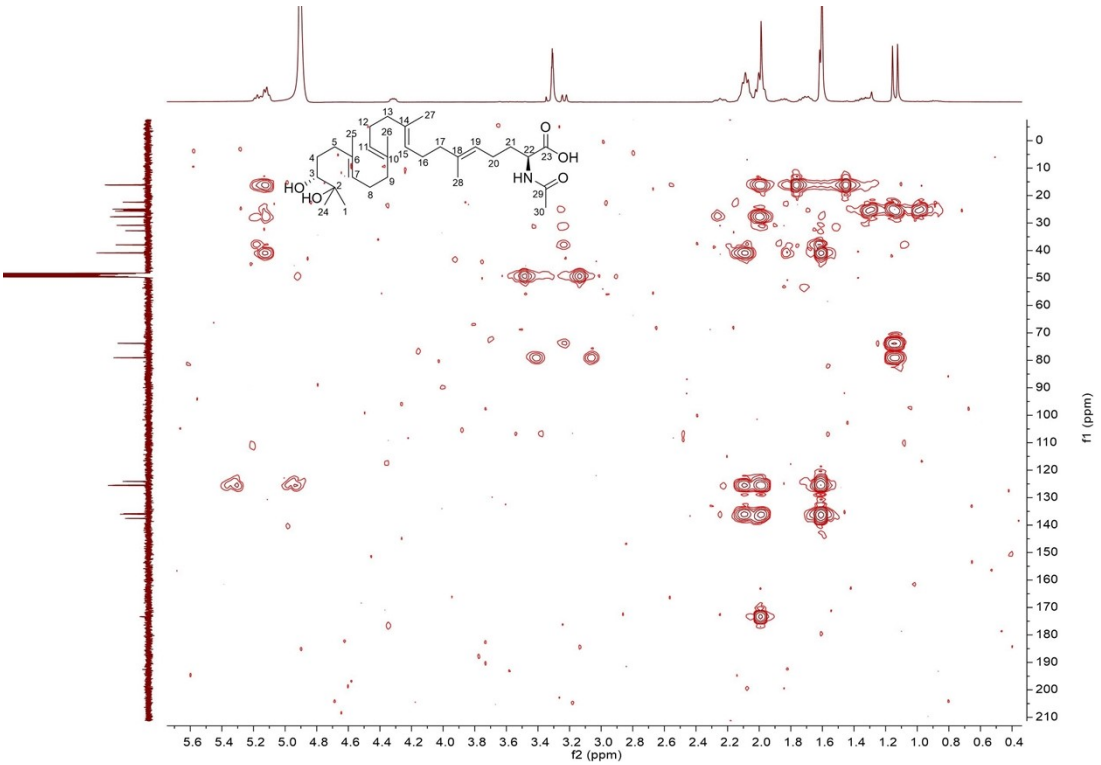

Figure S45. HMBC spectrum of **7** in methanol-d_4.

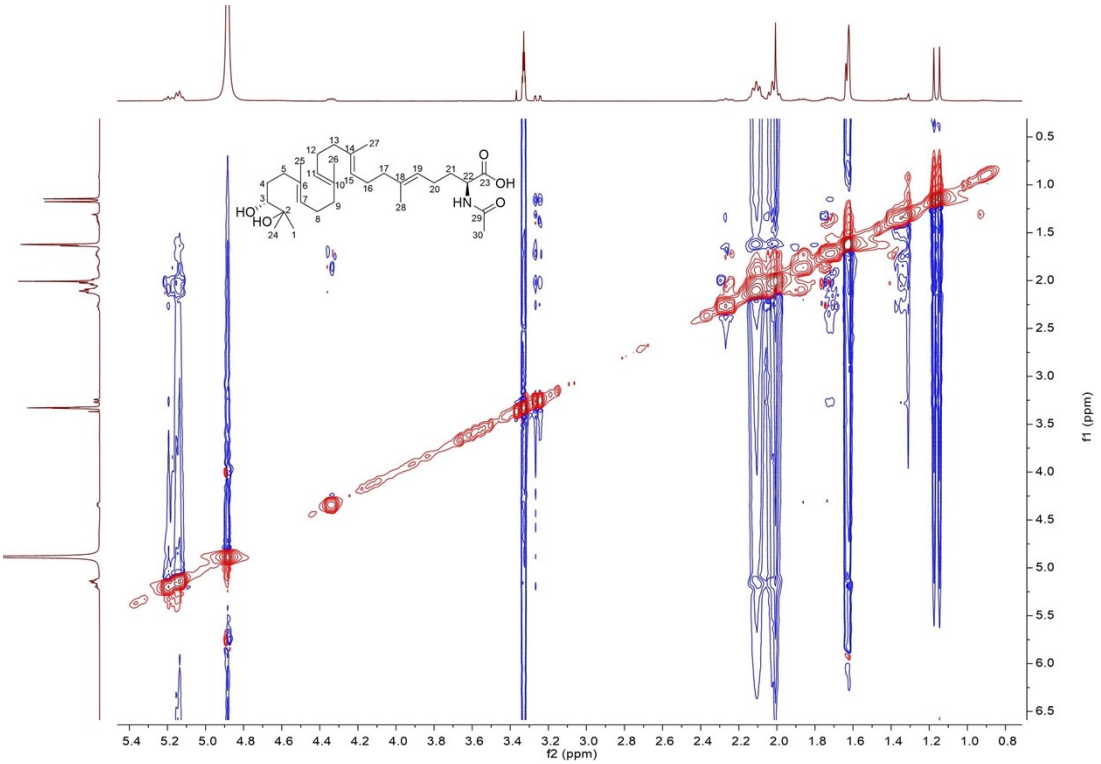

Figure S46. ROESY spectrum of **7** in methanol-d_4.

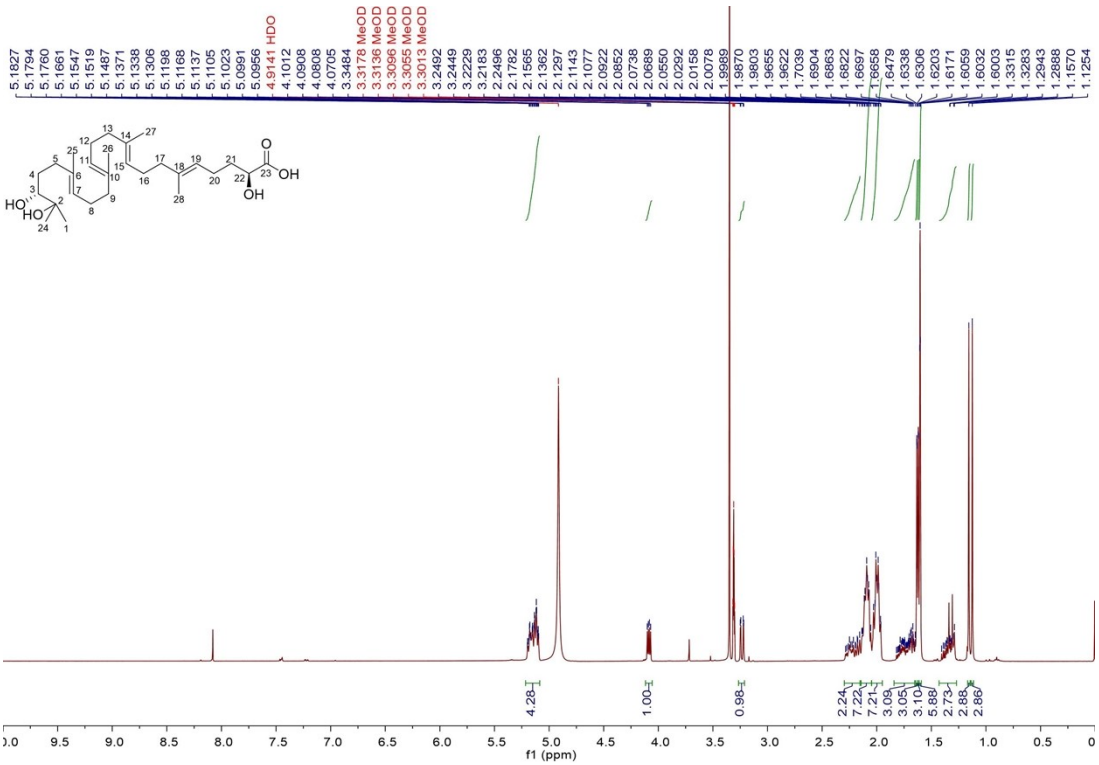

Figure S47. ^{1}H NMR spectrum of **8** in methanol-d_4 (400 MHz).

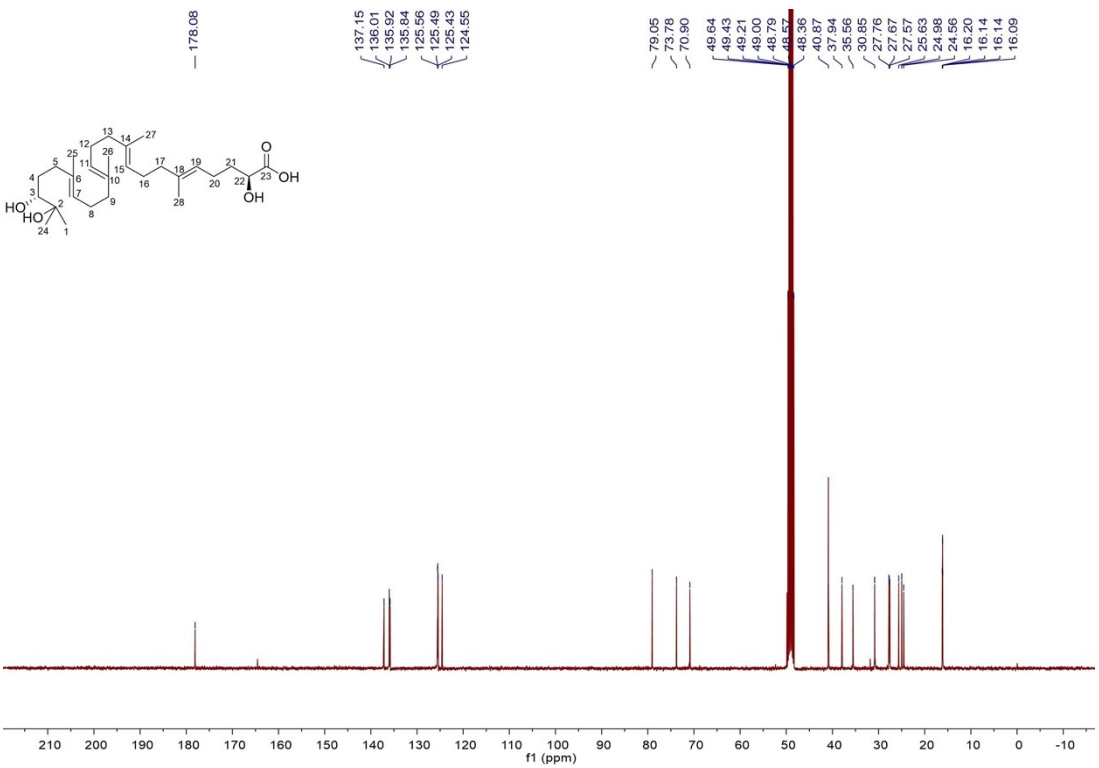

Figure S48. ^{13}C NMR spectrum of **8** in methanol-d_4 (100 MHz).

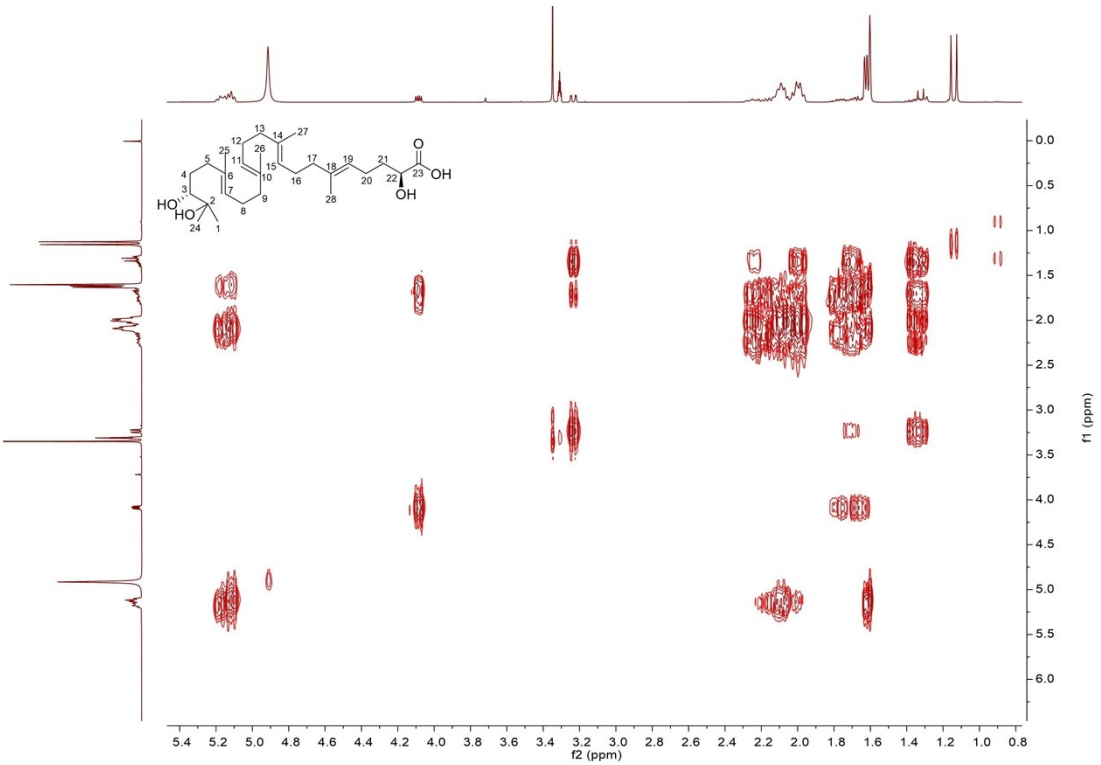

Figure S49. ^{1}H-^{1}H COSY spectrum of **8** in methanol-d_4.

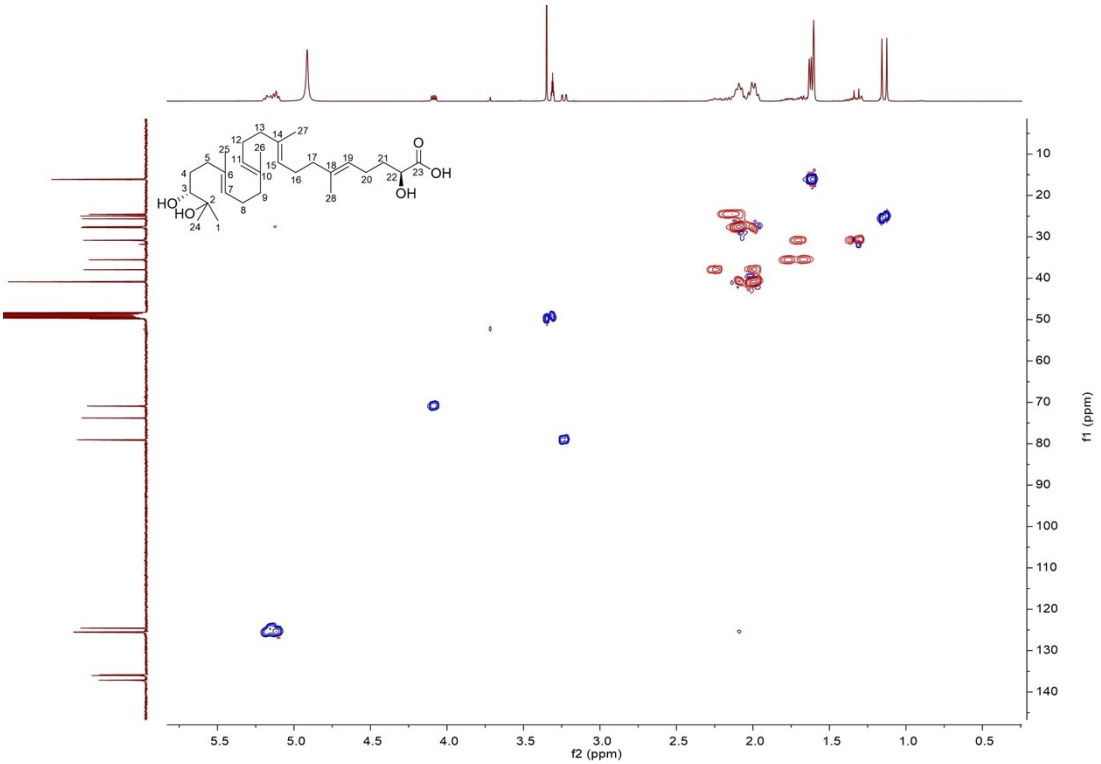

Figure S50. HSQC spectrum of **8** in methanol-d_4.

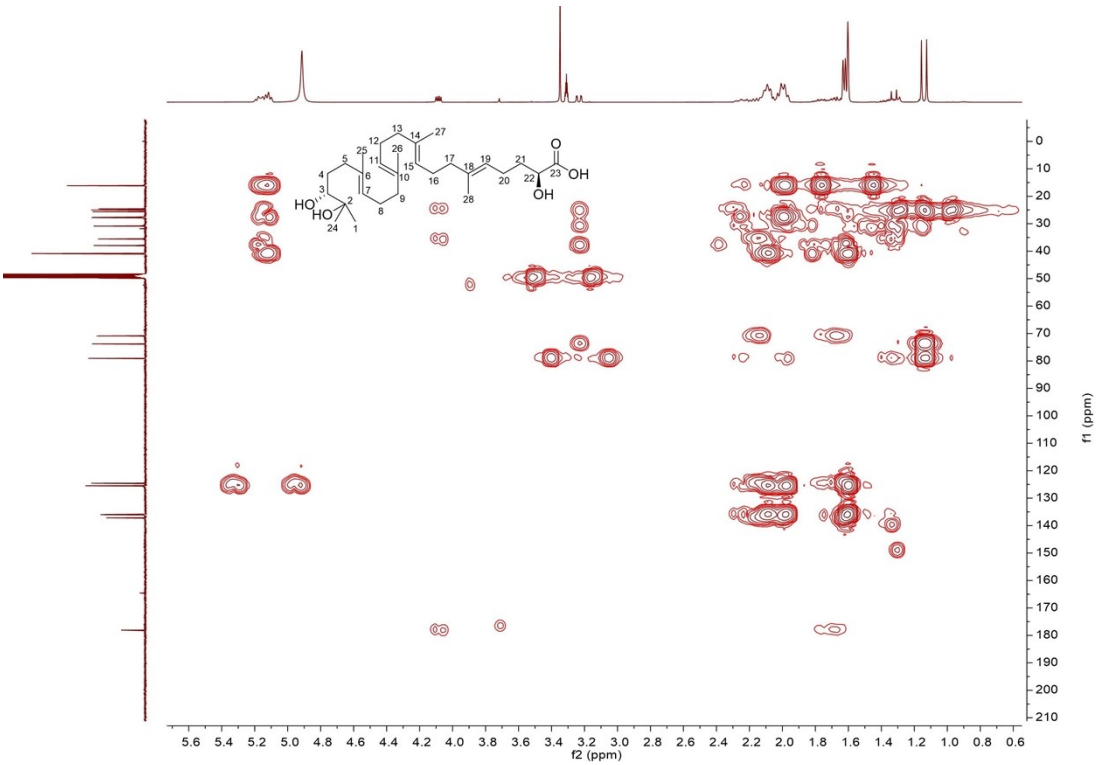

Figure S51. HMBC spectrum of **8** in methanol-d_4.

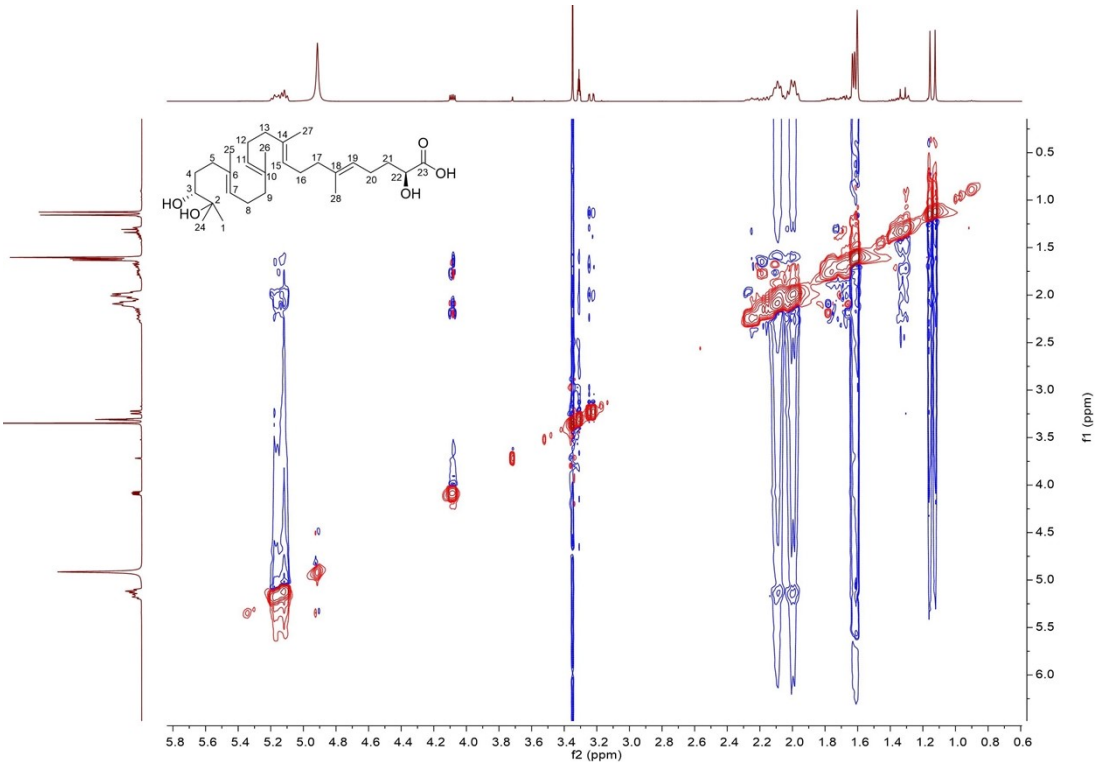

Figure S52. ROESY spectrum of **8** in methanol-d_4.

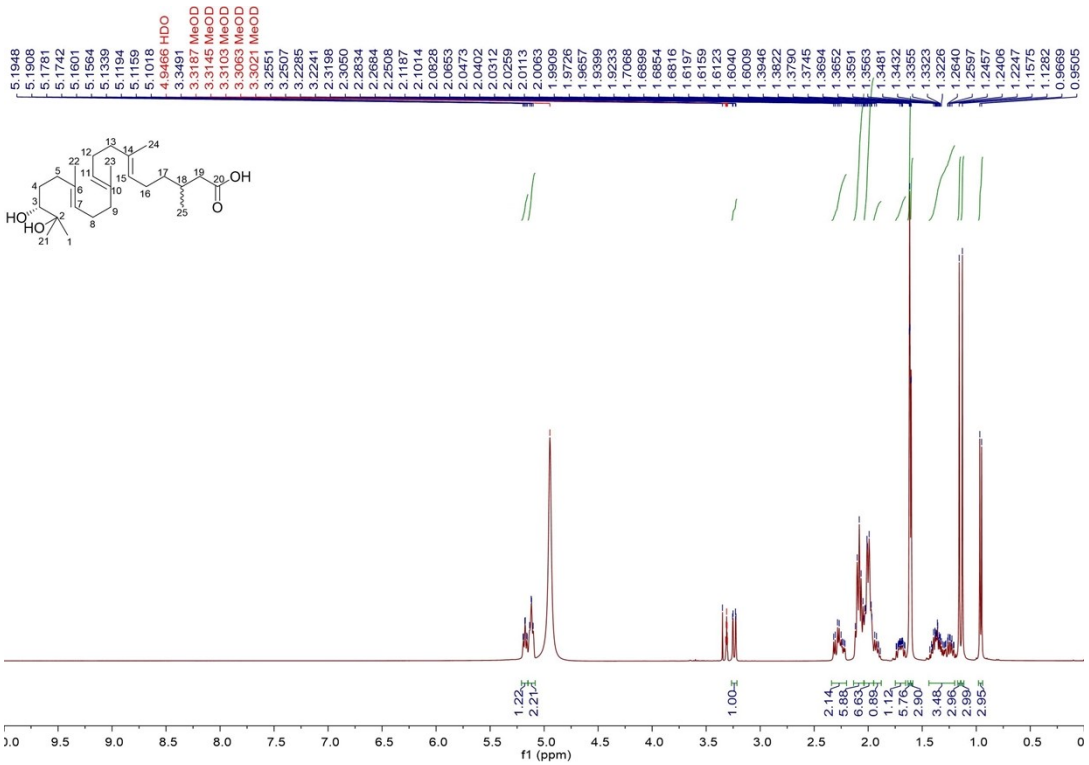

Figure S53. ^{1}H NMR spectrum of **9** in methanol-d_4 (400 MHz).

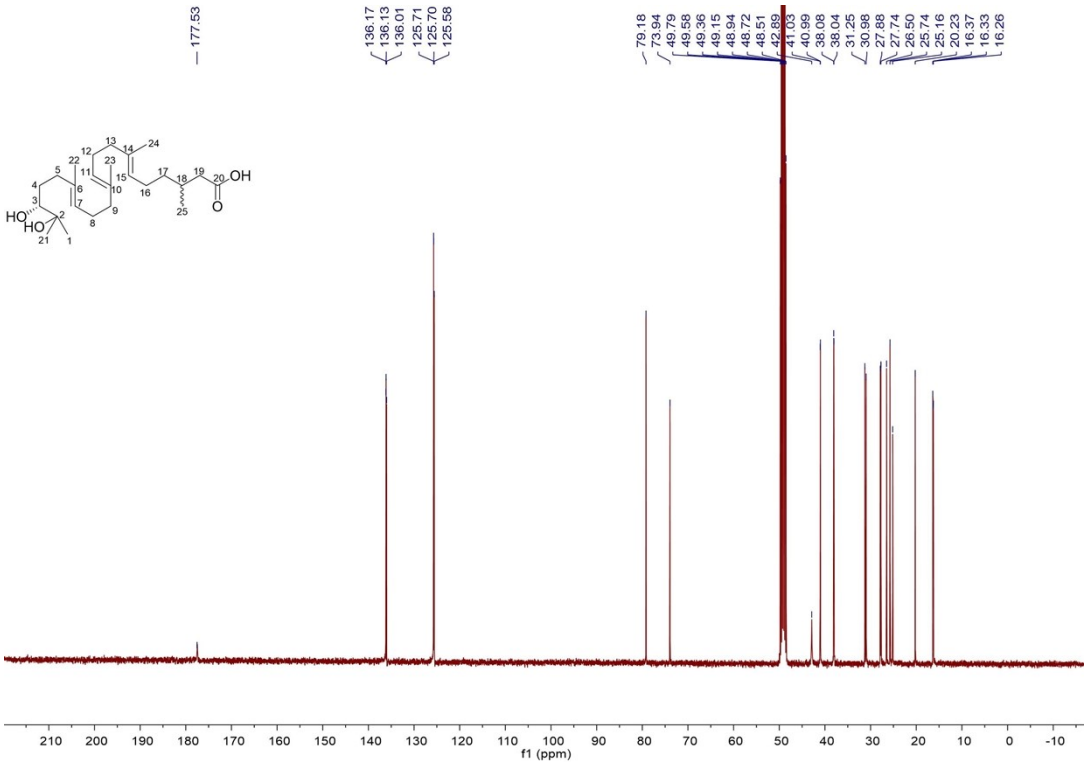

Figure S54. ^{13}C NMR spectrum of **9** in methanol-d_4 (100 MHz).

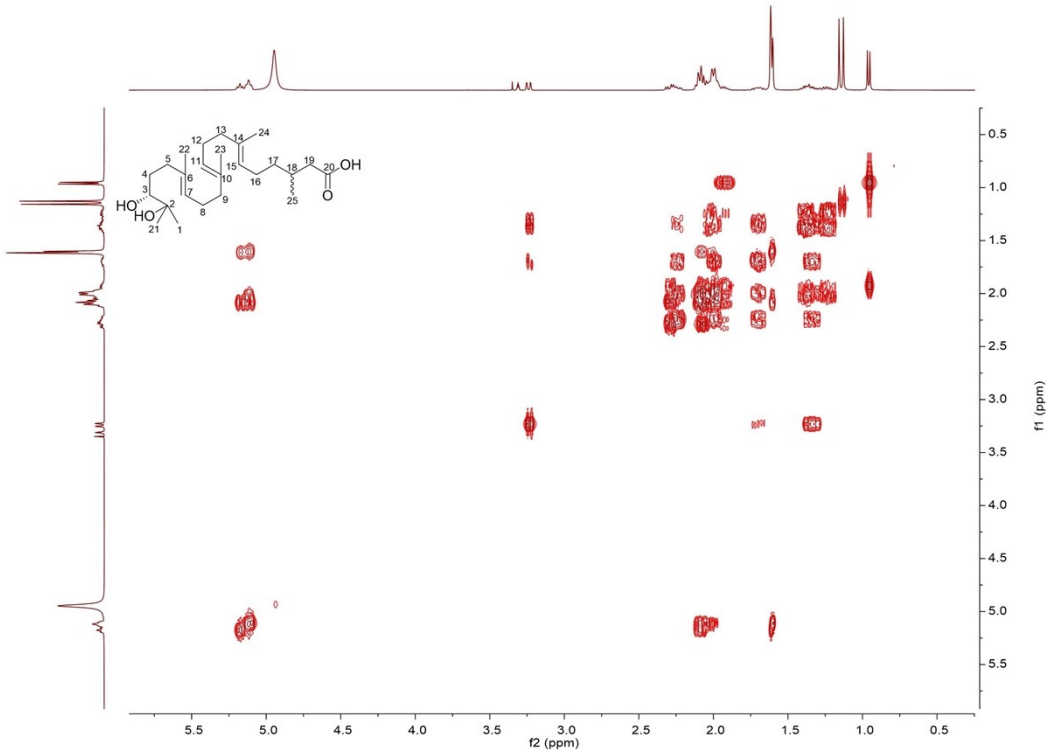

Figure S55. ^{1}H-^{1}H COSY spectrum of **9** in methanol-d_4.

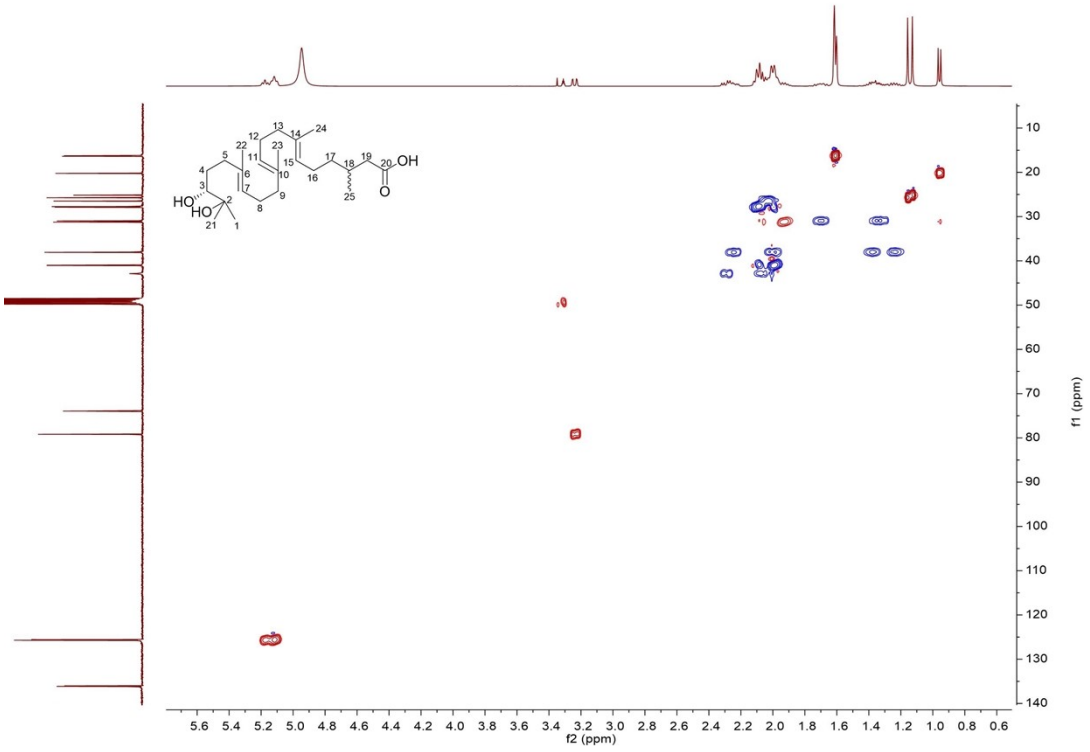

Figure S56. HSQC spectrum of **9** in methanol-d_4.

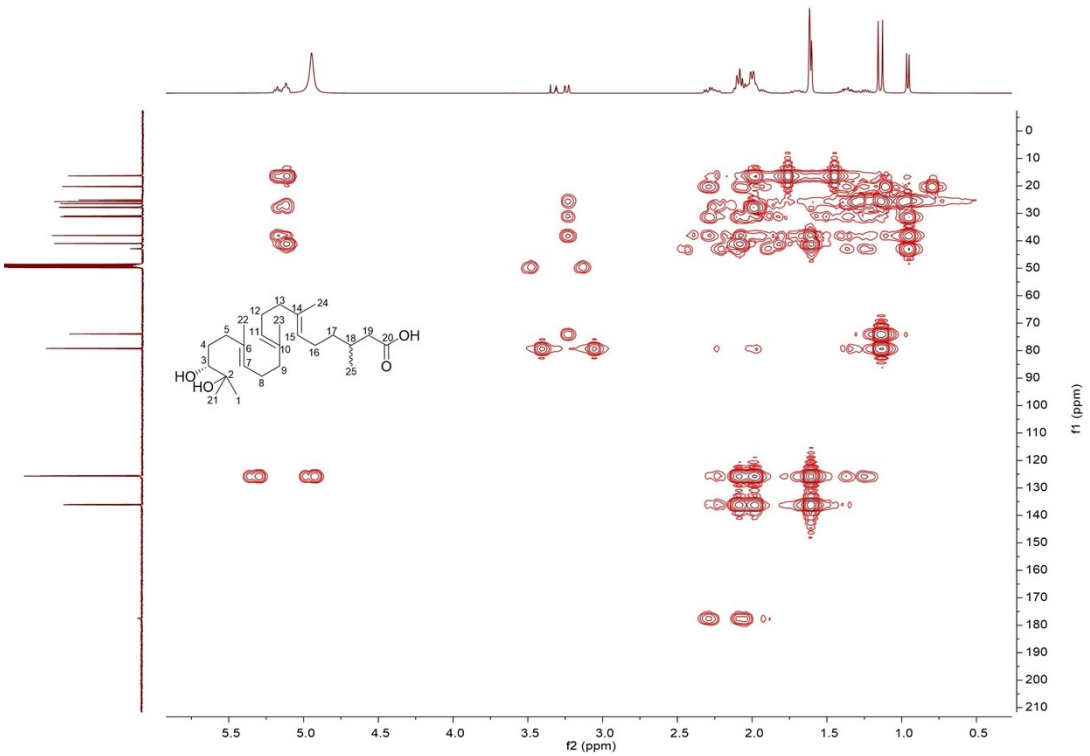

Figure S57. HMBC spectrum of **9** in methanol-d_4.

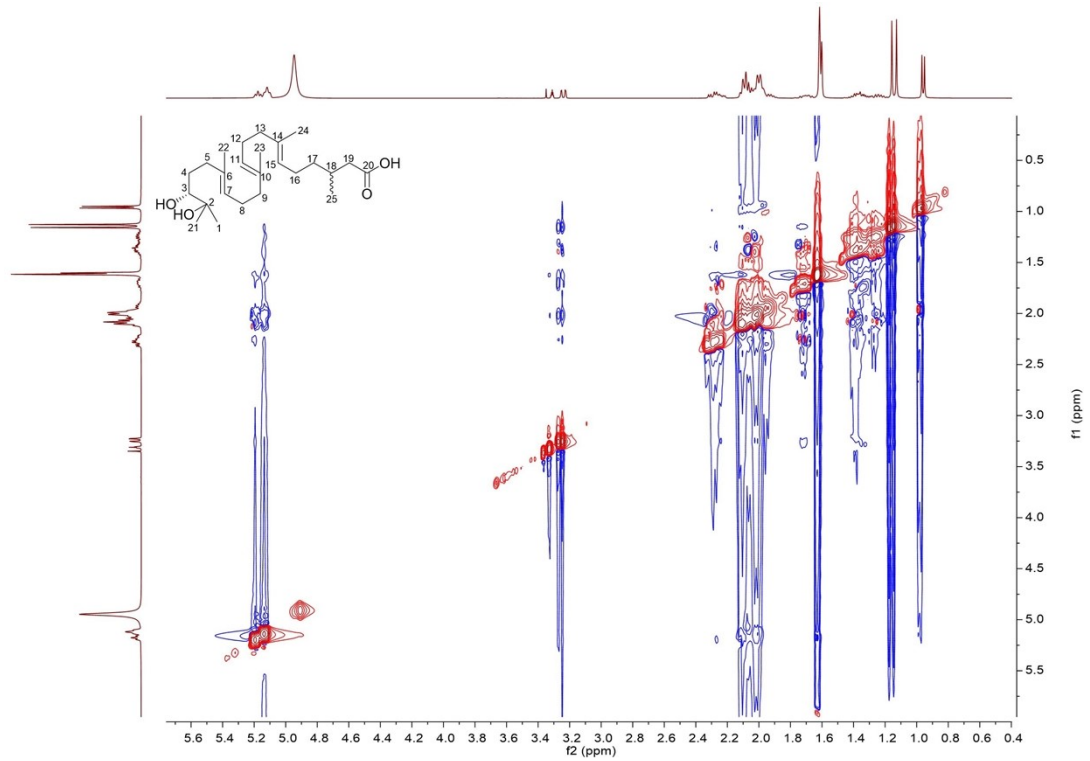

Figure S58. ROESY spectrum of **9** in methanol-d_4.

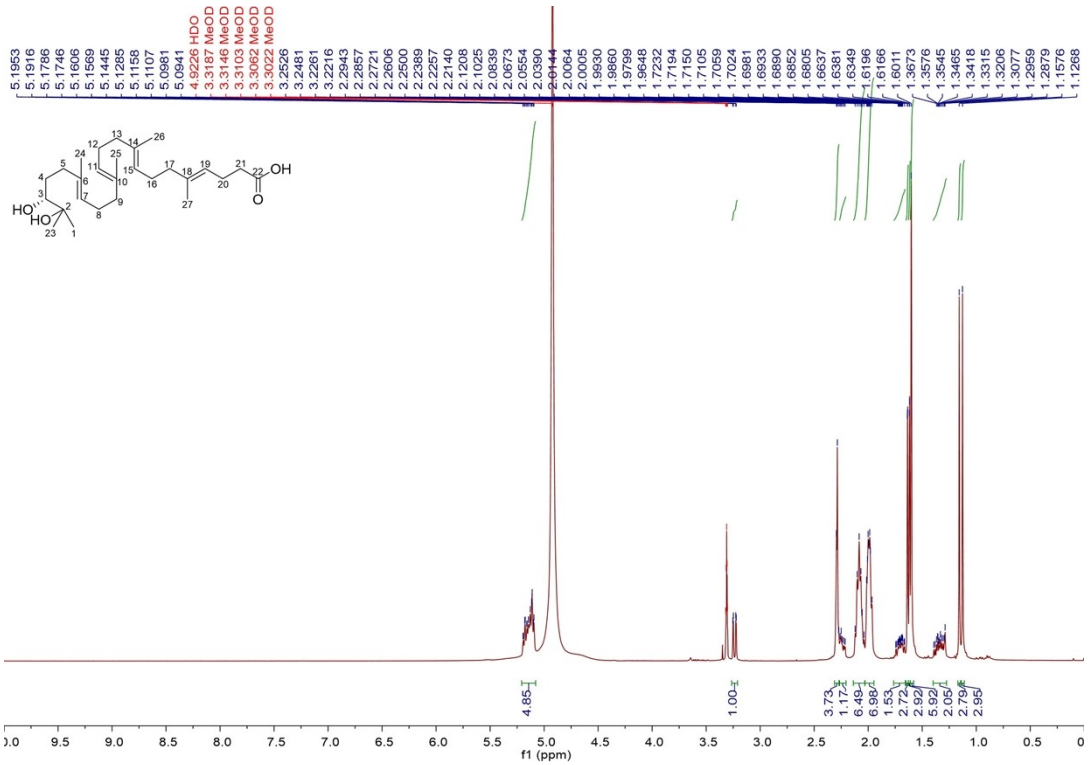

Figure S59. ^{1}H NMR spectrum of **10** in methanol-d_4 (400 MHz).

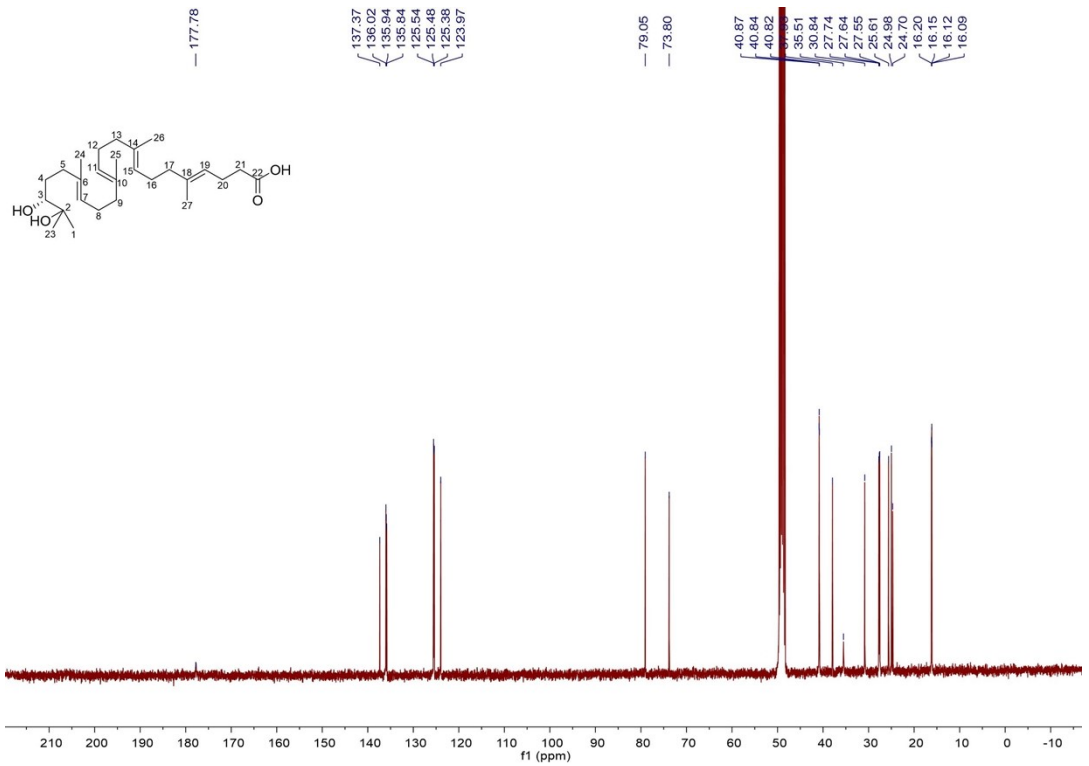

Figure S60. ^{13}C NMR spectrum of **10** in methanol-d_4 (100 MHz).

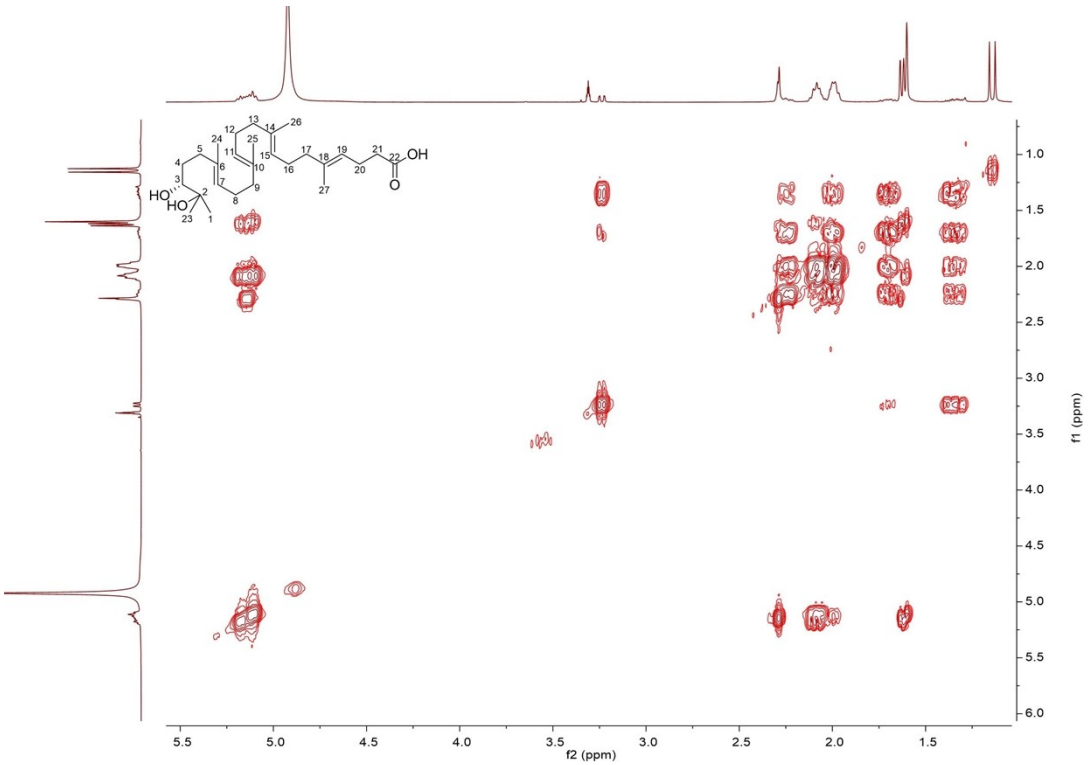

Figure S61. ^{1}H-^{1}H COSY spectrum of **10** in methanol-d_4.

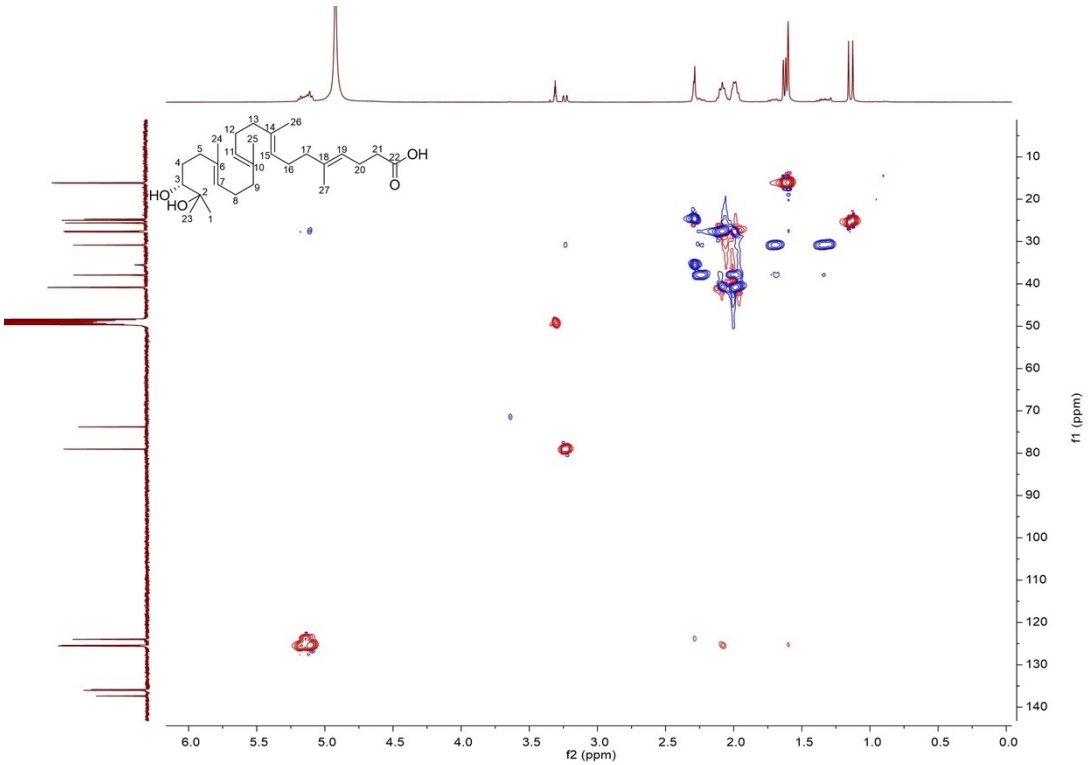

Figure S62. HSQC spectrum of **10** in methanol-d_4.

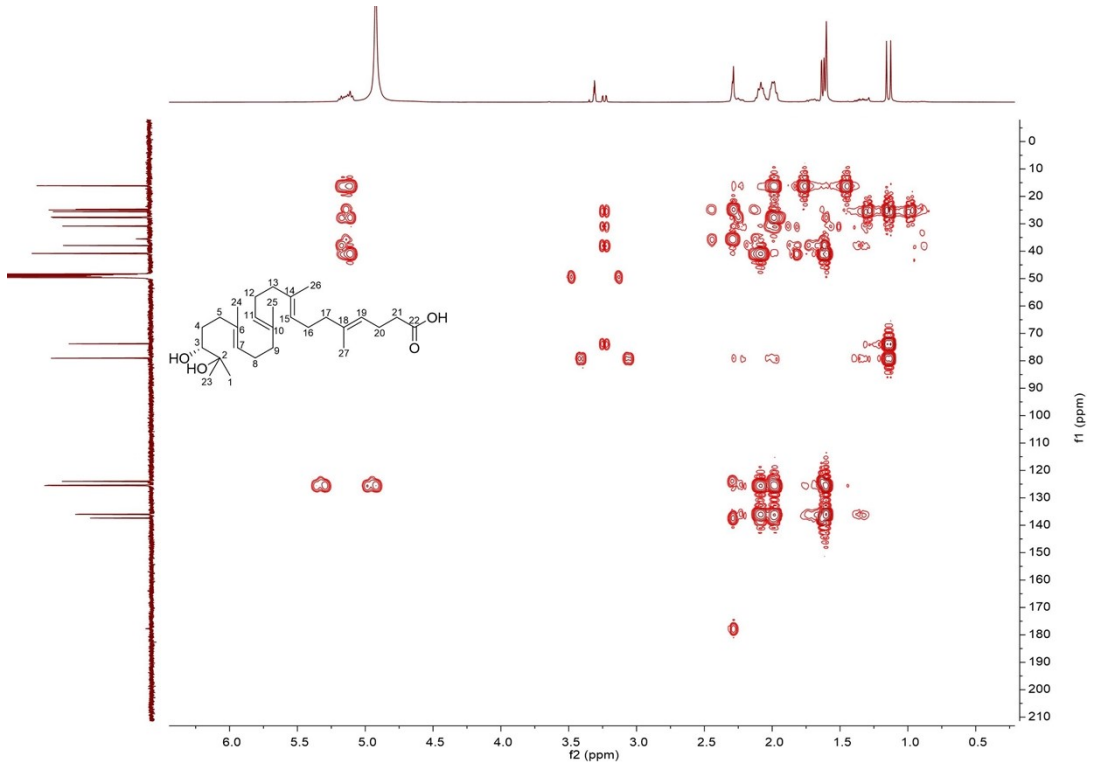

Figure S63. HMBC spectrum of **10** in methanol-d_4.

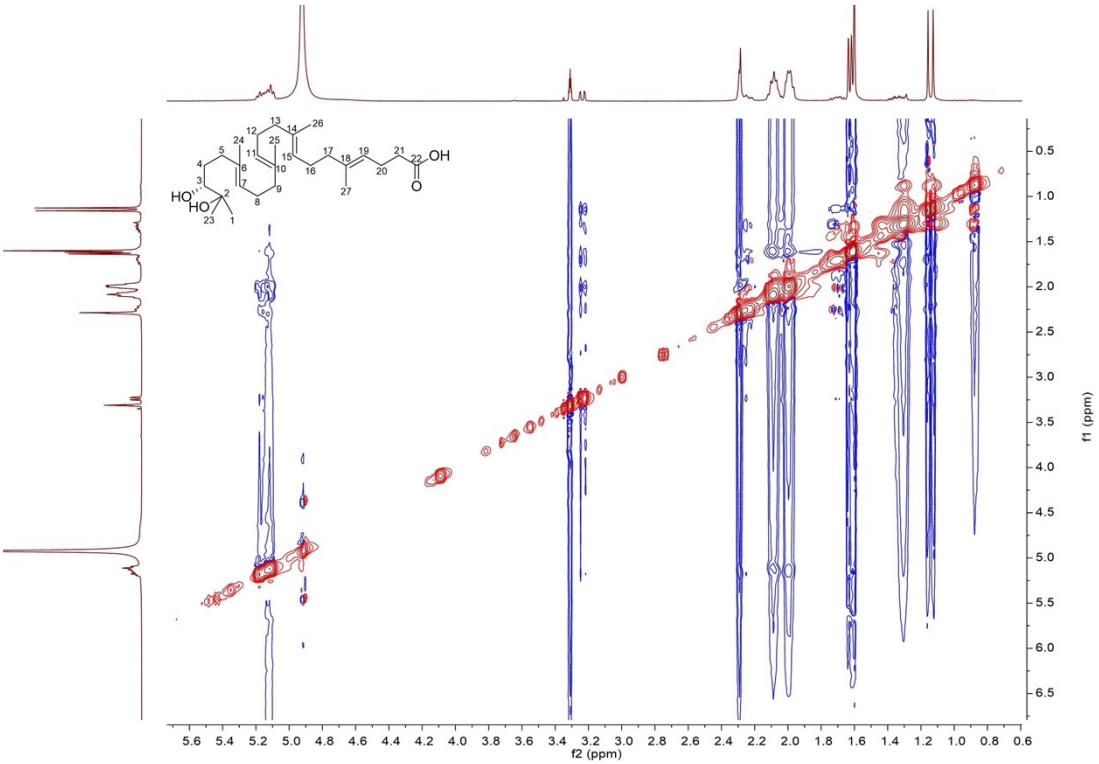

Figure S64. ROESY spectrum of **10** in methanol-d_4.

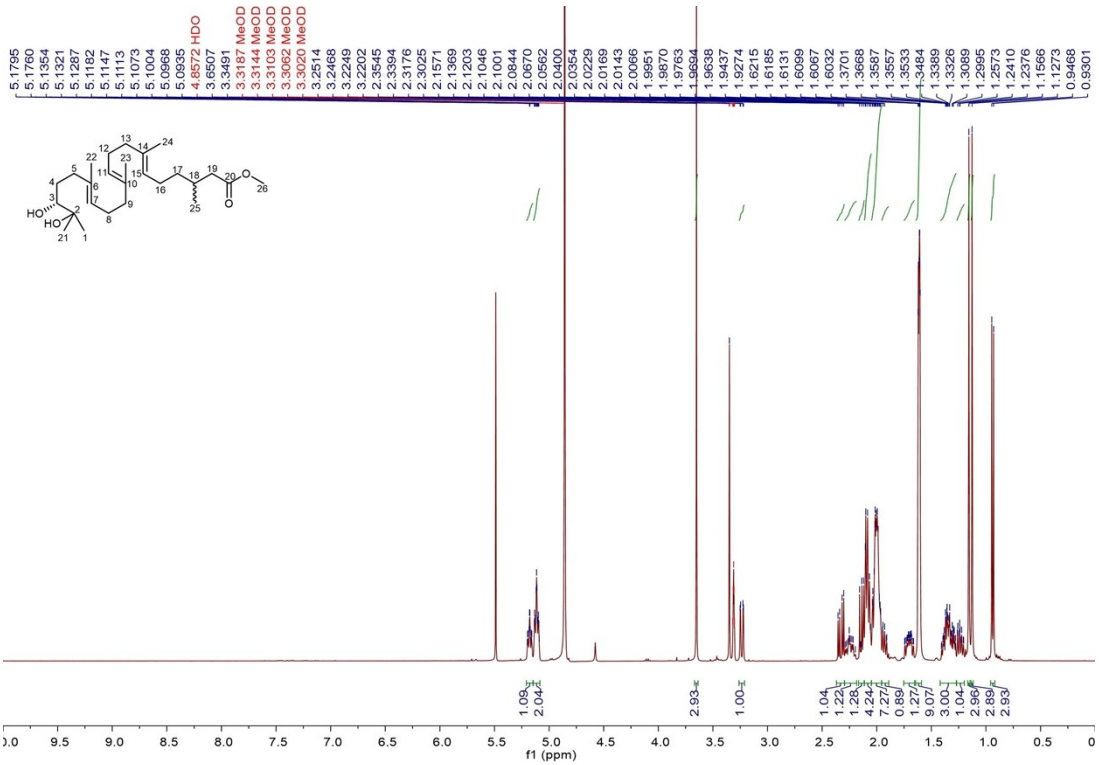

Figure S65. ^{1}H NMR spectrum of **9a** in methanol-d_4 (400 MHz).

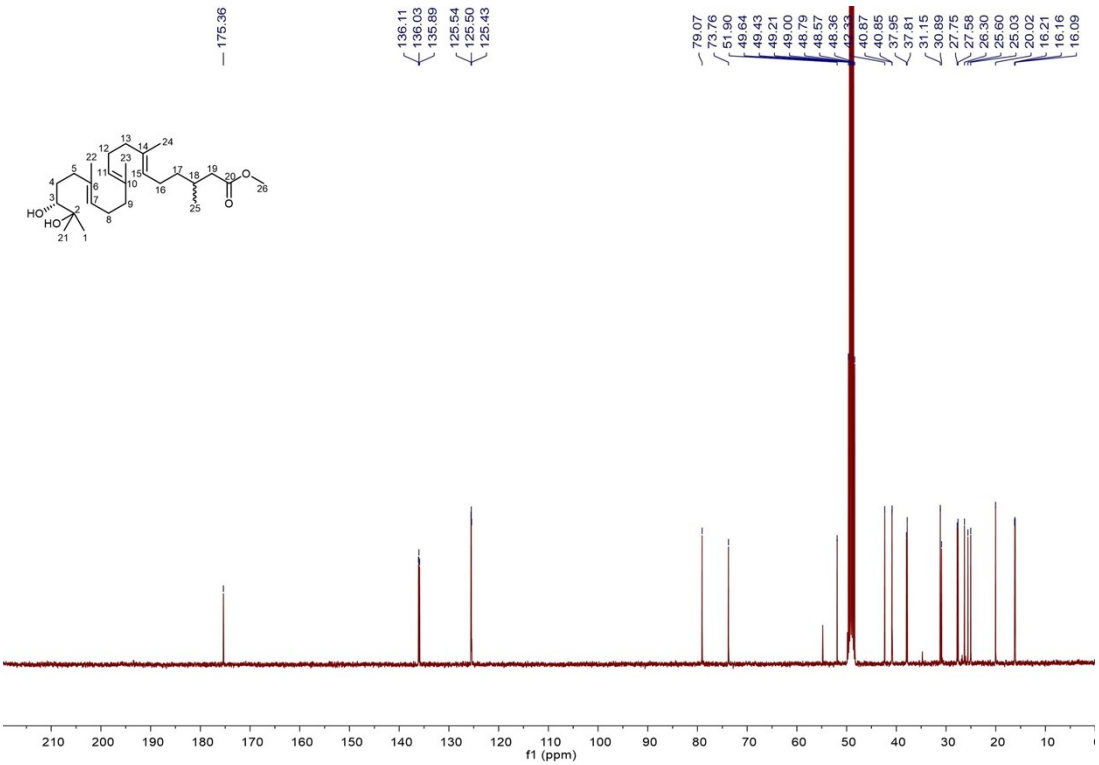

Figure S66. ^{13}C NMR spectrum of **9a** in methanol-d_4 (100 MHz).

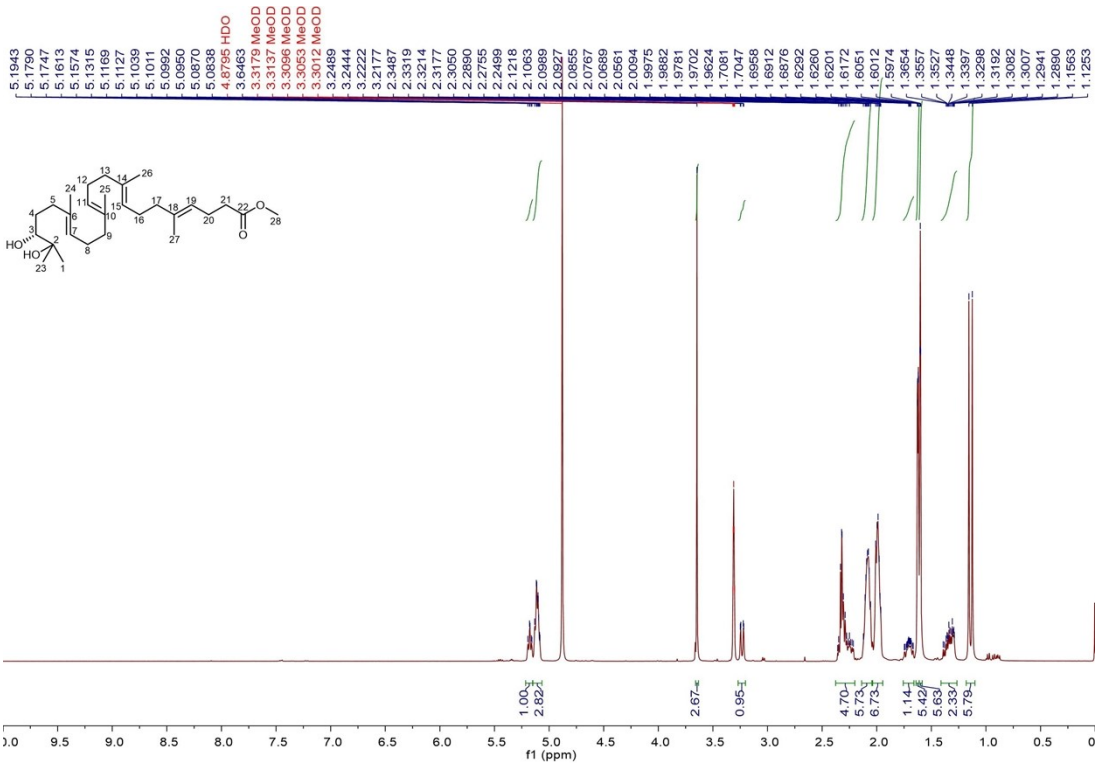

Figure S67. ^{1}H NMR spectrum of **10b** in methanol-d_4 (400 MHz).

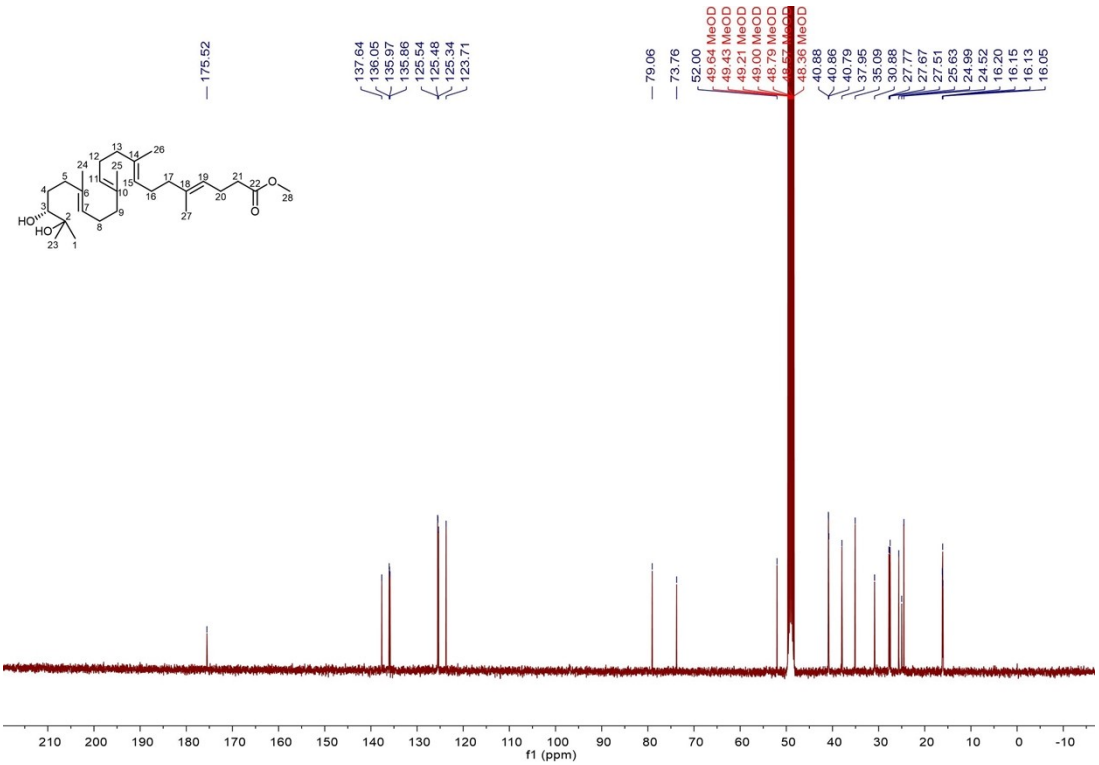

Figure S68. ^{13}C NMR spectrum of **10b** in methanol-d_4 (100 MHz).

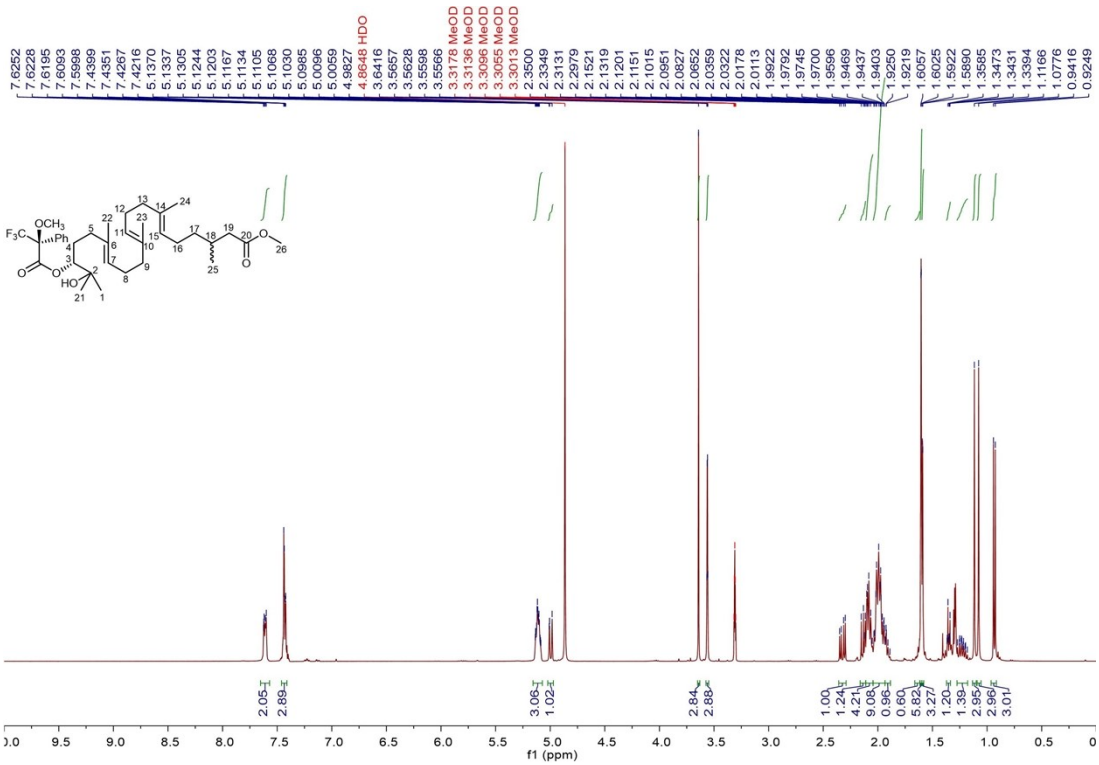

Figure S69. ^{1}H NMR spectrum of **9b** in methanol-d_4 (400 MHz).

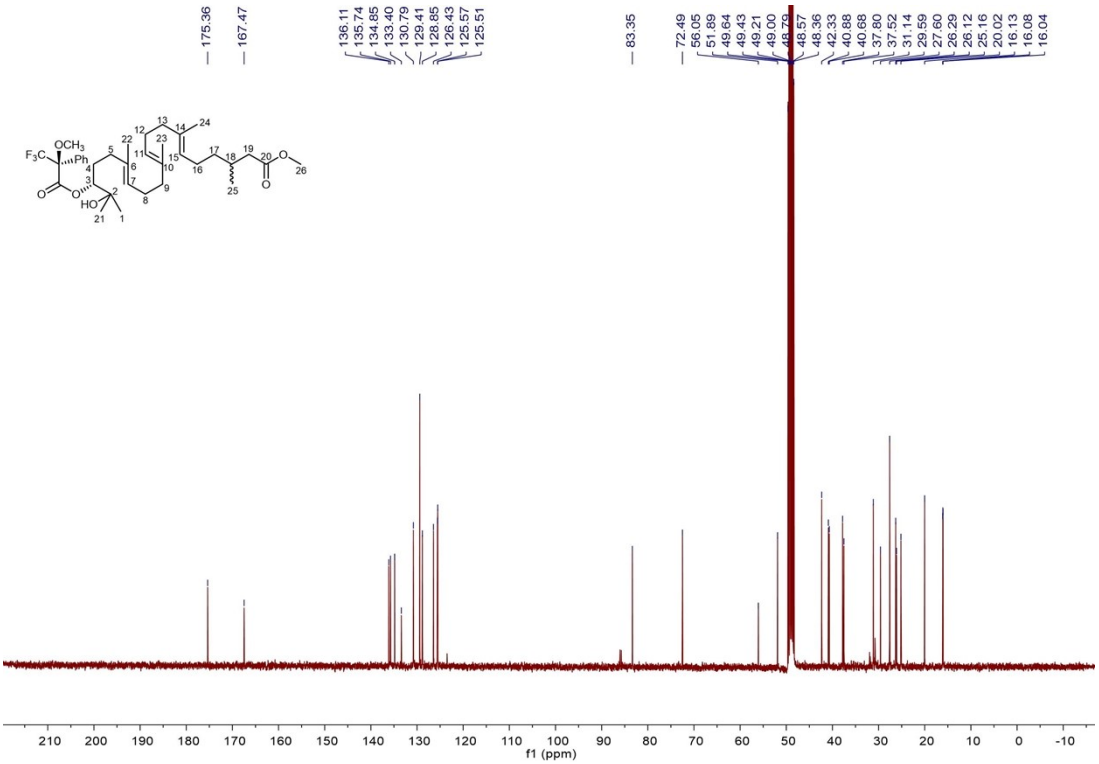

Figure S70. ^{13}C NMR spectrum of **9b** in methanol-d_4 (100 MHz).

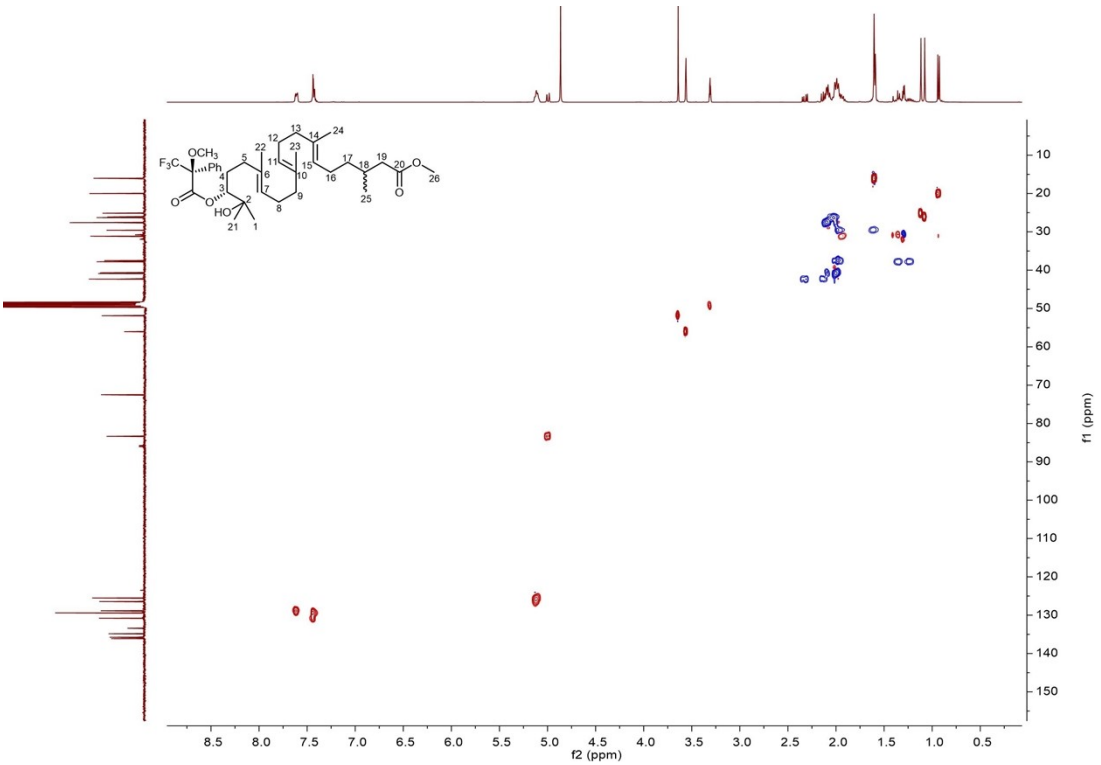

Figure S71. HSQC spectrum of **9b** in methanol-d_4.

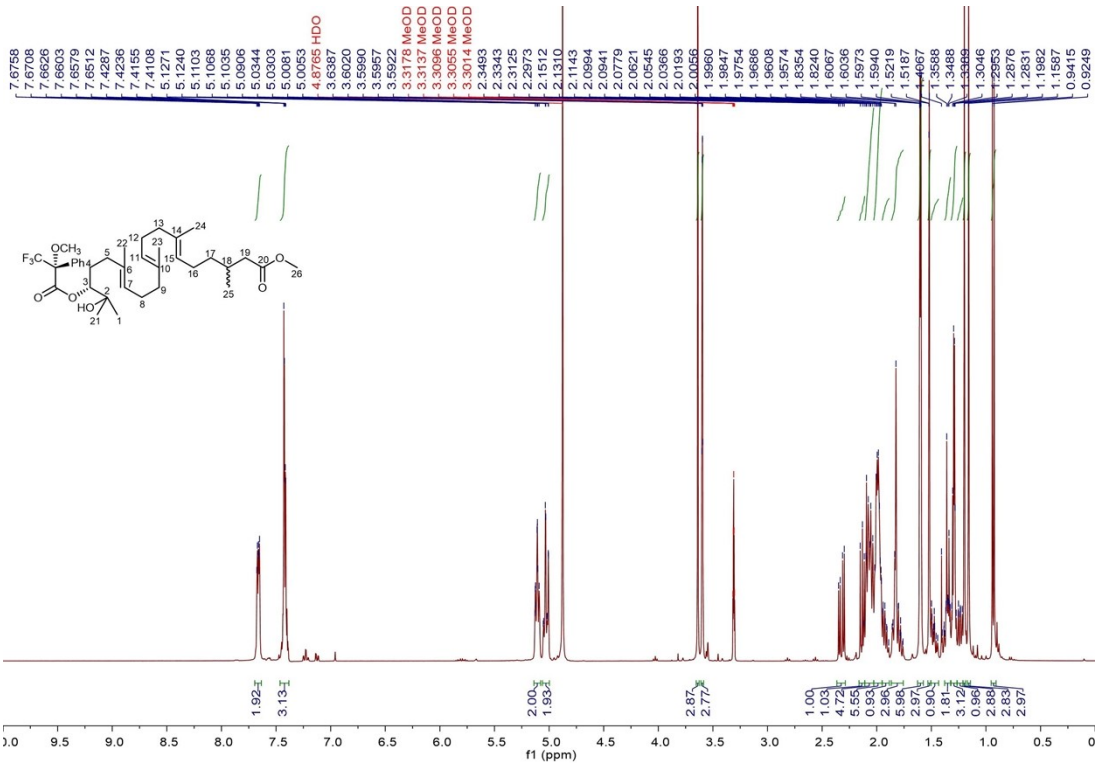

Figure S72. ^{1}H NMR spectrum of **9c** in methanol-d_4 (400 MHz).

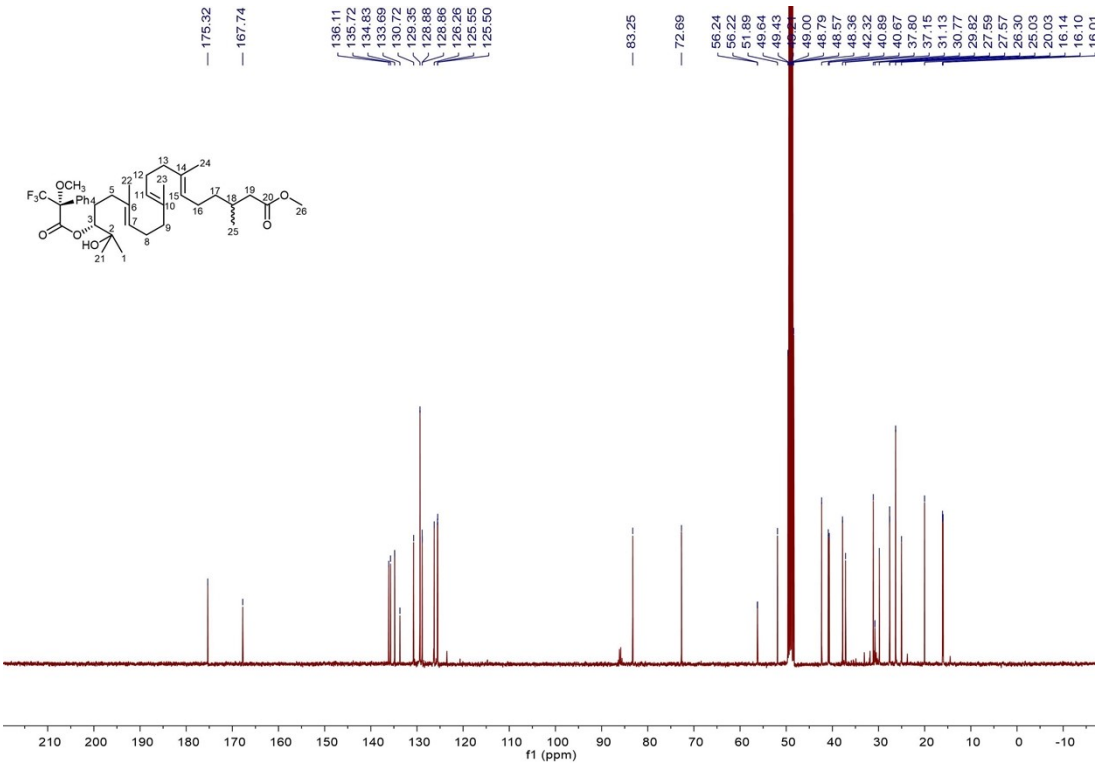

Figure S73. ^{13}C NMR spectrum of **9c** in methanol-d_4 (100 MHz).

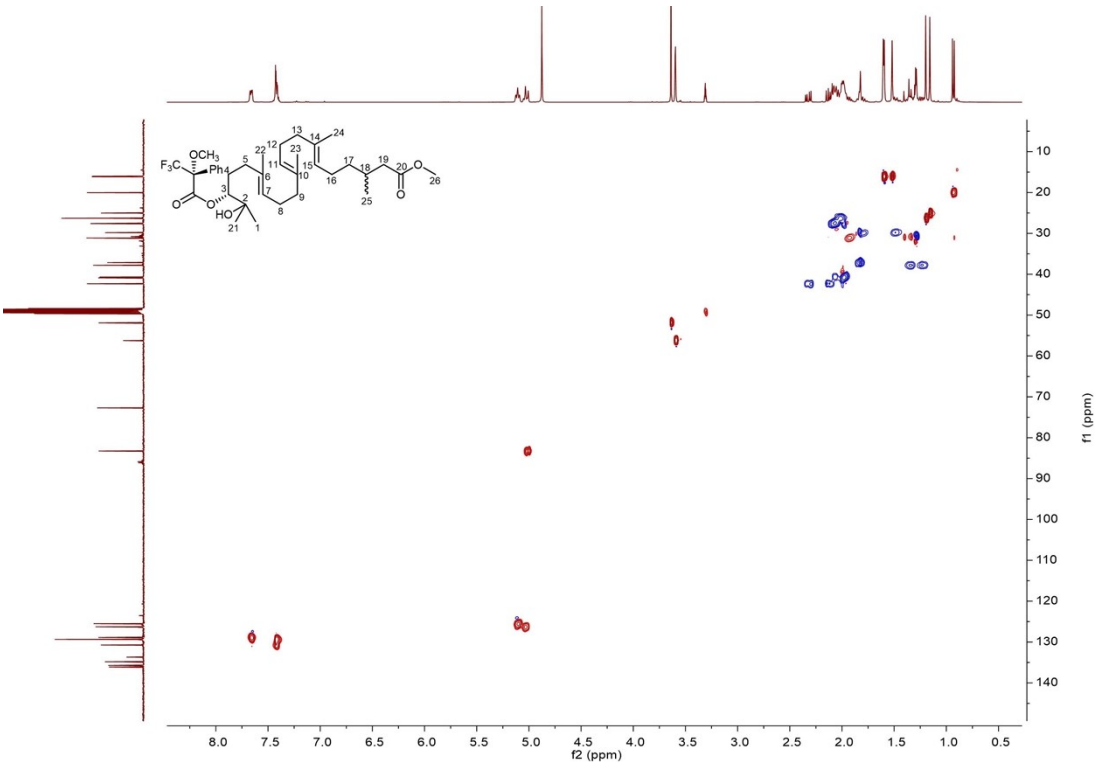

Figure S74. HSQC spectrum of **9c** in methanol-d_4.

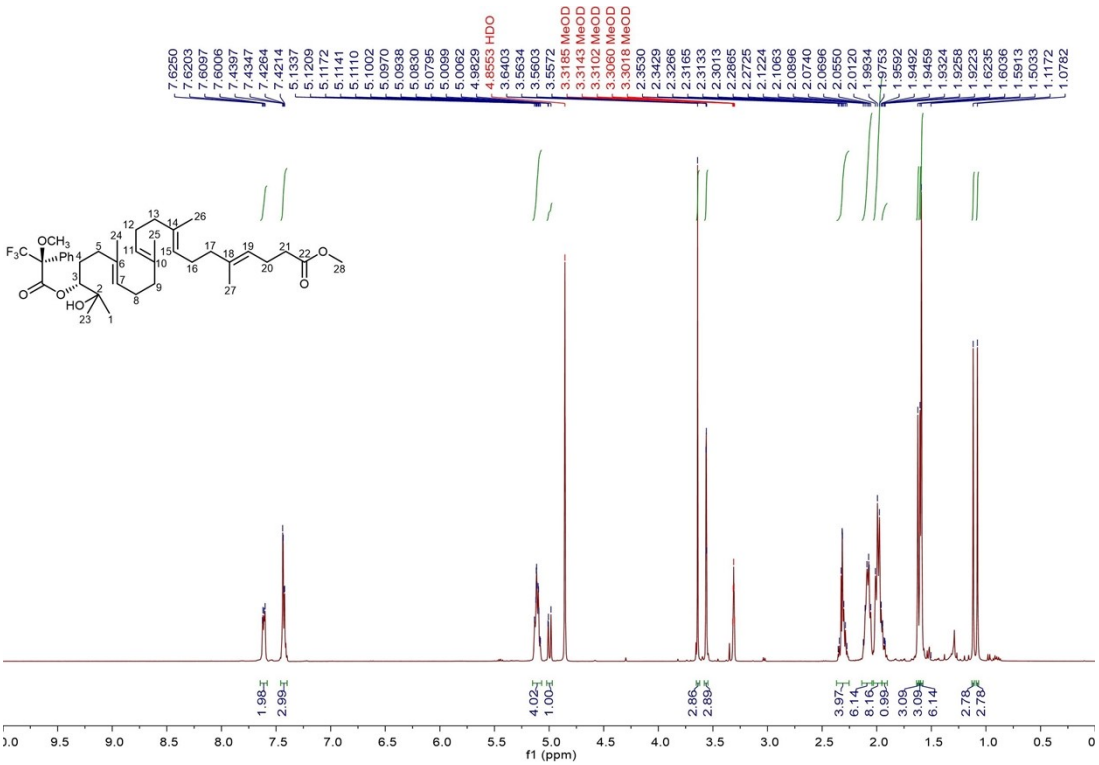

Figure S75. ^{1}H NMR spectrum of **10c** in methanol-d_4 (400 MHz).

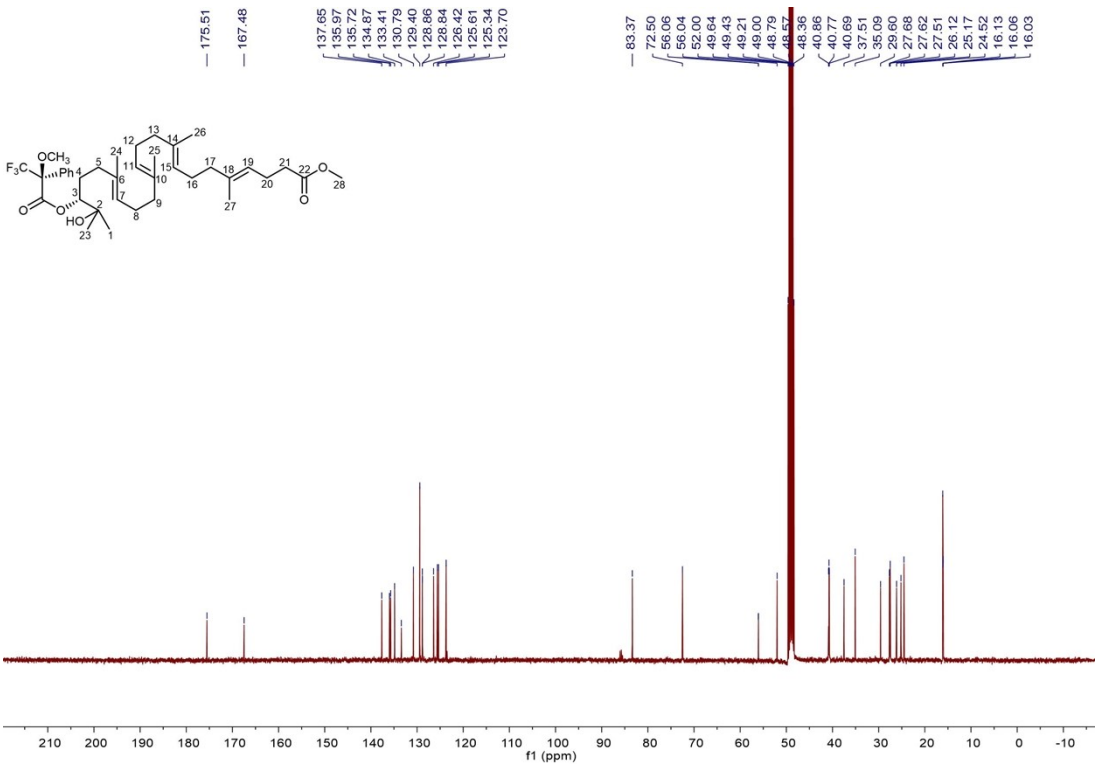

Figure S76. ^{13}C NMR spectrum of **10c** in methanol-d_4 (100 MHz).

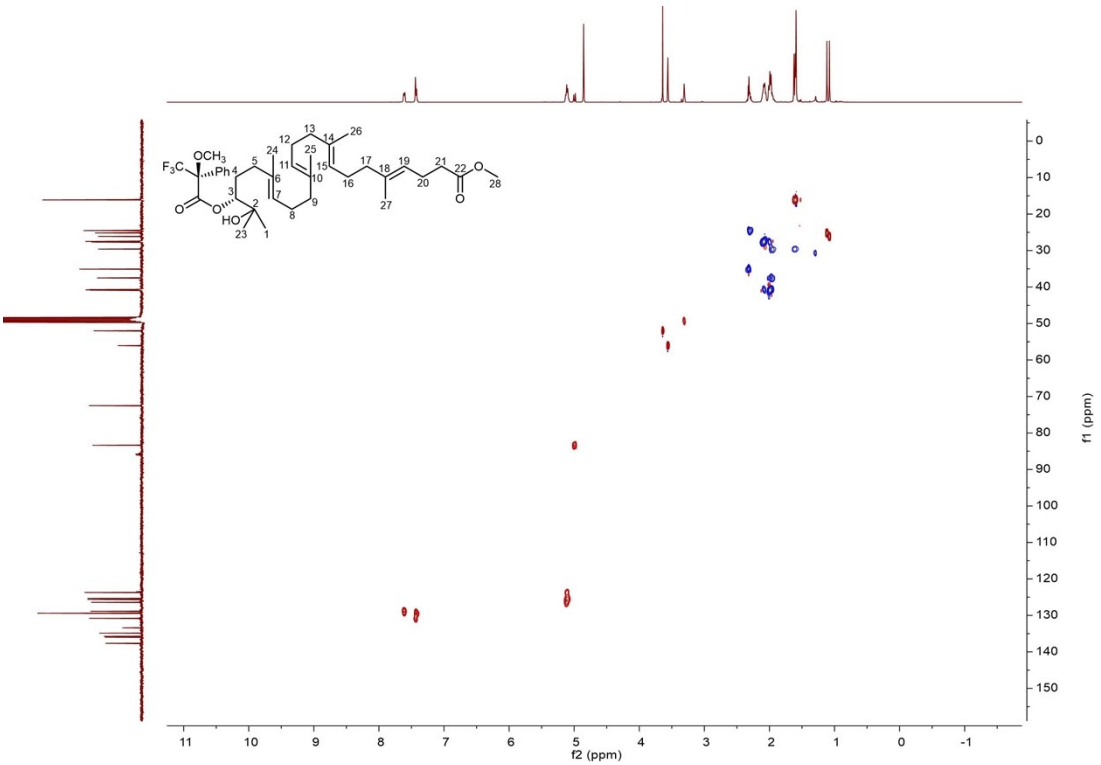

Figure S77. HSQC spectrum of **10c** in methanol-d_4.

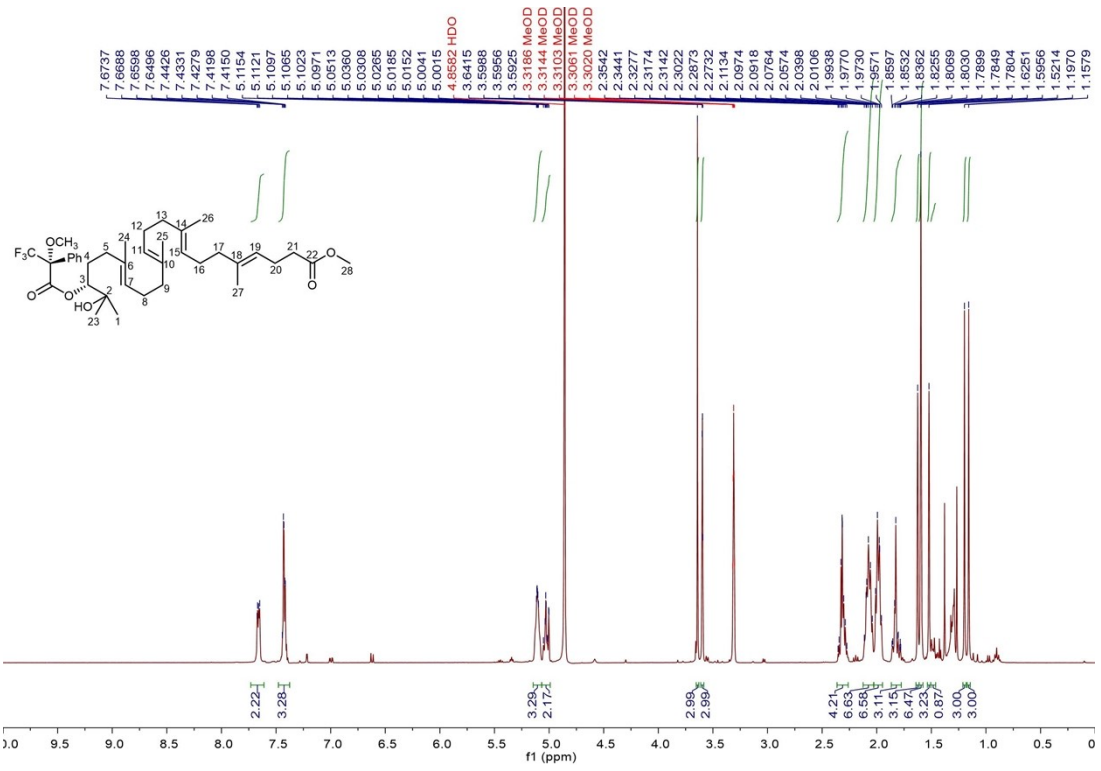

Figure S78. ^{1}H NMR spectrum of **10d** in methanol-d_4 (400 MHz).

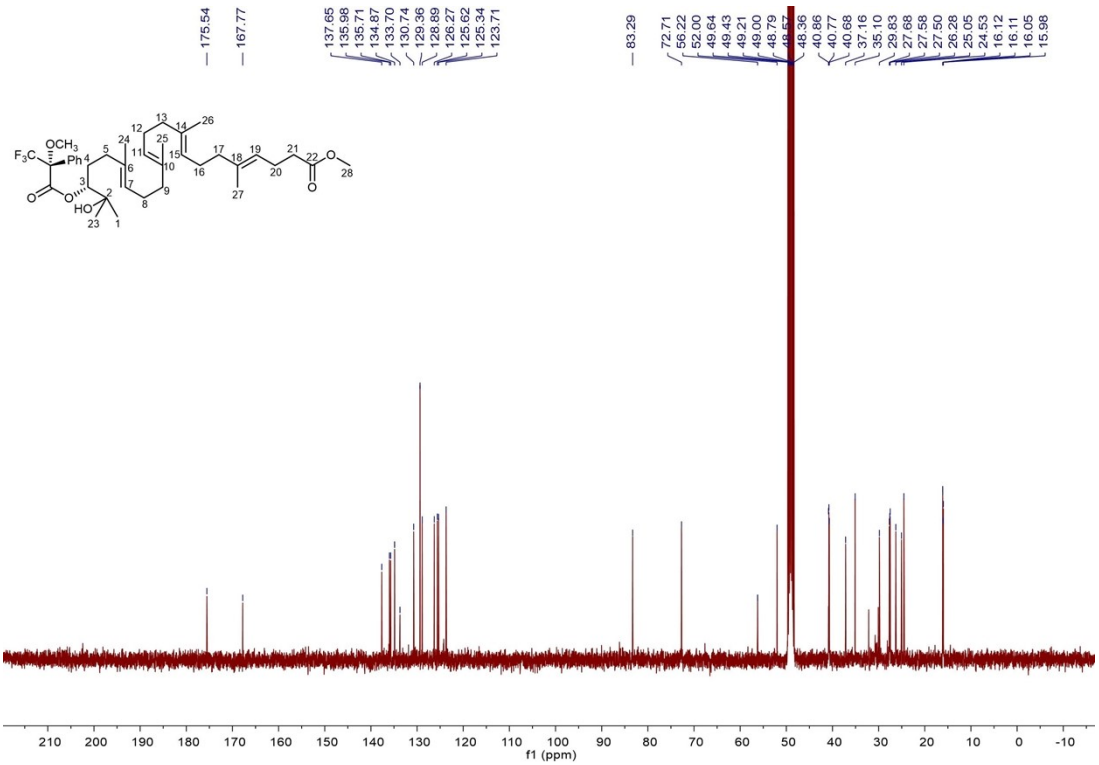

Figure S79. ^{13}C NMR spectrum of **10d** in methanol-d_4 (100 MHz).

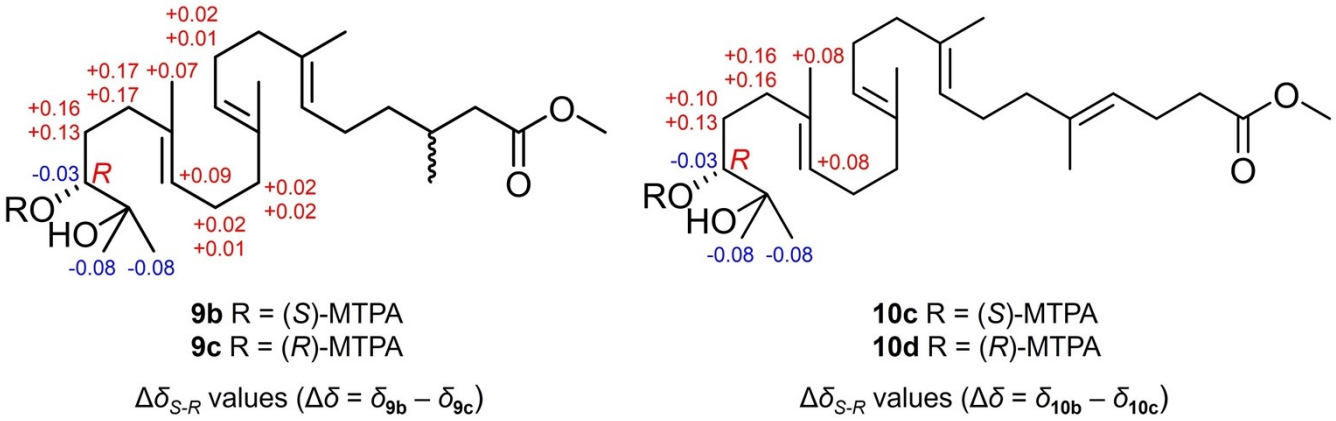

9b R = (*S*)-MTPA
9c R = (*R*)-MTPA

$\Delta\delta_{S\text{-}R}$ values ($\Delta\delta = \delta_{\mathbf{9b}} - \delta_{\mathbf{9c}}$)

10c R = (*S*)-MTPA
10d R = (*R*)-MTPA

$\Delta\delta_{S\text{-}R}$ values ($\Delta\delta = \delta_{\mathbf{10b}} - \delta_{\mathbf{10c}}$)

Figure S80. Absolute stereochemical determination at C3 of **9** and **10** using the modified Mosher method.

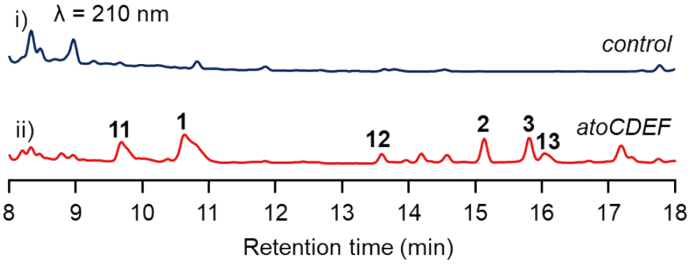

Figure S81. HPLC analysis of metabolites from *S. lividans* DLW1012 harboring the four genes *atoCDEF*. *S. lividans* SBT18 with empty pSET152 was used as a control.

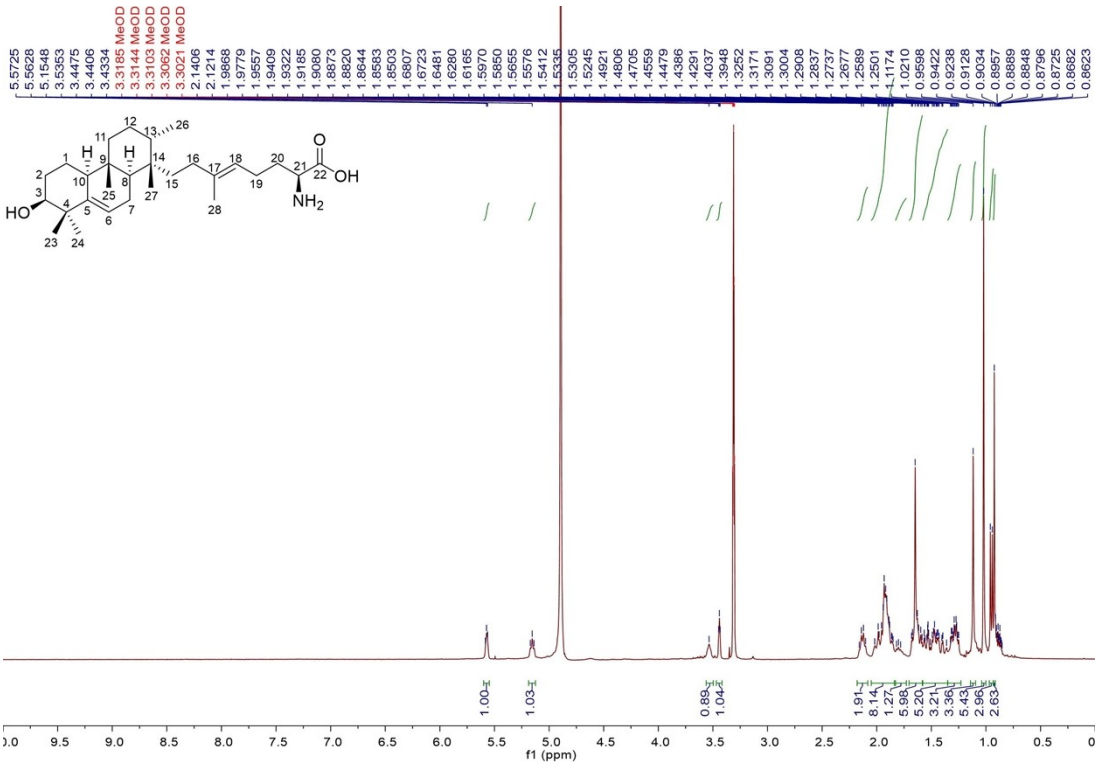

Figure S82. ^{1}H NMR spectrum of atolypene E (**11**) in methanol-d_4 (400 MHz).

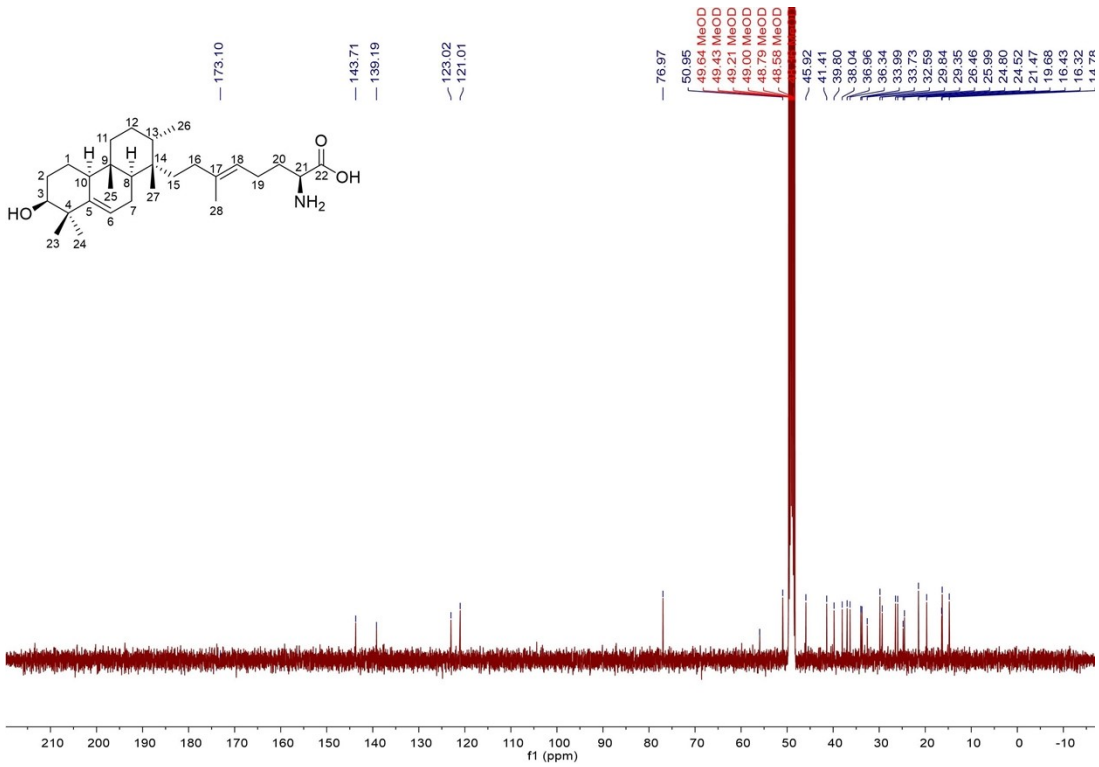

Figure S83. ^{13}C NMR spectrum of atolypene E (**11**) in methanol-d_4 (100 MHz).

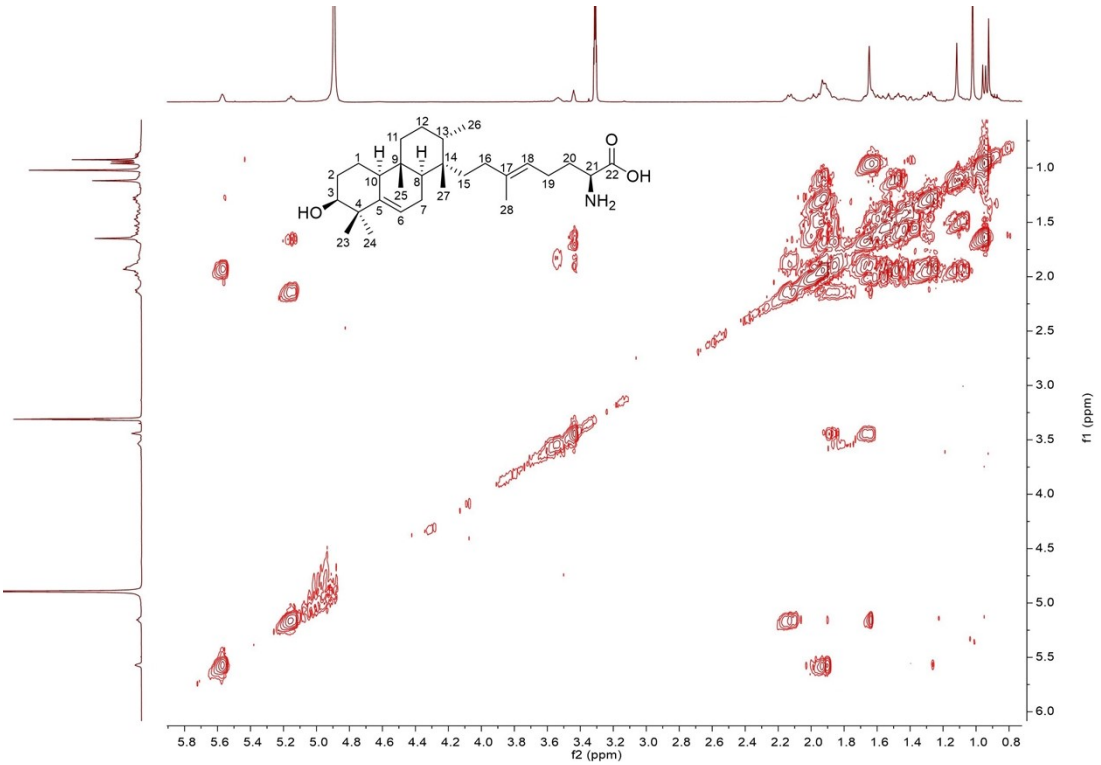

Figure S84. ^{1}H-^{1}H COSY spectrum of atolypene E (**11**) in methanol-d_4.

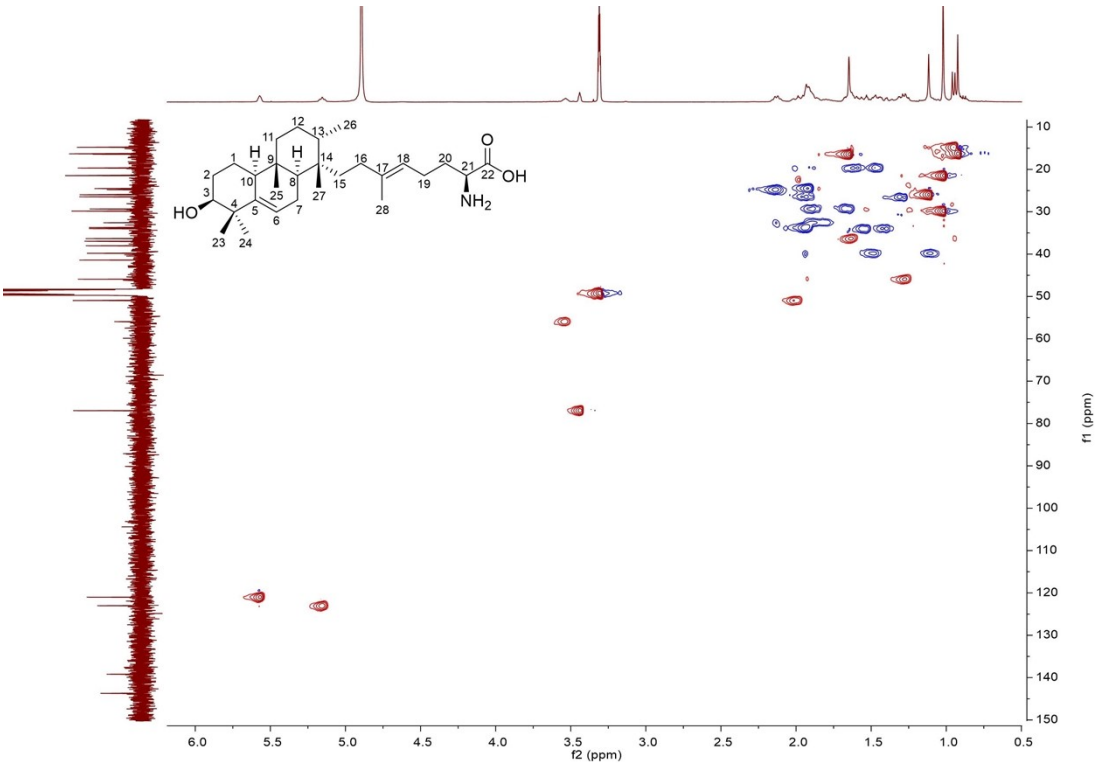

Figure S85. HSQC spectrum of atolypene E (**11**) in methanol-d_4.

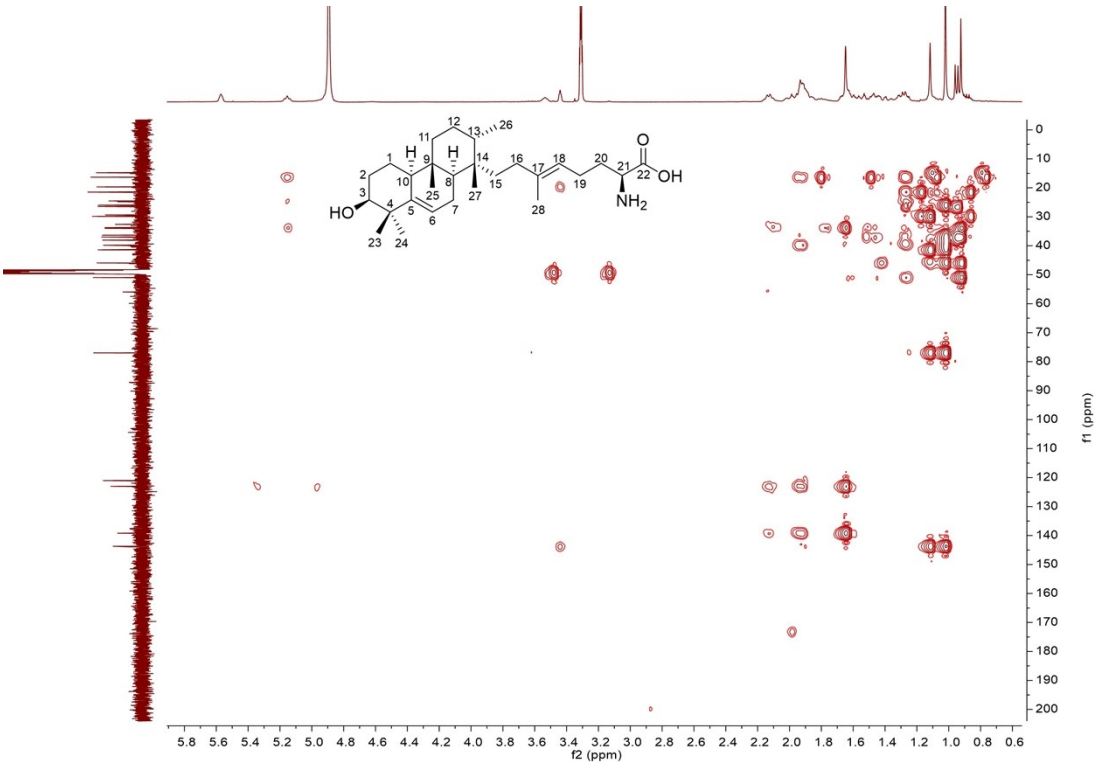

Figure S86. HMBC spectrum of atolypene E (**11**) in methanol-d_4.

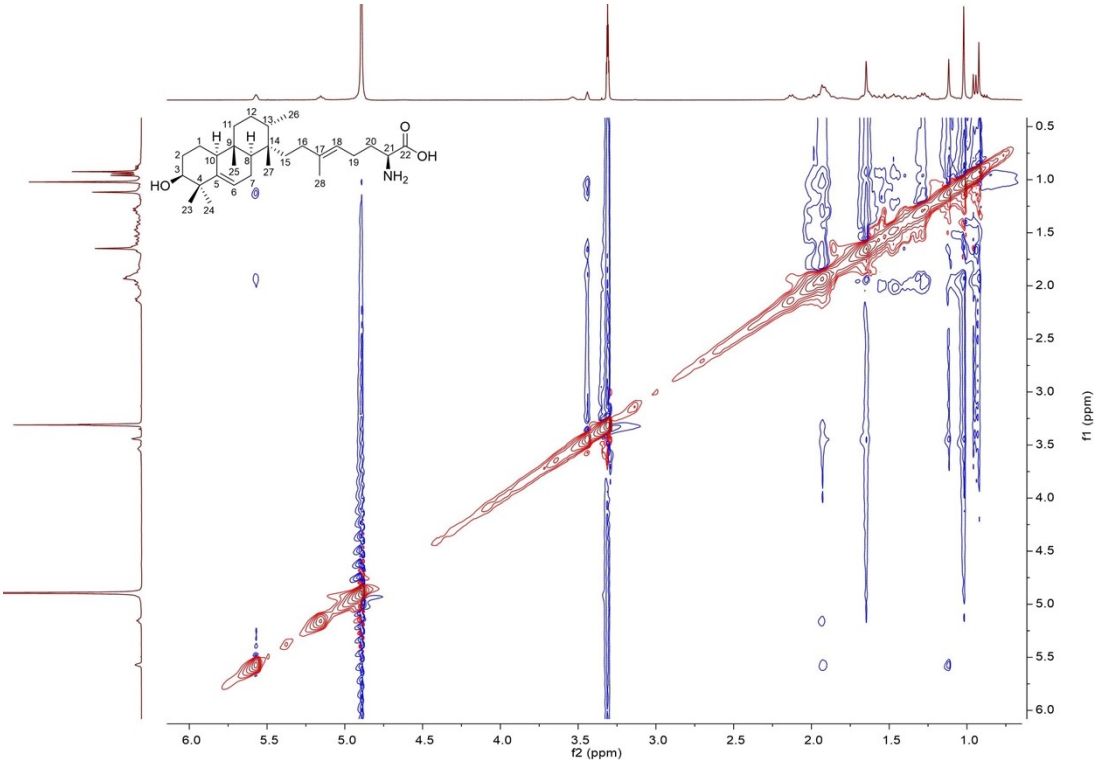

Figure S87. ROESY spectrum of atolypene E (**11**) in methanol-d_4.

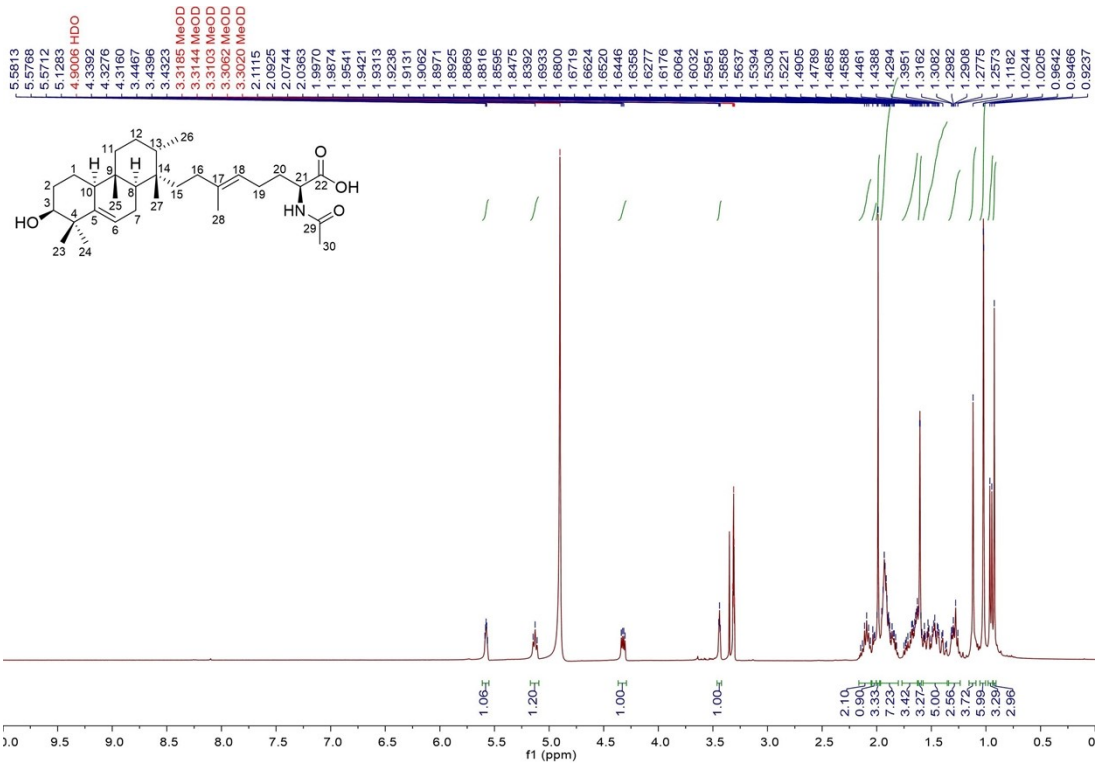

Figure S88. ^{1}H NMR spectrum of atolypene E (**11**) in methanol-d_4 (400 MHz).

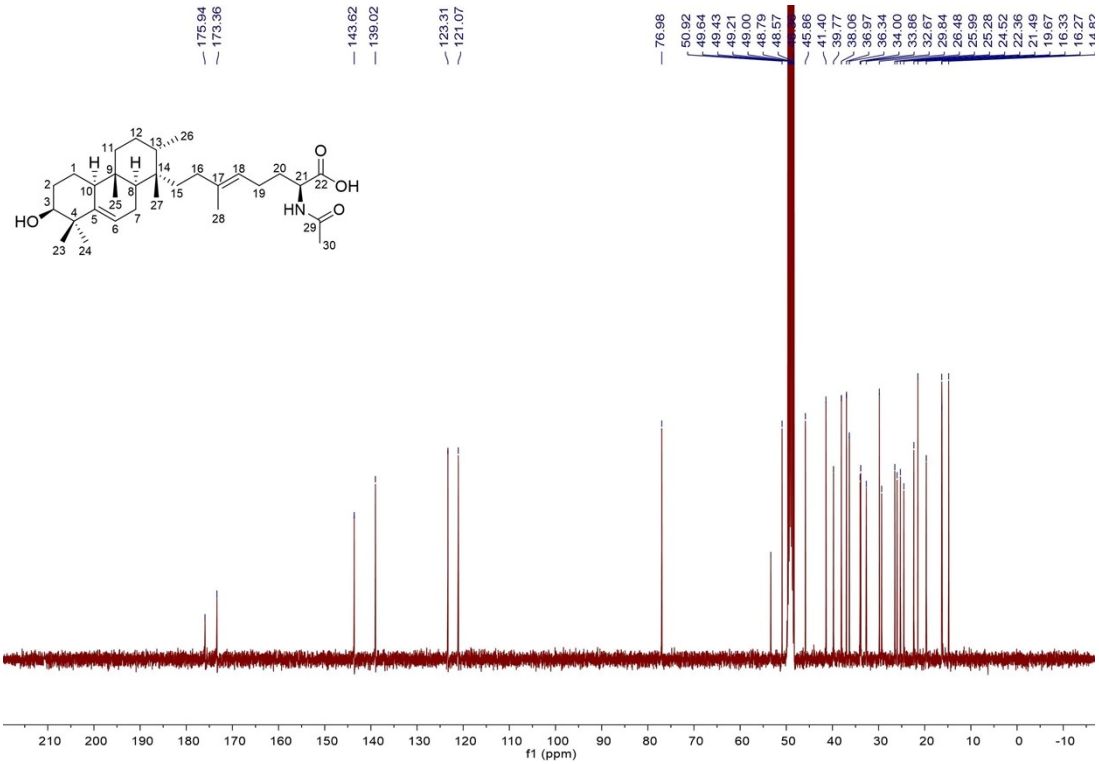

Figure S89. ^{13}C NMR spectrum of atolypene F (**12**) in methanol-d_4 (100 MHz).

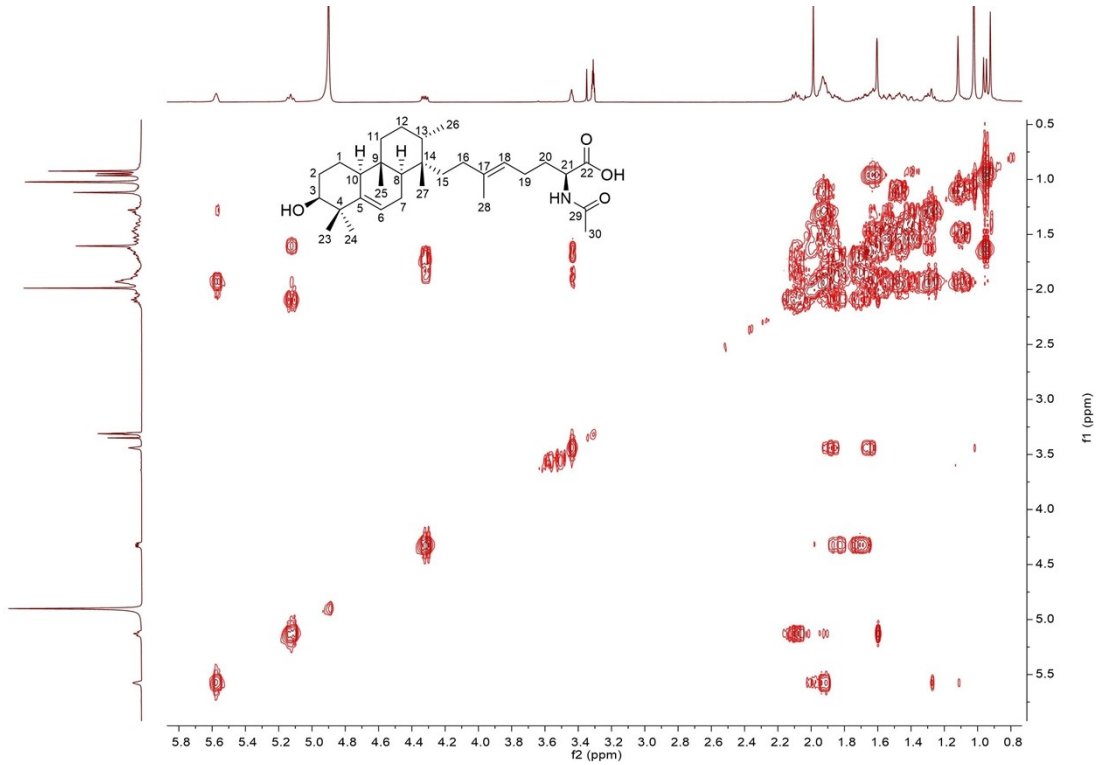

Figure S90. ^{1}H-^{1}H COSY spectrum of atolypene F (**12**) in methanol-d_4.

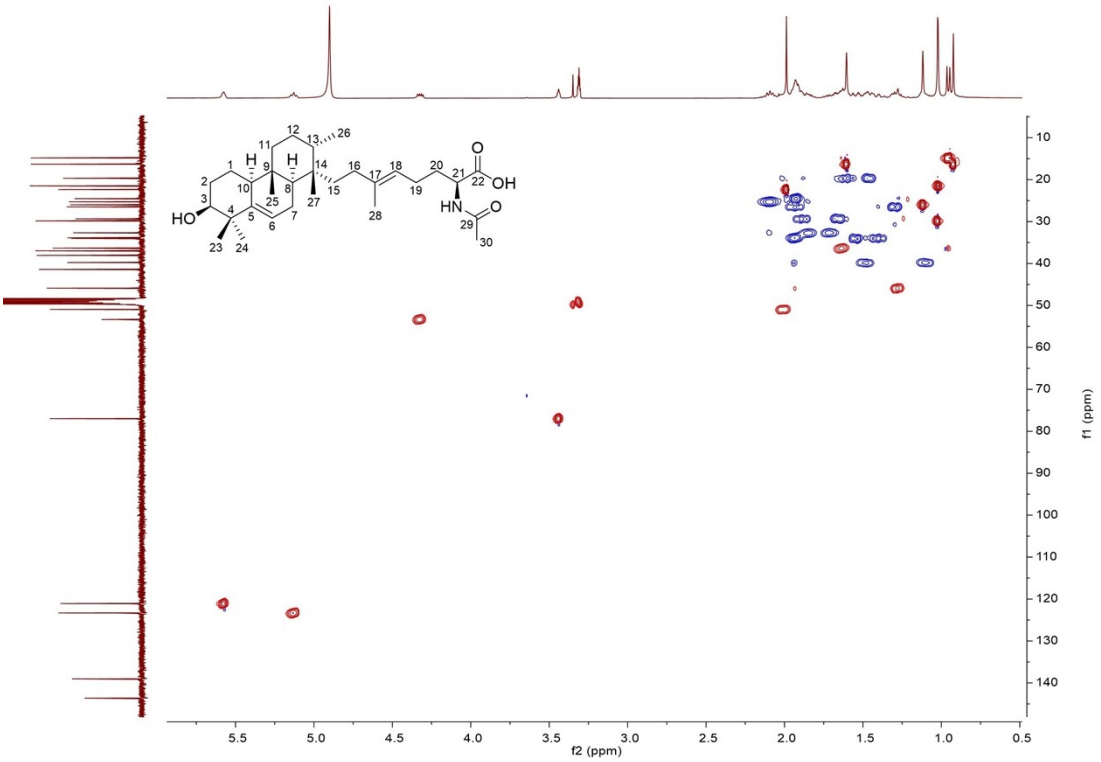

Figure S91. HSQC spectrum of atolypene F (**12**) in methanol-d_4.

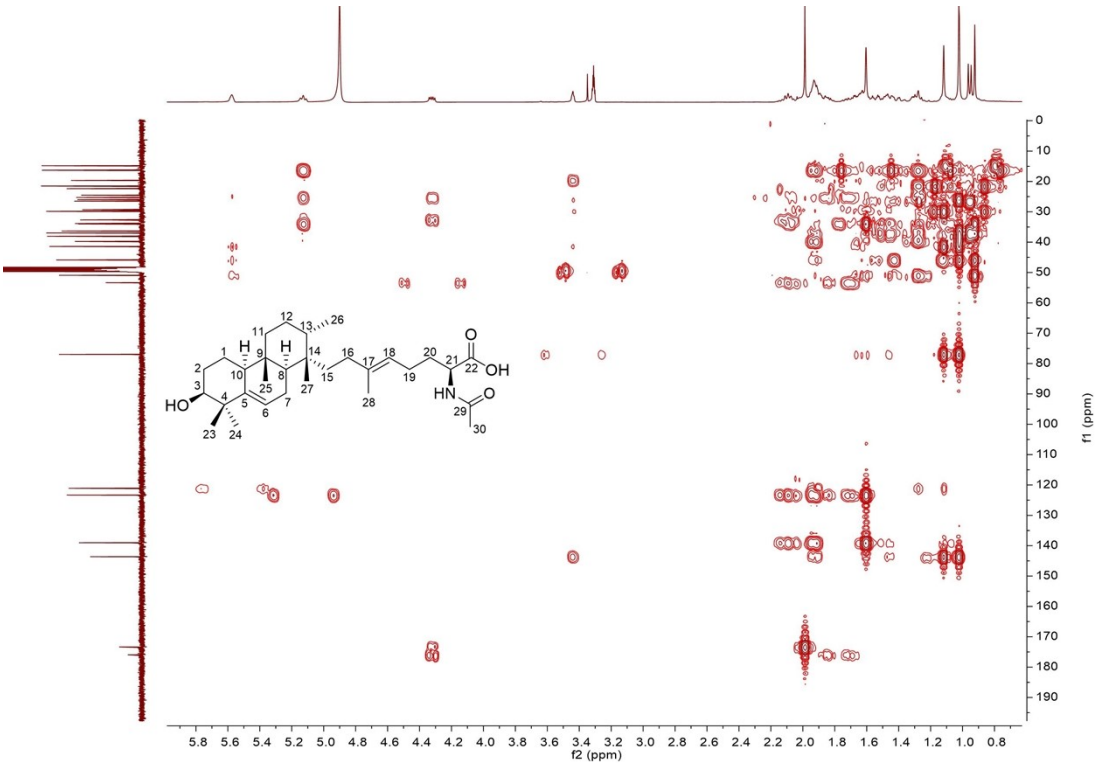

Figure S92. HMBC spectrum of atolypene F (**12**) in methanol-d_4.

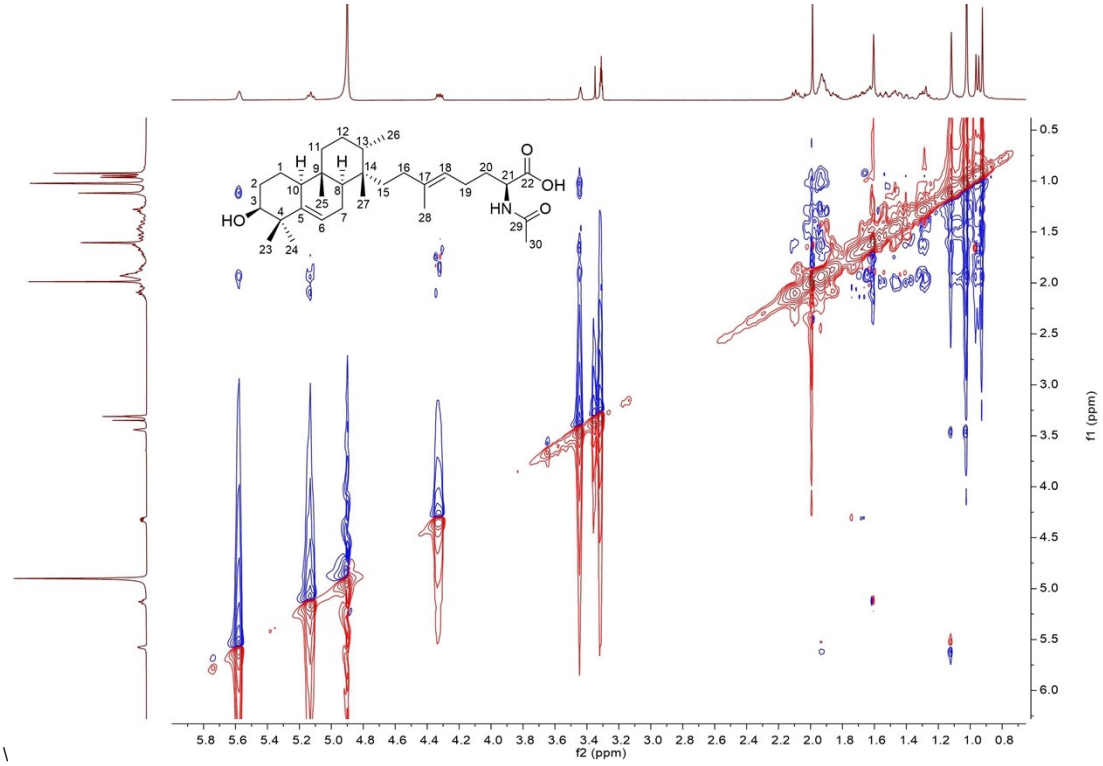

Figure S93. ROESY spectrum of atolypene F (**12**) in methanol-d_4.

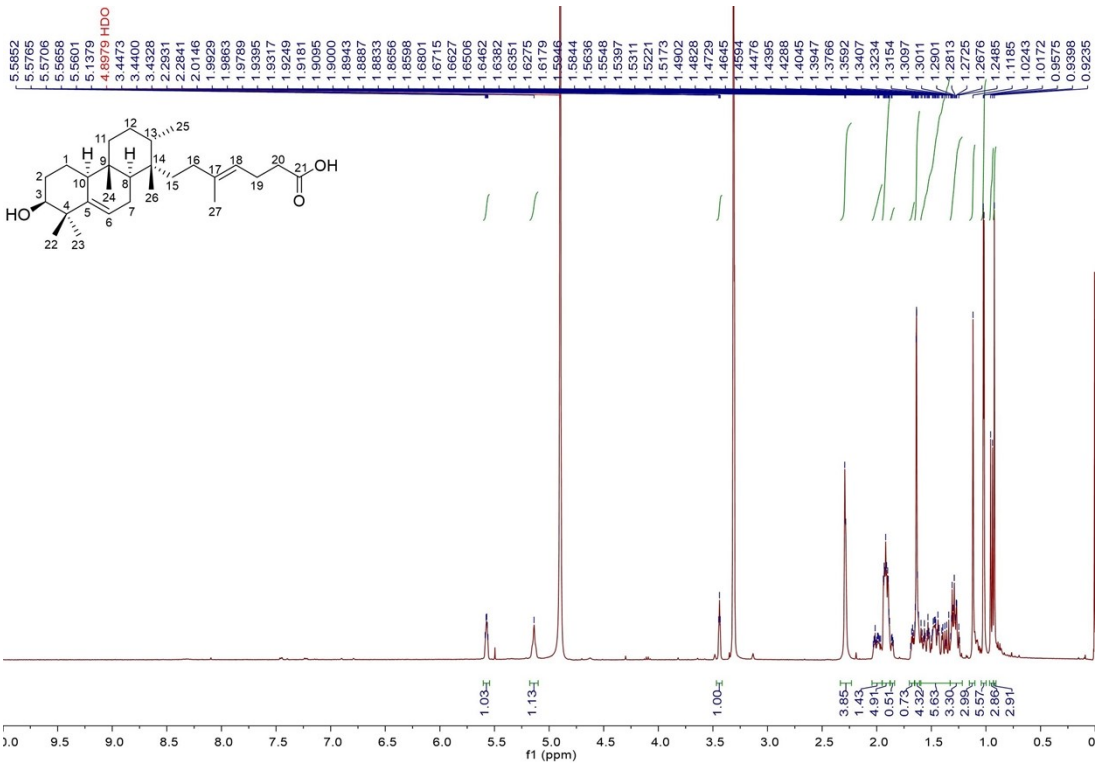

Figure S94. ^{1}H NMR spectrum of atolypene G (**13**) in methanol-d_4 (400 MHz).

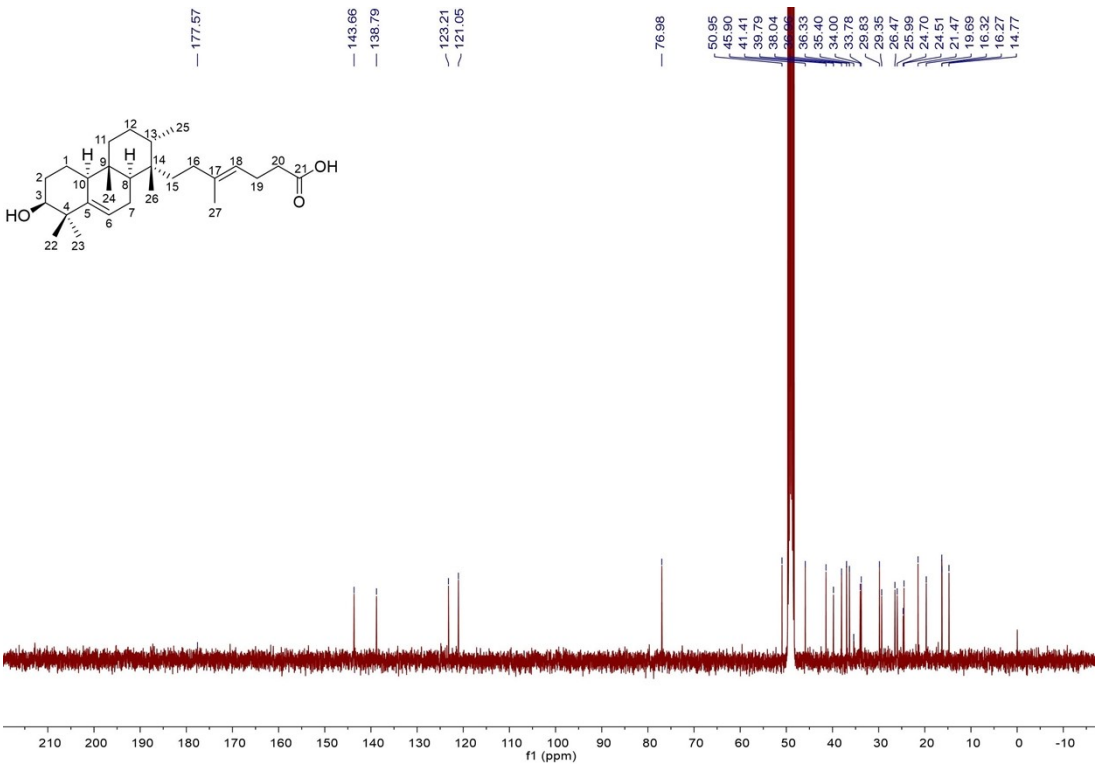

Figure S95. ^{13}C NMR spectrum of atolypene G (**13**) in methanol-d_4 (100 MHz).

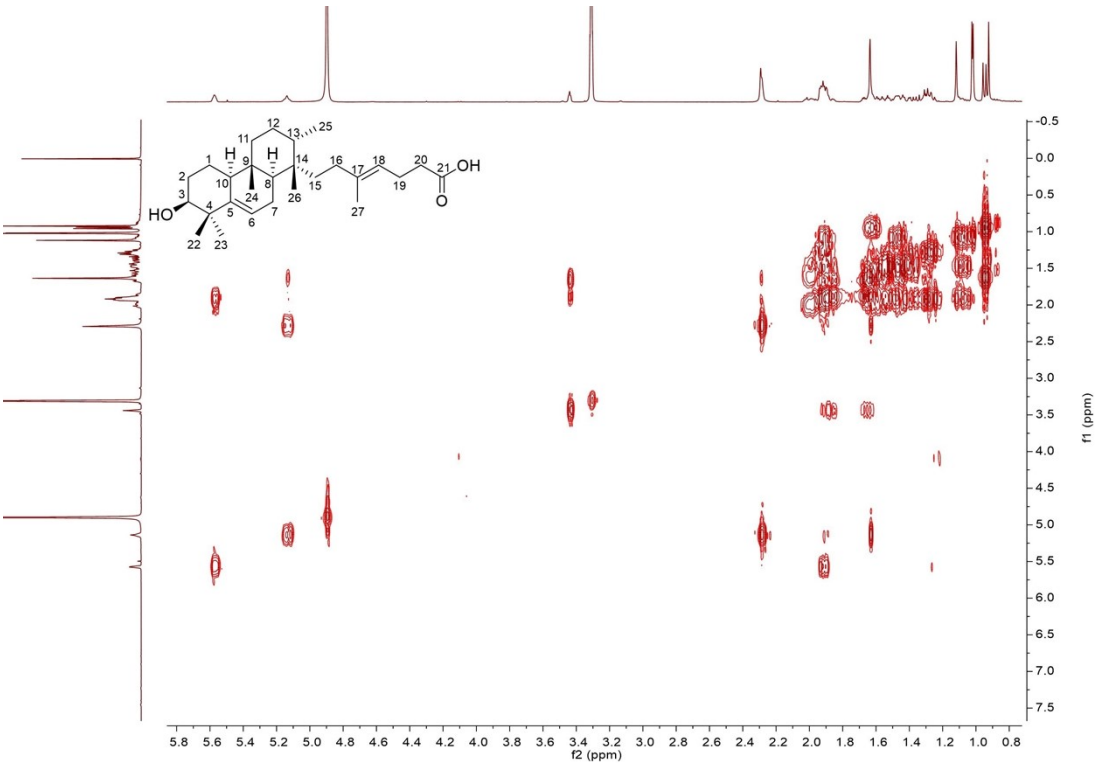

Figure S96. ^{1}H-^{1}H COSY spectrum of atolypene G (**13**) in methanol-d_4.

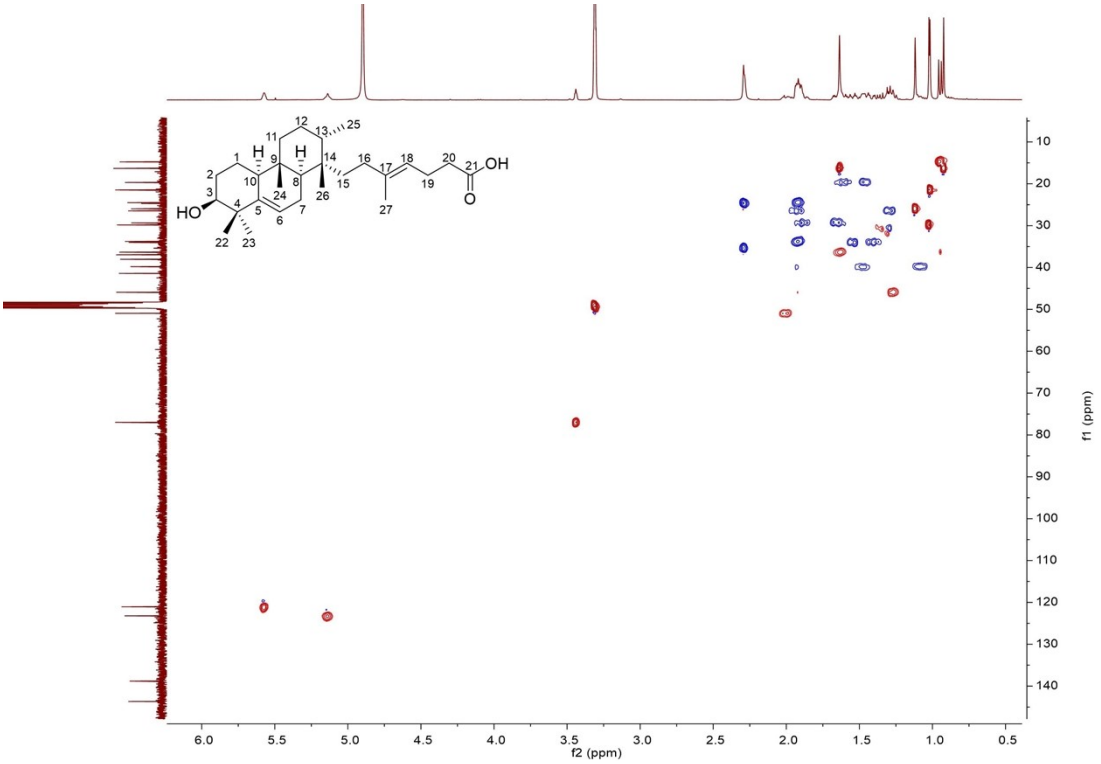

Figure S97. HSQC spectrum of atolypene G (**13**) in methanol-d_4.

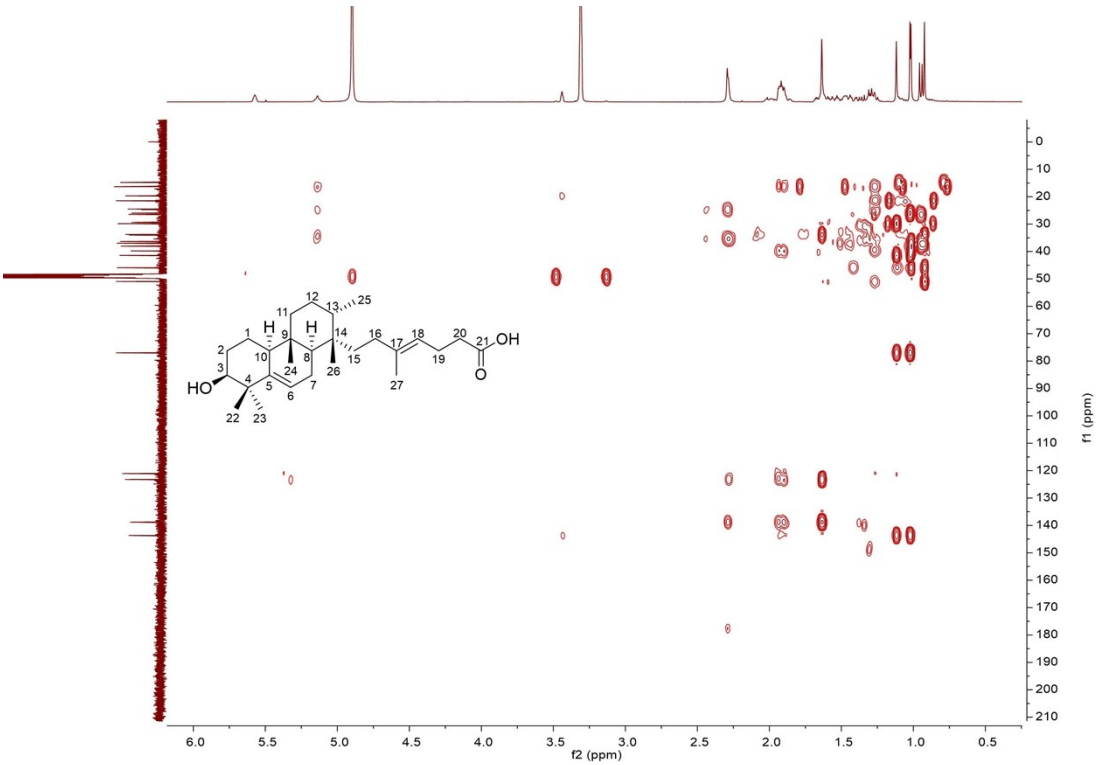

Figure S98. HMBC spectrum of atolypene G (**13**) in methanol-d_4.

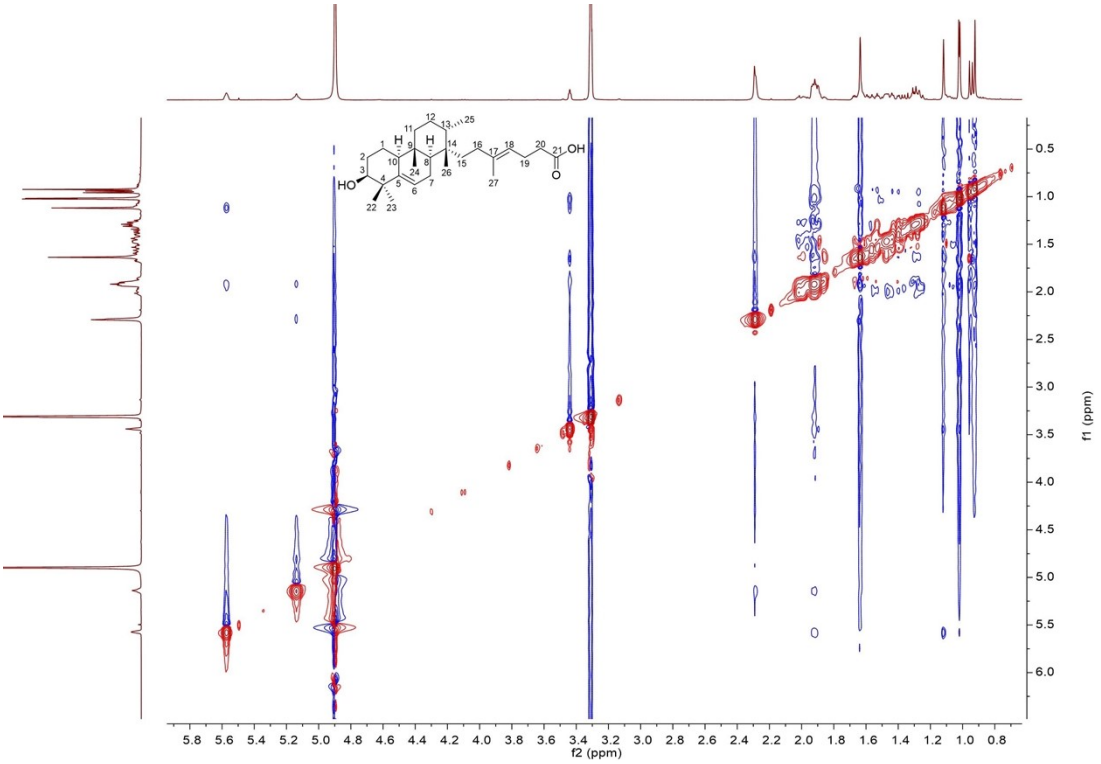

Figure S99. ROESY spectrum of atolypene G (**13**) in methanol-d_4.

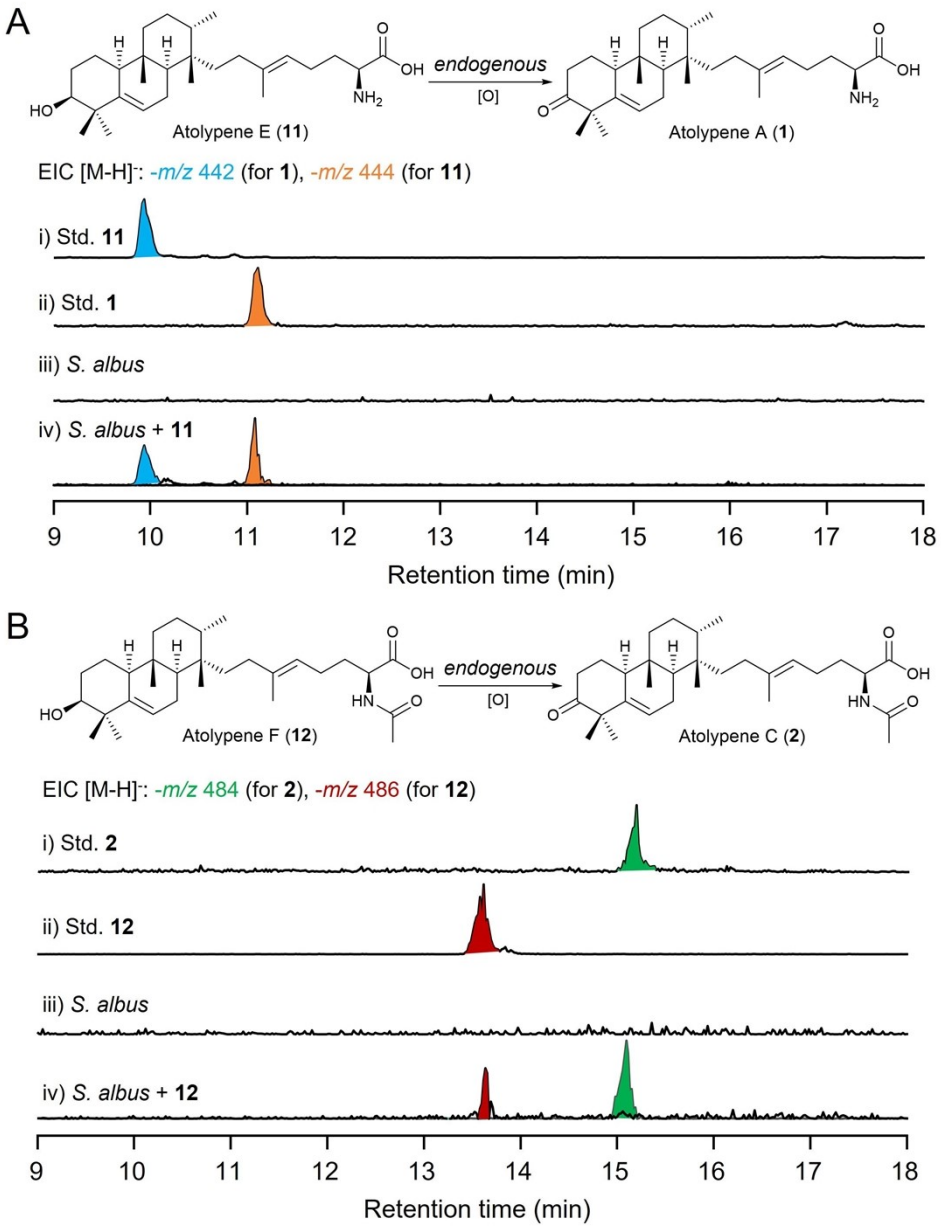

Figure S100. EIC analysis of wild-type *S. albus* that were supplemented with **11** and **12**, respectively.

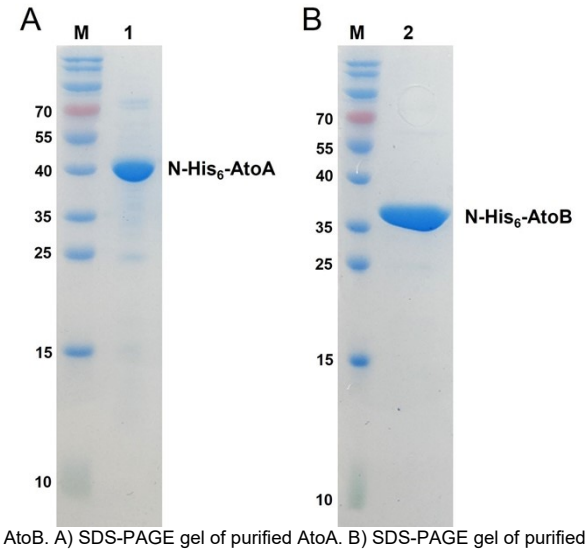

Figure S101. Protein purification of AtoA and AtoB. A) SDS-PAGE gel of purified AtoA. B) SDS-PAGE gel of purified AtoB. M, Prestained Protein Marker (Vazyme); lane 1, purified N-His_6-tagged AtoA (413 amino acids, ~45.0 KDa); lane 2, purified N-His_6-tagged AtoB (346 amino acids, ~36.8 KDa).

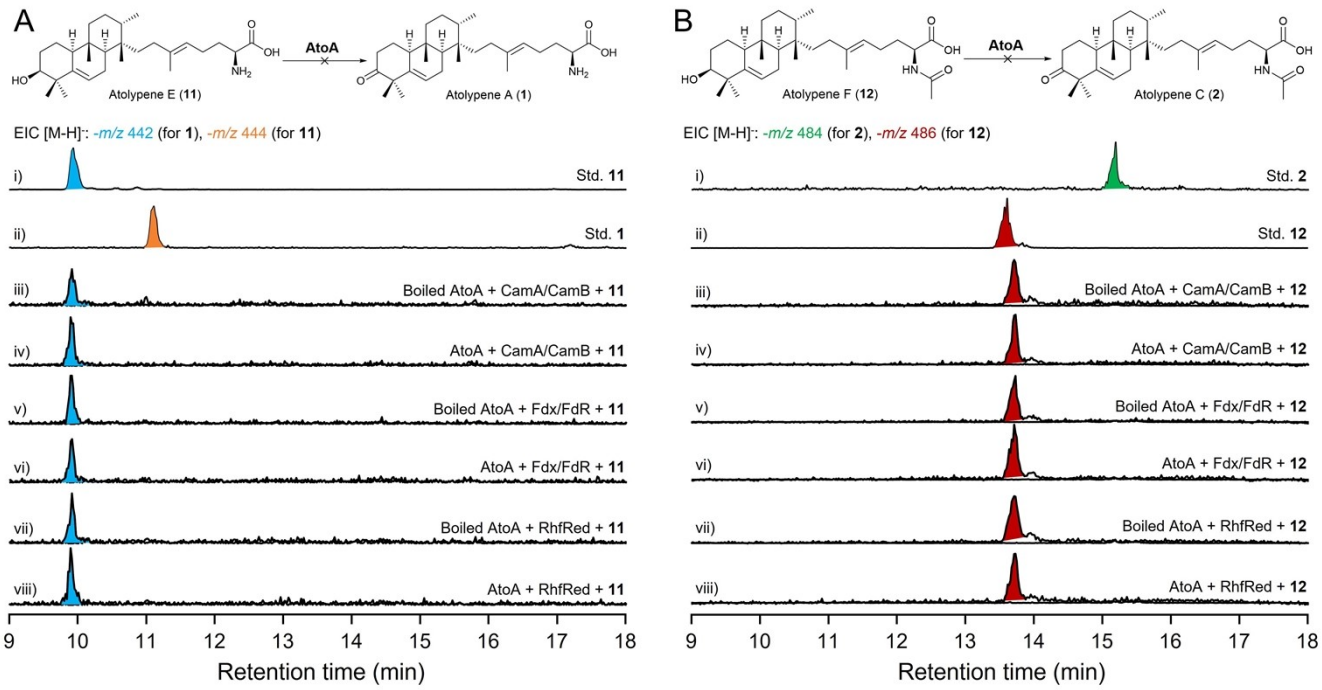

Figure S102. LC-MS analysis of the in vitro reactions of AtoA with **11** and **12**, respectively.

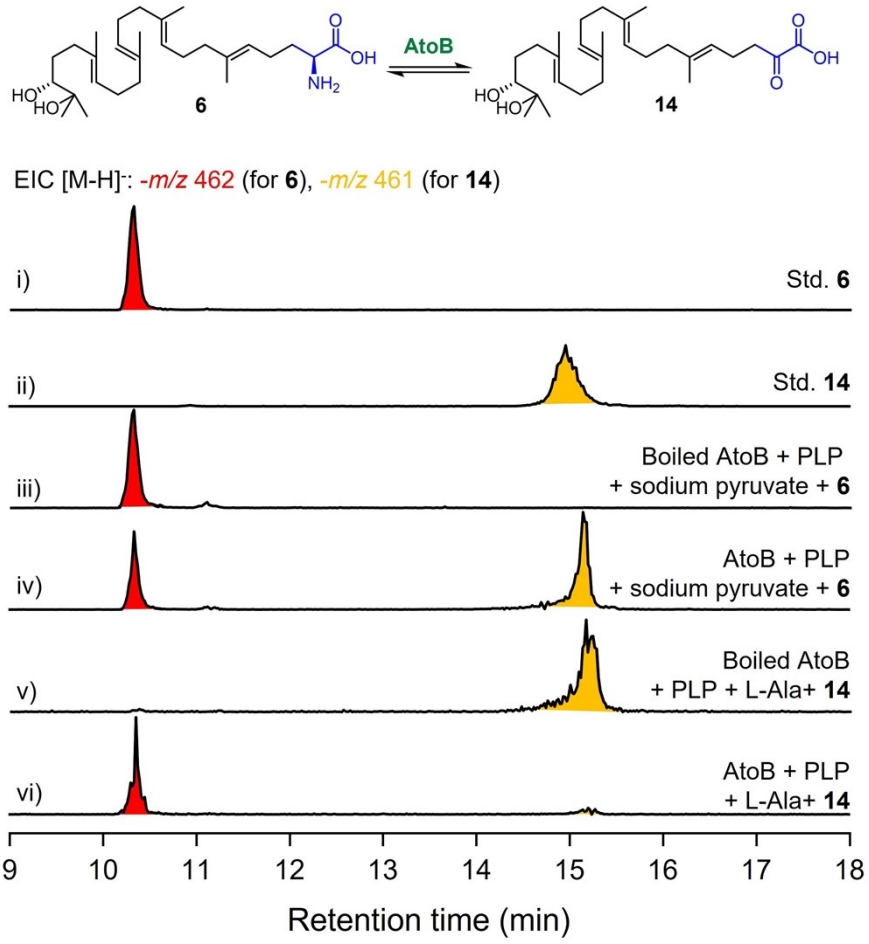

Figure S103. LC-MS analysis of the in vitro reactions of AtoB with **6** and **14**. PLP: pyridoxal phosphate; L-Ala: L-alanine.

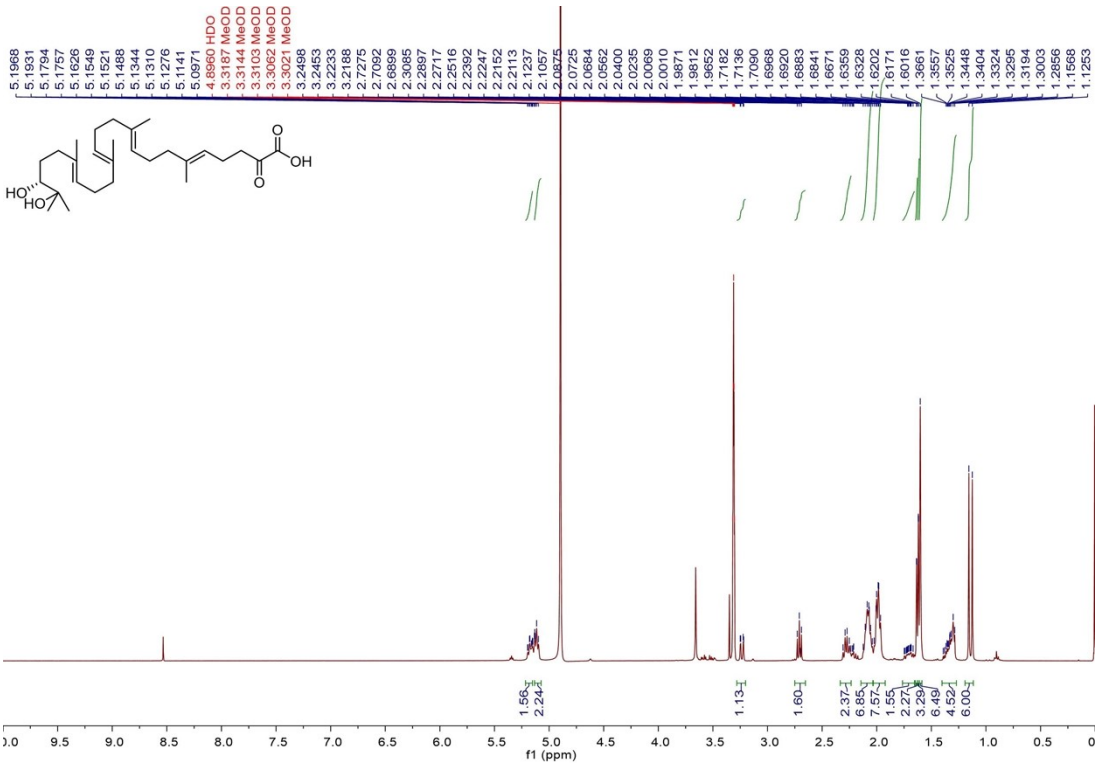

Figure S104. ^{1}H NMR spectrum of **14** in methanol-d_4 (400 MHz).

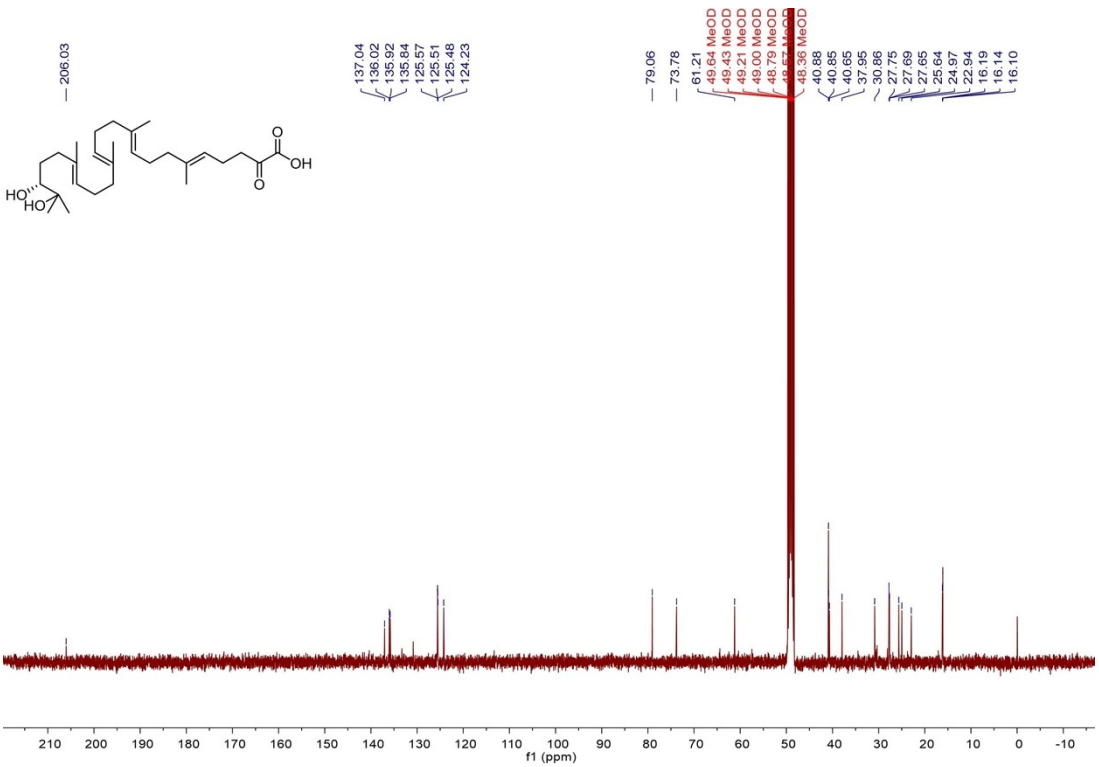

Figure S105. ^{13}C NMR spectrum of **14** in methanol-d_4 (100 MHz).

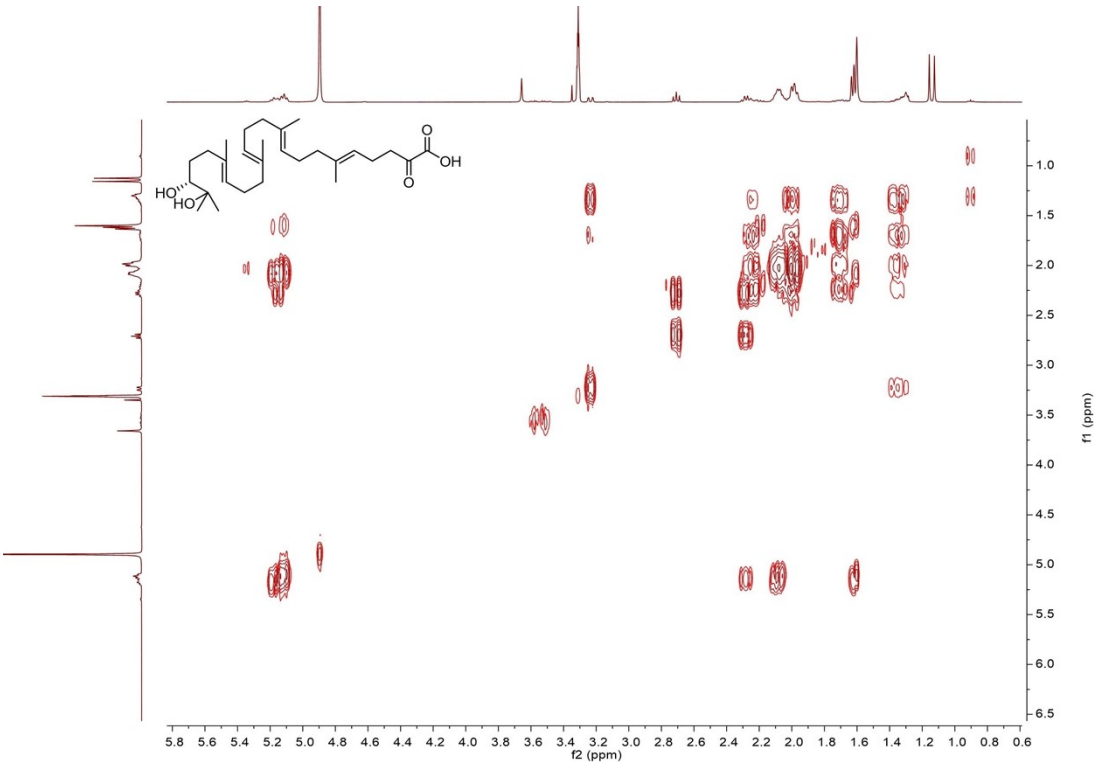

Figure S106. ^{1}H-^{1}H COSY spectrum of **14** in methanol-d_4.

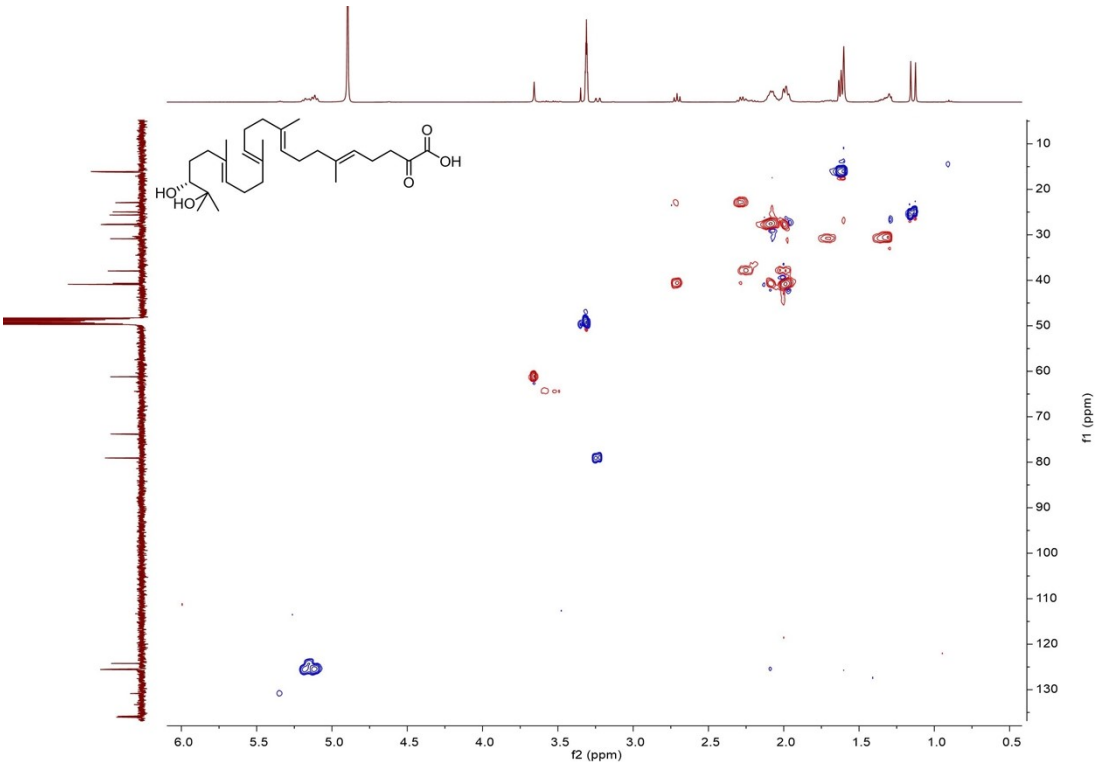

Figure S107. HSQC spectrum of **14** in methanol-d_4.

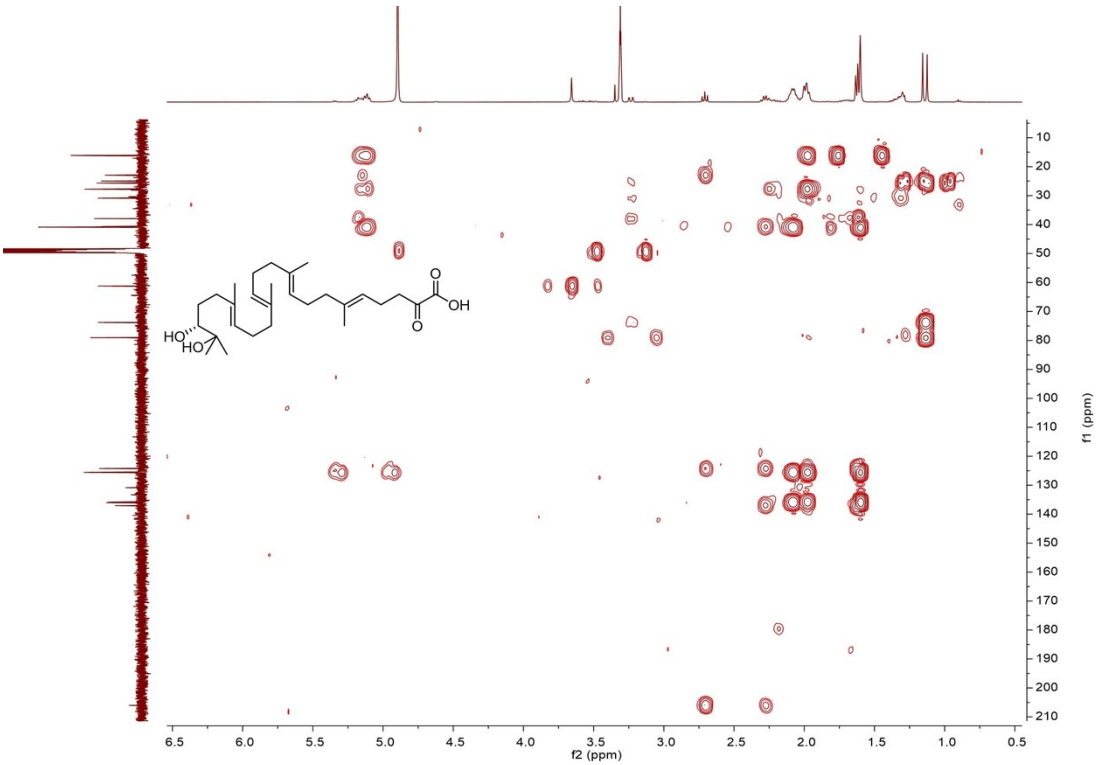

Figure S108. HMBC spectrum of **14** in methanol-d_4.

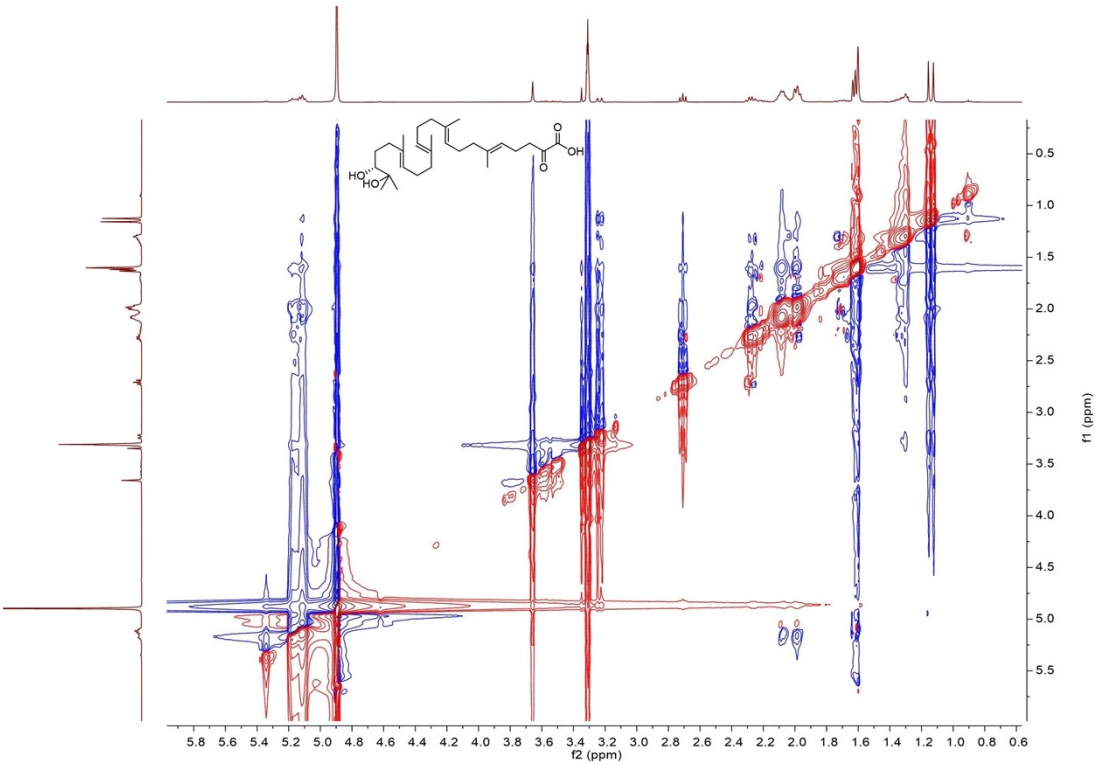

Figure S109. ROESY spectrum of **14** in methanol-d_4.

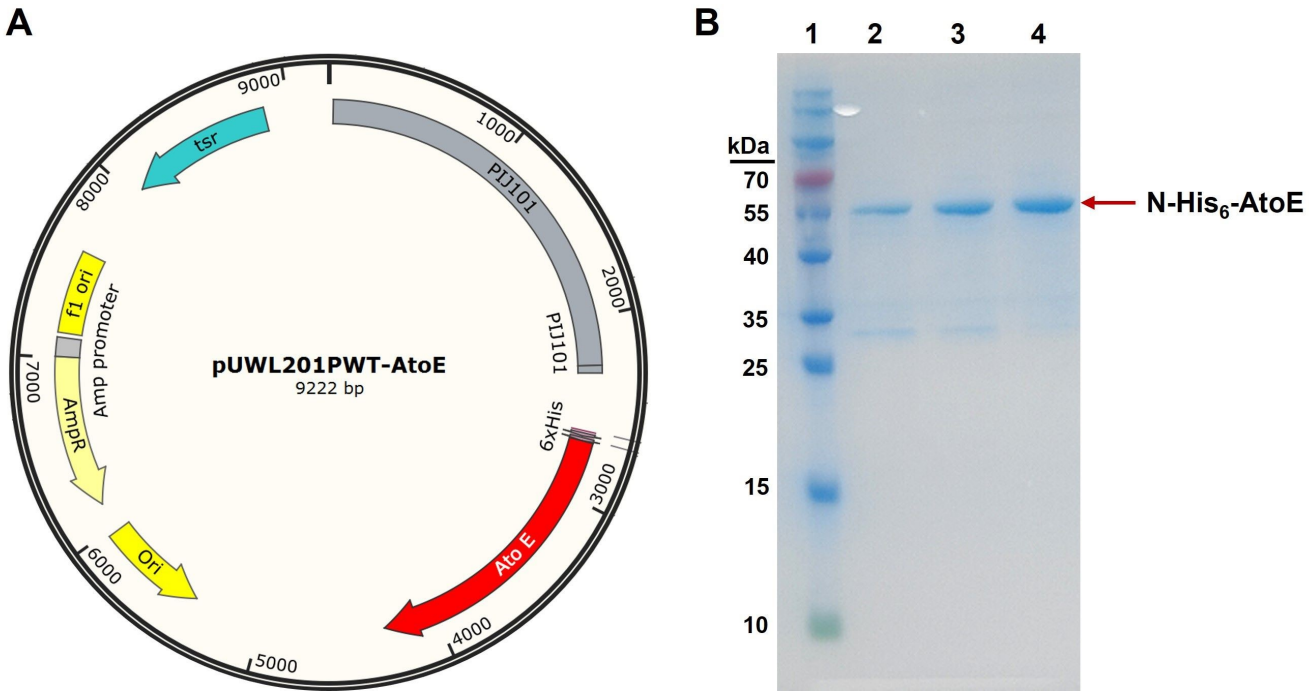

Figure S110. Plasmid construction and protein purification of AtoE. A) Plasmid map, gene *atoE* with His_6-tag were inserted into the *Nde*I and *EcoR*I restriction sites within the pUWL201PWT vector to construct the pUWL201PWT-AtoE. B) SDS-PAGE gel of purified AtoE. Lane 1, Prestained Protein Marker (Vazyme); lane 2-4, purified N-His_6-tagged AtoE (553 amino acids, ~59.3 KDa).

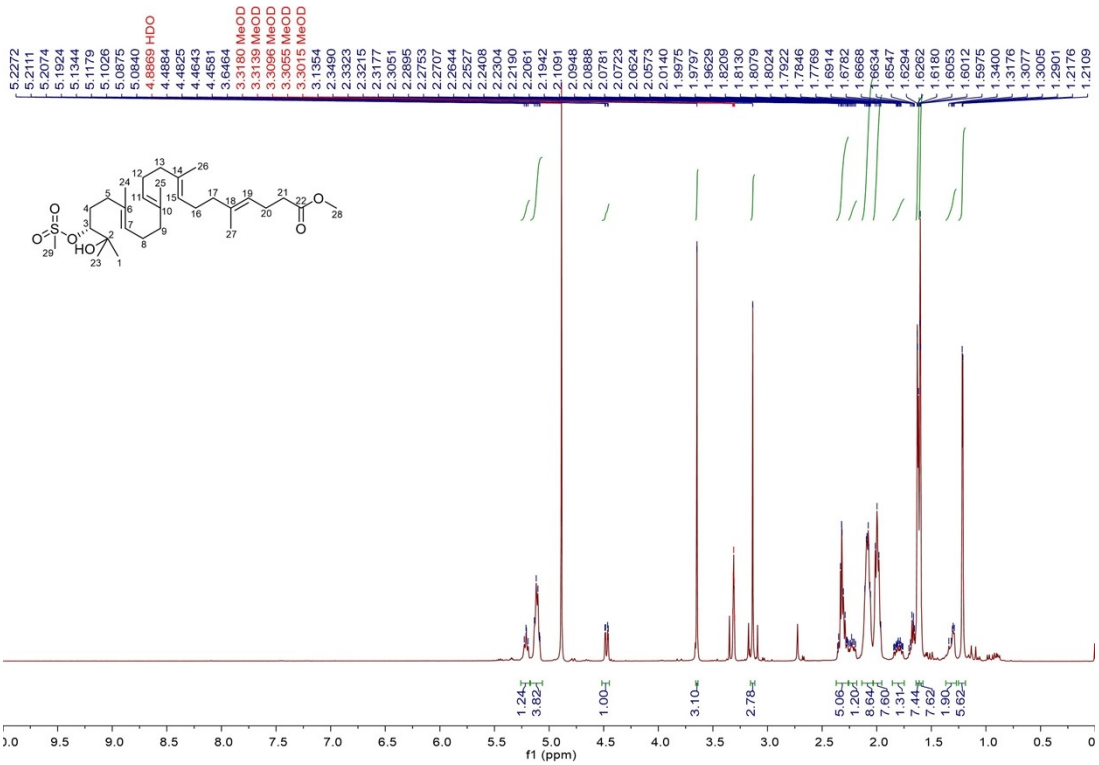

Figure S111. ^{1}H NMR spectrum of **10e** in methanol-d_4 (400 MHz).

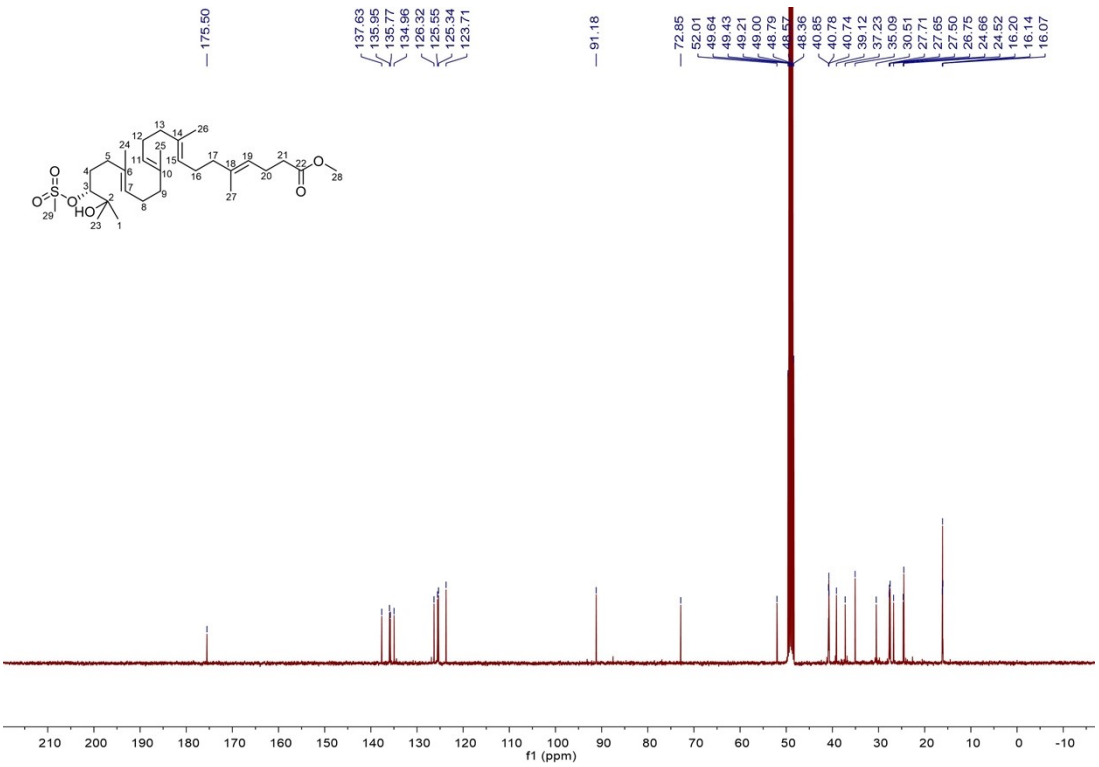

Figure S112. ^{13}C NMR spectrum of **10e** in methanol-d_4 (100 MHz).

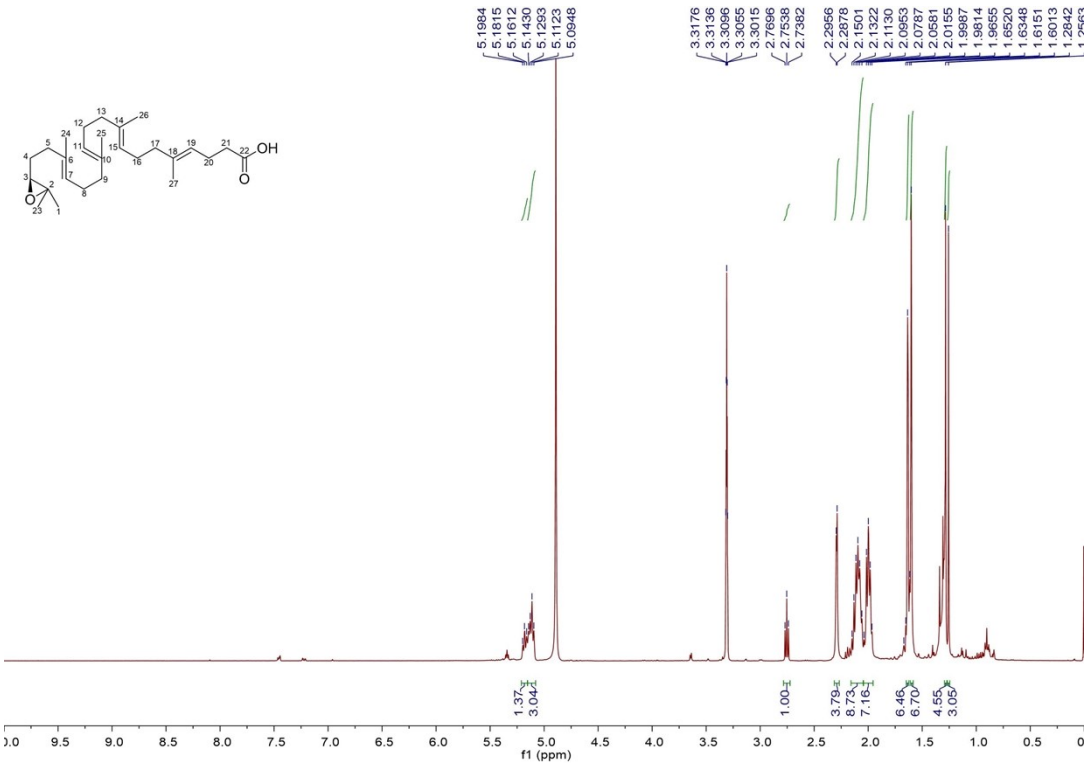

Figure S113. ^{1}H NMR spectrum of **10a** in methanol-d_4 (400 MHz).

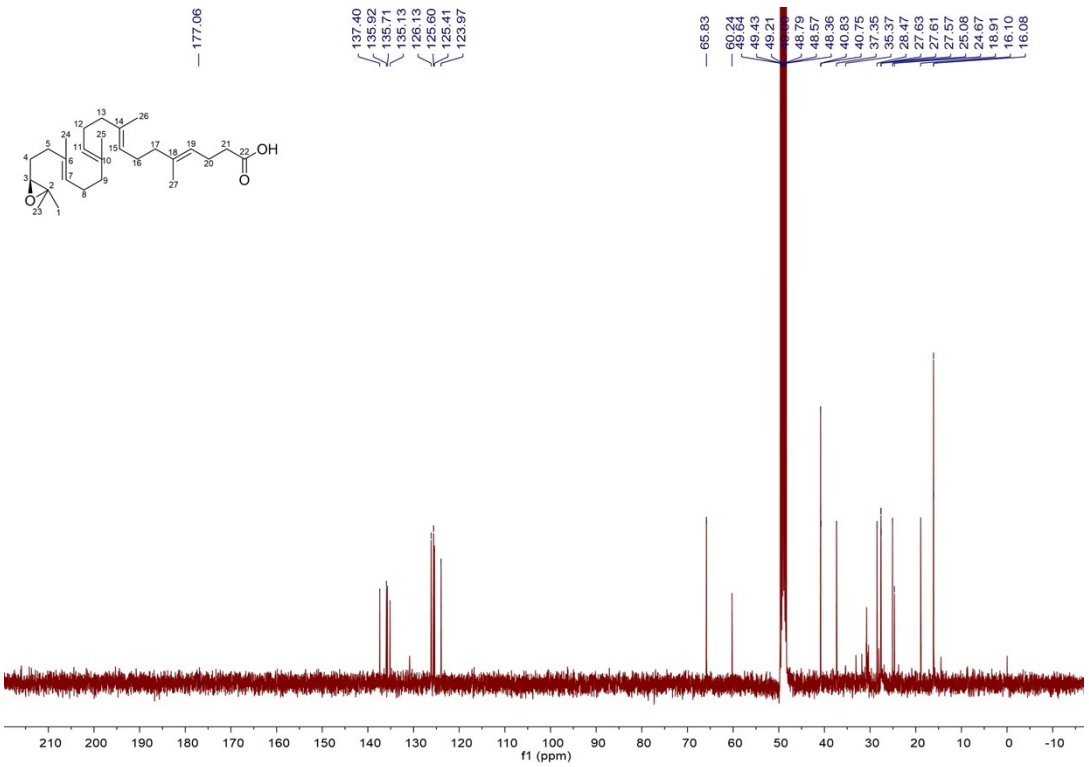

Figure S114. ^{13}C NMR spectrum of **10a** in methanol-d_4 (100 MHz).

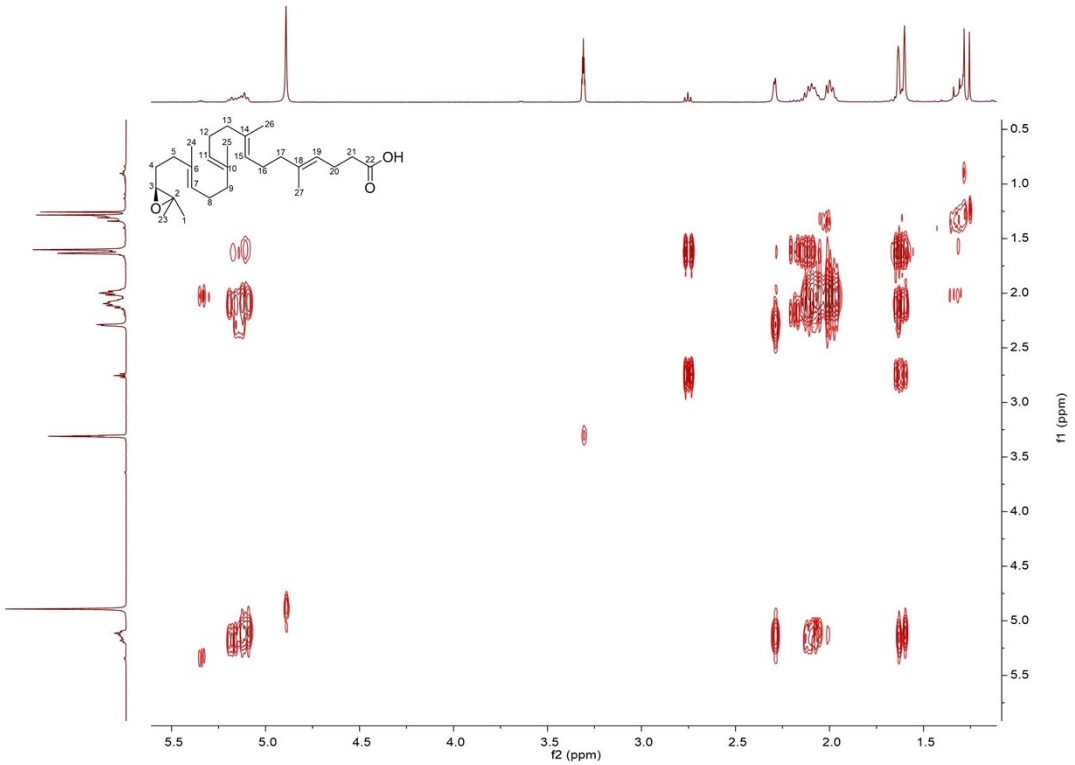

Figure S115. ^{1}H-^{1}H COSY spectrum of **10a** in methanol-d_4.

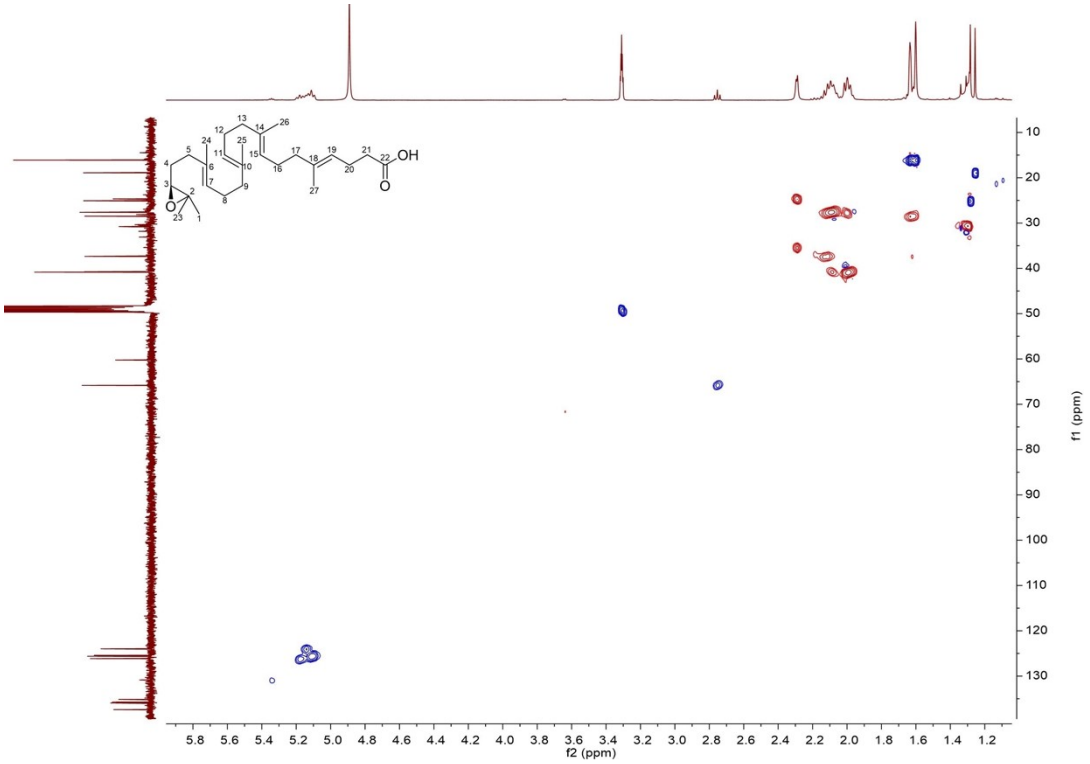

Figure S116. HSQC spectrum of **10a** in methanol-d_4.

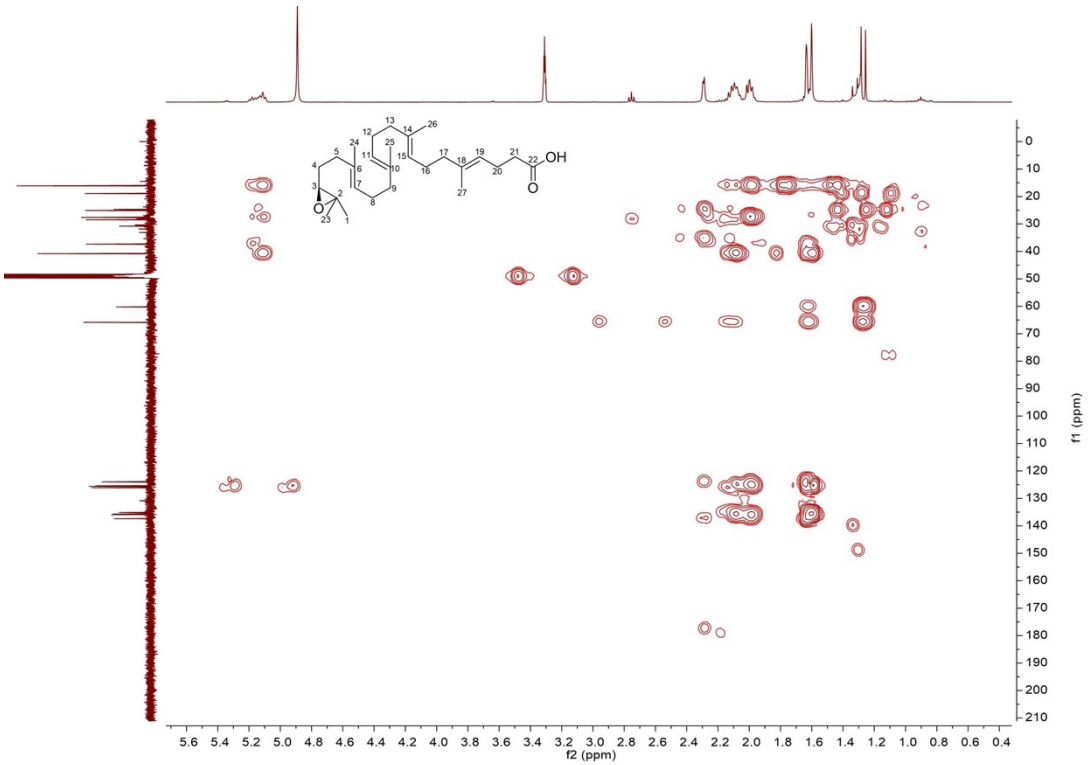

Figure S117. HMBC spectrum of **10a** in methanol-d_4.

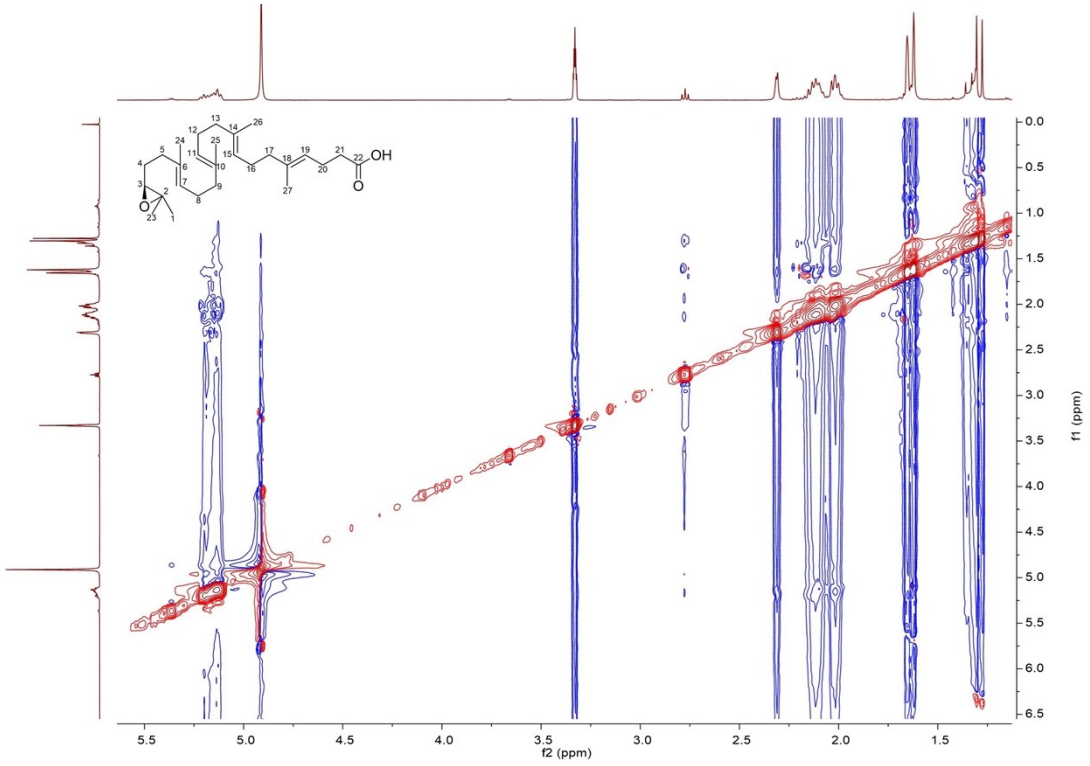

Figure S118. ROESY spectrum of **10a** in methanol-d_4.

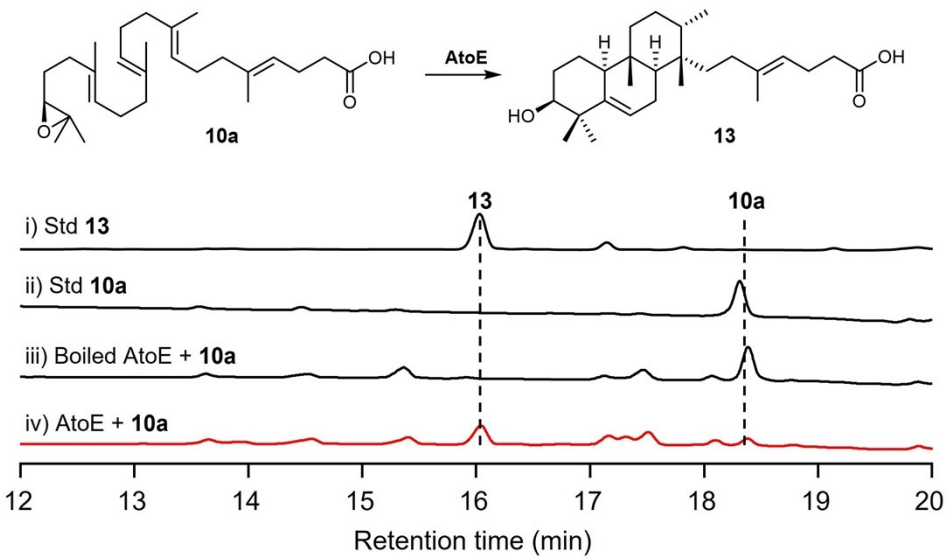

Figure S119. HPLC analysis of in vitro biochemical assay of AtoE with **10a** (λ_{max} = 210 nm).

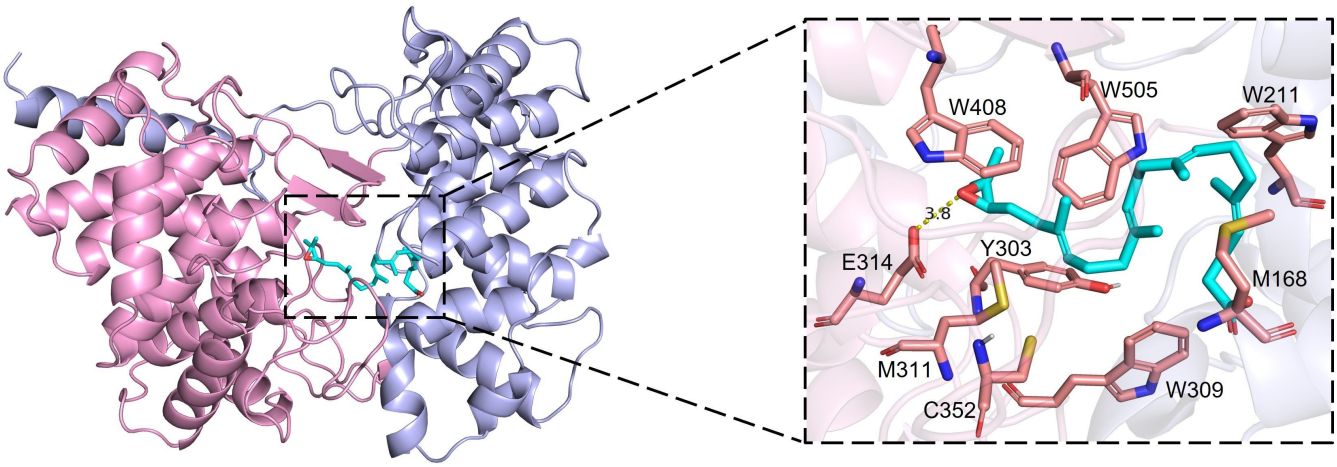

Figure S120. Structural model of AtoE with displaying key active site residues and a docking model of **10a**.

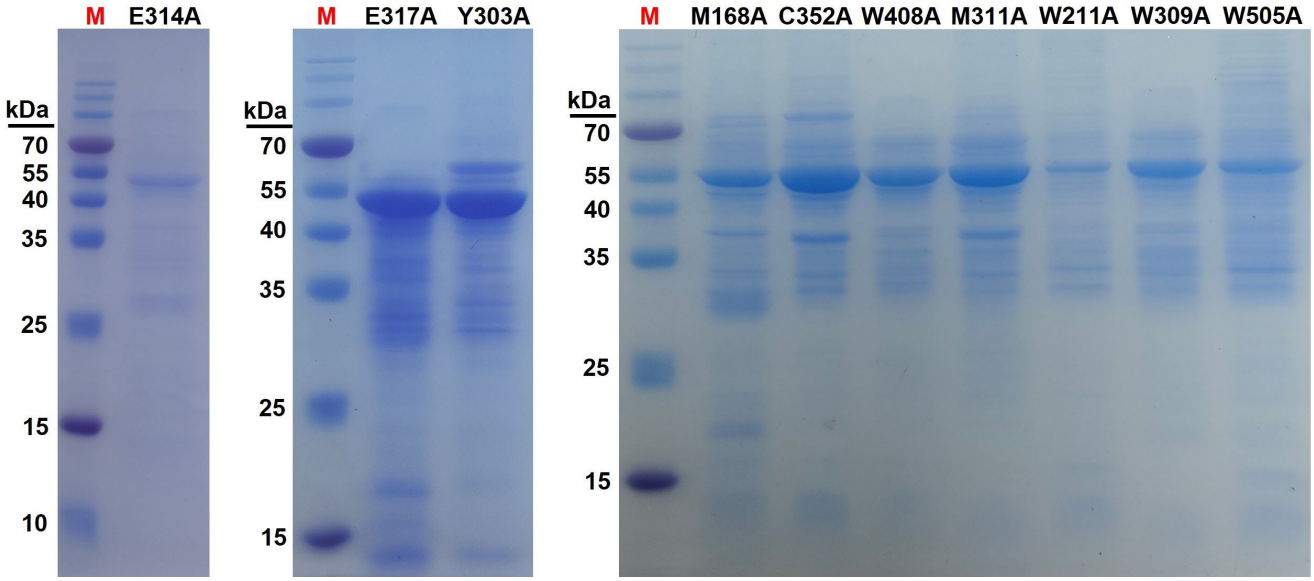

Figure S121. Protein purification of AtoE mutants. Each AtoE mutant was fermented in 4L cultures, and the resultant proteins were purified, yielding E314A, E317A, Y303A, M168A, C352A, W408A, M311A, W211A, W309A, and W505A. Lane M, Prestained Color Protein Ladder (Beyotime).

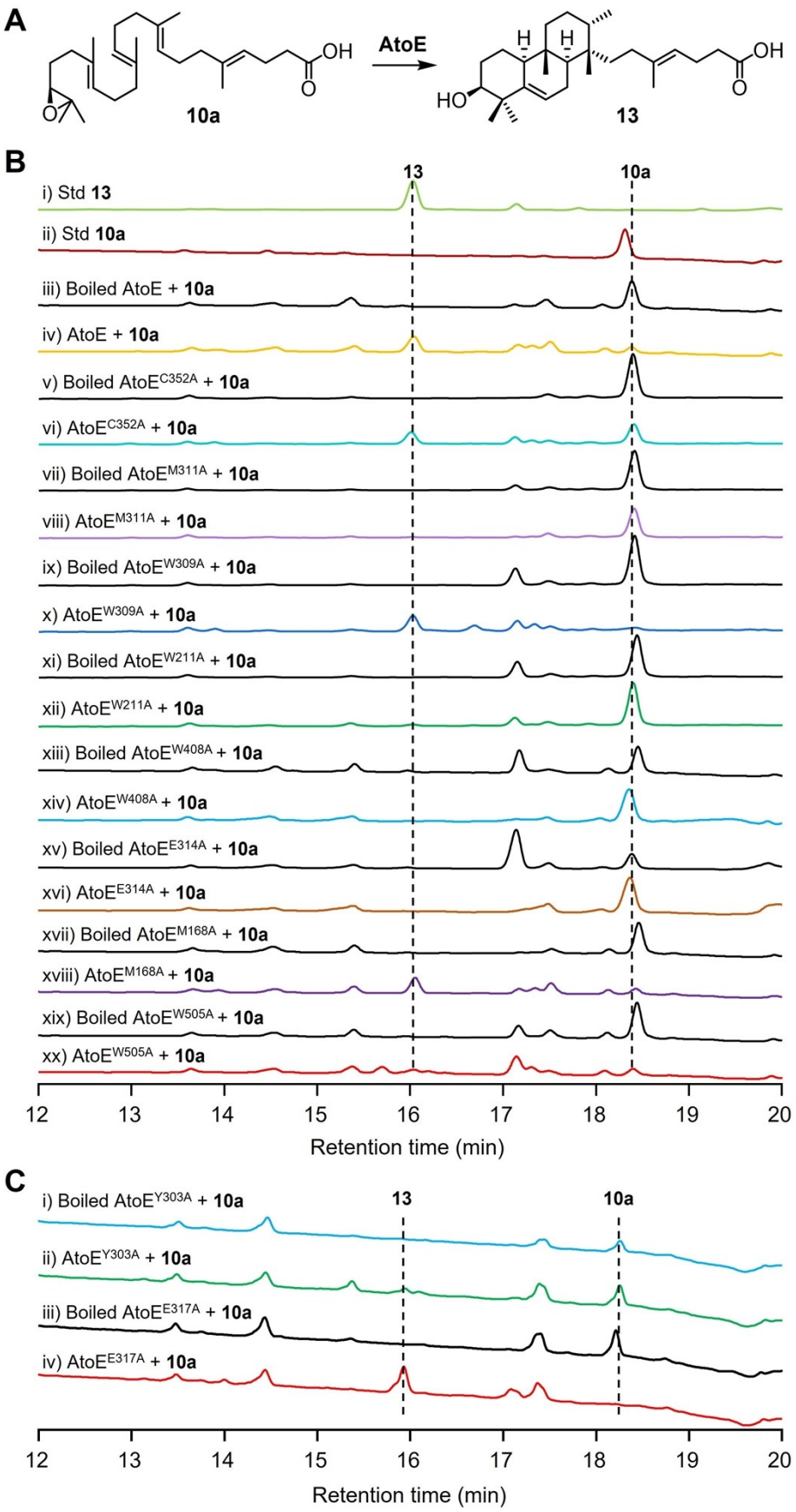

Figure S122. In vitro reactions of AtoE variants with the substrate **10a**. A) Cyclization of **10a** by MTC AtoE catalyzes the formation of **13**; B) HPLC profiles (λ_{max} = 210 nm) of the in vitro reactions of AtoE and its variants (C352A, M311A, W309A, W211A, W408A, E314A, M168A, and W505A) with the substrate **10a**; C) HPLC analysis of the in vitro reactions of variants (Y303A and E317A) with the substrate **10a**.

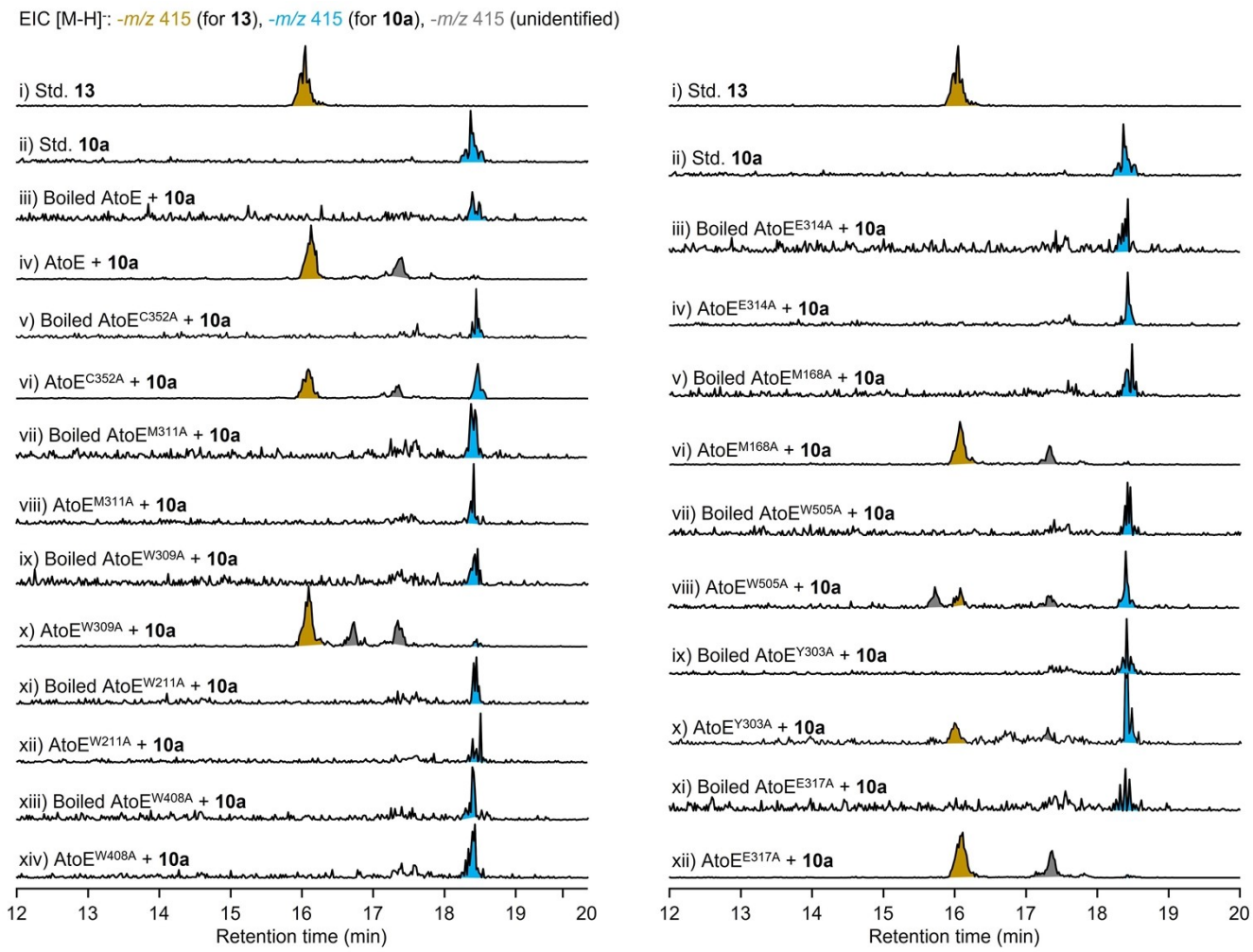

Figure S123. LC-MS analysis of the in vitro reactions of AtoE and variants with **10a**.

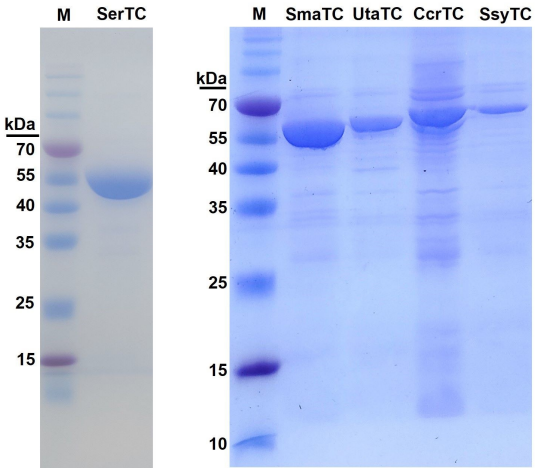

Figure S124. Protein purification of selected class II MTCs. M, Prestained Protein Marker (Vazyme); Purified N-His_6-tagged SerTC (572 amino acids, ~61.3 KDa); Purified N-His_6-tagged SmaTC (600 amino acids, ~63.7 KDa); Purified N-His_6-tagged UtaTC (588 amino acids, ~63.6 KDa); Purified N-His_6-tagged CcrTC (589 amino acids, ~65.3 KDa); Purified N-His_6-tagged SsyTC (585 amino acids, ~61.0 KDa). SerTC (Uniprot ID: A4FIP2); SmaTC (Uniprot ID: A0A515GD19); UtaTC (Uniprot ID: A0A2T0STH2); CcrTC (Uniprot ID: A0A7W7FUZ7); SsyTC (Uniprot ID: A0A5Q0H4Q7).

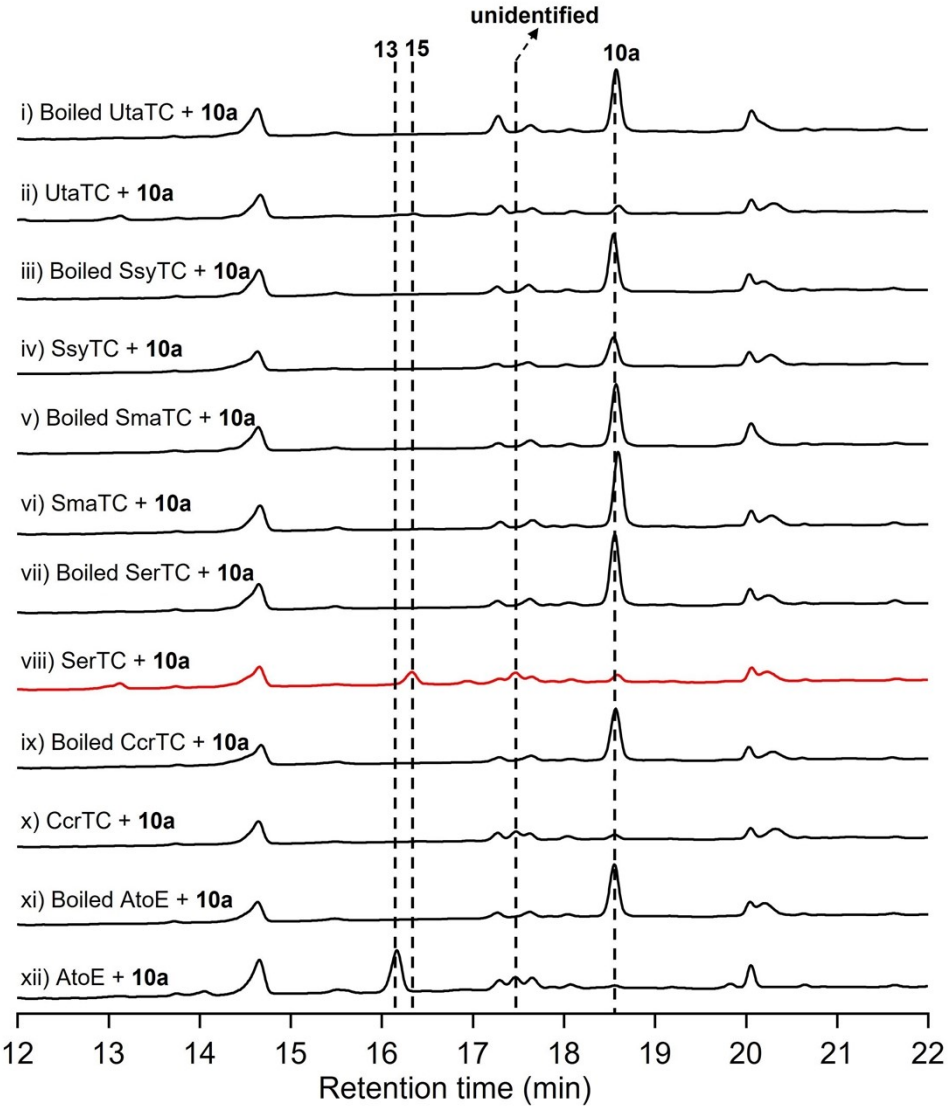

Figure S125. HPLC profiles (λ_{max} = 210 nm) of the in vitro reactions of class II MTCs (UtaTC, SsyTC, SmaTC, SerTC, CcrTC, and AtoE) with **10a**.

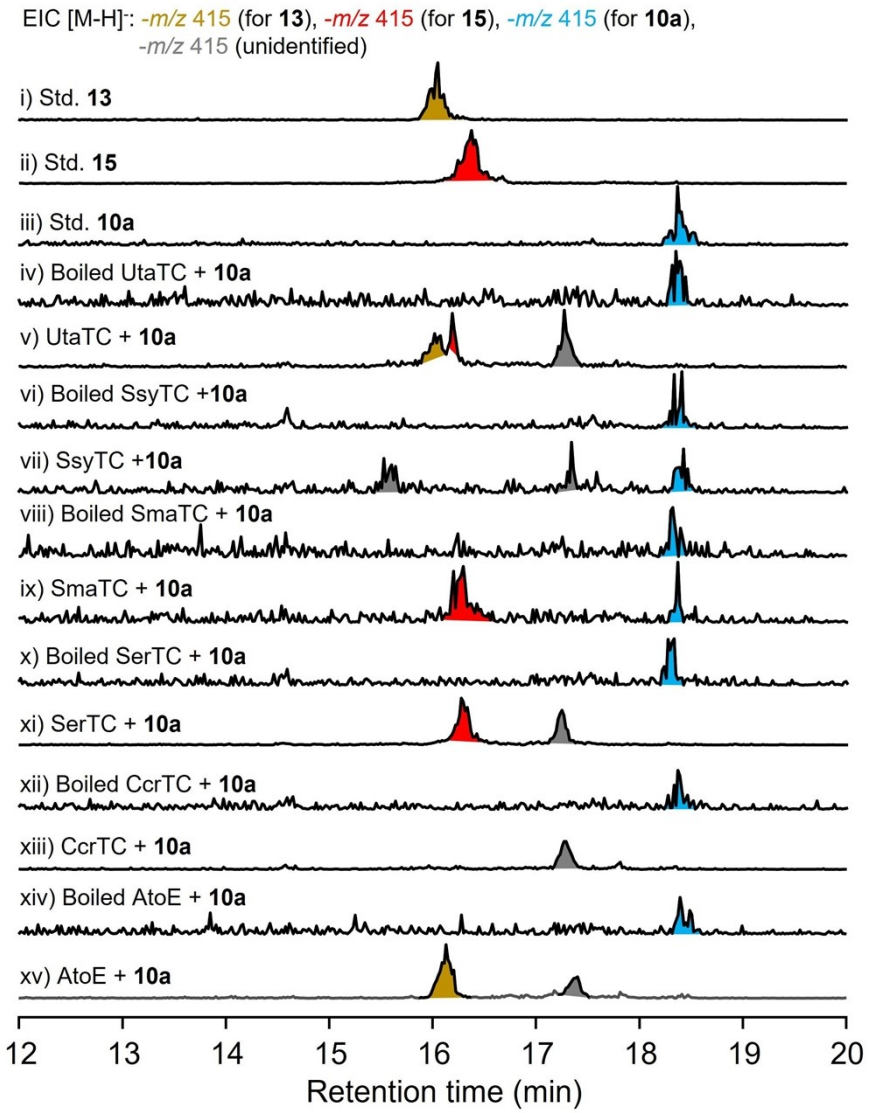

Figure S126. LC-MS analysis of the in vitro reactions of class II MTCs (UtaTC, SsyTC, SmaTC, SerTC, CcrTC and AtoE) with **10a**.

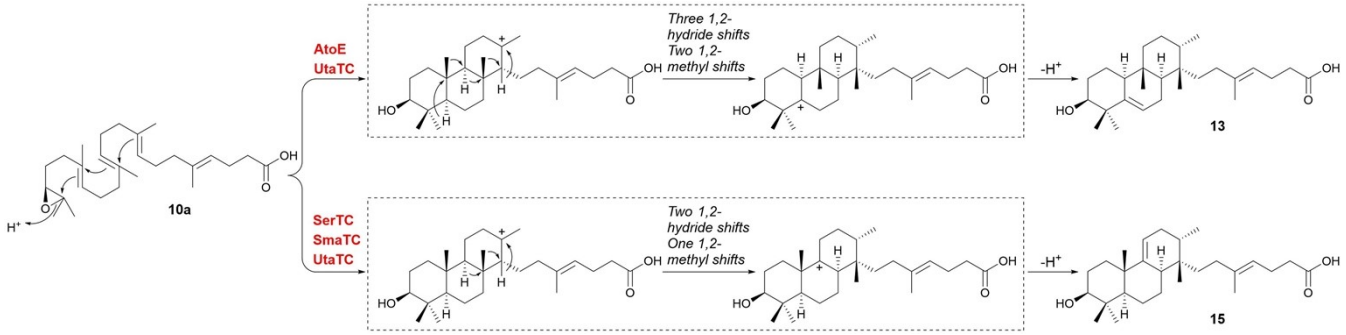

Figure S127. Proposed catalytic processes of the class II MTCs involving substrate **10a** to form **13** and **15**.

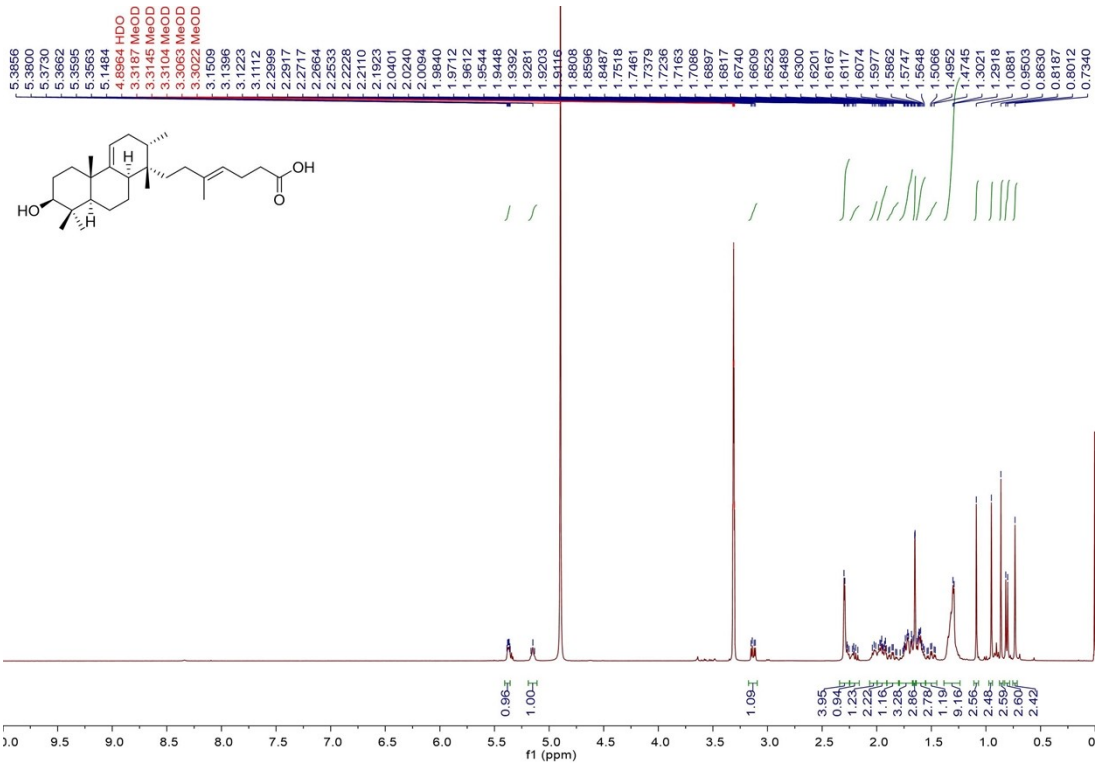

Figure S128. ^{1}H NMR spectrum of atolypene H (**15**) in methanol-d_4 (400 MHz).

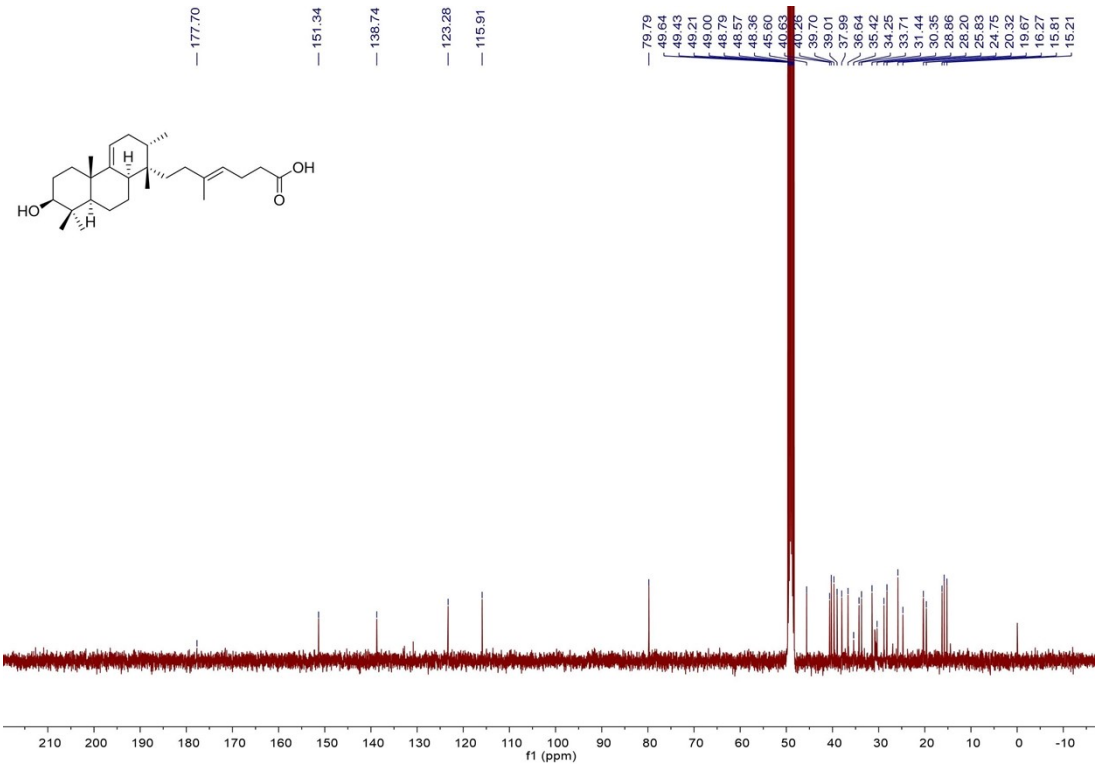

Figure S129. ^{13}C NMR spectrum of atolypene H (**15**) in methanol-d_4 (100 MHz).

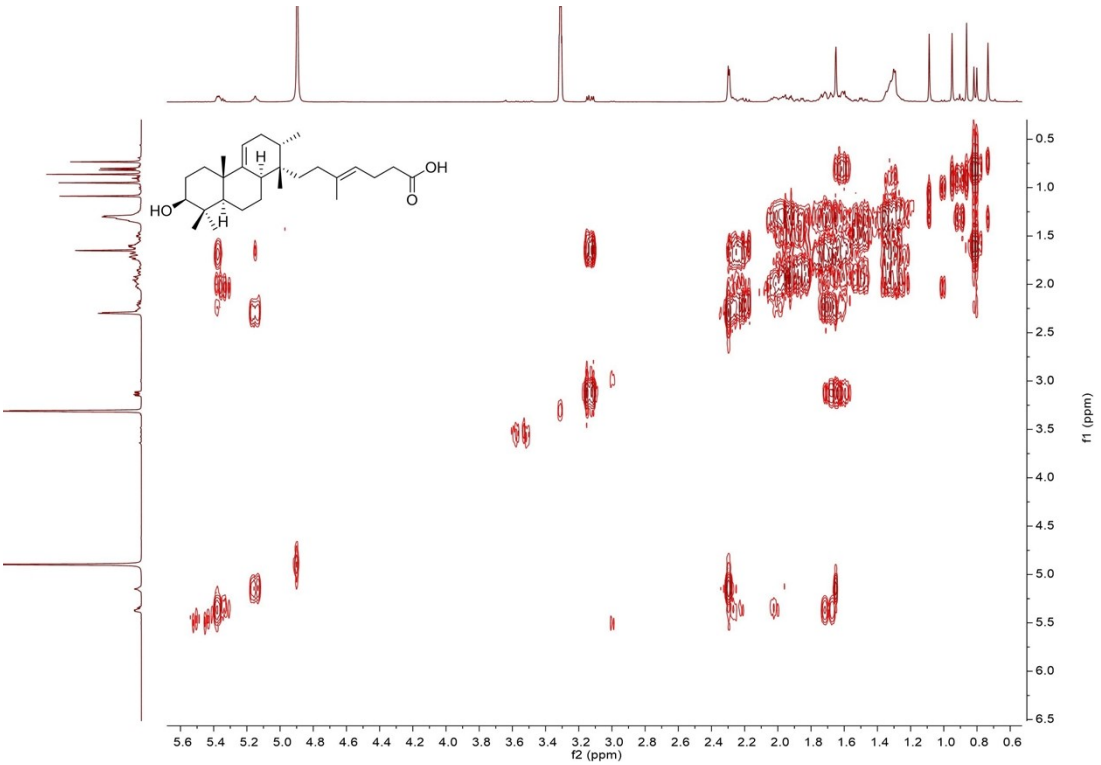

Figure S130. ^{1}H-^{1}H COSY spectrum of atolypene H (**15**) in methanol-d_4.

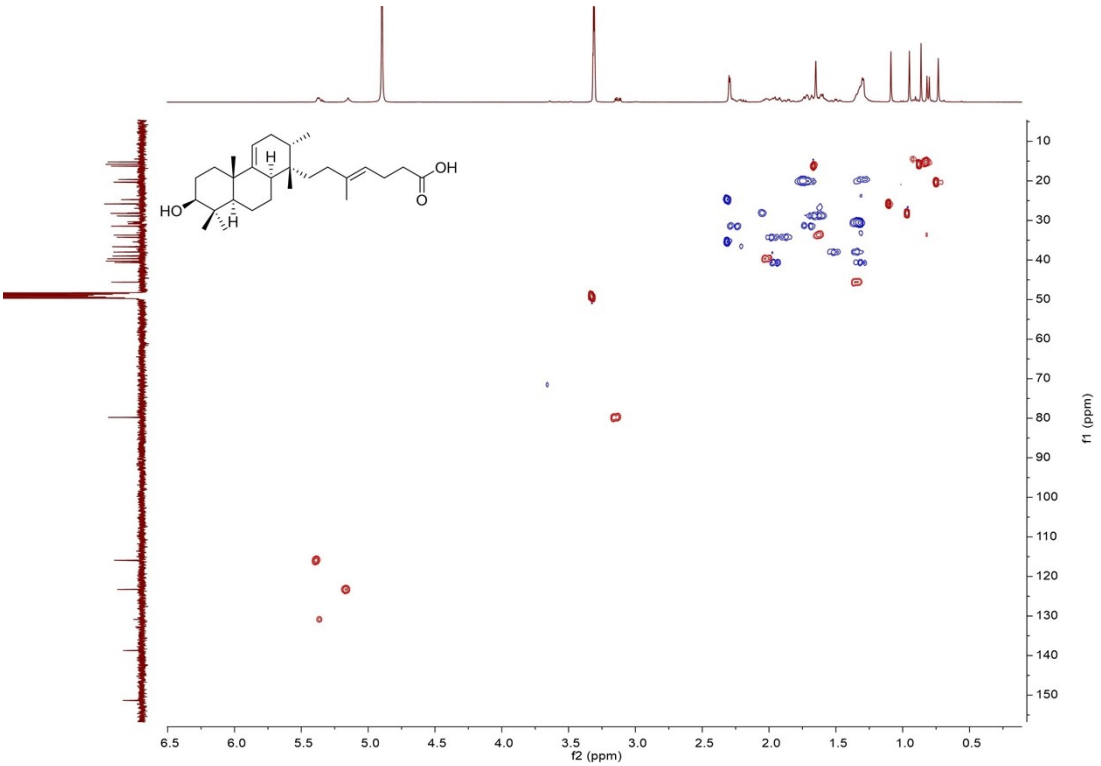

Figure S131. HSQC spectrum of atolypene H (**15**) in methanol-d_4.

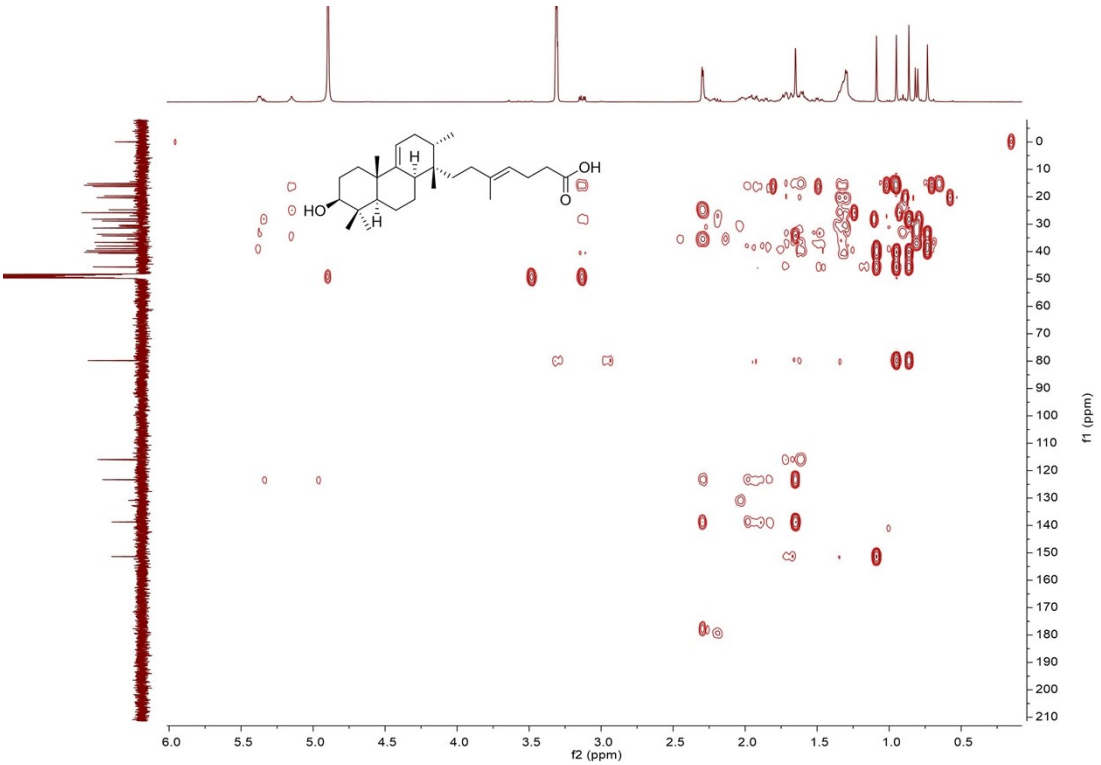

Figure S132. HMBC spectrum of atolypene H (**15**) in methanol-d_4.

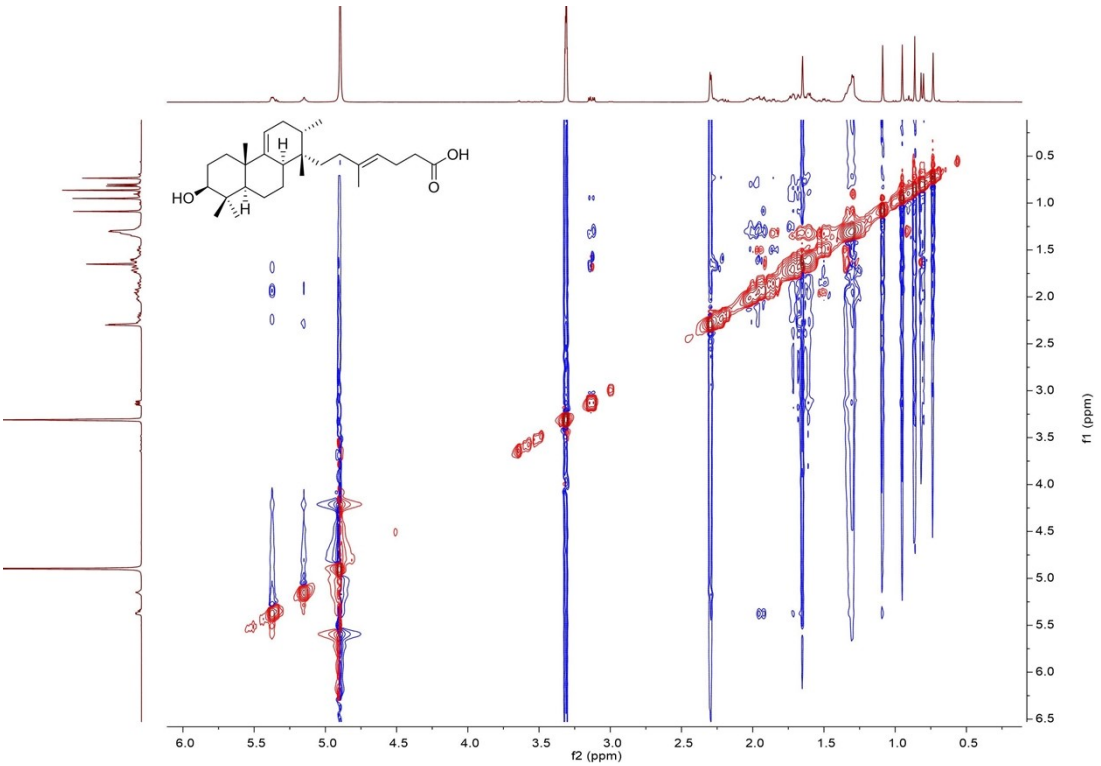

Figure S133. ROESY spectrum of atolypene H (**15**) in methanol-d_4.

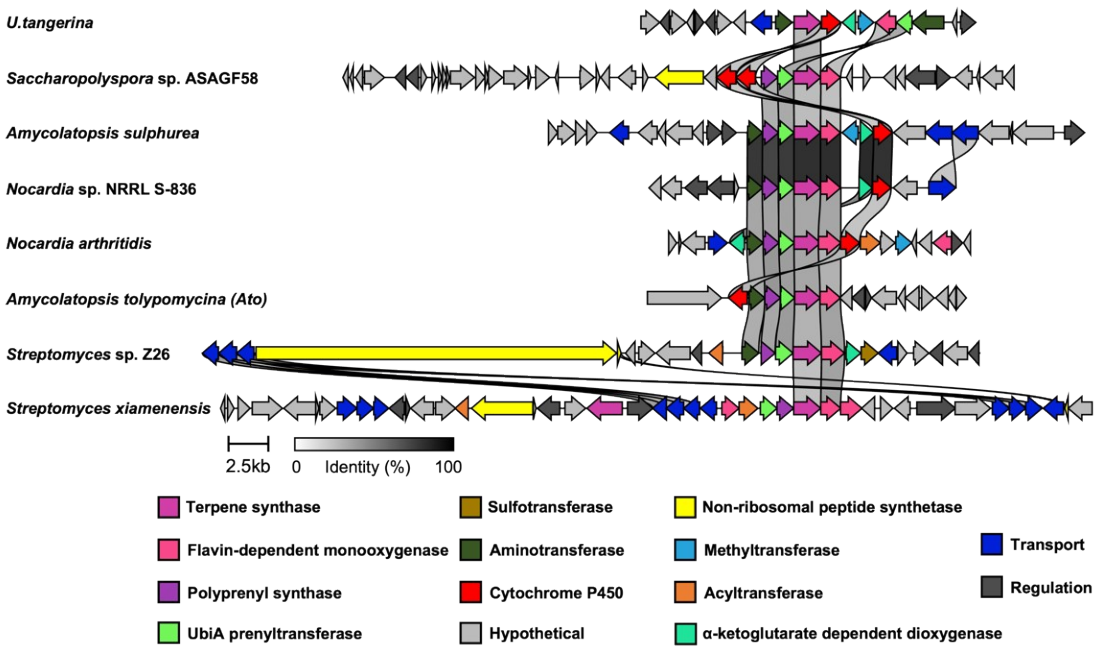

Figure S134. Analysis of selected *ato*-like BGCs. Links are drawn between genes if they share at least 30% identity. Genes are colored based on putative function.

References

[1] L.-B. Dong, X. Zhang, J. D. Rudolf, M.-R. Deng, E. Kalkreuter, A. J. Cepeda, H. Renata and B. Shen, *J. Am. Chem. Soc.*, 2019, **141**, 4043–4050.

[2] L.-B. Dong, J. D. Rudolf, D. Kang, N. Wang, C. Q. He, Y. Deng, Y. Huang, K. N. Houk, Y. Duan and B. Shen, *Nat. Commun.*, 2018, **9**, 2362.

[3] L.-B. Dong, J. D. Rudolf, M.-R. Deng, X. Yan and B. Shen, *ChemBioChem,* 2018, **19**, 1727–1733.

[4] S. Y. Hsu, D. Perusse, T. Hougard and M. J. Smanski, *ACS Synth. Biol.*, 2019, **8**, 2397–2403.

[5] P. Mazodier, R. Petter and C. Thompson, *J. Bacteriol.*, 1989, **171**, 3583–3585.

[6] L.-B. Dong, J. He, Y.-Y. Wang, X.-D. Wu, X. Deng, Z.-H. Pan, G. Xu, L.-Y. Peng, Y. Zhao, Y. Li, X. Gong and Q.-S. Zhao, *J. Nat. Prod.*, 2011, **74**, 234–239.

[7] X. T. Liang, J. H. Chen and Z. Yang, *J. Am. Chem. Soc.*, 2020, **142**, 8116–8121.

[8] E.J. Corey, M. C. Noe and W.-C. Shieh, *Tetrahedron Lett.*, 1993, **34**, 5995–5998.

[9] S. Kumar, G. Stecher, M. Li, C. Knyaz and K. Tamura, *Mol. Biol. Evol.*, 2018, **35**, 1547–1549.

[10] I. Letunic and P. Bork, *Nucleic Acids Res.*, 2021, **49**, 293–296.

[11] R. Zallot, N. Oberg and J. A. Gerlt, *Biochemistry*, 2019, **58**, 4169–4182.

[12] C. L. M. Gilchrist and Y.-H. Chooi, *Bioinformatics*, 2021, **37**, 2473–2475.

[13] M. S. Paget, L. Chamberlin, A. Atrih, S. J. Foster and M. J. Buttner, *J. Bacteriol.*, 1999, **181**, 204–211.

[14] S.-H. Kim, W. Lu, M. K. Ahmadi, D. Montiel, M. A. Ternei and S. F. Brady, *ACS Synth. Biol.*, 2019, **8**, 109–118.

[15] S. C. Chang, W. C. Yang and Y. H. Lee, *Biochim. Biophys. Acta.*, 1992, **1129**, 219–222.

[16] J. P. Gomez-Escribano and M. J. Bibb, *Methods Enzymol.* 2012, **517**, 279–300.

[17] M. Bierman, R. Logan, K. O'Brien, E. T. Seno, R. N. Rao and B. E. Schoner, *Gene*, 1992, **116**, 43–49.

[18] J. D. Rudolf, L.-B. Dong, T. Huang and B. Shen, *Mol. Biosyst.*, 2015, **11**, 2717–2726.

[19] T. Itoh, K. Tokunaga, Y. Matsuda, I. Fujii, I. Abe, Y. Ebizuka and T. Kushiro, *Nat. Chem.*, 2010, **2**, 858–864.

[20] Y. Hayashi, N. Matsuura, H. Toshima, N. Itoh, J. Ishikawa, Y. Mikami and T. Dairi, *J. Antibiot.*, 2008, **61**, 164–174.

[21] C. Dürr, H. J. Schnell, A. Luzhetskyy, R. Murillo, M. Weber, K. Welzel, A. Vente and A. Bechthold, *Chem. Biol.*, 2006, **13**, 365–377.

[22] T. A. Alsup, Z. Li, C. A. McCadden, A. Jagels, D. Łomowska-Keehner, E. Marshall, L.-B. Dong, S. Loesgen and J. D. Rudolf, *RSC Chem. Biol.*, 2024, **5**, 1010-1016.

[22] Y. Hayashi, H. Onaka, N. Itoh, H. Seto and T. Dairi, *Biosci. Biotech. Bioch.*, 2007, **71**, 3072–3081.